Università degli Studi di Pavia

Dipartimento di Scienze della Terra e dell'Ambiente

SCUOLA DI ALTA FORMAZIONE DOTTORALE

MACRO-AREA SCIENZE E TECNOLOGIE

DOTTORATO DI RICERCA IN SCIENZE DELLA TERRA E DELL'AMBIENTE

Chiara Amadori

3D architecture and evolution of the Po Plain - Northern Adriatic Basin since the Messinian salinity crisis through Pliocene-Pleistocene time

Anno Accademico 2014-2017
Ciclo XXX

Coordinatore
Prof. Roberto Sacchi

Tutor
Prof. Andrea Di Giulio

Co-tutors
Dott. Giovanni Toscani
Dott. Daniel Garcia-Castellanos

Official Acknowledgments

I want to sincerely thank everyone who contributed to the completion of this Ph.D Thesis. In particular, I want to thank Andrea Di Giulio and Giovanni Toscani for their constant presence, scientific and psychologic support (sometimes needed).

This Thesis gained substantially from the co-operation with Eni E&P that is why I am very (very) grateful to Manlio Ghielmi and Roberto Fantoni for supplying me with data and for helping familiarise me with the subsurface features of the Po Basin. These two guys, that I greatly admire, have infinite energy and passion for research; because of them, Academia should envy Eni.

Thanks also to Claudio Cattaneo for the funny moments spent during Data Room days.

I want also thank Nicoletta Mancin for performing the micropaleontological analyses, Francesco Maesano and Chiara D'Ambrogi for the helpful and productive discussions and, above all, the time-depth conversion modeling.

Special thanks go to the brilliant modelers: Daniel Garcia-Castellanos for his fundamental help in numerical modeling and Pietro Sternai, for his great care in paper writing!

I want also sincerely thank all the people I have met at the CSIC-ICTJA and the University of Barcelona for the very pleasant time spent together in Barcelona.

CHAPTER 1
INTRODUCTION

1.1. Aims

The proposed scientific project aims at reconstructing the Late Messinian-Pleistocene 3D architecture of the Po Plain-Northern Adriatic foredeep-foreland basin, studying its regional step-wise evolution. The foredeep-foreland basins evolution is a wide and fundamental topic for a number of geological studies and applications because their deposits architecture contains abundant information about tectonic, sedimentary and climate processes that occurred through times on the scales of the entire basin in collisional settings. The 3D shape of a foreland basin is, in fact, the result of the interaction among thrust belt deformation/uplift, consequent accommodation space creation, iv) sediment supply, erosion and eustacy/climate processes. All these processes are recorded in the study area which is the shared foreland-foredeep of two thrust belts (The Southern Alps and Northern Apennines) with opposite vergence. Moreover, the Po Plain has been one of the most important continental oil and gas province in the western Europe and is the most densely populated region in Italy. In such a region, basin architecture impacts, for instance, on water resources, seismic hazard and subsidence distribution (both natural and induced). All these elements ensure that a 3D reconstruction of the late Messinian-Pleistocene fill of the Po Plain and the study of its controlling processes can be not only an important scientific contribution but also a useful tool for different activities (land management, natural resources exploitation/protection, and seismic hazard assessment).

Thanks to the huge amount of subsurface data mostly provided by hydrocarbon exploration (Eni Upstream private property), the geodynamic system formed by the Po Plain foreland basin enclosed by the Southern Alps and Northern Apennines is an ideal laboratory to investigate the relationships between deep and surface processes in driving the architecture of foreland basins. Previous studies starting from the early 80s, different scientific projects and researches have been carried out to describe the structural framework of the Po Plain area (Pieri & Groppi, 1981; Bigi et al., 1986; Cassano et al., 1986; Bigi et al., 1990, Fantoni and Franciosi, 2010; Turrini et al., 2014, 2016). All these studies, mainly coming from or being devoted to hydrocarbon exploration, did not describe the most recent stratigraphic architecture of the Po Plain. All of them in fact, taking advantage of a limited number of seismic reflection profiles and cross sections, describe the main buried structures and the general architecture of the basin, without giving details about the most recent (last ca. 6 Ma) tectonic and stratigraphic evolution of the central Po Plain-Northern Adriatic basin. This lack of information

and data has been partially compensated in the last 10 years by recent papers that described in detail the facies distribution of the Plio-Pleistocene sediments of the Po Plain (Ghielmi et al., 2010, 2013; Rossi et al., 2015). Nevertheless, the basin-scale 3D architecture of the topmost part of the Po Plain-Northern Adriatic sedimentary infill remains largely undetermined.

The chief objective of this project is to perform and illustrate, for the first time, the central-eastern Po Plain and Northern Adriatic basin 3D stratigraphic model of the late Messinian-Pleistocene sedimentary infill, from 3D lithospheric to 1D scale with some focus on the Venetian Friulian basin. The main objects of the present Thesis are itemized as follow:

- Analysis of the 3D step-wise tectono-sedimentary evolution of the Po Plain-Northern Adriatic Basin subsurface by 2D seismic analysis, 3D time-to-depth conversion and reconstruction of isopach maps.
- Reconstruction of the paleotopography of the Po Plain during the Messinian salinity crisi maximum sea level drop through backstripping analysis.
- Description of the Venetian-Friulian and Northern Adriatic basin detailed Plio-Pleistocene stratigraphic evolution through 2D seismic interpretation, well correlation and 1D geohistory analysis.
- Discussion of the Tectonic Vs Climate control on sediment supply through time.

This Thesis is organized into chapters; the third, fourth and fifth ones are three different extended papers. They are scientifically independent, still related to the same study area but focusing on various aspects of the Po Plain-Northern Adriatic basin analysis by means of diversified methods (i.e., seismic interpretation, well-log analysis, 3D modeling, numerical modeling, backstripping analysis).

1.2. Research project relevance

A detailed description of the tectonostratigraphic architecture of the Po Plain area has filled a knowledge gap regarding the latest c. 6 Ma. Indeed, a detailed knowledge of this 3D stratigraphic record is of important for different aspects. It hosts important natural gas reservoirs, aquifers, and storage sites, it is also responsible for natural subsidence affecting the Po Plain and for seismic site effects (i.e. amplified surface ground motion) due to geotechnical conditions of surficial geological layers (e.g. Ronald Abraham et al., 2015).

The Po Plain subsurface has long been studied, described, explored and exploited, being of strategic relevance mainly for the oil and gas production. Up to less than 20 years ago, the Po Plain was one

of the main oil and gas province in Western Europe and also at present is a target for natural gas research and exploitation.

In this view and for these reasons, a vast scientific literature dealt with these sectors of the Po Basin (Lindquist, 1999; Casero, 2004; Ghielmi et al., 2008; Eni, 2009; Bertello et al., 2010; Ghielmi et al., 2010, 2013; Cazzini et al., 2015 and reference therein), where oil traps are located, typically structural highs and fault-related anticlines in Mesozoic carbonate sequences.

A more limited number of scientific researches dealt with the entire extension of the Po Plain and with its buried structures and subsurface architecture. Moreover, the few studies considering the whole Po Plain give a mostly qualitative description of the basin architecture providing a very general picture frame of the subsurface. The even more restricted number of studies concerning the Po Plain with a more detailed and quantitative approach, provide data with a resolution not sufficient for further studies devoted to volume calculations, seismic risk assessment, slip rates calculations.

In addition, since these detailed studies are carried out in different times, by different research groups, with different datasets, surveying different stratigraphic levels or time periods and taking advantage of different velocity models, all these studies are often intrinsically scientifically rigorous and sometimes also extremely detailed but very inhomogeneous among themselves. Moreover, these studies often do not contain the original data (i.e. seismic reflection profiles or well logs) but only redrawn wells, maps and cross sections, in many cases georeferenced with different coordinate systems and projections.

For all these reasons, the attempt of merging them in a coherent 3D model would not only be extremely time consuming but also scientifically impossible or extremely imprecise. Below, a list of some basin-scale studies dealing with the entire Po Plain is reported in order to give a general (but not exhaustive) view of the available scientific products. For each of them, a brief description of the data contained will be given, along with the explanation of the reason(s) why they are not suitable for a complete and detailed description of the late Messinian-Pleistocene architecture of the Po Plain.

- Pieri and Groppi, 1981: this paper contains 14 regional profiles that allow a good description of the buried structures in the Po Plain. It has been for years the reference publication dealing with the Po Plain as it contains also structural maps of the buried Northern Apennine main thrusts and structure contour maps of the bottom Pliocene. Notwithstanding the fundamental importance of this first complete description of the Po Plain subsurface, its level of resolution and the space between data does not allow any constrained 3D reconstruction of the Plio-Pleistocene stratigraphic sequence
- Cassano et al., 1986: a few years later Cassano et al. published 13 regional cross sections,

with similar (in some cases coincident) traces of those from Pieri and Groppi. In addition to this, Bouguer anomalies and gravimetric maps were provided in order to better constrain the deep structures, usually the goal for oil and gas exploration. Once again, given the purpose of the study and the object of the research, the Plio-Pleistocene interval have been detailed following the same approach of Pieri and Groppi.

- Bigi et a., 1992, Structural Model of Italy: this regional map provides a detailed picture of the buried faults in the Po Plain along with a structure contour map of the bottom Pliocene (contour lines every 500 m). Also in this case, only the base Pliocene surface has been reconstructed with a 1:500.000 scale, not suitable for quantitative detailed analysis.
- Fantoni and Franciosi, 2010: 8 regional profiles describe the main structures in the Po Plain and in the Adriatic foreland. 5 of these 8 regional cross sections are located in the Po Plain and the Plio-Pleistocene stratigraphic sequence is subdivided into 4 intervals. Anyway, also, in this case, the space between the regional cross sections is of tens of kilometres so that a 3D reconstruction starting from these data is impossible.
- Ghielmi et al. 2010 and 2013: these two recent papers describe the stratigraphic record and the tectonic evolution in the Po Plain and Northern Adriatic Sea area from Messinian to Middle Pleistocene times. The authors considered an impressive amount of seismic profiles and well logs and the result is the most detailed published facies distribution within the Plio-Pleistocene time interval. Nevertheless, no basin-scale information was given neither on the thickness of different units nor on the depth of the key stratigraphic horizons.
- Turrini et al. 2016: in this paper, the authors provide an isopach map of the Plio-Pleistocene deposits, useful for basin/regional analysis, but whose level of resolution (space between original data) is sufficient for qualitative descriptions, not for quantitative ones.

From this brief review of papers and maps regarding the entire Po Plain, it is evident that several deep stratigraphic levels (e.g. bottom Pliocene, top of Mesozoic carbonates) have been reconstructed and/or described by some of the previous authors (according to quality, spacing, and confidentiality of data). At the same time, an equally evident gap of knowledge regarding the 3D architecture of the Plio-Pleistocene deposits comes out also from a first scientific literature check. This is justified and comprehensible considering that Plio-Pleistocene deposits have been the main target for hydrocarbon exploration (especially for gas) in the Po Plain, thus dataset was not released to the scientific community. These deposits are of fundamental importance not only from the applied point of view but also from the scientific one. This project aims at filling the gap of knowledge regarding the most recent and shallowest levels in the Po Plain, in this way giving also a contribution to the

comprehension of the complex thrust-fold belt/foredeep and climate VS tectonic relationships. Further outcomes that can be taken into account after the end of the project, both from Academia and industry, are:

- to evaluate and study new geopotentials.
- the detailed 3D model can support further studies for subsidence analysis for hydrogeological and hydrocarbon extraction.

CHAPTER 2
GEOLOGICAL SETTING

2.1. Geodynamic Setting

The geological setting of the Po Plain-Northern Adriatic region (Fig. 1) has been deeply investigated and described by several authors through the last 40 years (Cuffaro et al., 2010; Fantoni and Franciosi, 2010; Turrini et al., 2016 and reference therein); this chapter tries to briefly summarize the state of art.

Figure 1. Digital elevation model of the study area: Po Plain and Northern Adriatic Sea (Fontana, 2012).

The Italian peninsula is defined as the result of complex geodynamics where both pre-Alpine (Mesozoic and pre-Mesozoic) and Alpine (mainly Cenozoic) tectonics have interacted through time to create the current, high-complex structural and stratigraphic puzzle (Castellarin, 2001; Castellarin and Cantelli, 2010; Cuffaro et al., 2010; Mosca et al., 2010; Carminati and Doglioni, 2012 and reference therein) (Figs. 2, 3). Within this inherited geological setting, the Po Valley (hereafter, also Po Plain or Po basin) together with the Northern Adriatic Sea, corresponding to the northernmost buried sector of the Adria plate, is approximately 40,000 km^2 large. This region is the shared foreland-foredeep domain of three different orogens: it represents the foredeep and foreland of the SW-directed Apennines subduction (Carminati et al., 2003) (Fig. 2), the retrobelt foreland of the SE-directed Alpine subduction (Doglioni and Carminati, 2002; Dal Piaz et al., 2003; Kummerow et al., 2004) and the foreland basin of the NE-directed Dinaric

subduction (Di Stefano et al. 2009) (Fig. 3). Each subduction is associated with different vertical motions, e.g., subsidence in the foreland basin and uplift in the belt. All three belts propagated toward the Adriatic lithosphere (Panza et al. 2003, Barbieri et al., 2004; Cuffaro et al., 2010 and reference therein), gradually reducing the area of the plate.

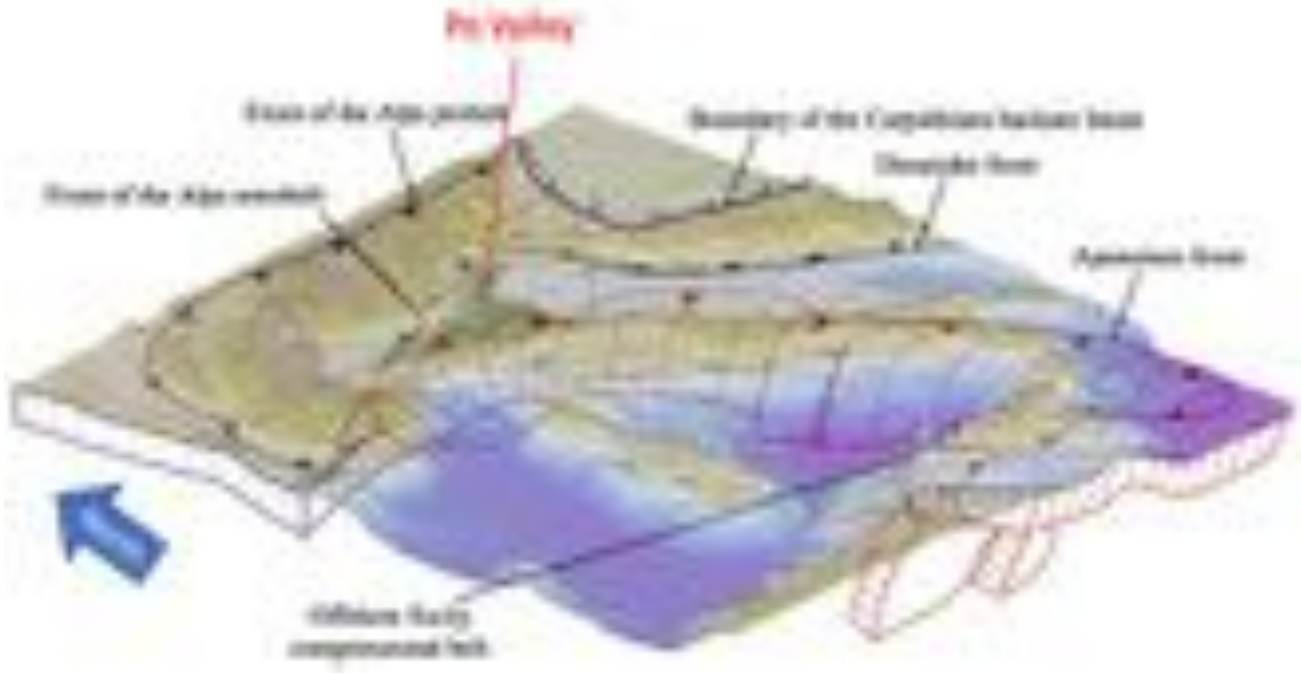

Figure 2. The Po Plain and surrounding tectonic units, Adria plate subduction in evidence (modified from Carminati and Doglioni. 2012).

Indeed, the tectonic history of the region likely started at the end of the Paleozoic and is still going on as accounted by recent studies and the latest earthquake-activity in the central and eastern parts of the basin: the Apennine front currently concentrates seismogenetic structures either along blind thrusts buried beneath the Po Plain, or along the partially exposed structures forming the mountain front that bounds the plain to the southwest (Burrato et al., 2003; Carminati et al., 2003, 2010; Toscani et al., 2006, 2009; Picotti and Pazzaglia, 2008; Livio et al., 2009; Fantoni and Franciosi, 2010; Maesano et al., 2013). Thanks also to this peculiar tectono-stratigraphic setting, the Po Plain-Northern Adriatic regions is one of the major hydrocarbon provinces of continental Europe (Casero, 2004; Picotti et al., 2007; Fantoni and Franciosi, 2010; Cazzini et al., 2015).

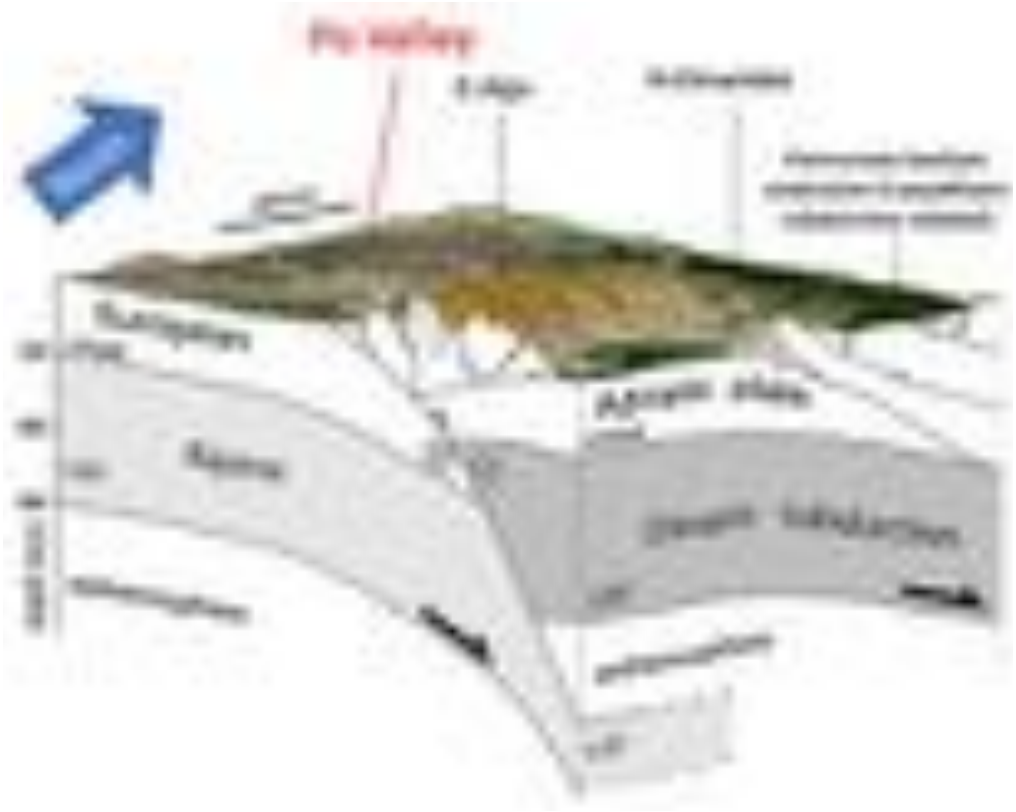

Figure 3. Interference between Alpine and Dinaric subductions (modified from Cuffaro et al. 2010).

Remarkably, a large part of the geological knowledge in the region is related, directly or indirectly, to the oil business (Pieri and Groppi, 1981; Bongiorni, 1987; Cassano et al., 1986; Mattavelli and Novelli, 1987; Mattavelli and Margarucci, 1992; Casero et al., 1990; Lindquist, 1999; Bello and Fantoni, 2002; Fantoni et al., 2004; Ghielmi et al., 2010, 2013).

The Po Valley deep subsurface architecture resulted from a Mesozoic extensional tectonic phase, developed in the western Tethys realm related to Upper Triassic-Lower Jurassic rifting, with evidence for Cretaceous to Paleogene structural inversion during Alpine pre- and syn-collisional tectonic phases (Bertotti et al., 1993; Masetti et al., 2012 and reference therein). Then, since late Miocene, compression affected the foreland and the surrounding orogenic belts, due to Apennine north-to-northeast migration (Fantoni and Franciosi, 2008; 2010; Ghielmi et al., 2013; Turrini et al., 2014).

The subsurface stratigraphic succession of the Po basin (Fig. 4) (Jadoul and Rossi, 1982; Lindquist, 1999; Argnani and Ricci Lucchi, 2001; Bertotti et al., 1993; Mellere et al., 2000; Fantoni and Franciosi, 2008, 2010 and reference therein) overlies the Variscan crystalline basement and, from base to top is made by:

i) late Paleozoic–Mesozoic evaporitic–siliciclastic sediments during the Lower Triassic rifting;

ii) Middle Triassic carbonate depositional system, articulated in platforms and intra-platform basins filled with mixed siliciclastics and carbonate sediments;

iii) pelagic systems developed during the maximum deepening and widening of the North-South-trending basins formed during the Upper Triassic-Jurassic extensional phase (Bertotti et al., 1993; Sarti et al., 1993);

iv) syntectonic Tertiary siliciclastics produced when the Alpine deformation involved the Mesozoic carbonates and the overlying clastic sequences;

v) high and low efficient turbidites during the entire late Miocene-middle Quaternary, time when the area was involved only in the Apennines deformation, causing the southward-dipping of the entire foreland and progressive depocenters filling (see geological sections in Pieri and Groppi, 1981; Bigi et al., 1986; Cassano et al., 1986; Fantoni and Franciosi, 2010; Toscani et al., 2014; Ghielmi et al., 2013 and reference therein).

Details on the late Messinian-Pleistocene tectono-sedimentary are contained in the following section *2.2*.

Figure 4. Schematic stratigraphic column of the Po Plain (modified from Linququist, 1999; Casero 2004 and Turrini et al., 2014). MS = major unconformity. On the right, only the hydrocarbon system related to the Mesozoic oils is described (Turrini et al., 2014). Colour code from International Stratigraphic Chart, 2017.

Across the region, the buried structural geometries mainly refer to the external domains of the Southern Alps and the Northern Apennines, created tectonic arches and controlled the sediment infilling geometries of the respective foredeep-basins (Pieri and Groppi, 1981; Cassano et al., 1986; Castellarin et al., 1985; Carminati and Doglioni, 2012; Argnani and Ricci Lucchi, 2001; Bartolini et al., 1996; Bertotti et al., 1997; Castellarin and Vai, 1986; Perotti, 1991; Perotti and Vercesi, 1991; Ricci Lucchi, 1986; Fantoni et al., 2014; Toscani et al., 2014; Scardia et al., 2015 and reference therein) (Fig. 5).

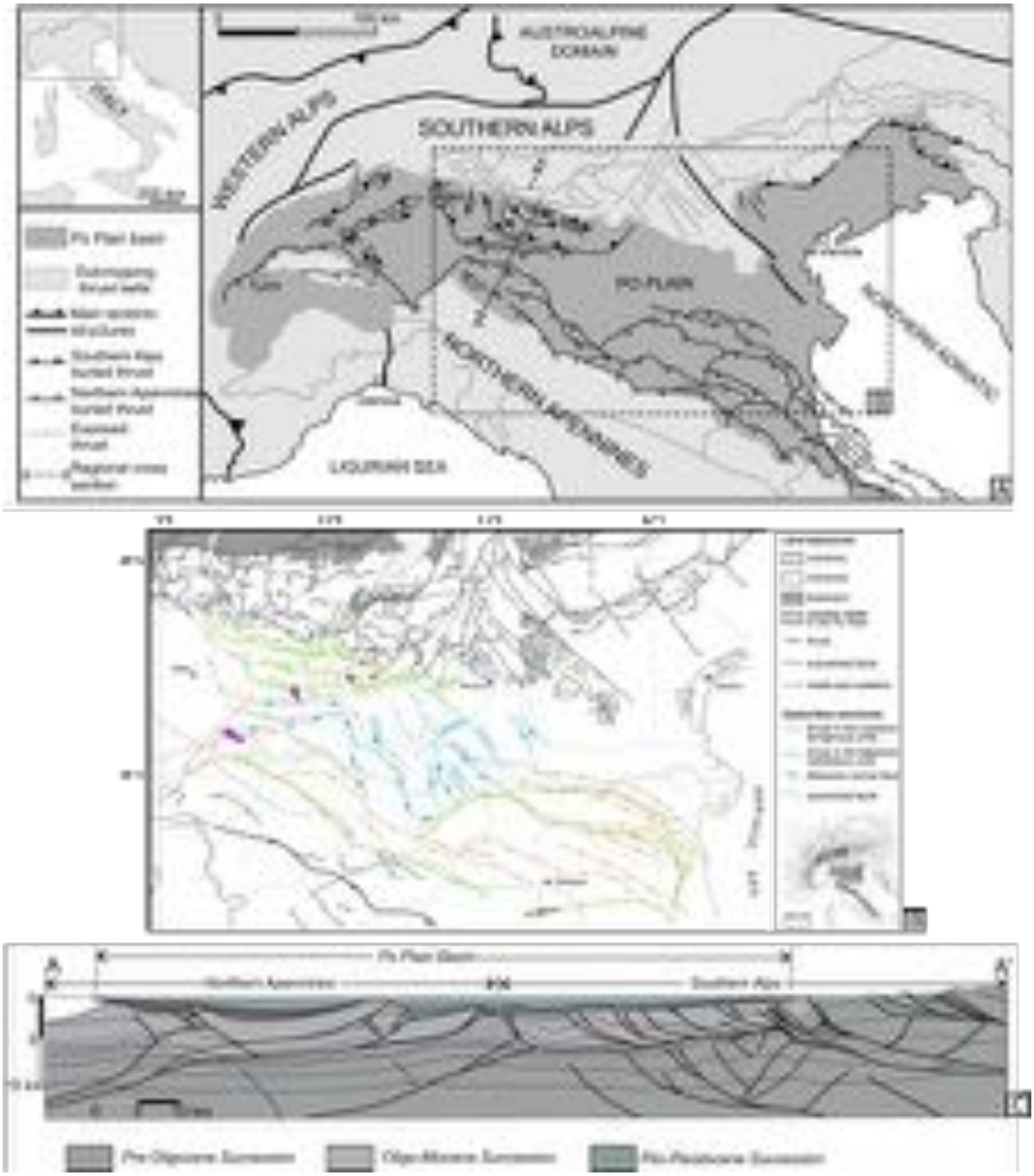

Figure 5. Po Plain - A: Northern Adriatic tectonic setting (modified from Toscani et al., 2014). B: structural map of the central-eastern Po Plain (modified from Scardia et al., 2015). C: Geological profile, see box A for location (modified from Toscani et al., 2014).

2.2. Late Messinian-Pleistocene tectono-stratigraphic evolution of the Po Plain-Northern Adriatic Basin

Recently, fundamental steps forward on the Po Plain-Northern Adriatic basin tectono-sedimentary architecture have been done thanks to new seismics and well-log data released by Eni's research group in a few papers collecting multidisciplinary results from the last 15 years of study (Fantoni and Franciosi, 2010; Ghielmi et al., 2010, 2013; Cazzini et al., 2015; Rossi et al., 2015). The main output is a detailed 2D basin-scale tectono-stratigraphic model described by several time-related lithofacies association maps.

This chapter attempts to summarize the state of the art from the papers above cited; the renewed overview of the Po Plain-Northern Adriatic Basin (hereafter PPAF) became also the fundamental starting point for this Thesis work and its outcomes.

The maps from Ghielmi et al. (2010, 2013) will be described separately and only the thrust fronts and faults which were active or present at the corresponding sequence time will be shown.

The late Miocene to Pleistocene tectono-stratigraphic setting of the PPAF has to be primarily attributed to the Northern Apennine structural evolution, therefore, in spite of the three competing subductions acting along the northern Adriatic plate boundaries, the flexure of the Apennines slab controlled almost completely the subsidence of the northern Adriatic area (Carminati et al., 2003, 2005). As a consequence of the severe Apennine compressional synsedimentary tectonics, the Adria foreland basin changed its shape through depocenter migration towards the foreland located to the northeastern regions, i.e. Veneto and the Northern Adriatic Sea, including the former Marnoso-Arenacea basin, located in the Emilia-Romagna Apennines, into the thrust-and-fold belt. According to Ghielmi et al. (2010, 2013), this migration occurred through alternating stages of simple and fragmented foredeep (Fig. 6).

The structural evolution of the Northern Apennine N to NE-verging blind arcs was not simultaneous across the whole Po Plain: while the Emilia arc started deforming in the Tortonian, experienced its maximum uplift activity in Piacenzian–Gelasian times and reached its present-day configuration in the Zanclean (Toscani et al., 2014 and reference therein), to the east the outward propagation of the Ferrara–Romagna arc was active since the Messinian and continued until the Zanclean–Piacenzian and the Gelasian, for the inner and for the outer Ferrara arcs respectively (Boccaletti et al., 1985; Bigi et al., 1992; Ghielmi et al., 2010, 2013: Maesano et al., 2015).

The continuing Quaternary tectonic activity, although associated with an elusive topographic expression, is recorded by deformation and tilting of river terraces and exposed syntectonic sediments (Boccaletti et al., 1985; Boccaletti et al., 2011; Picotti and Pazzaglia, 2008; Wegmann and Pazzaglia, 2009; Ponza et al., 2010). Conversely, out in the plain there are only a few exceptions to the general blind geometry of the buried outer fronts of both the SA and NA chains.

A partial exception is represented by the Mantova Monocline (MM) not involved in the foredeep migration during the Pliocene (the last migration took place during the Intra-Messinian Phase). This anomaly is probably related to the local presence of a rigid substratum (Trento Plateau) that hampered the thrust migration towards the foreland.

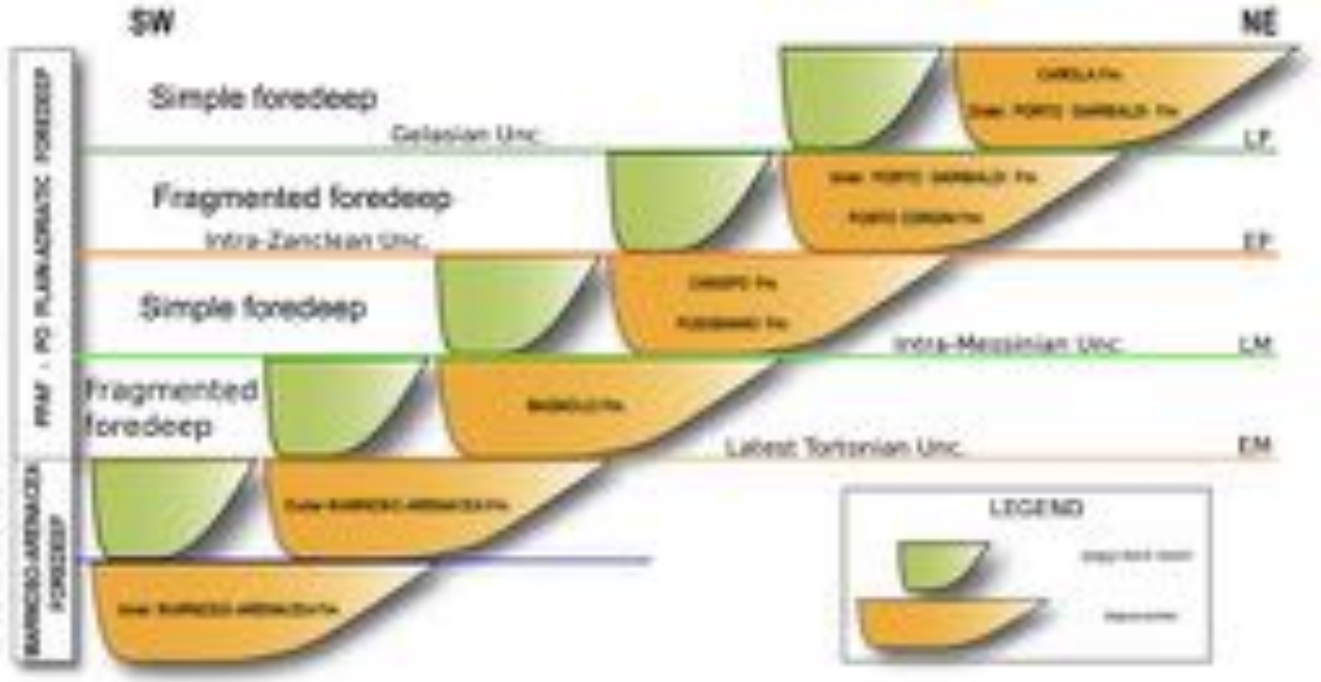

Figure 6. Model of the Po Plain-Adriatic Foredeep (PPAF) depocenters migration (modified from Ghielmi et al. 2010)

Ghielmi et al. (2010, 2013) and Rossi et al. (2015) based their tectono-stratigraphic analysis of the PPAF on the recognition of large-scale tectono-stratigraphic units, the allogroups (NACSN 1983). The allogroups are bounded by major tectonically induced unconformities produced by high magnitude basin modifying tectonic phases (Fig. 5, 6). Their boundaries also correspond to abrupt major changes in the type and gross distribution of depositional systems.

For instance, in the foreland and foreland ramp areas these major tectonic phases are marked by drowning-platform unconformities recording sharp relative sea-level rises in most of the areas; on the contrary, in the Northern Apennine thrust-and-fold belt, the same tectonic phases were responsible for severe uplift and tilting of the thrust-top basins, corresponding to abrupt relative sea level falls and by

sharp basinward shifts of the coastal and marginal marine depositional systems.

Component unconformity-bounded sub-units are the Large-Scale Sequences (LSS), according to Ghielmi et al. (2010, 2013). LSSs can be recognized within the allogroups and they are usually produced by lower magnitude tectonic phases corresponding to important sedimentary facies changes; during the middle-late Quaternary they are also influenced by climate driven sea-level fluctuations.

Allogroups and LSSs unconformities are synchronous along the basin, from the piggy-back basins through the foredeep and foreland ramp, because related to the same deformation phase. Accurate datation of the events and the unconformities corresponding to allogroup and sequence boundaries, were carried out by Eni's research group by means of paleontological analysis of foraminifera and nannoplankton assemblages and magnetostratigraphy (i.e. Muttoni et al., 2003), both for supporting and verifying the well and seismic correlations as well as the environmental interpretation. On Messinian succession, palynological analysis was also performed.

These deformative events generated four major tectonically controlled basin-scale unconformities: Latest Tortonian Unc. (not investigated during this Thesis), Intra-Messinian Unc. (ME3) at the base of allogoup LM, Intra-Zanclean Unc. (PL2) at the base of allogoup EP and base Gelasian Unc. (PL4) at the base of allogoup LP, plus four LSSs maps: base Pliocene (PL1), Intra-Piacentian (PL3), ca. base Calabrian (PS1) and base middle Pleistocene (PS2) (Fig. 7, 8).

The PPAF allogroups span in time 1.5–2.5 Ma and are represented by deposits which are some thousands of meters of present-day thickness in the foredeep depocenters; the LSSs instead, span in shorter time 0.15–1.3 Ma.

In order to avoid confusion with previous papers (Ghielmi et al., 2010, 2013; Rossi et al., 2015), in the following chapters, this Thesis will use same names and colour code for allogroups and LSSs.

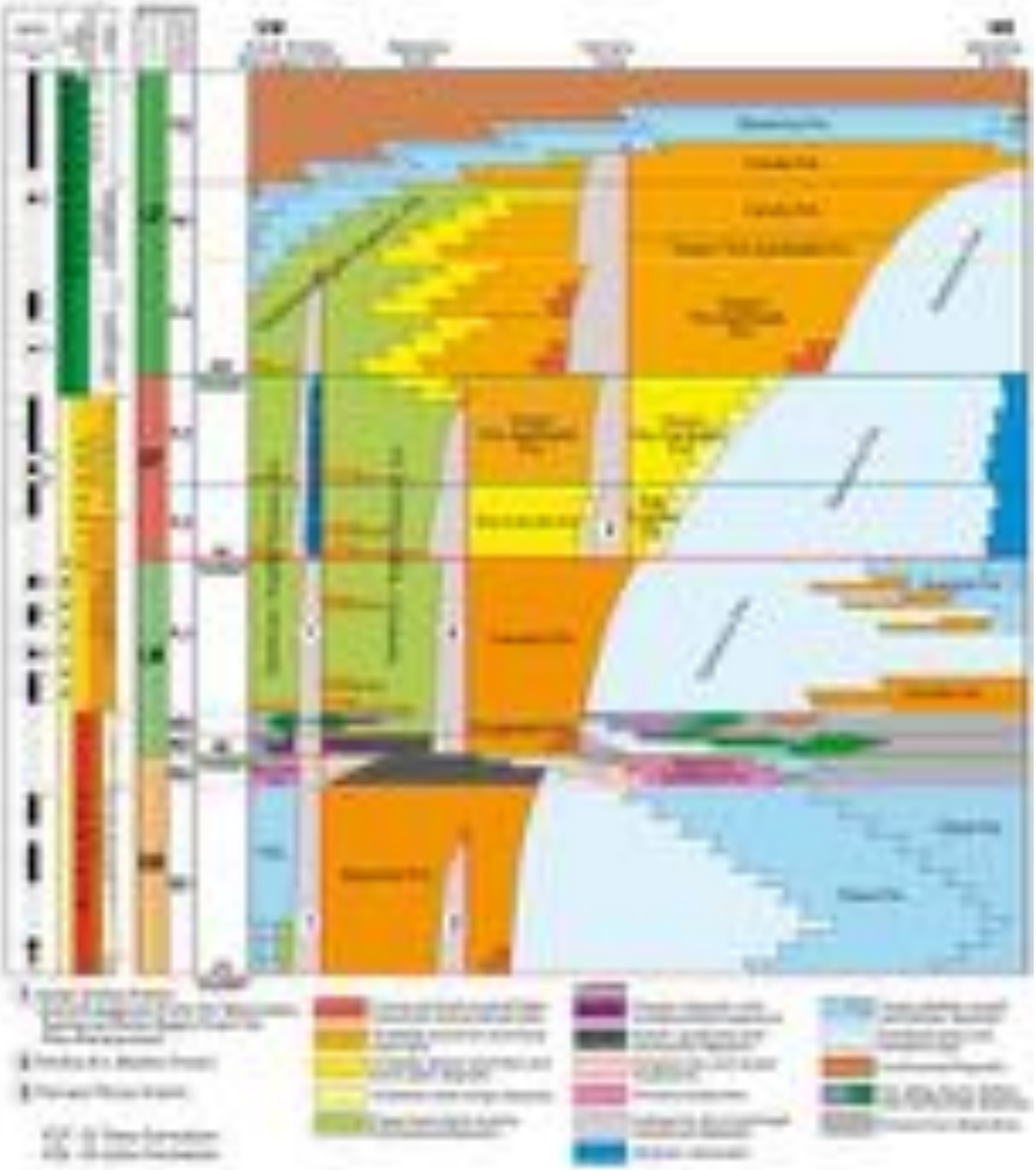

Figure 7. The Messinian-Pleistocene stratigraphic framework of the PPAF along an idealize oblique transect located in the central-eastern Po Plain from Emilia (SW) to Venetian Basin (NE) (modiefied from Ghielmi et al. 2013). Vertical scale in geological time. Quaternary base is modified after Gibbard et al. (2010).

From a sedimentological point of view, the Messinian–Pleistocene sedimentary infill of the PPAF is mostly represented by thick sequences of turbidites deposited in deep-marine environments (water depths usually exceeding 1,000 m) (Fig. 8).

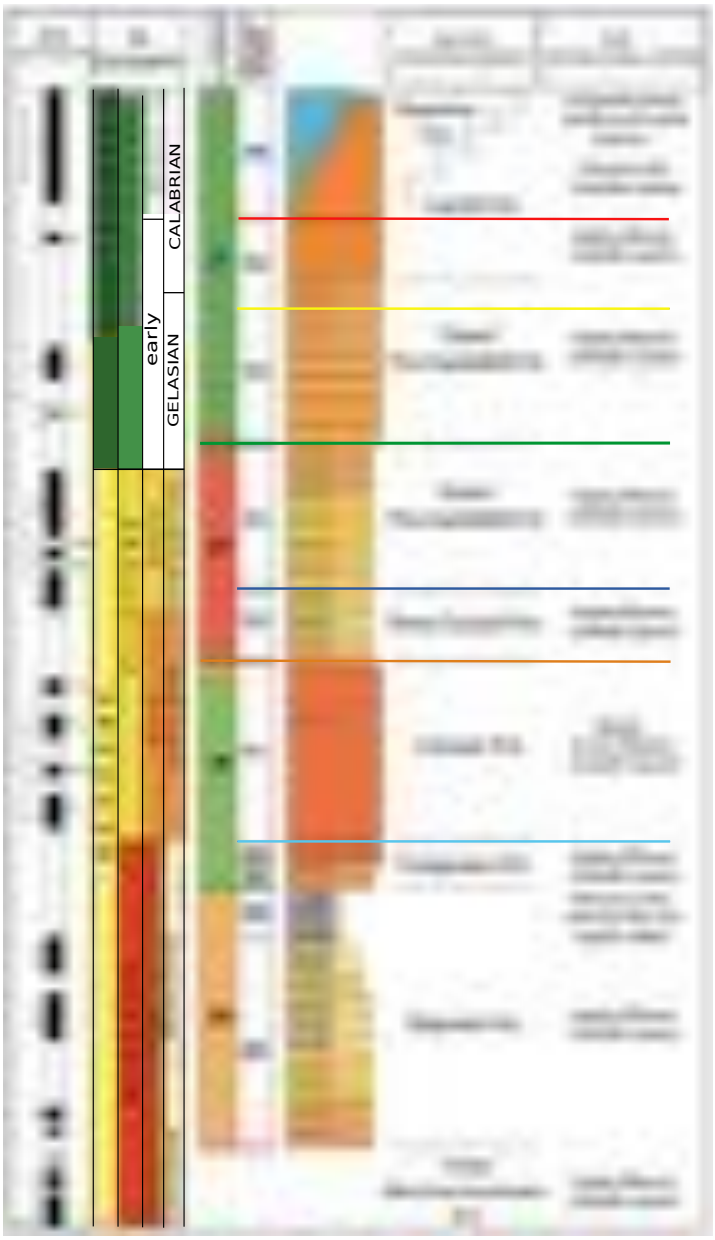

Figure 8. Simplified stratigraphy of the turbidite systems of the PPAF (modified from Ghielmi et al. 2013). Quaternary base according with Gibbard et al. (2010).

These turbidite deposits can be referred to two main types of turbidite systems: Type I and II (sensu Mutti, 1985; Mutti et al., 1999) (Fig. 9).

Sand-rich Type I highly-efficient turbidite systems (Fig. 9A) were volumetrically dominant in PPAF. These basin-scale systems were characterized by very large dimensions (basin-scale) and remarkably

tabular geometry, width up to 50–70 km and length usually exceeding 200/250 km, with thicknesses of several hundreds of meters.

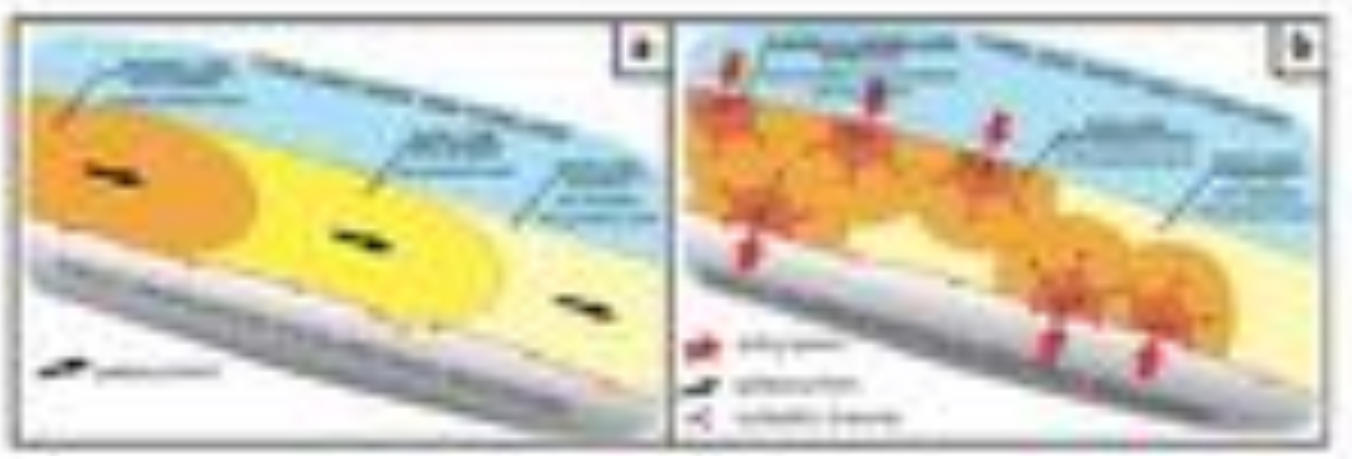

Figure 9. Depositional elements in turbidite systems of the PPAF. A) highly-efficient (Type I) turbidite system. B) Poorly-efficient (Type II) coalescing turbidite sustems (modified from Ghielmi et al., 2010).

They are almost entirely composed of sand/sandstone lobes (volumetrically largely predominant), expressed by thick-bedded sand/sandstone facies, passing downcurrent into basin plain deposits, made up of mud/mudstones with thin-bedded fine-grained sands/sandstones. The paleocurrents, parallel to the foredeep main axis, are from NW towards SE. Thin sequences of mud and marl deposited on the foreland and foreland-ramp may be present at the base of the turbidite succession.

Poorly-efficient Type II turbidite systems (Fig. 9B) fed by lateral entry-points are also present in PPAF. These turbidite systems predominated in the foredeep in the lower Pliocene (i.e Canopo Fm.) and mostly consist of thick-bedded coarse-grained channel-lobe transition deposits (thick-bedded coarse-grained sandstones and pebbly-sandstones extensively channeled and scoured) that grade downcurrent into lobe deposits.

Huge volumes of clastics were supplied by major fluvio-deltaic systems active along the Alps margins of Lombardia and Veneto and in particular by the paleo-Adda, paleo-Mincio and paleo-Adige rivers. Only a subordinate contribution of clastics was instead provided by the northern Apennine belt, mostly due to local submarine erosion and resedimentation of recent deposits from the active structural fronts.

The thrust fronts of the Apennine margin were entirely submerged until Calabrian time when the high condensed marine sedimentation was replaced by continental deposits, thus they were not affected by continental exposure and erosion during the entire Pliocene-early Pleistocene time.

Deep piggy-back basins, developed in the Reggio-Emilia-Bologna-Ravenna area, worked as sediment traps for the clastic detritus coming from exposed most internal southern margin thus, no important

sediment supply from the Apennine region contributed to the Po basin infilling.

The style of the depositional systems underwent dramatic changes particularly during the Messinian in relation to the combined effects of the salinity crisis (Hsü et al., 1978; Roveri et al., 2014; Sternai et al., 2017 and reference therein) and the morpho-structural reshaping due to tectonic basin modification (Artoni, 2003, Artoni et al., 2010; Ghielmi et al., 2013; Rossi et al., 2015). During the syn-evaporitic Messinian (Sequence ME2), the evaporative drawdown generated a basinward shift of the coastal onlaps over the toesets of the pre-evaporitic Messinian coastal wedges; basinward, in deep piggy-back basins and their transition toward the foredeep, gypsum and anhydrite change laterally to dolomicrite and anoxic mudstones in close stratigraphic relationships with turbidite systems. Well-log and seismic data suggest that the PPAF depocenters remained in relatively deep-water conditions and were mainly interested by turbiditic sedimentation during the whole Messinian salinity crisis (syn- and post-evaporitic Messinian). Nevertheless, the evaporative water loss since the onset of the salinity crisis promoted a network of incised valleys, submarine canyons and slump scars developed in relation to the Intra-Messinian unconformity, which can be seismically traced above the primary evaporites. This unconformity (corresponding to LM allogroup boundary) is overlain, at basin margins (in particular in the northern Apennine thrust-top basins) by chaotic complexes of the Sequence ME3 containing large amounts of Cretaceous to Miocene olistoliths and gypsum breccias. This was mainly in relation to the uplift generated by the Intra-Messinian Phase, leading to the erosion and destabilization of the primary evaporites. Along the Southern Alps margin, fluvio-deltaic systems turned from normal regression to forced regression. In the foredeep, this turning point is highlighted by a dramatic increase of sedimentation rates in post-evaporitic sequences, almost one order of magnitude higher than in the pre-evaporitic sequence. The erosive depressions are filled by upper Messinian systems when accommodation increased after the forced regression phase. More marginward, lower Pliocene deposits unconformably overlie lower Messinian or older rocks.

During the Pleistocene, the eastern Po Plain and the Northern Adriatic Sea were interested by the impressive progradation of slope, shelfal and coastal deposits of the Ravenna Fm., i.e. the Po Plain Prograding Complex. It rapidly advanced along the foredeep axis towards SE from the Lombardia as far as its present-day position just SE of Ancona causing the almost complete infilling of the PPAF (Ghielmi et al., 2010; Garzanti et al., 2011). During its fast advance towards SE, it progressively merged with the active Apenninic and Alpine-Dinaric lateral progradations from the inner and outer foredeep margins, respectively.

LM allogroup

The boundary of LM Allogroup (late Messinian–early Pliocene) corresponds to a marked tectonic unconformity produced by the so-called ‘‘Intra-Messinian Phase’’. This tectonic event was responsible for the reactivation and uplift of the Emilia and Romagna arcs with the migration of the foredeep toward the foreland.

The main consequences are i) the inner depocenter of the former fragmented EM foredeep is incorporated within the northern Apennine thrust-and-fold belt as a system of large piggy-back basins;

ii) the creation of a new simple foredeep in a more external position with respect to the Emilia and Romagna arcs and partially superposed on the outer depocenter of the former EM fragmented foredeep. During this time, the foredeep extended from the MM to the northern Adriatic Sea for over 200 km in length and 25–40 km in width.

In the LM allogroup, three component LSSs are identified: ME3, ME4 and PL1.

The post-evaporitic ME3 and ME4 Messinian foredeep deposits consist of 1,000 m of turbidite sandstones and conglomerates of the Fusignano Fm. These sediments are mostly referred to highly-efficient turbidite systems and are volumetrically dominated by sandstone lobes. The main source area was probably located along the outer foredeep margin in the eastern Lombardia, where both the fluvial valleys and the submarine canyons underwent reincision, while the fan delta systems became largely dominated by progradation and forced regression. Fluvial reincision of the early Miocene valleys occurred during the maximum sea level drop developing, across the Intra-Messinian Unconformity (ME3) an extremely thick, semi-arid, argillic paleosols (Minervini, 1999; Fantoni et al., 2001). Close to the ME4 sequence boundary instead, a change to semi-humid paleosols is recorded, suggesting the presence of a periodically higher water table. Other important entry-points have been recognized more eastward, where large incisions cut the foreland ramp. The steeper gradients recorded after the Intra-Messinian phase led to the local erosion and remobilization of primary evaporites and to a renewed clastic input; the uplift and consequent readjustment to a lower base level generated a network of incised valleys and canyons. The Sequence ME3 records a major basin-modification phase and an increasing rate of differential subsidence, whereas the Sequence ME4 records a dramatic reduction of tectonic subsidence at the regional scale.

The Sequence ME3 (Fig. 10) is mainly characterized by large and locally very thick chaotic complexes which form, where present, the lower stratigraphic portion of the Tetto Fm. (Selli, 1954), called also Colombacci Fm. (Selli, 1952), corresponding with post-evaporitic brackish-freshwater succession

(Bassetti et al., 2004) in the Apennine thrust-top basins (Gelati et al., 1987; Rossi and Rogledi, 1988; Ghielmi et al., 1998; Roveri et al., 1998; Rossi et al., 2002; Artoni et al., 2010).

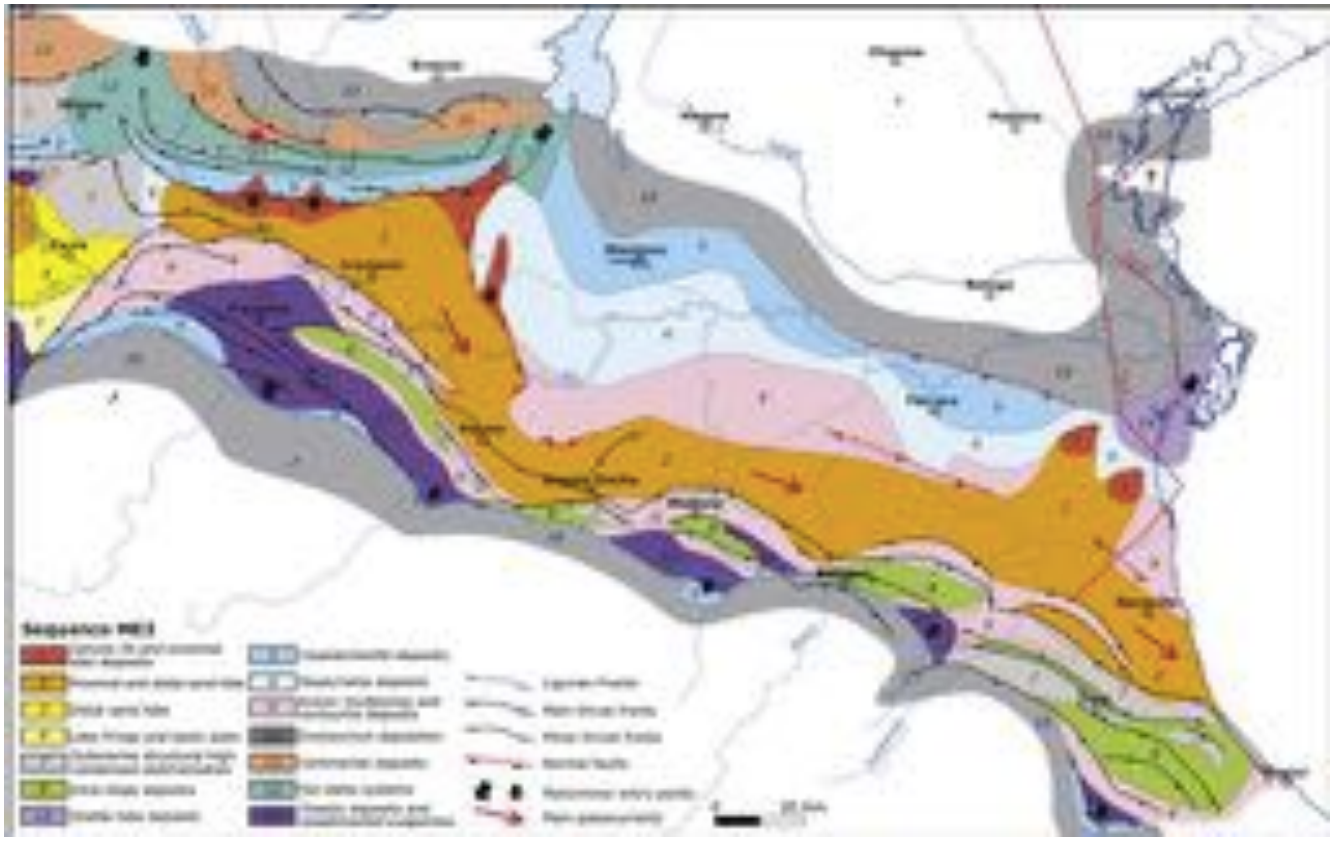

Figure 10. Facies associations distribution map of the post-evaporitic ME3 sequence (LM Allogroup) (Ghielmi et al., 2013)

These depositional units lie at the base of the tectonic slopes, typically containing slide blocks, slumps and large olistoliths made of evaporites and Epi-Ligurian rocks. The reworking index becomes very high in this setting, involving also Cretaceous Ligurian units. Typically, the mass-transport evaporites evolve downcurrent into high-density turbidites made of gypsorudites and then gypsarenites (Rossi et al., 2002; Minervini et al., 2008; Artoni et al., 2010). Anoxic mudstones occur both in the thrust-top and in the foredeep basins, and locally can be characterized by bottom current reworking. In the foreland of the Veneto Plain and the Northern Adriatic Sea, the allogroup boundary is represented by a deep erosional unconformity controlled by flexural tilting and local uplift over the peripheral bulge. This generated a relative base-level fall related to the Intra-Messinian phase. The erosion of large-scale incised-valleys developed over the whole area during the period of subaerial exposure, passing basinward into a network of submarine canyons. The truncated stratigraphic succession includes pre- and syn-evaporitic Messinian clastics and evaporites and older Miocene deposits, and locally reaches a maximum thickness of 400–500 m. This impressive system of valleys and canyons acted as by-passing areas for conveying large

volumes of coarse-grained clastics into deeper waters until it became filled in its more basinal portion since latest Messinian time (Sequence ME4).

In the foreland, the Sequence ME4 (Fig. 11) is represented only by thin sections of fluvial conglomerates deposited in the valley floors. Both in the northern Apennine thrust-top basins and in the Southern Alps margin, the Sequence ME4 records the deposition of fluvio-deltaic systems dominated by catastrophic fluvial floods and developed in relation to the combination of low-accommodation at basin margins and low-salinity of basin waters, brackish- to fresh-waters typical of the ‘‘Lagomare’’ event (Cita et al., 1975; Casati et al., 1976; CIESM, 2008). These deposits, referred in the subsurface as the Sergnano Fm. in the Southern Alps margin (Fantoni et al., 2001; Minervini et al., 2008) and as the Cortemaggiore Fm. in the northern Apennine margin (Rossi et al., 2002, 2015), formed active prograding wedges characterized by an increasing rate of by-passing and forced regression.

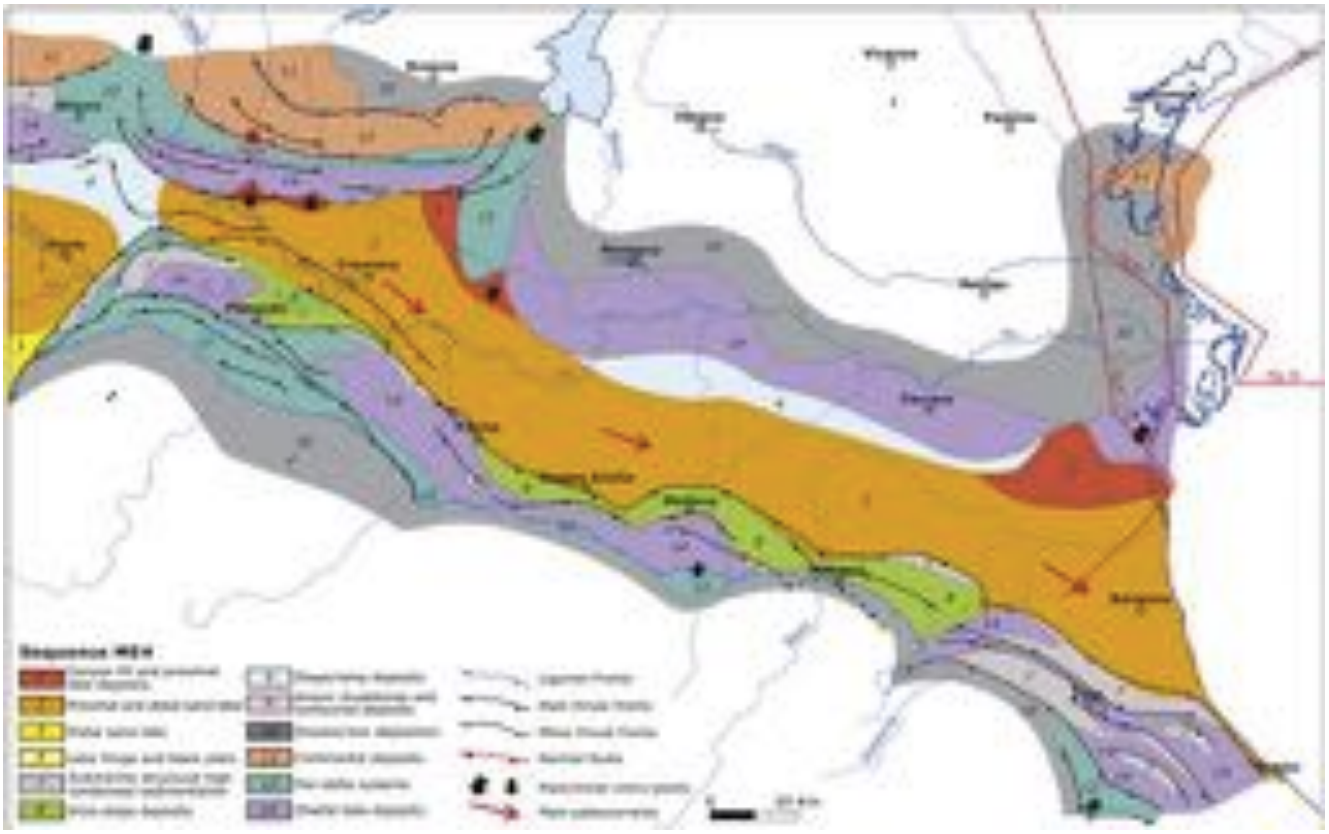

Figure 11. Facies associations distribution map of the post-evaporitic ME4 sequence (LM Allogroup) (Ghielmi et al., 2013)

The Miocene–Pliocene boundary represents a well-known regional marine ingression event, although its nature is not completely clear yet (Gennari et al., 2008; Garcia-Castellanos et al., 2009; Bache et al., 2012 and reference therein).

The PL1 sequence boundary (Fig. 12) corresponds to this impressive flooding surface along the inner and outer margins of the northern Apennine foreland basin, areas where the lower Pliocene

unconformably overlies the regressive wedge of the ME4 Sequence or older Messinian or pre-Messinian deposits. Basinward in the foredeep, where conformable relationships occur at the Miocene–Pliocene boundary, the basal portion of this lower Pliocene sequence probably contains also, topmost Messinian deposits.

The Sequence PL1 is represented, in the foredeep, by 500–700 m of alternating thick-bedded sand, sandstone and polygenic conglomerate of the Canopo Fm. These deposits were deposited in a 20/25 km-wide (35/40 km in MM) and more than 220 km-long foredeep extending from the MM (eastern Lombardia) to the Adriatic Sea. The coarse-grained channel-to-lobe transition deposits and the sand/sandstone lobes are the predominant facies associations. On the basis of the facies types and their distribution, these sediments may be interpreted as a complex of laterally coalescent sand-rich poorly-efficient Type II turbidite systems (Ghielmi et al., 2008). These systems were fed by several sedimentary entry-points located both on the inner and the outer margins of the foredeep generally with local paleocurrents transversal to the main foredeep axis. Two main source areas have been recognized: the MM foreland (the most important), and along the inner foredeep margin of the eastern Romagna area.

Figure 12. Facies associations distribution map of the Zanclean PL1 sequence (LM Allogroup). The map representative of the top of the sequence, shows the facies at ca. 4 Ma (Ghielmi et al., 2013).

In the meantime, a relatively thin section of clay interbedded with coarse-grained turbidite facies (Type

II systems) of the Caviaga Fm. (Dondi et al., 1982; Ghielmi et al., 1998, 2008) was deposited in the central Lombardia and in the western MM, which represented a relative paleo-high at this time, subdividing the PPAF from the westernmost depocenters of the Western Po Plain Foredeep.

After the basal Pliocene abrupt transgression, marine clays of the Santerno Fm. (Dondi et al., 1982) were deposited over a large area of the foreland. In the upper part of Seq. PL1, a predominantly southward progradation of slope, shelfal, coastal (Eraclea Fm., Eni subsurface lithostratigraphy) and continental depositional systems took place over the whole foreland area from Lombardia, in the W, to the northern Adriatic Sea, in the E. In a large area of the northern Adriatic Sea foreland, the Messinian incised- valleys were filled in by fine-grained turbidite sand and sandstone passing southward to alternating sand and clay of the Gisella Fm. (Eni subsurface informal lithostratigraphy). These deposits, 200/300 m-thick, are referred as belonging to sand lobe and lobe fringe/ basin plain depositional environments, respectively. The lower Pliocene prograding complex passes basinward to turbidites deposited in a deep-water foreland area, rich in dolostone and limestone rock fragments, provided by the prograding complex. In the piggy-back basins of the northern Apennine belt, the Seq. PL1 is predominantly represented by basinal turbiditic-emipelagic clays. A progradation from the southern basin margins developed towards NE in the upper part of the sequence also in this area.

EP allogroup

The unconformable boundary of the EP Allogroup (early-upper Pliocene) corresponds to a severe Pliocene Apennine tectonic event: the so-called Intra-Zanclean Phase. The main consequences of this tectonic phase are (Ghielmi et al. 2008): i) the deformation of the innermost structural element of the Ferrara fold-belt, which led to a significant change of the basin geometry with a partial migration of the foredeep that, in the Romagna sector, was split into two separate sub-basins (fragmented foredeep); ii) a phase of rapid subsidence (generating an abrupt relative sea level rise) in the Lombardia and Veneto foreland; iii) the activation of an important thrust front system in the Romagna offshore area; iv) a phase of severe uplift and tilting of the piggy-back basins of the northern Apennine thrust-and-fold belt.

In the EP allogroup, two component LSSs are identified: PL2 and PL3. During the deposition of the Allogroup EP the foredeep still extended from the MM to the northern Adriatic Sea with a total length of over 300 km and a total width of about 50 km. The western part of MM and the central Lombardia still represented a gentle paleo-high of the foredeep, where a mud-dominated turbiditic sedimentation was locally intercalated with coarse-grained turbidite facies (poorly-efficient Type II turbidite systems) fed by local entry-points located in the foreland. The Intra-Zanclean Phase was also recorded by a

dramatic change in the depositional regime with the sedimentation of the impressive Type I turbidite systems of Porto Corsini and ‘‘inner’’ Porto Garibaldi Fms. (Ghielmi et al. 2008b). About 2,000 m of stacked sand lobes were deposited in the present-day onshore portion of the foredeep. In the northern Adriatic Sea, these sediments grade downcurrent into muddier basin plain deposits.

The sedimentary infill of the Sequence PL2 foredeep (Fig. 13), 30-45 km wide and over 260 km long, comprises the lower-upper Pliocene turbidites of the Porto Corsini Fm. In the eastern Po Plain, this foredeep succession mostly consists of alternating thick-bedded coarse to fine-grained sands and mud with a maximum thickness in the foredeep depocenters of 1,100 m.

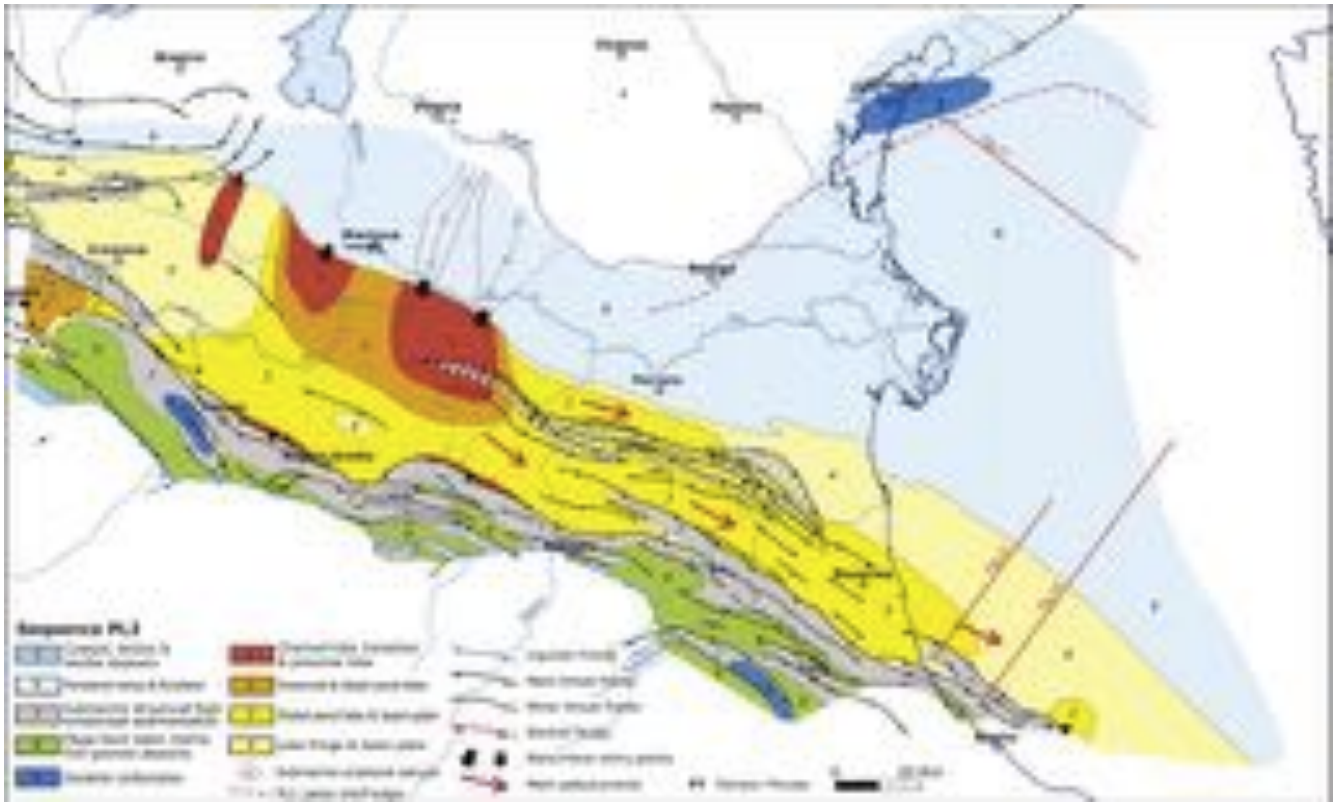

Figure 13. Facies association distribution of the Zanclean-Piacentian PL2 Sequence (EP Allogroup). The map representative of the top of the sequence shows the facies at 3.4/3.3 Ma. (Ghielmi et al., 2013)

These sediments are currently interpreted as proximal and distal turbidite sand lobe and basin plain deposits. The northern Adriatic Sea foredeep area was interested by the deposition of mud with intercalations of thin to thick-bedded fine-grained sand and referred to basin plain and distal sand lobe facies associations. In the Mantova Monocline (MM), close to the northern foredeep margin, thick-bedded coarse-grained turbidites of proximal lobe and channel-lobe transition have been recognized. In the MM and western Veneto foreland ramp, large-scale submarine canyons were incised into the PL1 lower Pliocene prograding wedge due to the turbidity currents erosional activity. During the Intra-

Zanclean Phase, the whole foreland area was interested by a major marine transgression related to the active subsidence. As a consequence, the PL1 prograding complexes were abruptly drowned. The foreland and foreland ramp were characterized by a non-depositional hiatus or by a condensed deposition of clay (Santerno Fm.). An up to 50 m-thick succession of skeletal packstone were deposited by relatively shallow-water carbonate systems in the Venice sector, a relative high area of the foreland away from the main clastic inputs. Along the inner foredeep margin, the Apennine belt underwent a severe phase of deformation during the Intra-Zanclean Phase with the reactivation of the already formed structural fronts. As a consequence, the sedimentation of condensed clay on large paleo-high areas occurred in this sector, while basinal fine-grained deposits were deposited only in narrow depocenters. Skeletal packstones of relatively shallow-water carbonate systems were deposited on top of the highest structural fronts (i.e. piggy-back margins and peripheral bulge).

The lower boundary of the Sequence PL3 is represented by a tectonic unconformity (Fig. 14). In the foredeep the deformative event caused to the formation of new structural fronts in the northern Adriatic Sea and in the easternmost onshore area, along with the reactivation of the former structures. Furthermore, this deformative event marked a sharp forestepping of the turbidite systems of the middle Pliocene ‘‘inner’’ Porto Garibaldi Fm. The deposition of thick-bedded coarse to fine-grained sand of proximal and distal sand lobes facies association occurred over most of the foredeep, while the basin plain deposits were limited to the northern Adriatic Sea. In the MM, turbidite coarse-grained sand and gravel of channel-lobe transition and proximal lobe were deposited. On the northern foredeep margin of this area, a large-scale channels complex has been identified through seismic interpretation and well data. The PL3 foredeep was, at this time, 45–50 km wide and over 300 km long and with a sedimentary infill about 1,000–1,100 m thick. In the Emilia area, due to the aggradation of a thick turbiditic succession, the thrust folds of the inner foredeep margin are gradually onlapped and, in the upper part of the sequence, finally overpassed with the foredeep turbidity currents overflowing also into the piggy-back basin. In the MM and western Veneto foreland and ramp domain, siliciclastic sedimentation started again after the period of non-deposition or condensation of the Seq. PL2.

The succession is represented by an overall regressive cycle with, in the lower part, ramp to shelfal clay (Santerno Fm.) and, in the upper part, predominantly southward prograding shelfal and coastal systems. On the contrary, the northern Adriatic Sea and the eastern Veneto ramp and foreland were still interested by very low sedimentation rates or by non-deposition and the sequence is represented by a thin section of marine clay (Santerno Fm.) or by a non-depositional hiatus.

In the piggy-back basins of the Emilia-Romagna area, the PL3 succession mostly consists of fine-grained

basin plain deposits. Only in the southeastern piggy-back depocenters, the upper part of the PL3 succession is represented by turbidite sand lobe deposits and basin plain interbedded clay and sand.

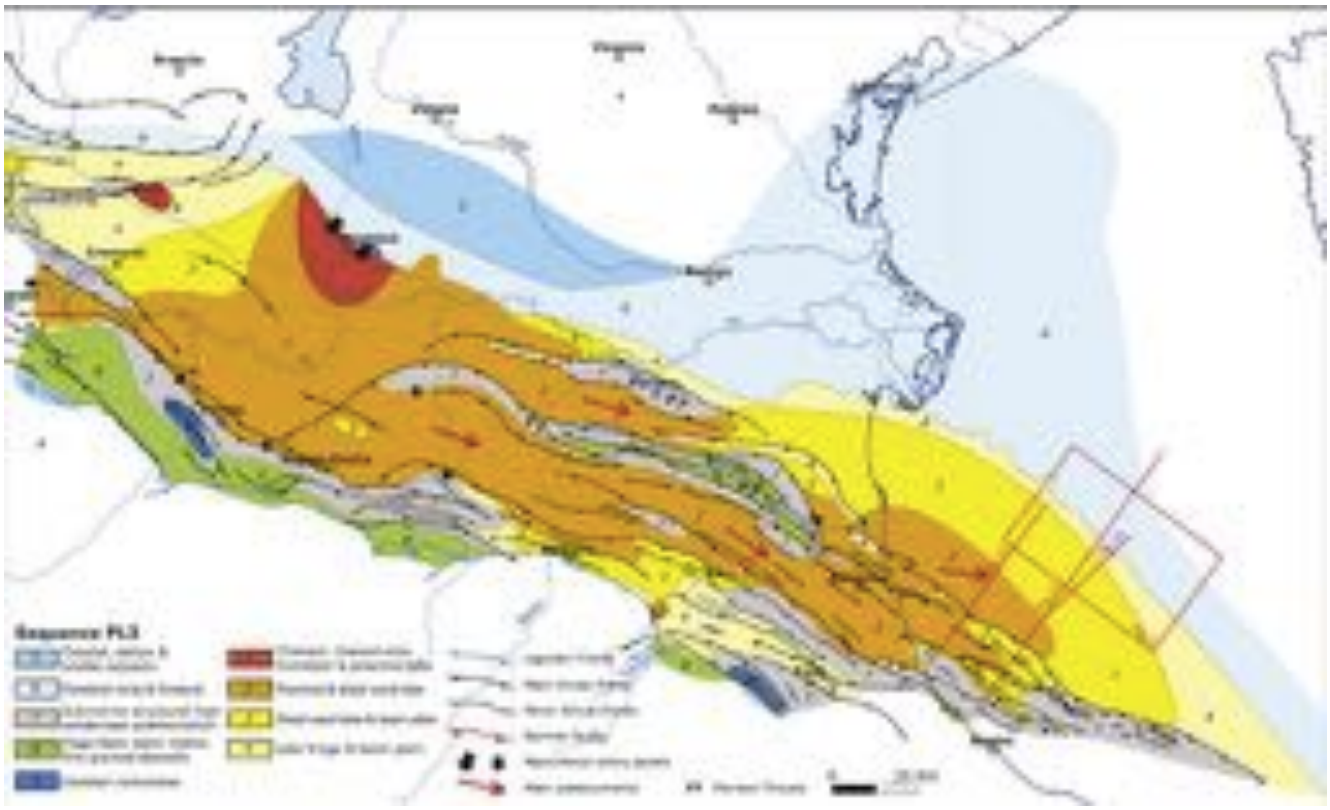

Figure 14. Facies association distribution map of the Piacentian-Gelasian PL3 Sequence (EP Allogroup). The map representative of the top of the sequence, shows the facies at about 2.4 Ma (Ghielmi et al., 2013).

The deposition of turbidite sands in this area was due to the local flowing of the foredeep sand-rich turbidity currents into the piggy-back basin and thus passing over the thrust fronts of the inner foredeep margin.

LP allogroup

The foredeep geometry dramatically changed again in relation to a regional tectonic event that marks the base of LP Allogroup (early Pleistocene according to the updated time scale, Gibbard et al. 2010): the Gelasian Phase.

In the LP allogroup, three component LSSs are identified: PL4, PS1 and PS2.

This event is correlated with the full structuration of the Ferrara fold-belt and the related uplift of its NW and SE lateral ramps and the uplifting/tilting toward SW of the whole present-day Bologna area (Ghielmi et al., 2008b); deeper carbonate units were also involved (Turrini et al., 2014). A severe phase of deformation also interested the northern Adriatic thrust-and-fold belt. The Gelasian Phase of deformation

produced a dramatic change of the Po Plain and the northern Adriatic Sea paleogeography. Most of the former foredeep area, including the onshore Emilia-Romagna sector and the south-western and inner sector of the northern Adriatic Sea, were isolated and incorporated within the Apennine thrust-and-fold belt as large piggy-back basins. To the west, the MM area was separated by the growth of the Ferrara NW lateral ramp and included in the westernmost Western Po Plain Foredeep (Minervini et al. 2008). A new foredeep (up to 350-km long, 80-km wide) formed to the east, in the area of the present-day eastern Veneto Plain and the northern Adriatic Sea (Ghielmi et al., 2008). Up to 2,800 m of mostly highly-efficient Type I turbidite sand lobes belonging to the ‘‘Outer’’ Porto Garibaldi (Sequence PL4) and Carola Fms. (Sequences PS1 and PS2) were deposited in the north-western sector of the foredeep. These proximal deposits grade towards SE into distal thin-bedded and fine-grained basin plain deposits. During the late Pliocene–early Pleistocene, the central-eastern Veneto foreland was the main source area for the foredeep turbidite systems of the Sequences PL4 and PS1 (Ghielmi et al. 2008). In the middle Pleistocene, as a consequence of eastward Po Plain progradation and the infilling of the MM, the main source area changed and the turbidite systems of the Sequence PS2 were fed directly from the Po River delta.

The Sequence PL4 (Fig. 15) is composed by early-middle Pleistocene sediments; the new foredeep, mostly located in the northern Adriatic Sea, overlie the external part of the former foredeep and the middle-late Pliocene foreland ramp. It shows a simple elongated shape and a length of over 200 km and a width of 35–45 km (20–25 km in the SE sector). The sedimentary processes were dominated by sand-rich highly-efficient turbidity currents. The entry-points were located in the south-eastern Veneto and the main paleocurrents were from NW, parallel to the main foredeep axis. Also, the PL4 foredeep succession, which reaches about 1,200 m of thickness, shows an evident down-current evolution towards SE from thick-bedded amalgamated coarse- to fine-grained sands of proximal and distal turbidite lobes to alternating clay and fine-grained sand of basin plain. Along the inner foredeep margin, submarine collapses from the active fronts of the northern Adriatic fold-belt provided minor volumes of sediments to poorly-efficient turbidite systems. In the foreland and foreland ramp the PL4 boundary was outlined by a transgressive episode generated by a tectonic tilting of the area (the Gelasian Phase).

In the northern MM, this transgressive episode was followed by a regressive cycle made up of ramp- to-foreland clay (Santerno Fm.) and by coarser-grained shelfal, coastal and deltaic deposits. In the northern Adriatic Sea ramp and foreland the Seq. PL4 is represented by condensed clays. A wide area of the Emilia-Romagna was included in a large piggy-back basin bordered by the Ferrara fold-belt to NE and by the Ligurian Units to SW.

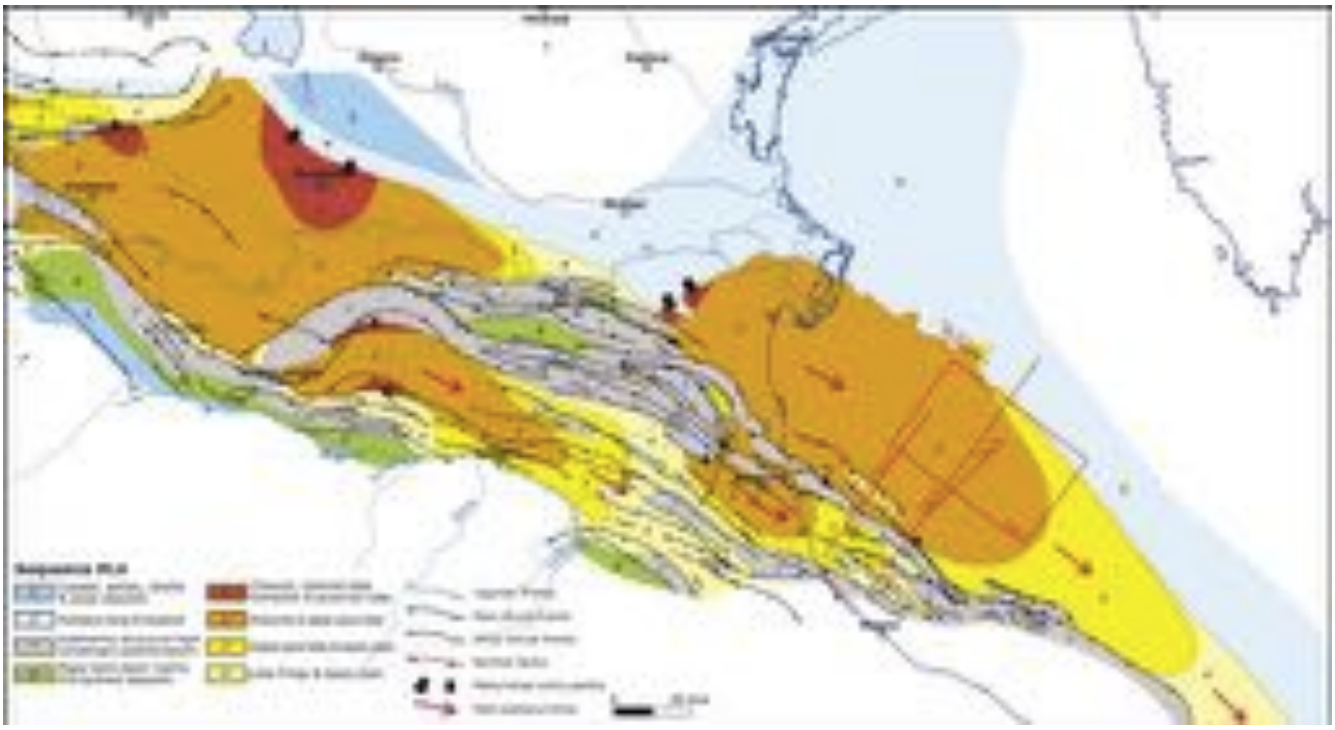

Figure 15. Facies association distribution map of Gelasian-Calabrian PL4 Sequence (LP Allogroup). The map representative of the top of the sequence, shows the facies at the Gelasian-Calabrian boundary (Ghielmi et al., 2013).

This basin was characterized by an exceptional extension in comparison to the other Messinian-to-Pleistocene thrust-top basins of the northern Apennine belt: about 140 km in length and 20–30 km in width. Its unusual extension was due to a middle Pliocene gradual tectonic deactivation of the Bologna thrust fronts which were completely onlapped by a thick aggradation of upper Pliocene-lower Pleistocene turbidites. Another large piggy-back basin is represented by the Ravenna Syncline. The infill of both depocenters (about 600-700 m thick in the Bologna depocenter) consists in the NW area of thick-bedded sand lobes that grade laterally (towards SE) into alternating fine-grained sand and clay of distal sand lobe and basin plain, and, finally, into distal basin plain mud.

These turbidites were deposited by highly-efficient turbidite systems fed by the Ferrara fold-belt lateral ramps. In the Emilia piggy-back basins a northeastward progradation of slope, shelfal and coastal systems occurred in relation to an important tectonic uplift of the northern Apennine margin, while basin plain mud was still deposited in the basin depocenters.

The Sequence PS1 (Fig. 16), is bounded at the base by a tectonic-controlled unconformity and consists of lower Pleistocene deposits. After the severe upper Pliocene tectonics, a gradual decrease of the Apennine compressional deformation occurred during the lower Pleistocene as indicated by a reduced growth of the existing structures and by the formation of only a few new structural fronts in the Veneto onshore area. As a consequence, the PPAF paleogeography of the Sequence PS1 was very similar to the

previous Sequence PL4 with a simple foredeep depocenter (50–70 km wide, over 260 km long) located in eastern Veneto Plain and the northern Adriatic Sea.

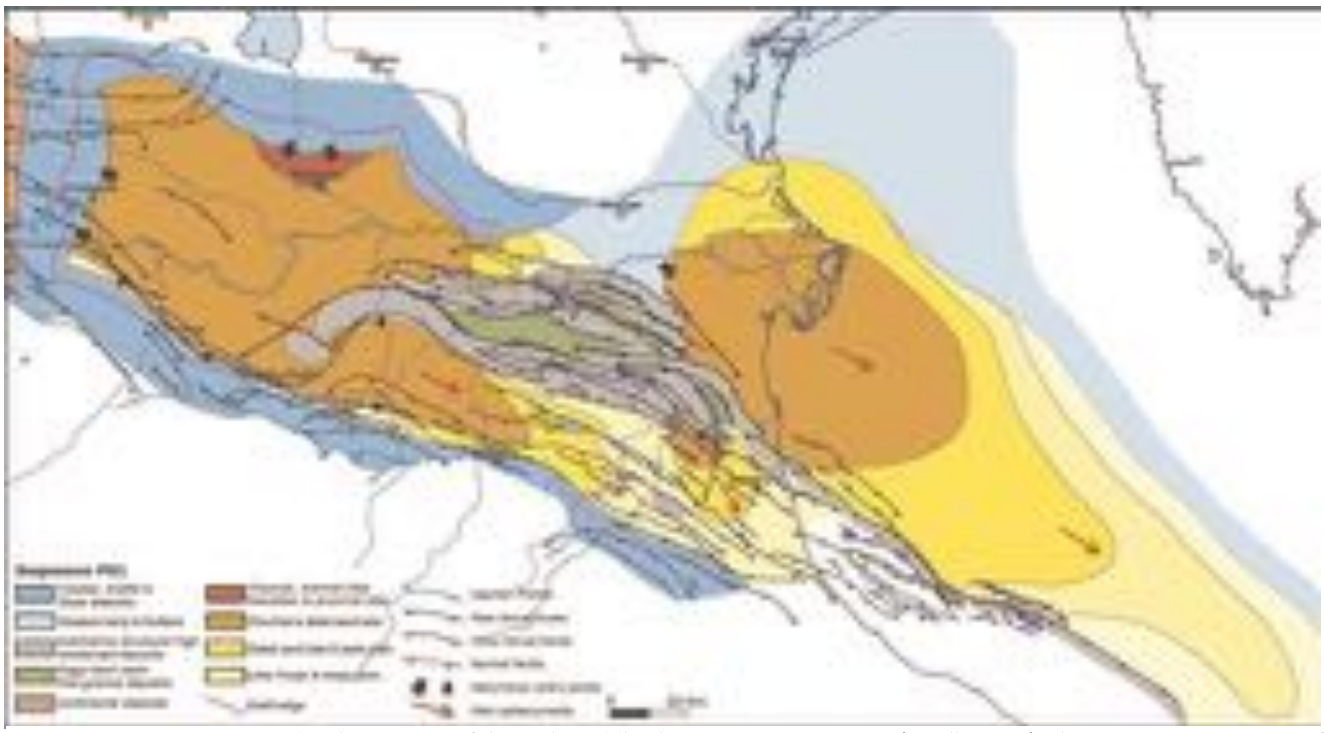

Figure 16. Facies association distribution map of the early-middle Pleistocene PS1 Sequence (LP Allogroup). The map is representative of the facies distribution of the middle-upper part of the sequence and is referred at about 1.2/1.1 Ma (Ghielmi et al., 2010).

The Ligurian Units of the Bologna-Reggio Emilia sector experienced an important northeastward displacement probably driven by thin-skinned gravity tectonics (Argnani et al., 2003). The foredeep succession, up to 700/800 m thick, consists of turbidite sand and mud of the upper part of the ‘‘outer’’ Porto Garibaldi Fm. and of the lower part of the Carola Fm. The Veneto foreland still represented the main source-area of the sediments and the main paleocurrents are still parallel to the foredeep axis. The PS1 sequence corresponds to the phase of minimum efficiency and backstepping of the foredeep Type I turbidite systems of the LP allogroup, as indicated by the limited extension of the sandier facies associations. The reduced efficiency was probably also related to the decreasing tectonic activity during lower Pleistocene. The Veneto and the northern Adriatic foreland were interested by the deposition of mud of the Santerno Fm. In the piggy-back domain most of the structural highs were progressively onlapped by the PS1 deposits due to the combination of reduced thrust fronts uplift and high turbiditic sedimentation rates. In the upper part of the lower Pleistocene, the combination of these factors generated a single depocenter (about 160 km long and 25–40-km wide) limited by the Ferrara thrust-and-fold belt to NE and by the emerged northern Apennines Chain to SW. Probably, also this large basin was predominantly characterized by highly-efficient turbidite systems with mainly longitudinal

paleocurrents. A partial connection with the MM, now included in the Western Po Plain Foredeep, took place during the lower Pleistocene. An active progradation of slope, shelfal and coastal/deltaic systems extensively occurred from the Apennine margin with the in- filling of the marginal depocenters behaving as piggy-back basins since the late Messinian. A coeval progradation is also recorded in the northern part of the MM.

The Sequence PS2 (Fig. 17) consists of middle-upper Pleistocene deposits. Also, the middle Pleistocene was characterized by a reduced Apennine compressional deformation and no new thrust front was activated. A remarkable exception is represented by the Bologna-Reggio Emilia Ligurian Units that still continue to move northeastward, probably driven by thin-skinned gravity tectonics (Argnani et al., 2003).

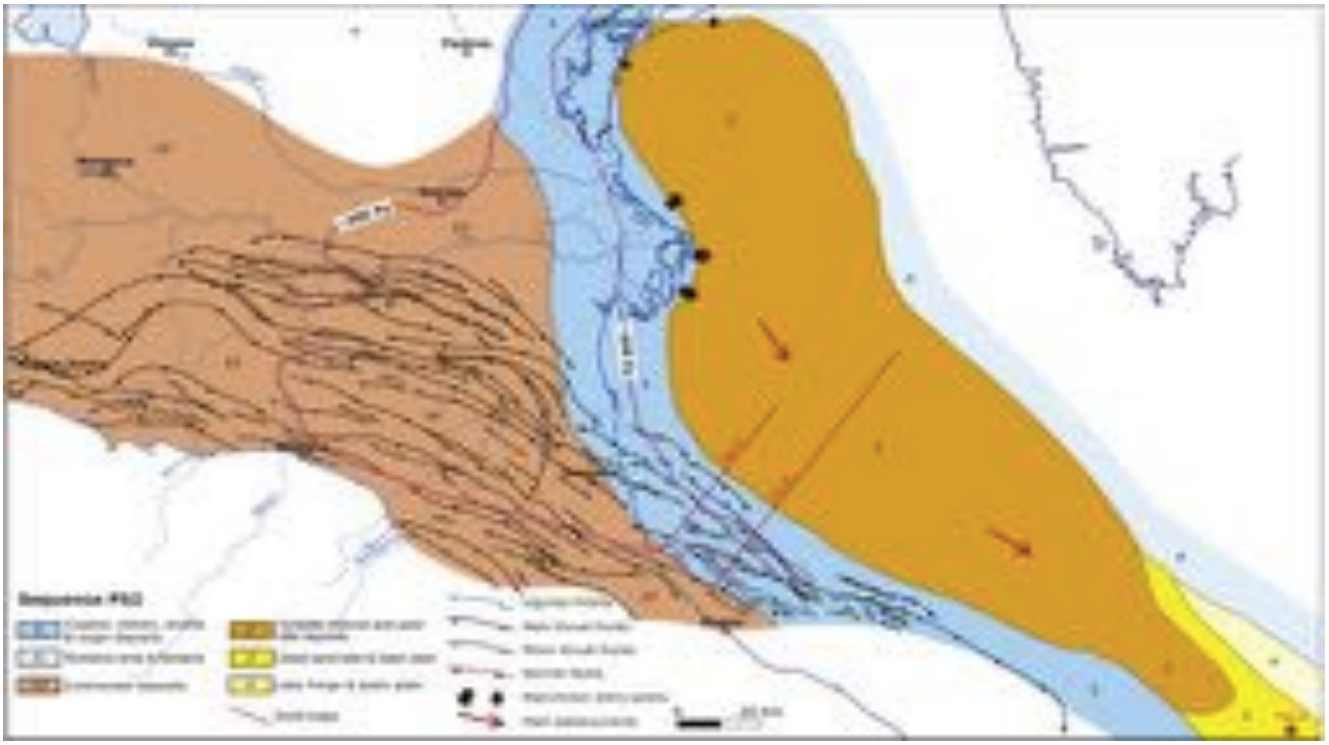

Figure 17. Facies association distribution map of the late Pleistocene PS2 Sequence (LP Allogroup). The map is representative of the facies distribution of the middle-lower part of the sequence (base of PS2b) and is refererred at about 0.6 Ma (Ghielmi et al., 2013).

In the foredeep, the PS2 sequence boundary is marked by an abrupt forestepping of the turbidite lobes as indicated by the superposition of sand lobes deposits on basin plain and distal lobe alternating clay and sand of the former Sequence PS1.

This sharp facies change was probably originated by a number of concurrent factors (in order of magnitude): i) the onset of Pleistocene glaciations in the Alps caused an abrupt increase of the grain-size and volume of the sediments (Muttoni et al. 2003); ii) during this time interval, the Po River system began to feed directly the PPAF, after the complete infill of the MM depocenter with turbidites, and with

slope-to-coastal deposits of Po Plain Prograding Complex (occurred during the Sequence PS1); iii) a minor Apennine compressional phase roughly coincident with the major climatic change.

The type of turbidite sediment grades towards SE into thinner-bedded and finer-grained basin plain deposits, with a dispersal pattern from NE still longitudinal to the foredeep axis.

The Sequence PS2 was affected by a progressive decrease of the turbidity currents efficiency, with highly-efficient Type I turbidite systems in the lower part of the sequence and deposits of lower efficient turbidite systems in the upper one. During the Sequence PS2, the progradation of slope, shelfal and coastal deposits of the Ravenna Fm. extensively occurred in the study area, as a consequence of the prolonged lowstand phases of the middle Pleistocene glacial episodes and of the huge volume of siliciclastic deposits produced during the stages of climatic degradation. Also, the reduced compressional deformation favored the progradation of the Po Plain Prograding Complex rapidly advanced southeastward along the foredeep axis reaching, from the central Veneto, its present-day position just SE of Ancona with an average shelf-edge advancement towards SE. As a consequence of the slope progradation, the foredeep depocenters of the Sequence PS2 rapidly migrated towards SE reaching the central Adriatic Sea. During its advancement towards SE, the axial progradation progressively merged with the active Apenninic and Dinaric lateral progradations from the inner and outer foredeep margins, respectively. During the Sequence PS2, the deep-water sedimentation was limited to the foredeep and to part of the ramp and foreland areas, while the deposition of continental (i.e. fluvial and floodplain deposits), coastal, shelfal and slope deposits took place over large areas. In the foredeep, the PS2 succession reached about 1,500 m of thickness, including turbidites and the overlying slope-to-continental deposits. During this interval, the inner and the outer foredeep boundaries were, respectively, represented by the toe of the slope of the lateral Apenninic progradation and by the onlap of foredeep turbidites on a low-angle dipping foreland.

The combination of the gentle dip of the foreland and of the high sedimentation rate was responsible for a rapid extension towards NE of the foredeep which rapidly reached its maximum extension with a width up to 75 km and a length of over 275 km. It is probable that the Po River flowed always to the north of the Ferrara thrust-and-fold belt with a lower-middle Pleistocene course roughly similar to the present day one. This assumption is supported by the available subsurface data: i) the large Bologna and Ravenna synclines were infilled during the lower-middle Pleistocene (Sequence PS1 and lower part of the Sequence PS2) by an Apenninic progradation towards NNE (and not towards SE); ii) in the same synclines the turbidites underlying the progradation are pre- dominantly fine-grained (Fig. 20); iii) on the contrary, the presence in the Pleistocene foredeep at NE of the Ferrara thrust-and-fold belt of a thick

turbiditic succession of amalgamated sand lobes confirm the presence of a major fluvio-deltaic system (the Po system) immediately to the west.

2.3. Late Messinian-Pleistocene hydrocarbon plays

The PPAF is one of the most prolific area for hydrocarbon (HC) exploration in Italy (the most important for gas). After a pioneering phase in the ’30 and ’40, Agip and its minor controlled oil companies conducted an intense exploration campaign in the PPAF between the ’60 and the ’90. The campaign result was the discovery and development of a large number of gas fields. At the present, the PPAF represent a mature area for HC exploration (Casero, 2004; Ghielmi et al., 2008; Eni, 2009; Cazzini et al., 2015 and reference therein).

Two plays are effective for gas exploration in PPAF: the Plio-Pleistocene Gas Play and the Messinian Play. The Plio-Pleistocene Gas Play is the main explorative target in the area. The targets are the turbidite sandstones of the Plio-Pleistocene Turbidite Systems of Canopo Fm. (Early Pliocene), Porto Corsini Fm. (Early Pliocene), Porto Garibaldi Fm. (Middle Pliocene-Early Pleistocene), Carola Fm. (Early-Middle Pleistocene). Thick-bedded sand lobes and thin-bedded fine-grained basin plain deposits are the main facies associations of the reservoirs. The Plio-Pleistocene turbiditic-hemipelagic clay interbedded to the turbidite sand is both the effective seal of sandy reservoirs and the source-rocks of the biogenic gas. The organic matter is vegetal of continental origin (kerogen type III). The gas accumulations are usually associated with seismic direct hydrocarbon indicator (DHI, i.e.: Bright Spot, Pull-down, Polarity Reversal, etc.) which represent a key support for exploration. The main traps are structural: 4-way closures in the fault propagation folds (e.g.: Selva-Minerbio, Alfonsine, Ravenna e Pomposa Gas Fields in the onshore area; Angela-Angelina, Porto Corsini, Porto Garibaldi, Cervia Gas Fields in the offshore area). In the offshore area, a second important structural trap is represented by 4-way closures due to the draping of the turbidite succession on highs of the pre- Pliocene substratum. The traps were subsequently generated by differential compaction.

The mixed (structural-stratigraphic) traps are the secondary target of the play in both onshore and offshore foredeep sectors. Two mixed trap types are present: the onlap of the turbidite reservoirs on the flanks of a fault propagation fold (dip closure toward the basin) (e.g.: San Potito, Tresigallo Gas Fields), and along the outer foredeep margin the turbidite sand onlap on the foreland ramp (e.g.: Naomi, Pandora Gas Fields). In both cases the trap shows a dip closure toward the basin. The residual potential of the

Biogenic Gas Play in the PPAF is mainly associated with mixed traps. The Messinian Play is an important play in the onshore area of the foredeep. The reservoirs consist of Messinian fluvio-deltaic to gravity-dominated shelf deposits of the Lanzano (Early Messinian), Sergnano and Cortemaggiore Fms. (Late Messinian). The Messinian reservoirs are sealed by the Early Pliocene clay (Santerno Fm.). The source rocks are the Oligocene and Miocene shales for the thermogenic hydrocarbons, Early Pliocene turbiditic-hemipelagic clay (Santerno Fm.) for the biogenic gas. The organic matter is vegetal of continental origin (kerogen type III). The HC phases are mixed (biogenic-thermogenic) gas and condensate. Due to the lithology of the Messinian reservoirs (conglomerate and sandstone) the HC presence is only occasionally supported by DHI. The main traps are structural: 4-way dip closures in the fault propagation folds (e.g.: Cortemaggiore, Bordolano Gas Fields), and Messinian erosional remnants sealed by Early Pliocene clay (e.g.: Sergnano, Romanengo Gas Fields) (Fantoni et al., 2001; Ghielmi et al., 2008, 2010; Bertello et al., 2010; Cazzini et al., 2015).

CHAPTER 3
BASIN-SCALE ARCHITECTURE OF THE PLIOCENE-PLEISTOCENE FILLING OF THE PO PLAIN-NORTHERN ADRIATIC FORELAND BASIN

3.1. Abstract

The Pliocene-Pleistocene tectonic and sedimentary evolution of the eastern Po Plain and northern Adriatic Foreland Basin (PPAF) (extended ca. 40,000 km^2) was the consequence of the severe Northern Apennine compressional activity and climate-driven changes of sea-level and sediment supply.

According with the 2D seismic interpretation, facies analysis and sequence stratigraphy approach by Ghielmi et al. (2013 and references therein), these tectono-eustatic phases generated six basin-scale unconformities referred to Base Pliocene (PL1), Intra-Zanclean (PL2), Intra-Piacenzian (PL3), Base Gelasian (PL4), base Calabrian (PS1) and Late Calabrian (PS2).

Here, it is presented a new 3D model of the PPAF derived from the mapping of these six unconformities by means of a dense network of ca. 8,000 km of seismic lines, correlated with more than 200 well stratigraphies (complete dataset provided confidentially by Eni Upstream).

The interpolated TWT surfaces have been depth-converted using the 3D velocity model calculated with Vel-IO3D, a tool for time to depth conversion. The obtained depth-converted surfaces

Up to date, the produced 3D depth-surfaces of the PPAF represent the largest and most detailed reconstruction of the Plio-Pleistocene architecture of the northern Italian subsurface. From the model, it is possible to calculate 6 isopach maps that are fundamental outputs to inspect step-by-step the basin paleogeographic evolution occurred through alternating stages of simple and fragmented foredeep together with high sedimentary supply and climate instability.

3.2. Introduction

The foreland-foredeep basins evolution is a wide and fundamental topic for a number of geological studies and applications. Foredeep deposits and their architecture contain abundant information about tectonic, sedimentary and climate processes that occurred at basin scale through time. The 3D shape of foreland and foredeep basins are, in fact, the result of the interaction among i) thrust belt tectonic load, ii) subsidence and consequent accommodation space creation, iii) sediment supply and iv) climate/eustacy processes. The interest in foreland-foredeep basins evolved also together with their incredible natural resources and geopotentials and geological knowledge increased as fast as the economic and scientific investments.

All these characteristics are recorded in the study area, the Po Plain-Northern Adriatic basin (PPAF), located in the Northern Italy, a nearly E-W elongated basin which developed as the foreland of the Northern Apennines to the South, and the retro-foreland of central Alps to the North. The PPAF is also one of the largest European onshore-offshore strategic targets for oil and gas exploration (Ghielmi et al., 2008; Cazzini et al., 2015).

3D modeling techniques are the most advanced frontiers of geological representation and basin analysis, considered as key tools in the understanding of the subsurface geological structures, evaluation and sustainable management of the subsurface resources (water, geothermal energy, oil and gas) and potential usages (e.g. storage activities, i.e. CO_2 and CH_4). The Northern Apennine region has to deal also with seismic hazards, as demonstrated by the Emilia seismic sequence of May-June 2012 with M_W max 6.1, and coseismic induced effects at the surface, such as the liquefactions related to an overpressure of shallow-depth aquifers (Di Manna et al., 2012; Emergeo Working Group, 2013).

Due to this complex socio-economic and geological framework, the sedimentary succession and tectonic setting of the study area have been the target of several studies (i.e. Basili et al., 2008; Fantoni and Franciosi, 2010; Fantoni et al. 2010; Ghielmi et al. 2010, 2013; Toscani et al., 2014; Turrini et al., 2014; DISS Working Group, 2015; Maesano et al., 2015; Maesano and D'Ambrogi, 2016 and reference therein). Nevertheless, very few depth-converted 2D and 3D reconstructions of the Po Plain subsurface at basin scale are presently available. Unfortunately, some of them focus on the base Pliocene only, others refer to deeper layers and are derived from a sparse 2D lines seismic coverage (i.e. Pieri & Groppi, 1981), which is not appropriate to investigate with high-resolution the Po basin evolution through the recent time.

In the following, the most important key studies are reported:

- Pieri & Groppi (1981): 2D cross- and along strike depth converted seismic sections of the entire stratigraphic succession (Mesozoic to recent) and base Pliocene map (1 km contouring) which is the only one completely mapped over the entire Po Plain and Northern Adriatic Sea. Up to date this remains the key reference for every study of the Po Plain subsurface.
- Bigi et al. (1992): Base Pliocene isobaths map (0.5 km contouring) from "Structural Model of Italy and Gravity map" 1:500,000.
- Fantoni and Franciosi (2010): 2D depth converted seismic sections.
- Turrini et al. (2014, 2016): 3D depth converted Mesozoic geometries and base Pliocene surface by means of public dataset only.

Although a complete review of the literature on the subject since the last decade is beyond the scope of this Thesis work, for more details, it could be worth to mention D'Ambrogi et al. (2010) and Turrini et al. (2014, 2016) and all reference therein.

New data were provided by EU-funded GeoMol project (www.geomol.eu) (Diepolder et al., 2014, GeoMol Team, 2015; Maesano & D'Ambrogi, 2015; Maesano et al., 2015). The project used a newly designed and implemented workflow for 3D model management and 3D time-to-depth conversion (i.e. Vel-IO 3D by Maesano and D'Ambrogi, 2017). One of the project's pilot area to investigate was a portion of the central Po Plain (about 5,700 km^2 wide area) by means of very dense seismic grid provided confidentially by Eni Upstream. The result was a very accurate depth-converted 3D model that include 15 horizons, from the top of Permian-Triassic to Pleistocene and more than 150 faults. Moreover, when these results were compared with precedent models, they demonstrated the inaccuracy and limitations of previous investigations.

It's clear, then, that a complete 3D detailed stratigraphic and velocity for the entire Po Plain-Northern Adriatic basin is still missing. This Thesis attempts to fill this knowledge gap for the Plio-Pleistocene stratigraphic interval, presenting a new 3D model of the PPAF (about 40,000 km^2 wide area) based on the interpretation and mapping of six basin-scale unconformities on ca. 8,000 km seismic lines, calibrated with more than 200 wells (complete dataset provided confidentially by Eni Upstream).

The Plio-Pleistocene sedimentary framework traced in seismic is consistent with the PPAF tectono-eustatic driven allogoups and large-scale sequences recognised by Ghielmi et al. (1998, 2010, 2013) and Amore et al. (2004). These unconformities are referred to Base Pliocene (PL1), Intra-Zanclean (PL2), Intra-Piacenzian (PL3), Base Gelasian (PL4), Base Calabrian (PS1) and Late Calabrian (PS2).

The 3D architecture derived from TWT seismic lines has been depth-converted using of the Vel-IO 3D software developed by Maesano and D'Ambrogi (2017) and successfully tested in the GeoMol project area (GeoMol Team, 2015; Maesano & D'Ambrogi, 2015; Maesano et al., 2015).

The final result is an accurate depth-converted reconstruction of the 3D stratigraphic architecture of

the Po Plain-Northern Adriatic basin during the latest ca. 6 Ma and the sediment thickness during each evolutionary step which are both fundamental in petroleum geoscience and in seismotectonic analysis.

3.3. Dataset

3.3.1. Seismic dataset

The input dataset used in this study (courtesy of Eni Upstream) is part of the impressive subsurface database, property of Eni Upstream collected over 60 years of exploration activity on the entire Po Plain and northern Adriatic basin. It consists of about 5,000 seismic lines and thousands of wells (Ghielmi et al., 2008; Fantoni and Franciosi, 2010). About 8,000 km of seismic lines have been selected as the basis for the geological model; in detail, the seismic grid is composed of 327 regional TWT seismic lines, covering ca. 43,000 km^2 of the central-eastern Po Plain and the northern Adriatic Sea (Fig. 18).

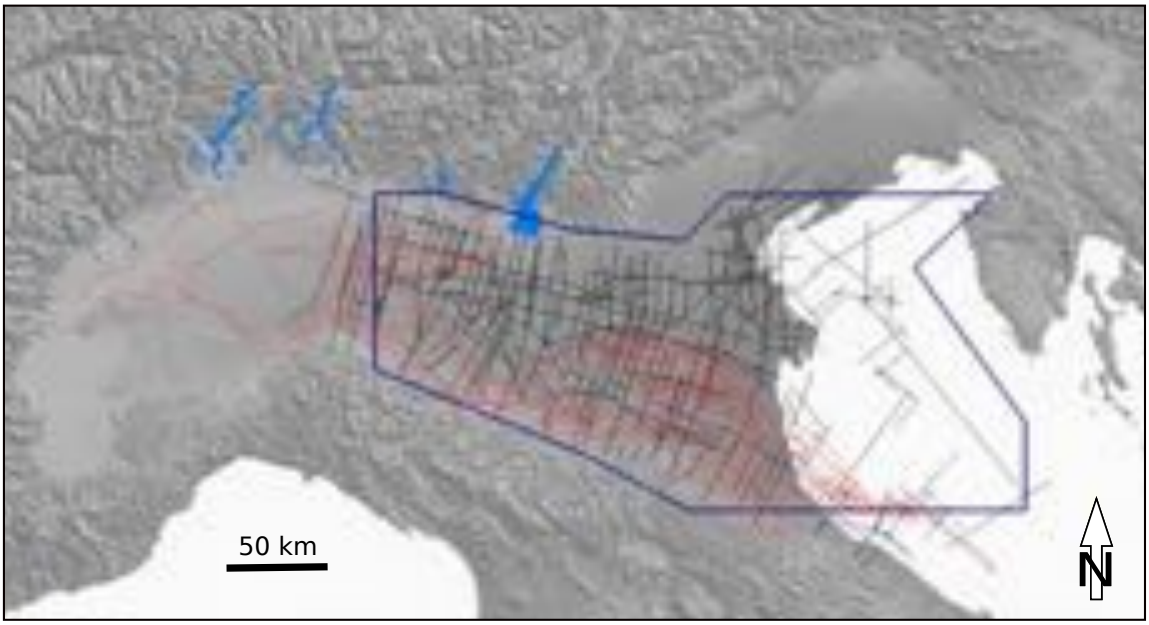

Figure 18. Black lines: Seismic line dataset provided by Eni Upstream. Red lines: tectonic framework of the Northern Apennine and Southern Alpine after Ghielmi et al. (2010). Bold blue line: perimeter of the study area.

The mapped key horizons correspond to the six main unconformities (allogroups and LSSs) defined by Ghielmi et al. (1998, 2010, 2013) and Amore et al. (2004), according with the stratigraphic scheme and correlation used by Regione Lomabrdia & ENI (2002), Muttoni et al. (2003), Garzanti et al. (2011) through Plio-Pleistocene succession. The intra-Messinian unconformity (ME3 unc.) has been also traced and included into the 3D time-model. Unfortuntaly it could not be depth converted because

the late Messinian is rarely recordered into the wells located into the deeper portion of the foredeep and poorly preserved in foreland.

The seismo-stratigraphic interpretation of the seismic lines is based on the description and interpretation of well logs coupled with the analysis of seismic geometries and facies. Bounding surfaces of different order and importance were correlated, at the basin scale, using well and seismic data and applying principles (Vail et al., 1977) and procedures (Catuneanu et al., 2009 and references therein) of seismic stratigraphy.

3.3.2. Well dataset

The interpretation and the time-domain stratigraphic calibration of the seismic profiles has been done by more than 200 explorative wells stored into the Eni Upstream's database and ViDEPI Project (available from http://unmig. sviluppoeconomico.gov.it/videpi/); thus (Fig.19). It was possible to integrate the seismic interpretation with stratigraphic markers and well-log curves (e.g. resistivity, spontaneous potential and sonic log).

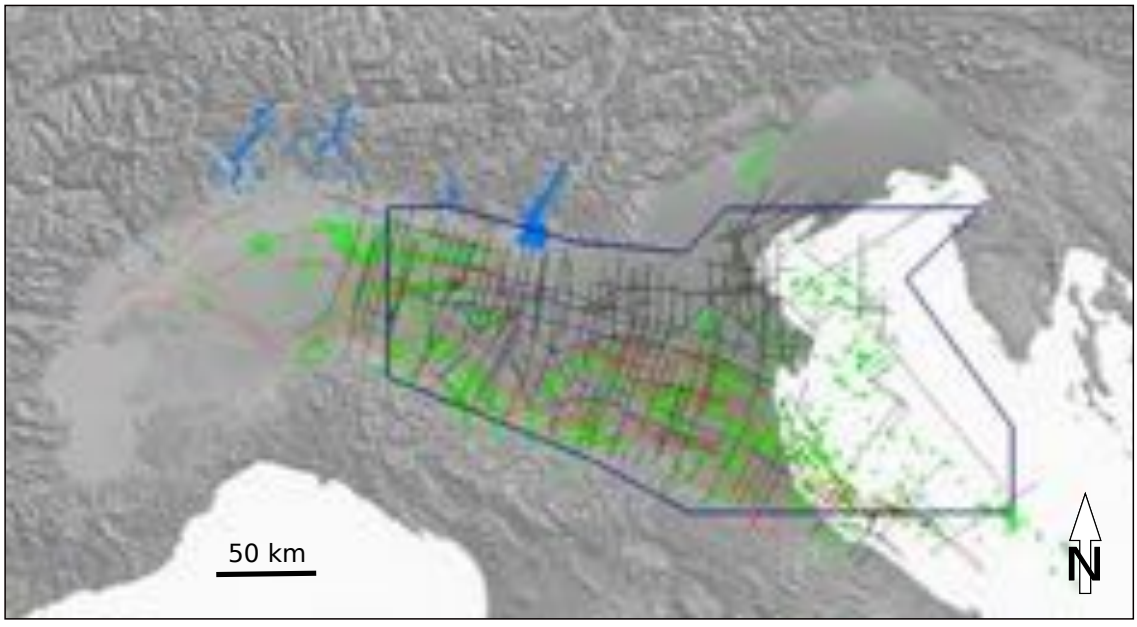

Figure 19. Green points: hydrocarbon wells from Eni's private dataset and ViDEPI Project. Black lines: Seismic line dataset provided by Eni Upstream. Red lines: tectonic framework of the Northern Apennine and Southern Alps after Ghielmi et al. (2010). Bold blue line: perimeter of the study area.

Eni's dataset is a coherent source of information and the 3D model building process did not require harmonization. The well data are digitized and stored in a database; they are marked by some primary keys like seismic unit, formation name, age and sometimes foraminifer biozones that enable the

correlation between well logs and data deriving from the seismic picking. This integrated approach supports the check of the line drawing during seismic interpretation, using a swift depth-time conversion of the well markers.

3.3.3. Seismic velocity dataset

Due to the large amount of seismic survey acquired and the onshore and offshore well fields, the Po Plain and the northern Adriatic Sea have a unique seismo-stratigraphic record, in particular of the Plio-Quaternary clastic succession, showing a great potential for 3D modeling analysis.
Moreover, 65 wells were used in order to support the 3D velocity model construction and optimization (Fig. 20). The extracted well log include velocity data i.e. interval velocity and average velocity, from which velocity-depth curves and all the parameters needed as input values for Vel-IO 3D, the tool used for 3D velocity model construction, optimization and time-depth conversion (Maesano and D'Ambrogi, 2017)

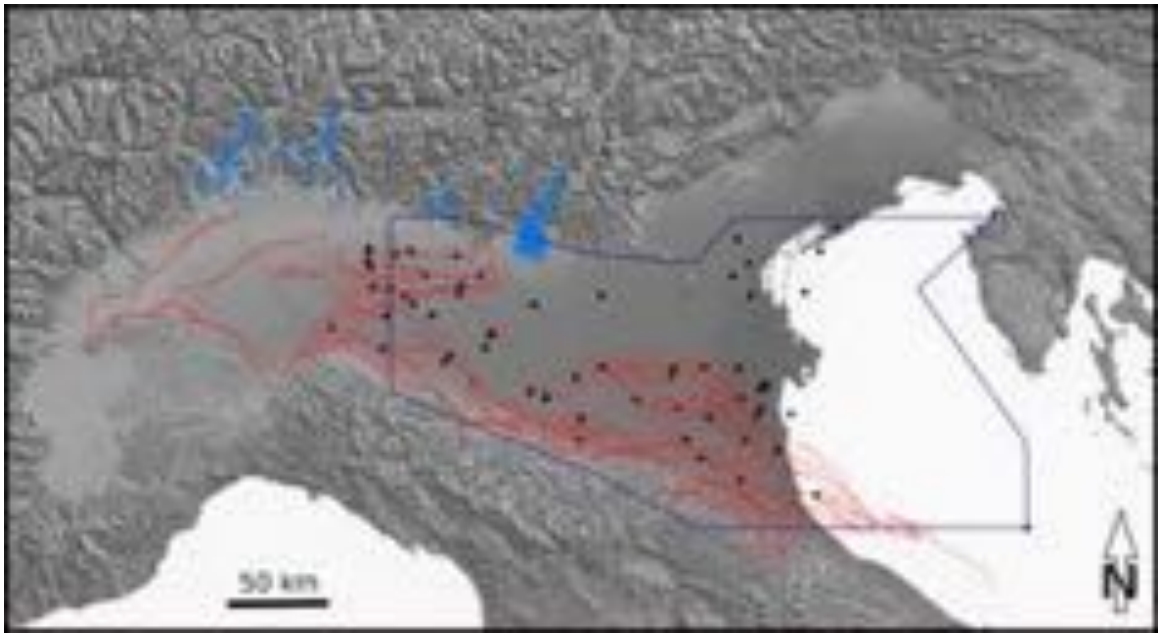

Figure 20. Black points: wells with velocity data used for 3D velocity model, from Eni's private dataset. Red lines: tectonic framework of the Northern Apennine and Southern Alpine after Ghielmi et al. (2010).

3.4. Methods

3.4.1. Workflow

The methodological approach is based on the construction of a 3D model using interpretation of a dense grid of seismic lines calibrated and converted with well log data and time-depth tables. The designed workflow (Fig. 21) is articulated in two different domains of the vertical Z axis, time and depth. Each domain is characterized by separate successive steps, sometimes connected.

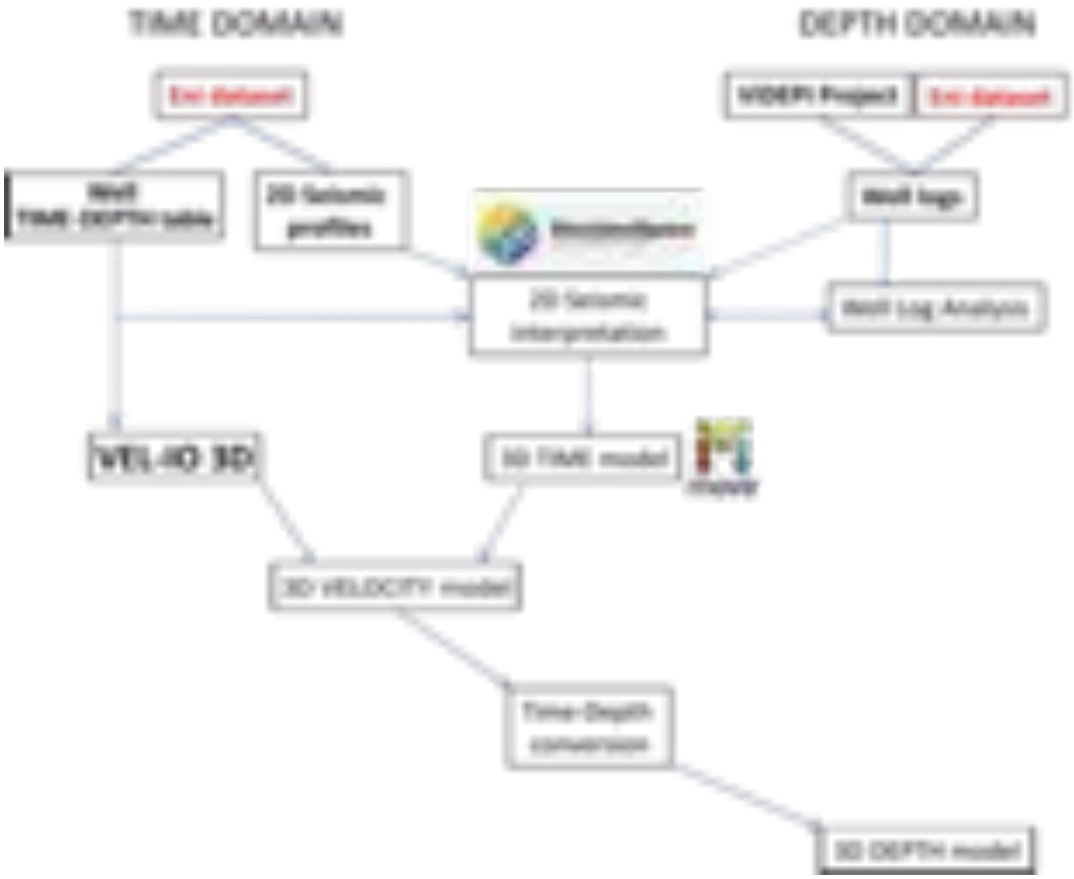

Figure 21. 3D model production workflow and software used during each step.

The main phases of the workflow can be summarized as follows:

1. Seismic and well log data selection from private (Eni Upstream) and public database (ViDEPI Project)
2. Interpretation of the key horizons in 2D seismic lines and well log analysis.
3. Interpolation of the 3D model in time domain (Delaunay Triangulation)
4. Calculation of the 3D velocity model.
5. Time-depth conversion.
6. Construction of the final 3D depth-converted model and refinement.

3.4.2. 2D seismic interpretation

The first step of the 3D modelling in depth domain is the construction of a 3D model in time based on the picked points, from 2D seismic reflection grid interpretation (Fig. 17, 21). Seismic line selection (from the huge Eni's private database composed of almost 5000 profiles) and complete interpretation were performed during 60 days at the Eni's Data Room only (offices located in San Donato Milanese, Milan) (Fig 22).

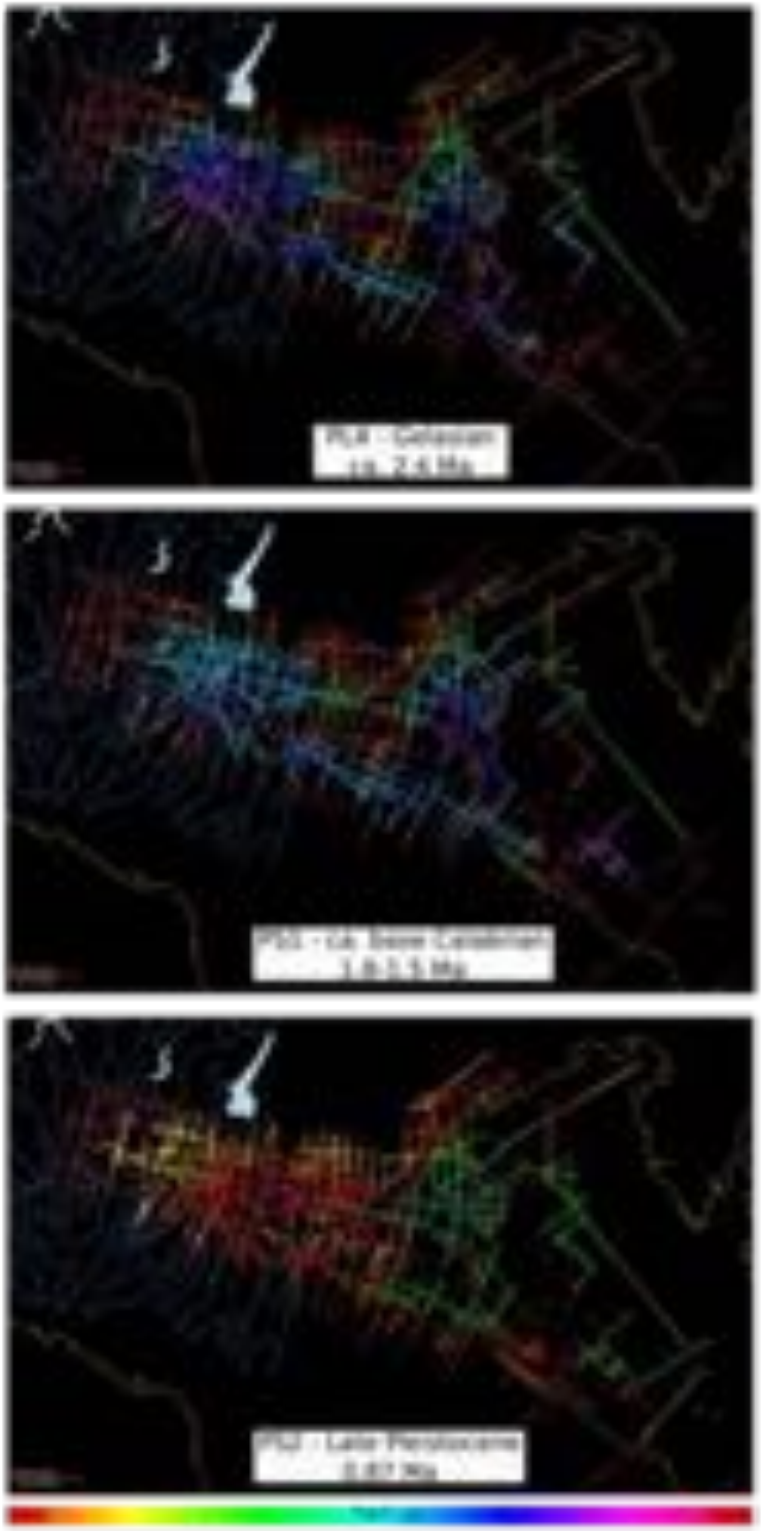

Figure 22. Geographic maps with seismic grid where is shown in colour the TWT interpretation of the key-horizon. Each map corresponds to one Plio-Pleistocene allogoup or LSS boundary. Name and age are indicated into the maps according with Ghielmi et al. (2010, 2013). Light blue lines: Po river drainage pattern.

Horizon interpretation was realized following seismic stratigraphy principles (Vail et al., 1977) and sequence stratigraphy according to Mutti et al. (1994), Catuneau (2006). Seismic sequences first needed to be defined by recognizing the surfaces of unconformity or correlative conformity from

reflection terminations, i.e. allogoups and Large Scale Sequence (LSS) boundaries, described by Ghielmi et al. (2010, 2013). The Intra-Messinian (ME3) unconformity is not shown in Fig. 22 because fragmented and not extended basin scale as the other Plio-Pleistocene surfaces. These key-horizons separate packages with concordant reflections whose parameters (configuration, amplitude, continuity, frequency and interval velocity) differ from adjacent groups. Each seismic sequence represents a depositional sequence with its own particular stratal geometry, thickness pattern, recording step by step the basin evolution.

Eni Upstream research groups dated physically the sequences by means of biostratigraphy (nannofossils and forams, pollen) and magnetostratigraphic methods integrated with log data as lithology, velocity and depositional facies (Muttoni et al., 2003, 2007; Ghielmi et al., 2010, Garzanti et al., 2011; Ghielmi et al., 2013, Scardia et al., 2015; Rossi et al., 2015). Improved accuracy results because a grid of seismic sections, although having considerably lower resolution than electric logs, provides a continuous profile of stratigraphy. However, electric logs must be correlated from well to well to depict the stratigraphy. All information has been applied also to environmental setting, depositional environments and the potential sand-shale content of the strata generating the seismic facies reflection pattern (see section 2.2, this Thesis, or full detail in Ghielmi et al. 2010, 2013) (Fig. 23).

In seismics, these units, with genetically related strata and geometry, are bounded by: Intra-Messinian unc. (ME3) (Fig. 23A), Base Pliocene (PL1) (Fig. 23B), Intra-Zanclean unc. (PL2) (Fig. 23C), Piacentian unc. (PL3) (Fig. 23D), Gelasian unc. (PL4) (Fig. 23E), Calabrian unc. (PS1) (Fig. 23F) and late Pleistocene unc. (PS2) (Fig. 23G). Delineation of allogroups and LSSs boundaries is repeated on all intersecting lines in the grid of seismic data until the boundaries have been correlated and tied throughout the entire grid. This process tends to verify the regional extend of major discontinuity surface.

Figure 23 (next pages). Seven lithofacies maps (from Ghielmi et al., 2010, 2013) showing the geological setting of the PPAF basin during the seven tectono-eustatic events occurred in the area since the late Messinian (section 2.2, this Thesis). A) Intra-Messinian (ME3) unconformity and base of LM allogroup. B) base Zanclean (PL1) unconformity. C) Intra-Zanclean (PL2) unc. and base of EP allogroup. D) Piacentian (PL3) unc. E) Gelasian (PL4) unc. and base of LP allogroup. F) Calabrian (PS1) unc. G) late Pleistocene (PS2) unc. Blue line: study area perimeter. Bold black lines: seismic profiles in figs. 24, 25, 26. Orange line: cross correlation section Fig. 25O. Green points: hydrocarbon wells Fig. 25P.

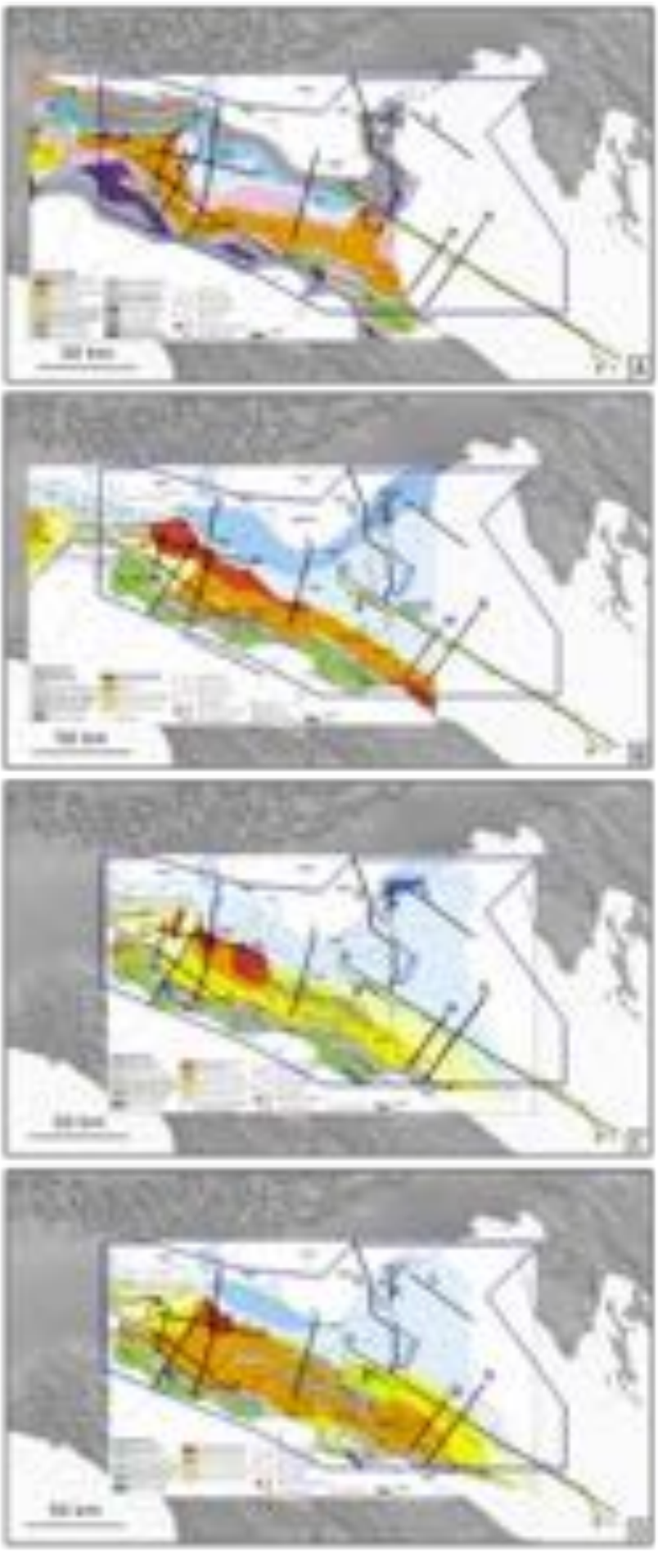

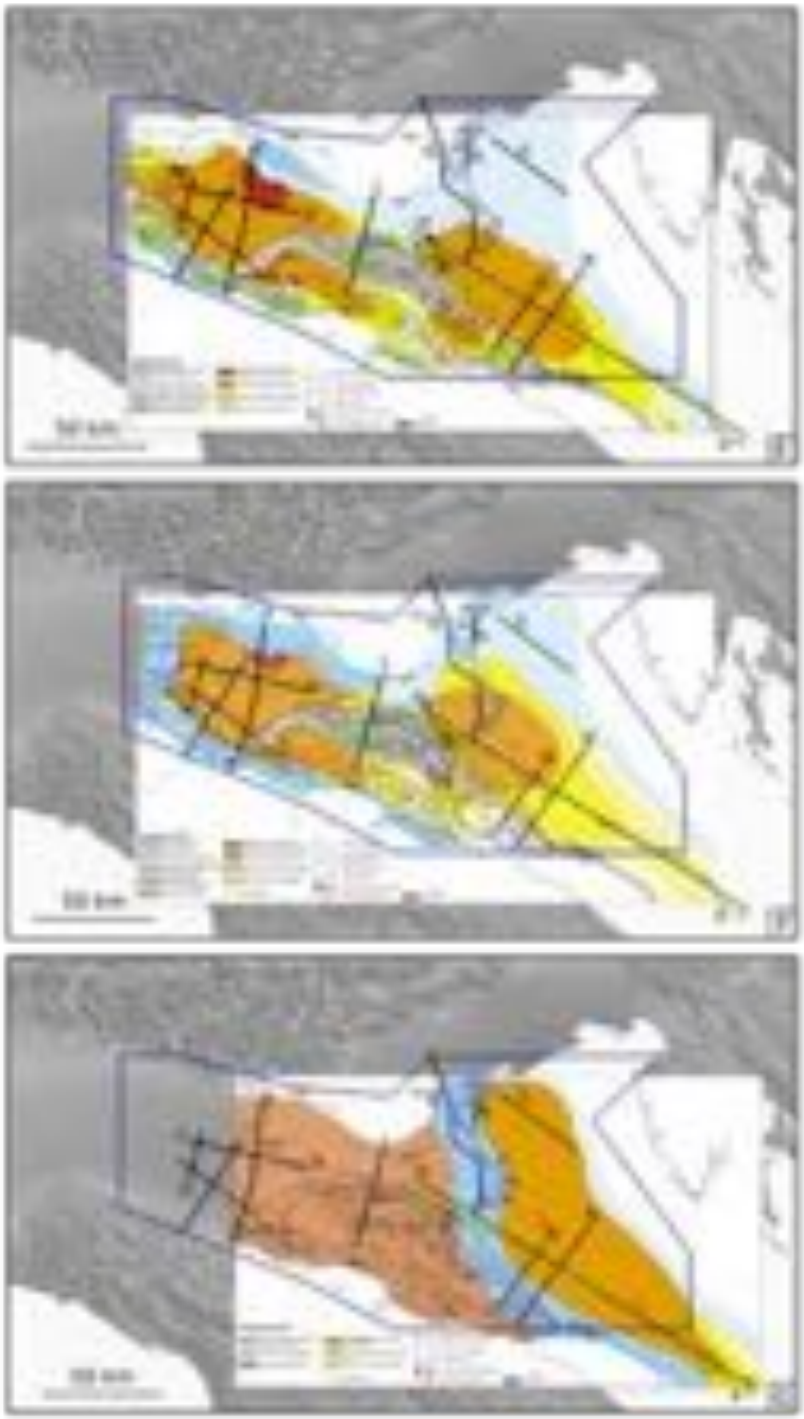

Figure 23. Seven lithofacies maps (from Ghielmi et al., 2010, 2013) showing the geological setting of the PPAF basin during the seven tectono-eustatic events occurred in the area since the late Messinian (section 2.2, this Thesis). A) Intra-Messinian (ME3) unconformity and base of LM allogroup. B) base Zanclean (PL1) unconformity. C) Intra-Zanclean (PL2) unc. and base of EP allogroup. D) Piacentian (PL3) unc. E) Gelasian (PL4) unc. and base of LP allogroup. F) Calabrian (PS1) unc. G) late Pleistocene (PS2) unc. Blue line: study area perimeter. Bold black lines: seismic profiles in figs. 24, 25, 26. Orange line: cross correlation section Fig. 25O. Green points: hydrocarbon wells Fig. 25P.

In this sub-paragraph, some published and unpublished 2D seismic lines, and a cross section, are shown (Figs. 24, 25, 26, 27, 28, 29) and described in order to give a few examples of the most meaningful features of the studied sequences in terms of seismic facies and geometries. Particular relevance is given to the seismic facies of turbidite deposits, useful to predict sand-shale content.

Seismic traces are distributed in the study area in order to give examples of each sector of the PPAF basin, i.e. onshore depocenters (Figs. 24-25-26), deformed Northern Apennine buried chain (Figs. 24-25-26-27), offshore Adriatic foreland ramp (Figs. 27-28) and Venetian-Adriatic foreland (Fig. 29). Each panel will be described separately in the following. Seismic lines from Eni private database (Figs. 24-25-26) are cut below 3000 ms to respect the industry policy for data publication. Names and colour code of the unconformity horizons according with Ghielmi et al. (2010, 2013).

Figure 24. (next page). A) geographic map for location. Blue line: study area perimeter. Red lines: buried tectonic architecture after Ghielmi et al. (2010). Black lines: seismic lines traces. Orange line: cross correlation profile in Fig. 25P. Green points: hydrocarbon wells from Eni private database, details in Fig. 25P. B-I) 2D seismic lines from Eni private database. Horizon colour code in according with Ghielmi et al. (2010, 2013). Light green line: Intra-Messinian (ME3) unconformity and base of LM allogroup. Light blue line: base Zanclean (PL1) unconformity. Orange line: Intra-Zanclean (PL2) unc. and base of EP allogroup. Dark blue: Piacentian (PL3) unc. Dark green line: Gelasian (PL4) unc. and base of LP allogroup. Yellow line: Calabrian (PS1) unc. Red line: late Pleistocene, PS2a unconformity (ca. 900 kyr). Dark red line: latest Pleistocene, PS2b unconformity (ca. 600 kyr). Dashed red lines: faults.

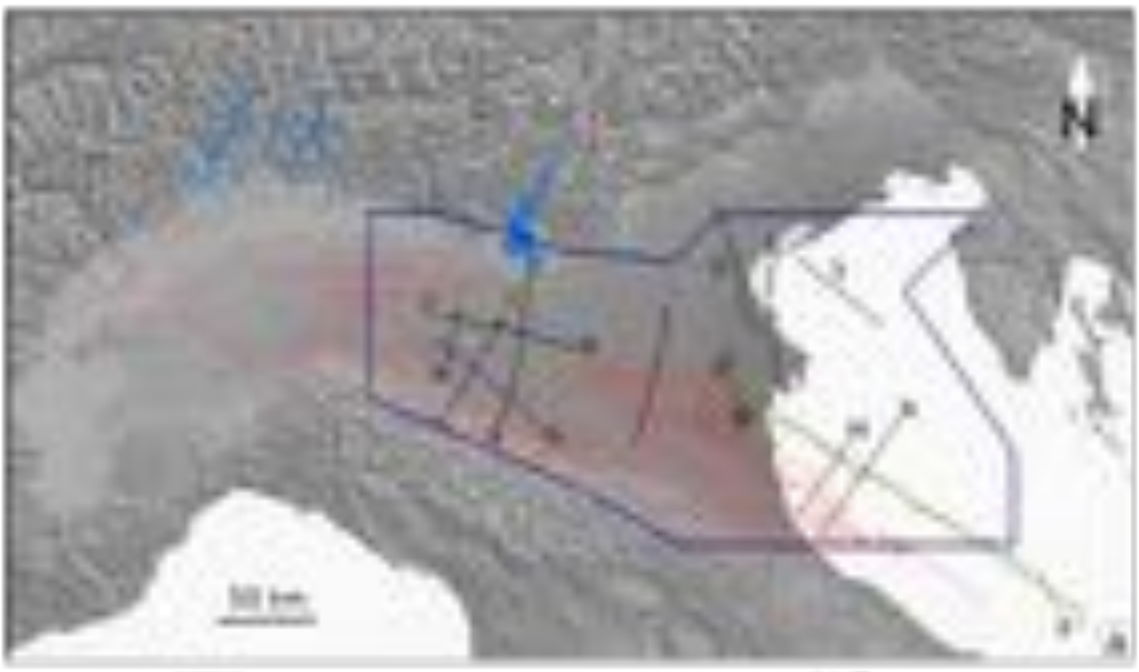

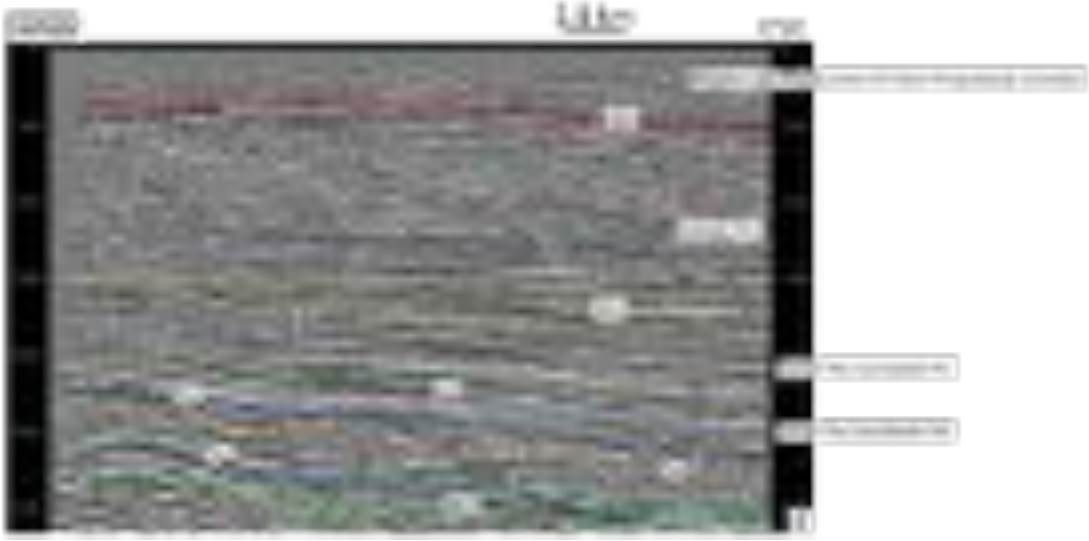

Fig. 24 B: this seismic line (see Fig. 24A for location) along the most external Apennine thrust front, migrated to N-NE sector during the early-middle Pleistocene tectonic phase (Fig. 23F).
Note: deformed onlap surface of the Plio-Pleistocene sequences on the thrust anticline. The late Messinian sequence is represented by coastal, shelfal and slope deposits (Fig. 23A) with complex subparallel and converging seismic reflector. The Pliocene turbidite deposits (PL1, PL2, PL3: Canopo, P.to Corsini, "inner" P.to Garibaldi Fms. respectively) are thinner to the NW because during the entire Pliocene, the area near the present-day Po river mouth was a south-dipping foreland ramp. Since the early Pleistocene instead, the deposition of PL4-PS1 sequences ("outer" P.to Garibaldi and Carola Fms. respectively) appear highly condensed to the NW because deposited on a submarine structural high. Vice versa, the sequences thicken to the SE with high amplitude and continuity subparallel reflection configuration pattern. During the Gelasian tectonic phase the eastern foredeep depocenter moved to the NE, reaching the present Po river mouth area. Pleistocene turbidites are fed from a major entry point to the NW with depositional direction to the SE (Fig. 23E).
The PS2 unconformity lies at the base of the middle-late Pleistocene Po Plain prograding Complex (Ravenna Fm.) because the profile shows the basin plain setting, far from the PS2 shelf-edge located to the west, in the Bologna-Ferrara area (Ghielmi et al., 2010, 2013) (Fig. 23G). Prograding clinoforms are very well visible because the trace is nearly perfectly parallel to the direction of progradation. Bottomset beds evolve in distal deep-water sand-rich turbidites (at ca. 1 sec TWT). Dashed red line: Apennine inverse faults.
Fig. 24 C: this seismic line located into the central depocenter, almost E-W oriented (see Fig. 24A for location), near to the Piadena anticline (Maesano & D'Ambrogi, 2015). Strong differences in amplitude and seismic pattern are visible. The late Messinian ME3 sequence is composed of subparallel to hummocky reflection configuration pattern with the highest amplitude to the west, thinning and grading low amplitude phases to the east. This heterogeneous seismic sequence corresponds to the west to a proximal sand lobe (Fig. 23A) and to slope ramp deposits to the east. PL1 unit (Canopo Fm.) appears completely different from the others, characterised by converging reflectors with high noisy signal. On the basis of the facies types and their distribution, these sediments may be interpreted as a complex of laterally coalescent sand-rich and coarse grained poorly-efficient Type II turbidite systems (Fig. 23B-C), fed by a main entry-point located on the outer margin, south-east to the Garda Lake, probably Adige-Mincio paleo system. PL3, PL4, PS1 sequences pattern changed to parallel reflector with high lateral continuity, corresponding to fine grained lobe fringe and basin plain deposits of the "inner" P.to Garibaldi Fm. (PL3 sequence) and proximal and distal (subordinated) sand lobe of "outer" P.to Garibaldi (Fig. 23D) and Carola Fm.

(PL4 and PS1 sequence respectively) (Fig. 23E, F). The PS2 unconformity lies above the prograding complex topsets.

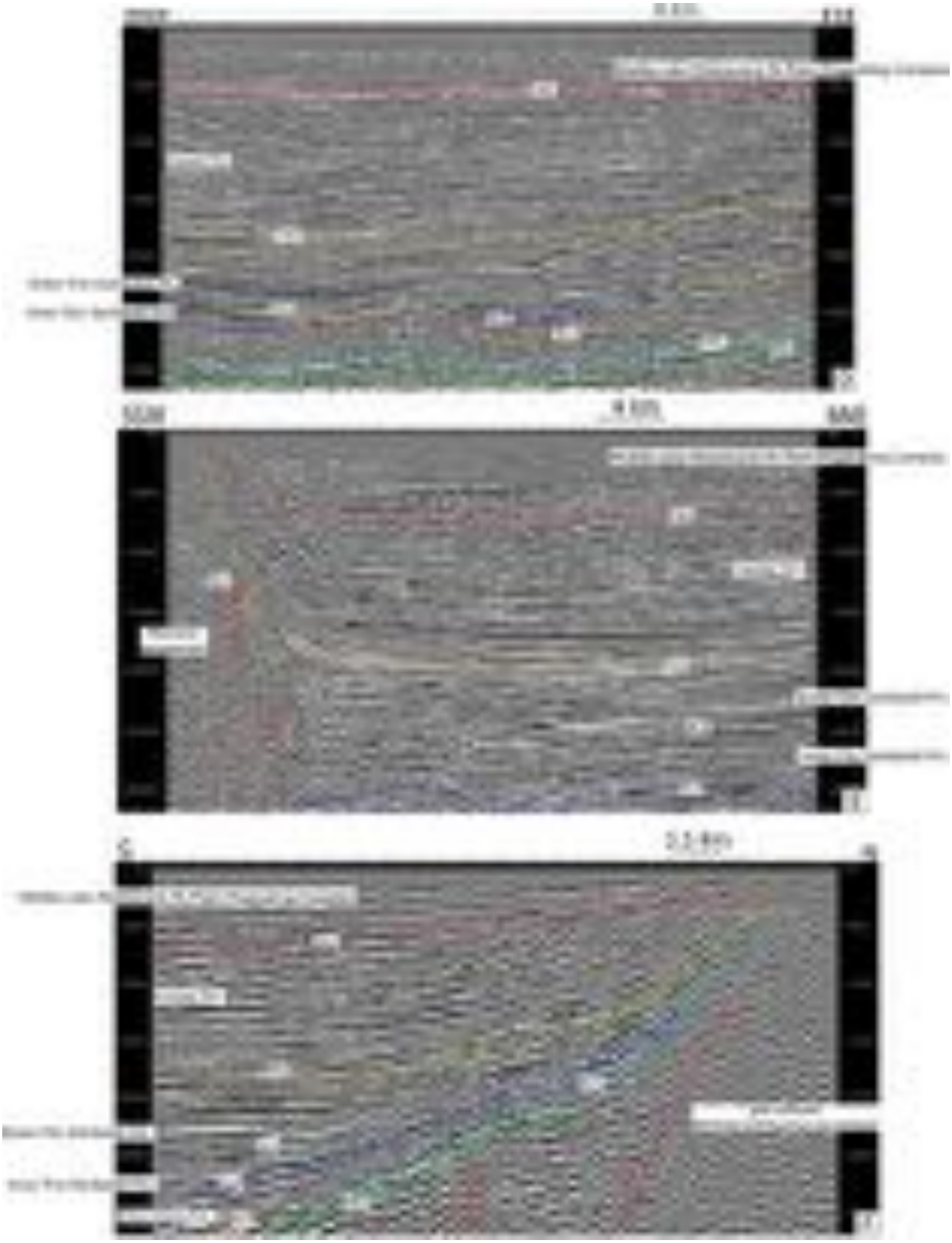

Figure 25. See Fig. 24A for location. D-E-F) 2D seismic lines from Eni's private database. Horizon colour code in according with Ghielmi et al. (2010, 2013). Light green line: Intra-Messinian (ME3) unconformity and base of LM allogroup. Light blue line: base Zanclean (PL1) unconformity. Orange line: Intra-Zanclean (PL2) unc. and base of EP allogroup. Dark blue: Piacentian (PL3) unc. Dark green line: ca. base Gelasian (PL4) unc. and base of LP allogroup. Yellow line: Calabrian (PS1) unc. Red line: late Pleistocene, PS2 unconformity (ca. 900 kyr). Dashed red lines: faults.

Fig. 25 D: this seismic line is the eastern prolongation of the seismic profile in Fig. 24C, crossing the north margin of the basin. In fact, all the units show similar reflection pattern features like the high amplitude PL1 and PL2 sequences made by coarse-grained proximal lobe, fed by entry points along the Mantova Monocline (MM) (stable source during the Zanclean-Calabrian time) and parallel, lateral continuous Pleistocene PL4 and PS1 seismic sequences, due to turbidite sand and shale interbedded layers.

Fig. 25 E: to the S, there are two reverse faults, probably splaying from the same thrust plane, belonging to the most external front of the Emilia arcs. In this area, the tectonic deformation started during late Tortonian (EM Allogroup, Ghielmi et al., 2010). The submarine structural high, caused condensed sedimentation until Calabrian, when the top of the anticline was overlain by coastal, shelfal and slope deposits. To the NE, during Messinian-Calabrian time evolved a deep foredeep depocenter filled mostly with highly-efficient sand-rich turbidite systems.

Fig. 25 F: this seismic line is the northward prolongation of the seismic line in Fig. 25E, covering from the south, the deformed Apennine chain with the depocenter and northward the foreland ramp (Garda Monocline). The foreland ramp, with pre-Messinian extensional faults, has Messinian and early Pliocene drowning unconformities occurred because of the increasing rate of subsidence related to the outward shift of new foredeep depocenter. The Pleistocene Prograding Complex (upper PS1 and PS2 sequence) have an apparent opposite progradation direction, visible in in figures 25 E and 25 F. The system from the Apennine margins and the north one from the South Alps, both prograding towards the foredeep centre. The overall Pleistocene Prograding Complex migration is to E-SE. The basement is characterized by chaotic seismic patter corresponding to the pre-collision Permian basement and Mesozoic carbonate succession.

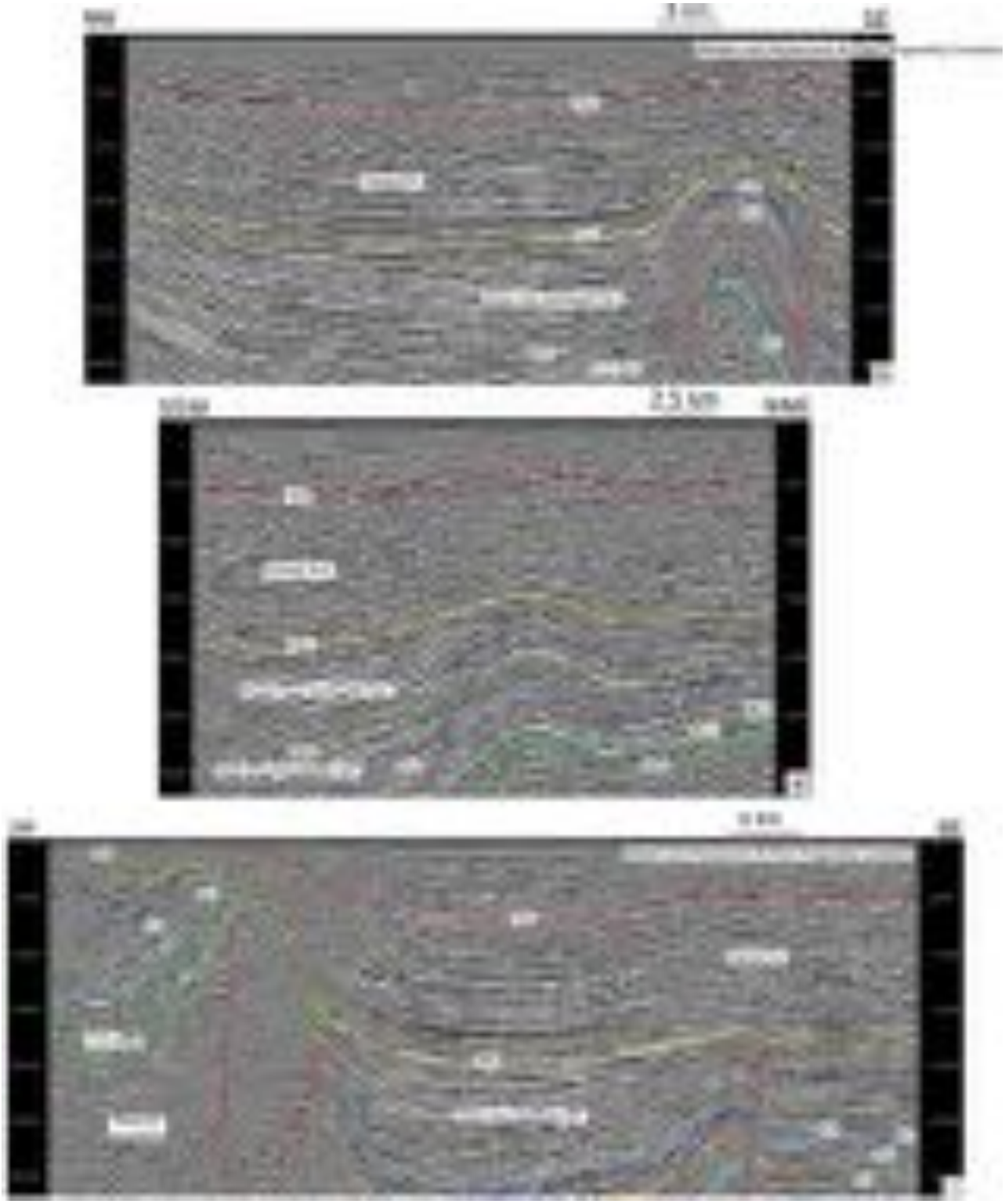

Figure 26. See Fig. 24A for location. G-H-I) 2D seismic lines from Eni's private database. Horizon colour code in according with Ghielmi et al. (2010, 2013). Light green line: Intra-Messinian (ME3) unconformity and base of LM allogroup. Light blue line: base Zanclean (PL1) unconformity. Orange line: Intra-Zanclean (PL2) unc. and base of EP allogroup. Dark blue: Piacentian (PL3) unc. Dark green line: ca. base Gelasian (PL4) unc. and base of LP allogroup. Yellow line: Calabrian (PS1) unc. Red line: late Pleistocene, PS2 unconformity (ca. 900 kyr). Dashed red lines: faults.

Fig. 26 G: this seismic line shows thrust-fold in the subsurface near to the Reggio Emilia town is shown, with syntectonic sedimentation demonstrated by deformed onlaps and growth strata at the top of the anticline. The anticline, with steep limbs, was growing since early-middle Pliocene (PL2 Intra-Zanclean phase) until recent time. The PS2 fully continental sequence is folded with lateral onlaps on the crest (visible at 300-400 ms), this deformation has also led to differential compaction. There are two high angle reverse faults, evolved in different periods as evidenced by different unit thicknesses at the footwalls. First, the SE-dipping one migrated in the middle Pleistocene (PL3 sequence) while the N-dipping back-thrust formed only in the early Pleistocene (Fig. 25E). Because the seismic section is cut under 3 seconds it is not visible the S-dipping basal thrust, required to accommodate the shortening at depth.

Fig. 26 H: the seismic section is located between the most external Emilia thrust front and the southern Alps, close to the Piadena anticline. From the SW, the large syncline near to the southern margin corresponds to Apennine thrust footwall. The anticline instead, is the lateral expression of Piadena structure (Fig. 26I). The Piacentian-Calabrian parallel-bedded, high-amplitude and high-continuity reflectors represent the turbidite infill. The early Pleistocene clinoforms (upper PS1 seq.) of the prograding complex appear not well developed due to the profile orientation, parallel to the shelf-edge and almost perpendicular to the progradation direction (Fig. 25F). The progressive upward anticline widening denotes reduction of the Piadena tectonic activity thought time.

Fig. 26 I: this seismic section (modified from Ghielmi et al., 2013) shows the Messinian–Pleistocene succession in the Cortemaggiore piggy-back basin of the Apennine thrust -fold belt (see Fig. 24A for location). It is possible to observe the following features:

i) the prominent angular unconformities, caused by the uplift of the Cortemaggiore front (to the SW), that characterized in particular the LM (ME3 unc.) and EP (PL4 unc.) allogroup boundaries;

ii) the presence at the base of the LM allogroup (ME3 unconformity) of a thick chaotic complex consisting of Ligurian and Messinian units resedimented through mass-transport processes (Artoni et al., 2010);

iii) the condensation that characterized the Cortemaggiore submarine high during Pliocene as indicated by the convergence of the PL2, PL3 and PL4 sequence boundaries;

iv) the progradational seismic geometries of the Pleistocene succession (sequences PS1 and PS2);

v) the local direction of the Pleistocene progradation are towards NE. Pliocene thrust faults related to the NE-ward propagation of the Apenninic deformation;

vi) the Piadena structure, forming an anticline, is clearly controlled by the underlying thrust and the PS1 horizon shows also the closures of the anticline towards NW and SE. The ongoing activity of the fold during the Calabrian is recognizable by the presence of syntectonic growth strata during this time

interval;

vii) Plio-Pleistocene turbidite sandstone lobes and lobe fringes are recorded by parallel-bedded, high-amplitude and high-continuity reflectors.

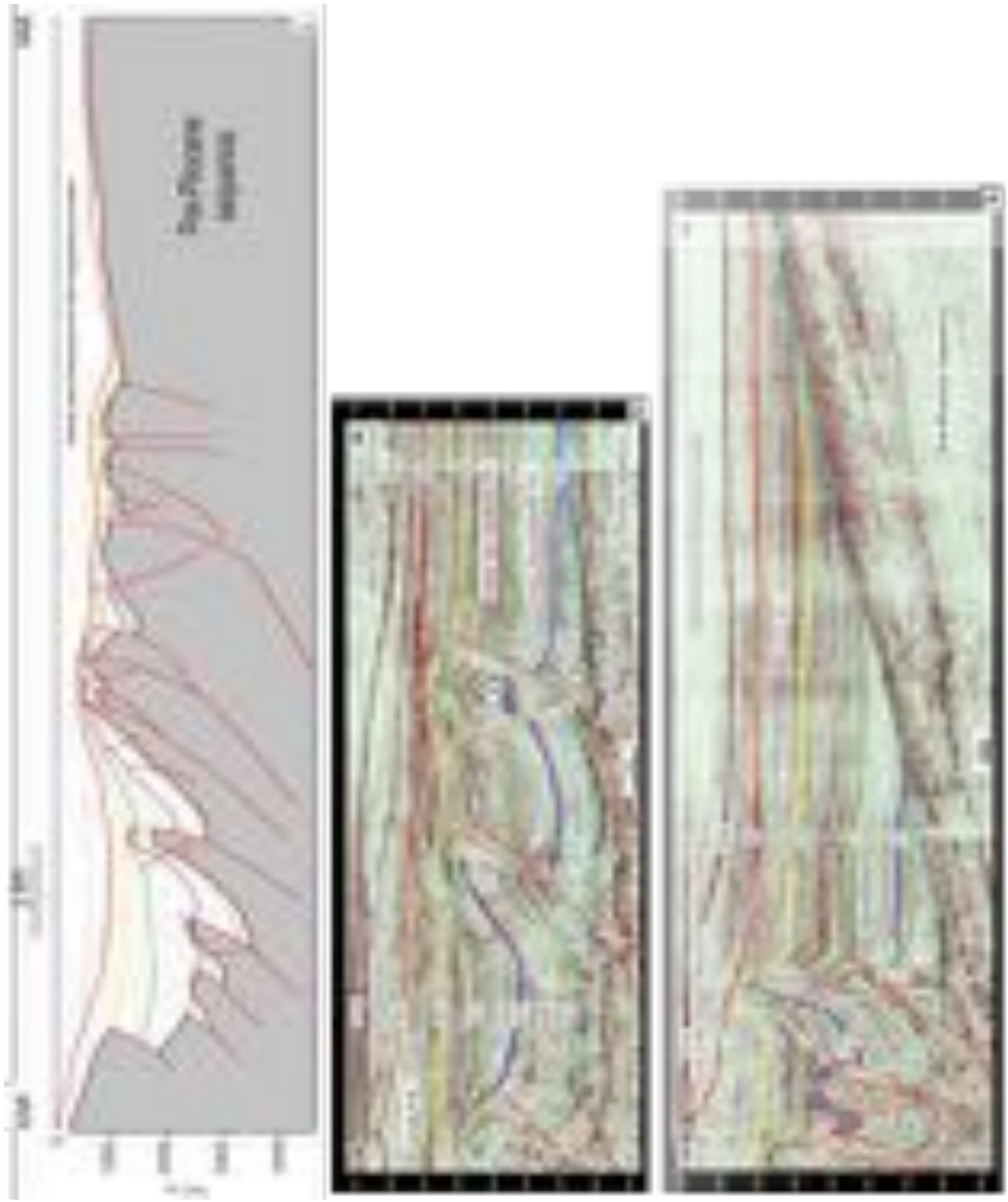

Figure 27 (above and next pages). Unpublished (L) and published seismic profiles and well log cross section (M-P) (Modified from Ghielmi et al., 2013; Cazzini et al., 2015). See text for details. Horizon colour code in according with Ghielmi et al. (2010, 2013). Light green line: Intra-Messinian (ME3) unconformity and base of LM allogroup. Light blue line: base Zanclean (PL1) unconformity. Orange line: Intra-Zanclean (PL2) unc. and base of EP allogroup. Dark blue: Piacentian (PL3) unc. Dark green line: Gelasian (PL4) unc. and base of LP allogroup. Yellow line: Calabrian (PS1) unc. Red line: late Pleistocene, PS2a unconformity (ca. 900 kyr). Dark red line: latest Pleistocene, PS2b unconformity (ca. 600 kyr).

Fig. 27 L: linedrawing of a composite seismic profile, SSW-NNE oriented, across the Bologna-Ferrara thrusts toward the foreland ramp on the Veneto region (see Fig. 24A for location).

Note: i) to the SW is evident a deep piggy-back basin, subsiding since the early Pliocene, filled with remarkable thickness of Plio-Pleistocene sequences;

ii) high sediment condensation and deformation at the top of the Ferrara arcs which started uplifting since the intra-Zanclean (PL2) tectonic phase;

iii) the progressive tectonic activity decreasing since Calabrian time. In this location, the most recent PS2 continental sequence, middle-late Pleistocene Po Plain Prograding Complex, is deformed (e.g. folded or tilted) but not displaced by thrust faults. In grey is the pre-Pliocene, Meso-Cenozoic substratum, deeply involved in the tectonic deformation (Fantoni & Franciosi, 2008, Toscani et al., 2009; Fantoni & Franciosi, 2010).

Fig. 27 M: this seismic section shows the Plio-Pleistocene succession in the northern Adriatic Sea fold belt (vertical scale in milliseconds, modified from Ghielmi et al., 2013) (see Fig. 24A for location).

It is possible to observe: i) the frontal part of the northern Apennine thrust and fold belt;

ii) the substantially undeformed foredeep of the LP allogroup (PL4, PS1 and PS2 sequences);

iii) the progradational seismic geometries of the Pleistocene Progradation Complexes. Note also the partial submarine truncation of the PL3 seq. along the thrust front n.2 occurred mainly during the Base Gelasian phase (Ghielmi et al., 2013). PS2b late Pleistocene surface, is the base of the youngest prograding sequence and is robustly dated in the Adriatic offshore at ca. 600 kyr, just above the Gephyrocapsa sp. 3 LO (Ghielmi M. personal communication). This youngest depositional sequence is best recognized at the eastern edge of the Po Plain, e.g. in the Venetian area (Kent et al., 2002).

Fig. 27 N: this Seismic section shows the Plio-Pleistocene succession in the northern Adriatic Sea (modified from Ghilemi et al., 2013) (see Fig. 24A for location).

Note: i) the most external and recent thrust-propagation folds of the northern Apennine thrust and fold belt;

ii) the undeformed to slightly deformed foredeep of the LP allogroup limited along the inner margin by the thrust front system n. 3;

iii) the onlap of the turbidites of the P.to Corsini (PL2 seq.), “inner” and “outer” Porto Garibaldi (PL3 seq. and PL4 seq. respectively), and Carola (PS1 seq.) Formations on the SW-dipping foreland ramp;

iv) the remarkable high lateral continuity and tabular geometry of the highly-efficient turbidite systems of the same formations and sequences listed above;

v) the Messinian sequences reduce in thicknesses moving to NE, towards the shelf-coastal area of the foreland domain where also evaporitic sediments deposited;

vi) the seismic progradational geometries of the Pleistocene progradations (upper part of seismic section).

It is possible to observe also the merging between Pleistocene Apenninic Prograding Complex (Calabrian-middle Pleistocene in age at this location) from the southwest margin of the basin, and the axial Po Plain Progradation Complex (middle Pleistocene), the local directions of progradation are towards the NE and towards the SE respectively. Both the progradations consists of slope, shelfal and coastal deposits of the Ravenna Formation. The thrust front n. 1, uplifted during the Intra-Zanclean Phase, represented during the Zanclean-lower Gelasian the inner limit of the EP allogroup foredeep (PL2 and PL3 sequences). The more external thrust front system n. 3 was involved in a first phase of activity at PL3 sequence boundary but reactivated and completely uplifted during the Gelasian Phase, representing the inner limit of the Pleistocene LP allogroup foredeep (PL4, PS1 and PS2 sequences). The gradual decrease of the thrust propagation in the PPAF area during Pleistocene, after the latest Tortonian-Gelasian intense activity, is suggested by the gradual onlap of the PS1 turbidites on the front n. 3, and by the substantially undeformed sediments of the PS2 seq. deposited above the same front (Ghielmi et al., 2013).

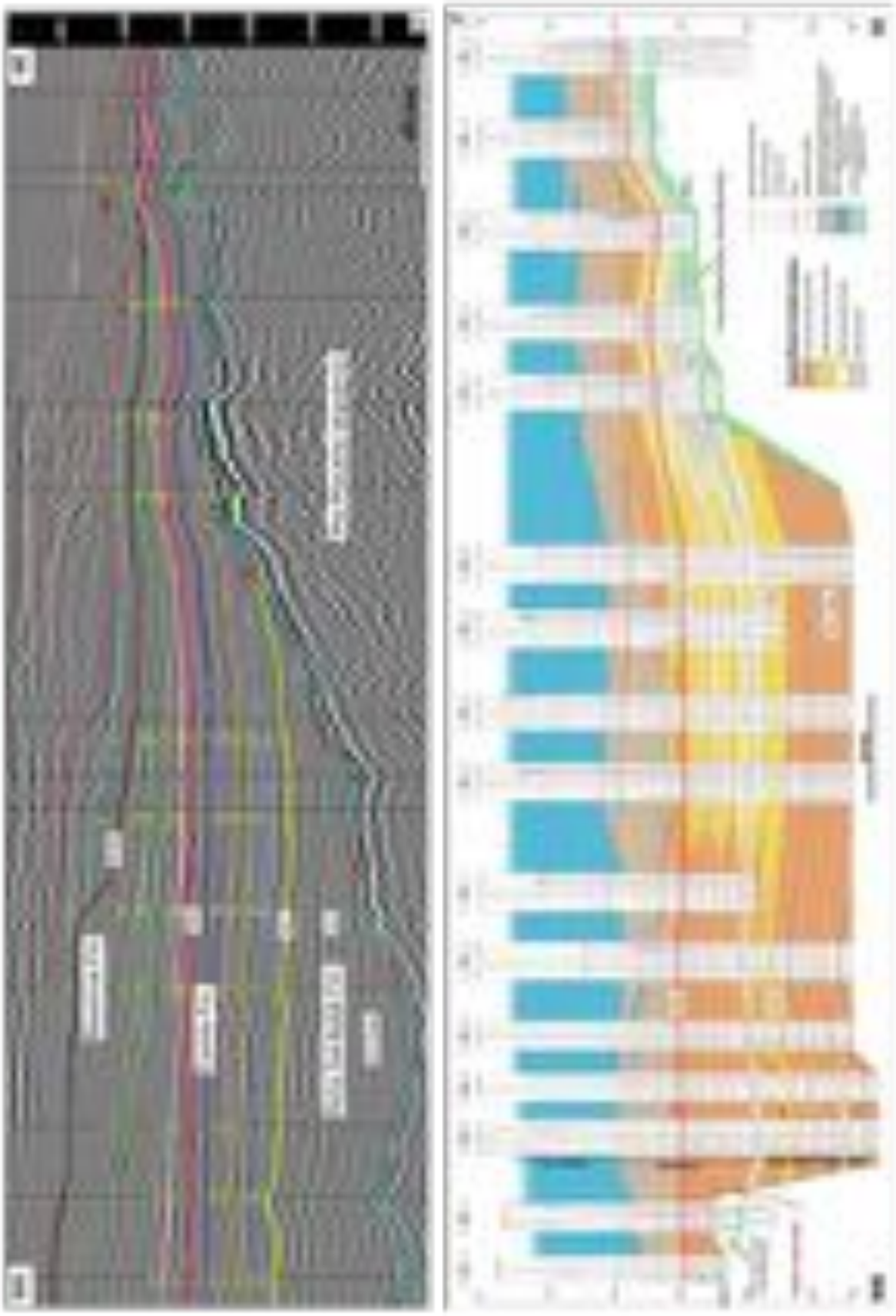

Figure 28. See Fig. 24A for location. O) Seismic lines modified from Ghielmi et al. (2010), P) Cross correlation panels modified from Cazzini et al. (2015). Horizon colour code: see Fig. 24 caption. See text for details.

Fig. 28 O: composite seismic section of the Pleistocene turbiditic succession of the LP allogroup foredeep (sequences PL4, PS1 and PS2) (see Fig. 24A for location). This seismic section runs parallel to the well correlation of Fig. 25P and extends for about 220 km roughly parallel to the main foredeep axis.

Note: i) the remarkable high lateral continuity and tabular geometry of the highly-efficient turbidite systems of the ‘‘outer’’ Porto Garibaldi and Carola Fms.;

ii) the onlap onto the foreland ramp of the “outer” P.to Garibaldi turbidites (Sequence PL4);

iii) the gradual progradation towards SE of the Po Plain Prograding Complex made up of slope, shelfal and coastal deposits of the Ravenna Fm. (Ghielmi et al., 2010).

Fig. 28 P: well correlation (vertically exaggerated) of the Pleistocene turbiditic succession of the allogroup LP foredeep (sequences PL4, PS1 and PS2). The correlation extends for about 220 km roughly parallel to the main foredeep axis and to Fig. 25O (see Fig. 24A for location) (modified from Cazzini et al., 2015).

Note: i) the remarkable high lateral continuity and tabular geometry of the highly-efficient turbidite systems deposits of the ‘‘outer’’ P.to Garibaldi and Carola Fms;

ii) the progressive downcurrent transition (towards SE) from proximal thick-bedded sand lobes to thin-bedded fine-grained distal basin plain deposits;

iii) the gradual progradation towards SE of the Po Plain Prograding Complex consisting of slope, shelfal and coastal deposits of the Ravenna Fm.

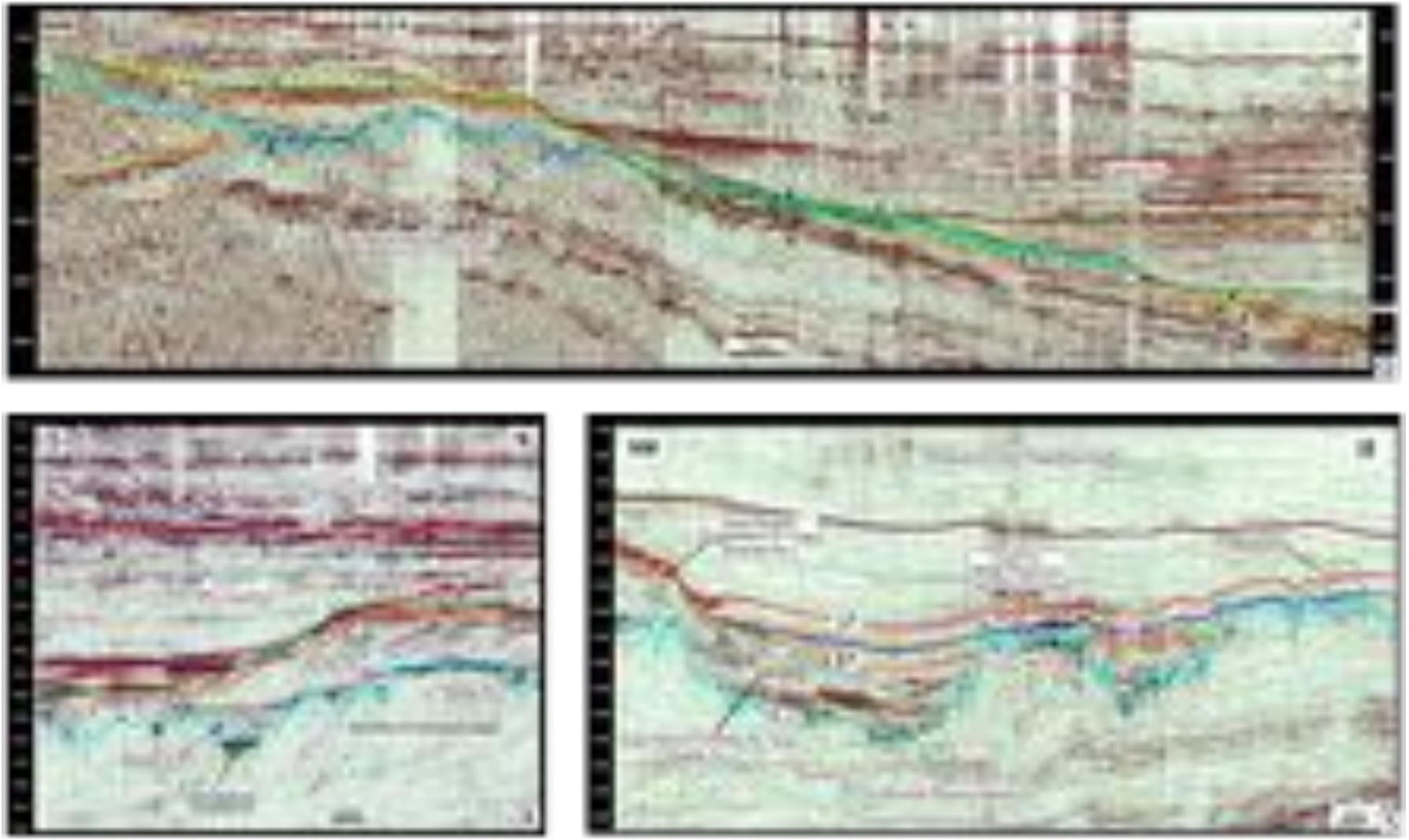

Figure 29. Seismic lines modified from Ghielmi et al. (2013). See text for details and Fig. 24A for location. Horizon colour code in according with Ghielmi et al. (2010, 2013). Light green line: Intra-Messinian (ME3) unconformity and base of LM allogroup. Light blue line: base Zanclean (PL1) unconformity. Orange line: Intra-Zanclean (PL2) unc. and base of EP allogroup. Dark blue: Piacentian (PL3) unc. Dark green line: Gelasian (PL4) unc. and base of LP allogroup. Yellow line: Calabrian (PS1) unc. Red line: late Pleistocene, PS2a unconformity (ca. 900 kyr). Dark red line: latest Pleistocene, PS2b unconformity (ca. 600 kyr).

Fig. 29 Q: regional composite seismic profile (see Fig. 24A for location) (modified from Ghielmi et al., 2013) showing the stratigraphic relationships between coastal wedges developed from latest Tortonian to Zanclean (Early Pliocene) around the peripheral bulge separating the Southern Alps and the Northern Apennines foredeeps. High-magnitude relative base-level changes can be estimated (see text for discussion). The coastal wedges are later onlapped by Plio-Pleistocene aggradational turbidite systems of the PPAF.

Fig. 29 R: 2D seismic section (modified from Ghielmi et al., 2013) of the uppermost Messinian-Pleistocene succession in the Venice Lagoon (see Fig. 24A for location). The local directions of progradation are towards S for the lower Pliocene (e.g. Eraclea Fm.) and towards NE for the middle Pleistocene Po Plain Prograding Complex. The LM, EP and LP allogroup boundaries are laterally interpreted to a greater extent than the boundaries of the component PL1 and PS2 large-scale sequences. Note the high amplitude Upper Messinian conglomeratic incised valley fill.

Fig. 29 S: Seismic section (vertically exaggerated) of the uppermost Messinian-to-Middle Pleistocene succession in northern Adriatic Sea (see Figs. 24A for location) (modified from Ghielmi et al., 2013). Note: i) the irregularity of the LM unconformity produced by the Late Messinian subaerial exposure;
ii) the Lower Pliocene Progradation (PL1 seq.) whose local direction is towards the SSE;
iii) in this offshore foreland area, the Early Pliocene turbidite sedimentation (PL1 seq.) was confined into the Messinian paleo-valleys. These poorly-efficient turbidites, directly fed by the progradating wedge, were deposited in a foreland setting;
iv) in this area, the LP allogroup boundary is represented by a surface of no deposition-condensation. At this location, the hiatus/condensed section comprises the sediments of the PL4 and PS1 sequences and of the basal part of the PS2 sequence.

3.4.3. From 2D to 3D-time modeling

Correlation though the seismic grid results in an accurate framework of superposed seismic sequences. The widespread use of three-dimensional modelling software, capable of processing and displaying large quantities of different surface and subsurface geological data, allows the user to view and understand the spatial relationships among structural or stratigraphic features (among many others, De Donatis, 2001, 2002; D'Ambrogi et al., 2004; Dhont et al., 2005; Fernandez et al., 2004; D'Ambrogi & Doglioni, 2008; Kaufmann & Martin, 2008; Fernandez et al., 2009; D'Ambrogi et al., 2010).

In the present Thesis, the software used to manage data, to perform seismic interpretation and to construct 3D geological models in time and depth domain, are:

- Move™ by Midland Valley Exploration Ltd.
- DecisionSpace® (Landmark) by Halliburton

The Delaunay triangulation is the chosen method to create a three-dimensional time-surface from the 2D interpretation. This method honours all the input points, optimizes the geometry of the triangles and fulfills the nearest neighbour relation. The 3D model in time includes also some fault segments, but they were not interpolated in surfaces and not converted in depth domain because a detailed structural analysis was not the aim of this Thesis.

To respect the tectonic deformation, footwall and hangingwall geometries have been traced continuously, producing single 3D surface per each horizon.

After the triangular interpolation, the surfaces have been smoothed and resampled with 1 km cell size. Smoothing is a common technique useful to improve the quality and eliminate some punctual errors derived from previous steps. The points of gridded surfaces (e.g. XYZ coordinates) will be the input data for the time-depth conversion (3.4.3 section, this Thesis). Both Move™ and DecisionSpace® software allow to honor the multi-scale approach proposed in this work combining, in a single 3D environment, different types of spatially referenced data from local to regional, enabling the user to integrate data across a wide range of scales within a single comprehensive model.

3.4.4. 3D Time-to-depth conversion

Maesano & D'Ambrogi (2017) designed a workflow for 3D velocity model production only from subsurface data: Vel-IO 3D. The tool, developed in ArcGIS, allows the management of velocity data and the calculation of a 3D instantaneous velocity model, that are the most difficult steps for the 3D model building. Furthermore, Vel-IO 3D workflow was tested already in a portion of the central Po Plain during GeoMol Project (2014) (Maesano & D'Ambrogi, 2015) thus, it seems to be the ideal tool for the present case study, according to the abundant availability of subsurface data.

The idea behind Vel-IO 3D script is to assign the velocity model parameters to each point of X and Y coordinates within the 3D model in time domain and then perform the calculation and interpolation of the depth value (Z). The tool works following three main steps:

i) 3D instantaneous velocity model building;

ii) velocity model optimization and

iii) depth conversion.

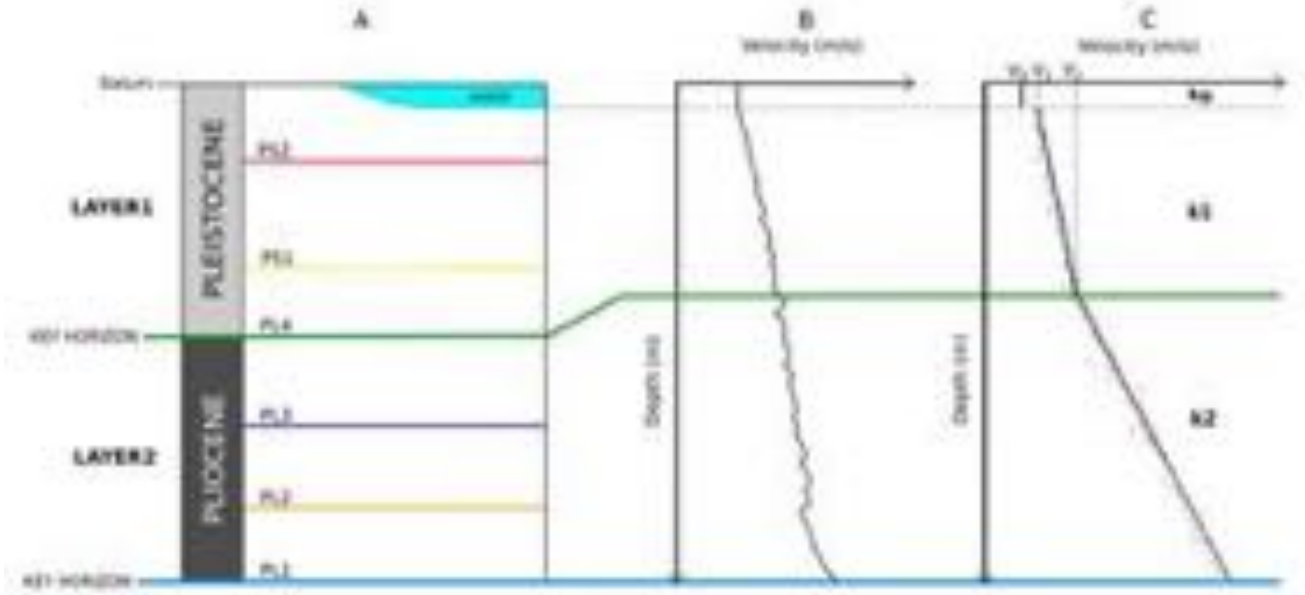

Figure 30. A) Velocity two layer-cake scheme used for the velocity model: key-horizon and unit names refer to the main unconformity surfaces (see section 2.2, this Thesis or Ghilemi et al., 2013). B) example of the interval velocity plot of well. C) Example of instantaneous velocity model; V and k are respectively the initial velocity and the velocity gradient of each layer.

The PPAF subsurface 3D instantaneous velocity model performs velocity analysis and interpolation; to simulate the Po Plain-Northern Adriatic basin a two layer-cake model has been chosen, dividing the Pliocene from the Pleistocene volume by selected key-horizons (Fig. 30A).

After the 3D TIME model building, the chosen key-horizons are: the base of allogroup LP, the PL4 unconformity surface, base Gelasian in age (corresponding to the top of the second one) and the base Pliocene PL1 unconformity, that is the base of the entire model.

In order to convert correctly the offshore area, the bathymetry of the Adriatic Sea is added into the 3D TIME model as an uppermost layer (Fig. 31).

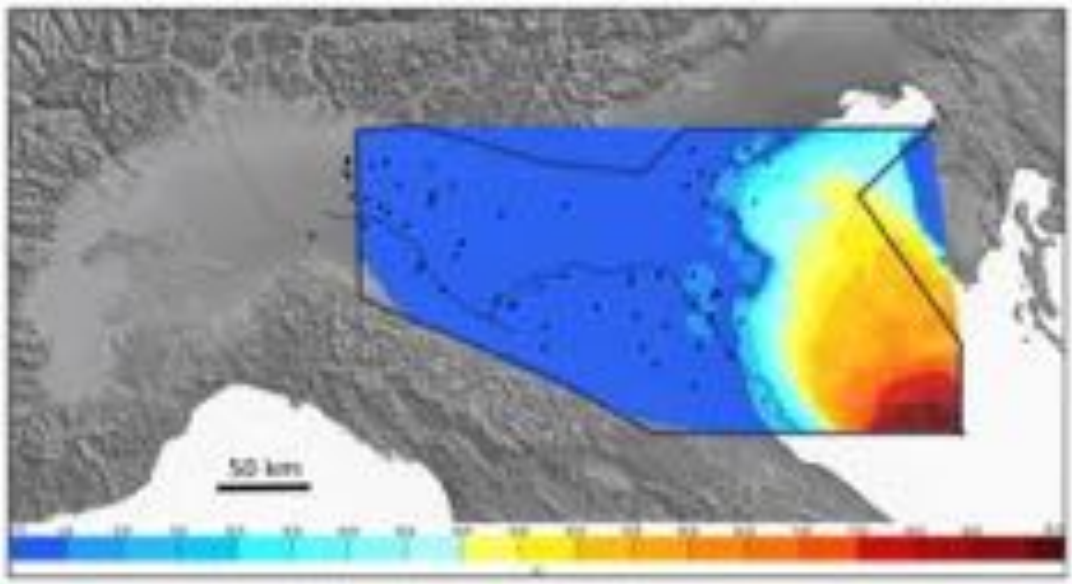

Figure 31. Bathymetry of the northern Adriatic Sea converted in time domain. Black points: wells with velocity attributes used for the depth-conversion. Black lines: external buried thrust fronts of the northern Apennine. Blue line: study area perimeter.

The 3D bathymetry in time domain has been obtained from the conversion of the bathymetry in depth domain from SRTM30 (Becker et al., 2009) using the constant velocity of the sound in water: 1500 m/s.

To make use of Vel-IO 3D and perform velocity analysis some inputs are requested, i.e.: velocity parameters and their spatial variation for each key-horizon, calculated from velocity analysis on the selected wells (Fig. 20), following the linear equation (1) and respective Correlation coefficients ($\mathbf{R^2}$) are applied to each layer to be converted:

$$\mathbf{V(Z) = V_0 + kZ} \qquad \mathbf{(1)}$$

Where V(Z) is the velocity (m/sec) at Z depth (m) and V_0 and k (1/sec) are respectively the initial velocity at the top of the considered layer (i.e. at the key horizon) and the gradient describing the velocity variations with depth (Ravve and Koren, 2006) (complete theory of the method in Maesano & D'Ambrogi, 2017 and supplementary materials).

In the present study, the cake model is composed of two main layers thus, the velocity parameters and correlation coefficients are:

- V_0 = acoustic velocity in water, 1500 m/s
- K0 = constant gradient of the water velocity-depth curve.
- V_1 = initial velocity at the top of the Pleistocene layer: at the surface datum or well.
- K1 = gradient of the velocity-depth curve into the Pleistocene thickness.
- R^2_1 = coefficient of correlation of the layer1 (Pleistocene), accepted only if $\geq$0.5.
- K2 = gradient of the velocity-depth curve into the Pliocene thickness.
- V_2 = initial velocity at the top of the Pliocene layer (PL4 unc.) in well.
- R^2_2 = coefficient of correlation of the layer2 (Pliocene), accepted only if $\geq$0.3.
- PL4 in twt: Pleistocene key-horizon, unconformity surface from 3D TIME model.
- PL4 depth in well: depth calibration of the unconformity.
- PL1 in twt: Pliocene key-horizon, unconformity surface from 3D TIME model.
- PL1 depth in well: depth calibration of the unconformity.

The southern margin of the Po basin is an area with the litho-facies and thickness variations due to the irregular geometry produced by the northern Apennine fronts. During the 3D velocity model building, the major problems were encountered, where the tectonic setting is more articulated and generate abrupt velocity changes and high gradients. To not affect the more regular and homogeneous depocenter zone (in terms of less variability both in the initial velocity values and in the gradient) with errors derived during velocity interpolation, a barrier is imposed located along the external

fronts, to divide and isolate the model calculation into two different settings: the foredeep-foreland to the north-east and the thrust anticlines, thrust-top basins to the south (Fig. 32).

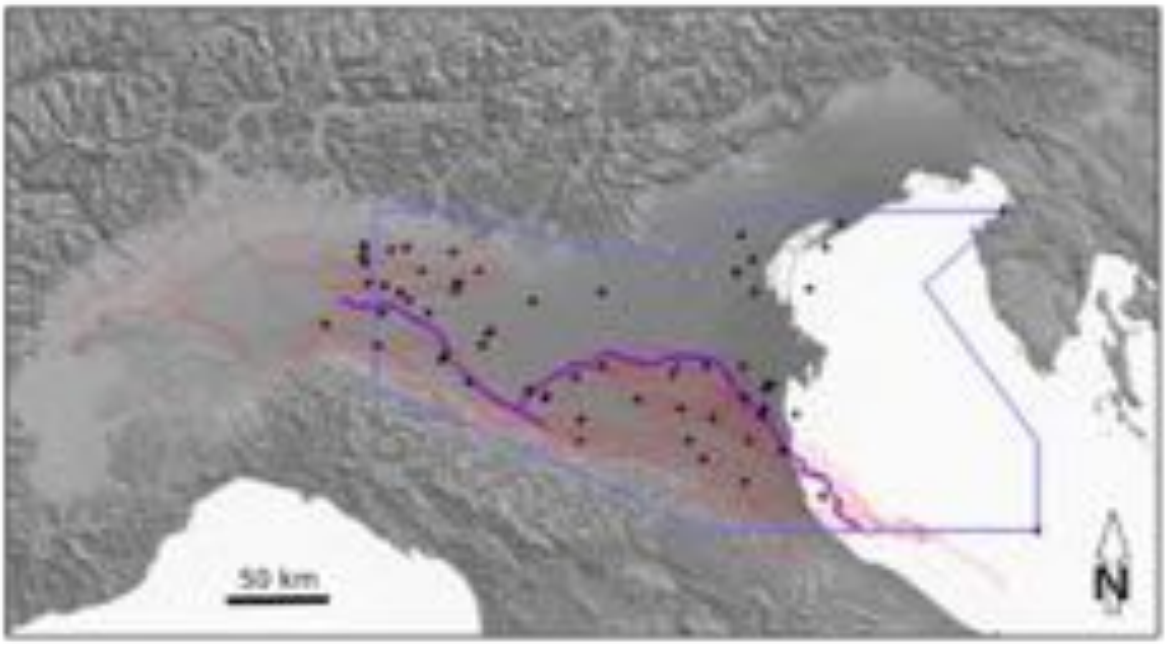

Figure 32. Purple lines: velocity model barrier located along the most external Apennine buried thrust fronts. Blue line: study area perimeter. Black points: wells with velocity attributes used for the depth-conversion. Red lines: tectonic setting after Ghielmi et al. (2013).

A model optimization follows the first velocity model building. In order to improve the consistency of the obtained velocity model. During the optimization, new independent points (V_0 and k values derived from measured depths in wells) are added to the model to reduce the geometrical uncertainties in the areas located far from the original velocity data. These additional points (e.g. wells) works as "control points"; the best V and k values found for each horizon during the optimization are then associated to the control points coordinates and are used, together with the existing velocity data, to calculate optimized grids of the velocity model.

During the optimization, data were accepted only into a vertical range of 50-100 m. This vertical resolution is chosen because relative to the vertical seismic resolution, which is the raw data of the model.

Eventually, the tool runs the time-depth conversion of any object (all the six unconformities described by Ghiemi et al. 2013 and reconstructed in the 3D TIME model, see section 3.4.2, this Thesis). The input data are the optimized velocity model and the surfaces from 3D TIME model to be depth converted.

Since the points of each surface represent a node obtained after the time-depth conversion procedure they can be re-imported into the 3D environment, for instance Move, DecisionSpace, ArcGIS software, as meshes with preserved boundaries and no further basic editing is needed.

3.5. Results

3.5.1. TWT-maps

In this chapter, the basin-scale distribution and geometry of the stratigraphic units forming the 3D building blocks of the late Messinian-Pleistocene sedimentary infill (Fig. 33) are described by means of isochronous maps of each key surfaces.

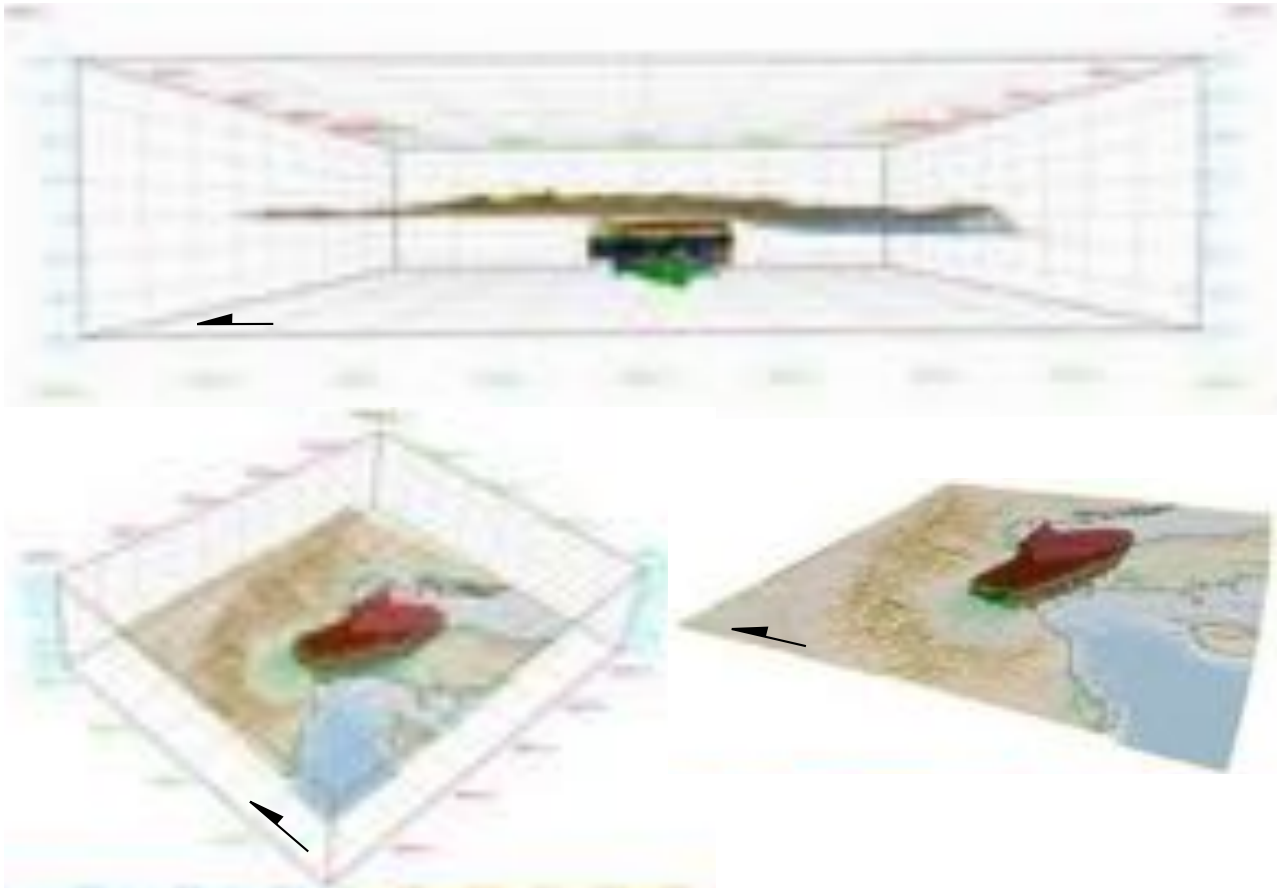

Figure 33. 3D block in different views, x20 vertical exaggeration. Top: vertical lateral view from the west. Bottom left and right: tilted 3D block. The seven key surfaces are in time domain. The topography is from TOPO30 (30 arc-sec resolution) Black arrow: north direction. From the bottom of the 3D model: light green surface: ME3 unc.; Light blue surface: PL1 unc.; Orange surface: PL2 unc.; Blue surface: PL3 unc.; Green surface: PL4 unc.; Yellow surface: PS2 unc.; Red surface: PS2 unconformity.

The surface grid of the unconformities coming out from the interpolated seismic interpretation need to be carefully checked and refined in order to avoid intersections between surfaces or inconsistencies due to interpolation. It's possible that two unconformities overlap or cut each other, in particular near the study area boundaries or even in sectors where lack of seismic reflection profiles force the interpolation algorithms to work with few/sparse data. In these cases, structure contour lines and/or cross-sections need to be carried out and modified in order to obtain geologically consistent results. Here, only the obtained maps that homogeneously cover the whole basin area are shown, contour lines are every 500 ms for the ME3, PL1, PL2, PL3 and PL4 unconformities and every 250 ms for

the Pleistocene PS1 and PS2. In the case of the Messinian surface (ME3), only the western depocenter can be converted into a continuous surface.

The 3D maps in figs. 34-40, show the interpolated maps corresponding to the seven studied unconformities. Nevertheless, even in time domain, some qualitative considerations can be made on the basis of the stratigraphic record and of the mapping results.

The deeper unconformity, the Intra-Messinian unconformity (ME3 unc. and base of LM allogroup) (Fig. 34), and the above late Messinian depositional sequence are not everywhere preserved. In fact, in most of the basin margin and the foreland the entire post-evaporitic Messinian succession is missing (due to erosion or non-deposition) or highly condensed thus, in that areas the late Messinian unconformity corresponds to the base Pliocene (PL1 unc.). In the western foredeep, on the contrary, late Messinian deep-water turbidites filled the local basin left after the sea level drop, occurred during the Messinian Salinity Crisis acme (Hsü et al., 1977; Rossi et al., 2015; Vai, 2016 and reference therein).

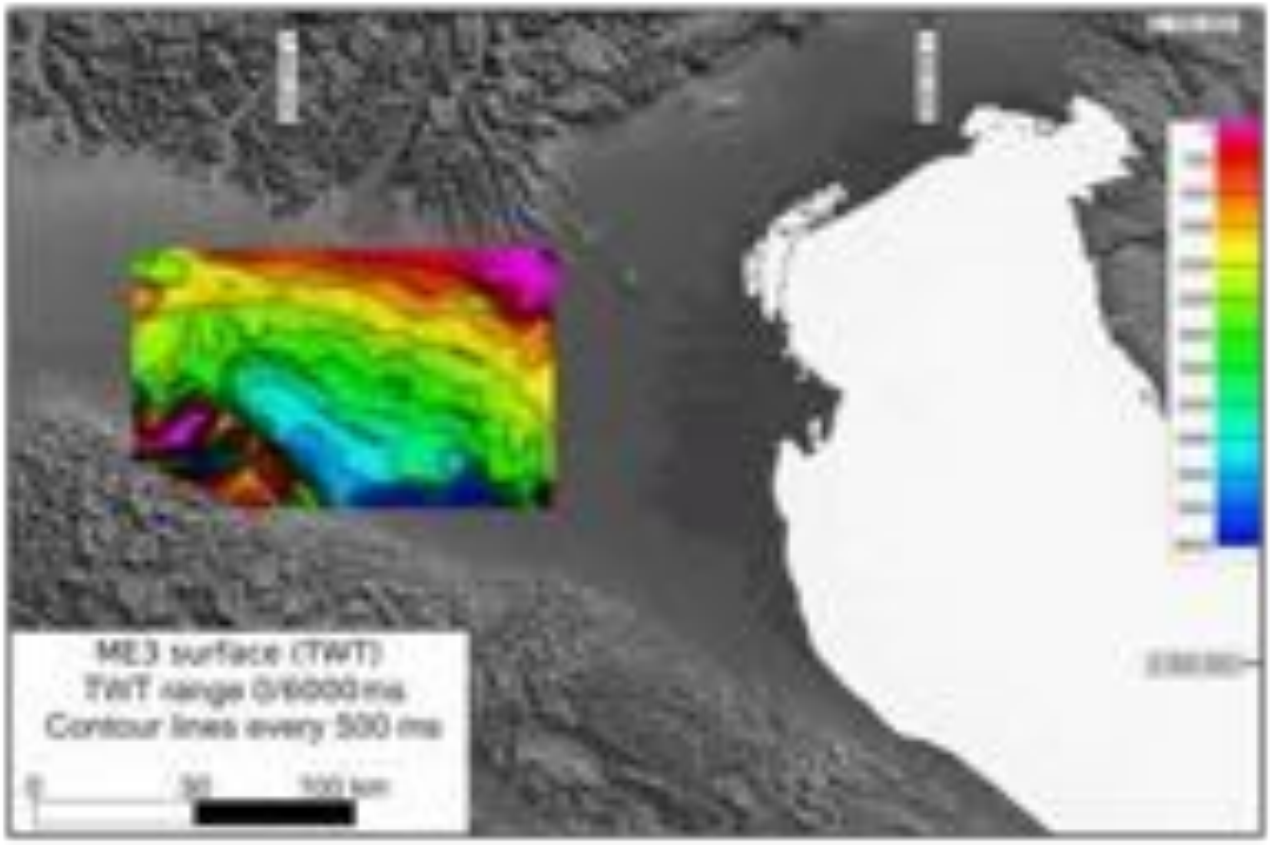

Figure 34. Map view of the 3D Intra-Messinian unconformity (ME3) in time domain, interpolated after seismic interpretation.

In fig. 35, the base Pliocene (PL1) surface is reported. This unconformity corresponds to the regional Zanclean marine ingression, following the end of the Messinian Salinity Crisis in the whole Mediterranean basin. The most of the Apennine deformation has already involved the relieves to the southern margin of the basin, near the boundary of the study area.

A foreland ramp is located to the north, i.e. southern Alps margin, the present-day Veneto region and

northern Adriatic Sea; these areas remained almost completely undeformed during the successive tectonic events. The deformation, in fact, acted only into the central sector of the study area, stacked to the north by the Trento Plateau.

In fig. 36, the PL2 Intra-Zanclean unconformity and base of EP allogroup is shown. During this intense early Pliocene tectonic phase, the PPAF recorded a strong change in basin shape and geometry. To the west, the Piadena thrust-fold deformed the early Pliocene PL1 depocenter. To the SE, the Ferrara most external arc migrated towards NE, fragmenting the foredeep and starting forming a deep basin, at that time still connected with the foredeep axis. The foreland ramp and foreland is similar to the previous scenario because the PL2 sequence ends on the PL1 top sequence in onlap or is preserved with minor thickness.

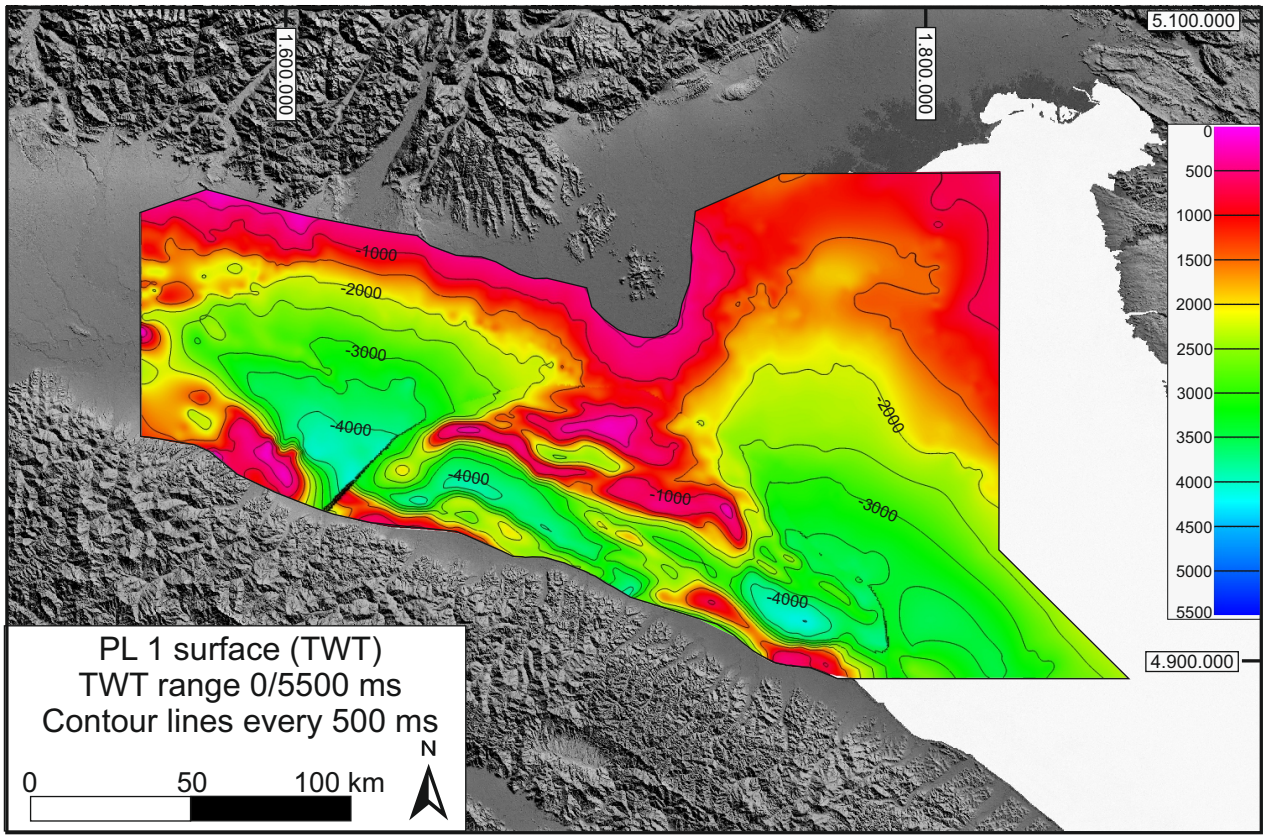

Figure 35. Map view of the 3D base Pliocene (PL1 unc.) in time domain, interpolated after seismic interpretation.

In fig. 37 is mapped the Intra-Piacentian (PL3) unconformity and its shape, testifies the ongoing NE Apennine migration and depocenters deepening. Due to the PL2 and PL3 tectonic phases, it is evident the almost complete separation between the western depocenter (south the Garda Lake) and the eastern Adriatic one.

In fig. 38, the base Gelasian (PL4) unconformity and base of the LP allogroup is shown. It marked the return to a simple foredeep after the fragmentation of the foredeep axis due to the evolution and uplift of the Bologna-Ferrara arcs and the progressive infill of the isolated piggy-back basins.

In fig. 39 the early Calabrian PS1 unconformity is represented. This surface is also labelled as *Qm1* in Maesano and D'Ambrogi (2015). This horizon is particularly important to date the tectonic activity into the western depocenter because it does not show a displacement due to Piadena fault propagation. The contouring is every 250 ms to appreciate the irregularities, even if the surface appears smoothed respect the deeper ones.

The map in fig. 40 describes the PS2 late Pleistocene horizon, named also "*R* or *Red* Unconformity" (Regione Emilia-Romagna and ENI-Agip, 1998; Muttoni et al., 2003; Garzanti et al., 2011) or *Qc1* in Maesano and D'Ambrogi (2015). This is the upper and youngest 3D surface reconstructed. As for the PS1 horizon, the contouring is every 250 ms.

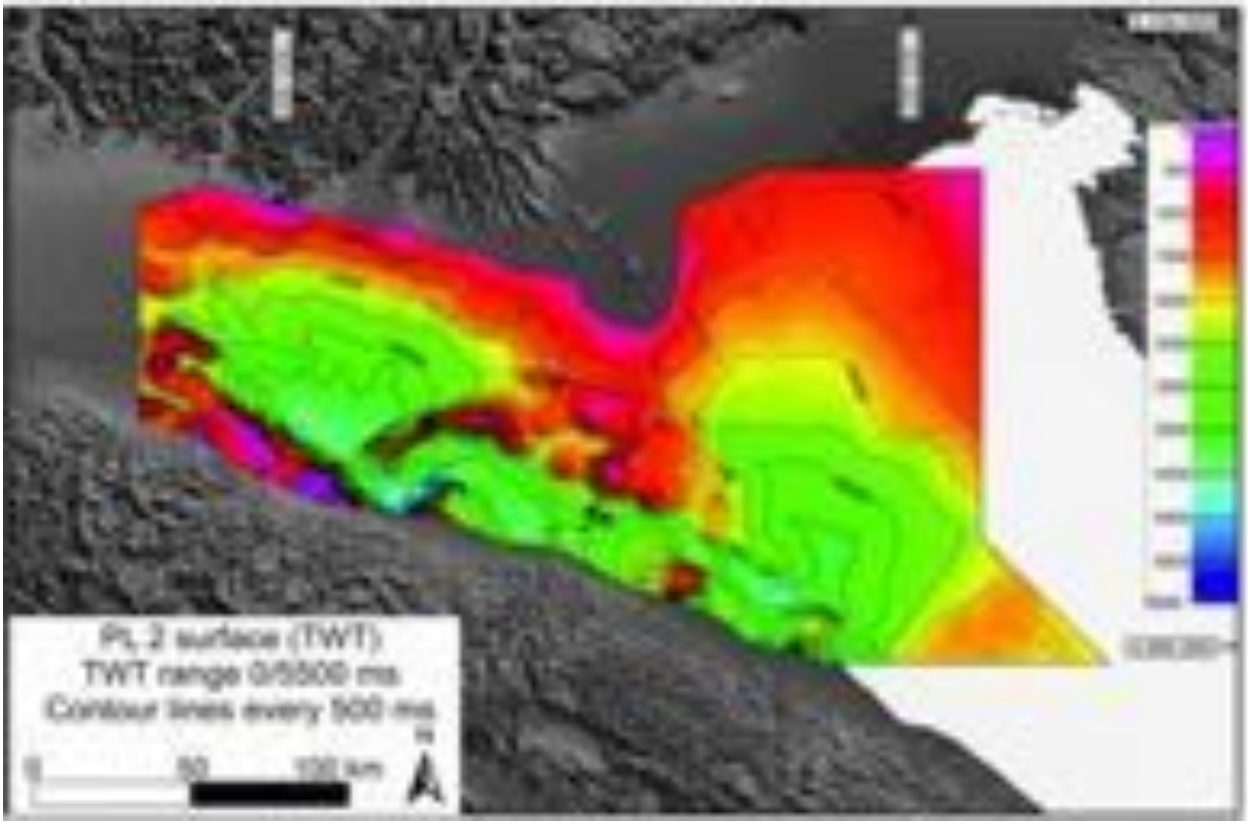

Figure 36. Map view of the 3D Intra-Zanclean surface (PL2 unc.), base of EP allogroup, in time domain, interpolated after seismic interpretation.

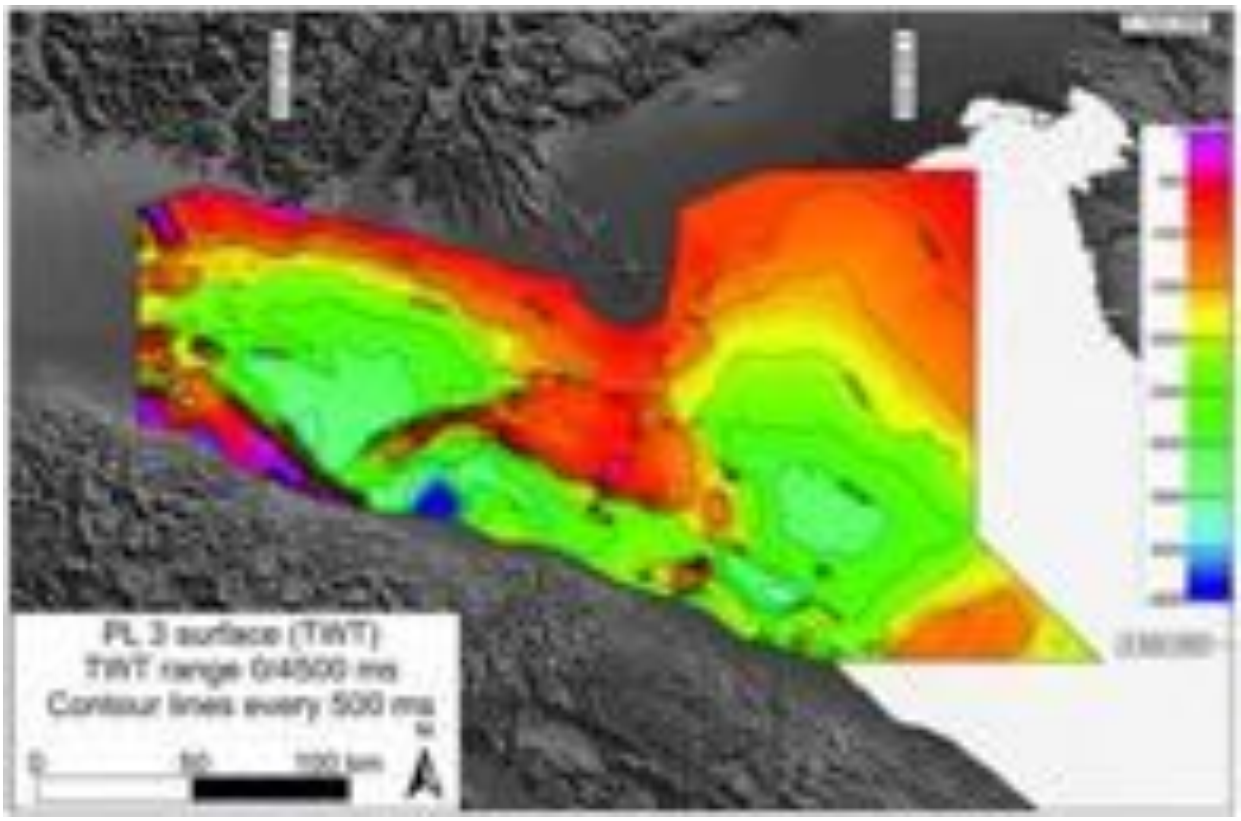

Figure 37. Map view of the 3D Piacentian surface (PL3 unc.), in time domain, interpolated after seismic interpretation.

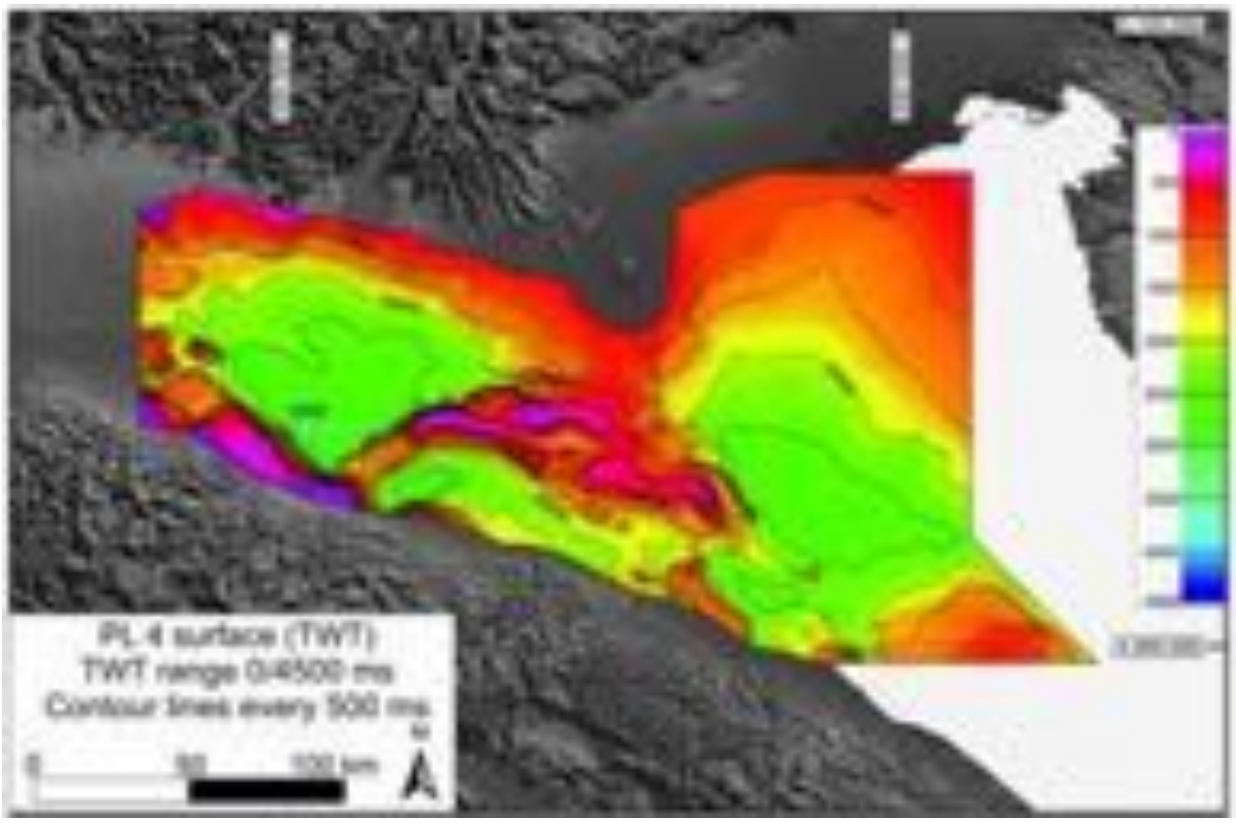

Figure 38. Map view of the 3D base Gelasian surface (PL4 unc. and base of LP allogroup), in time domain, interpolated after seismic interpretation.

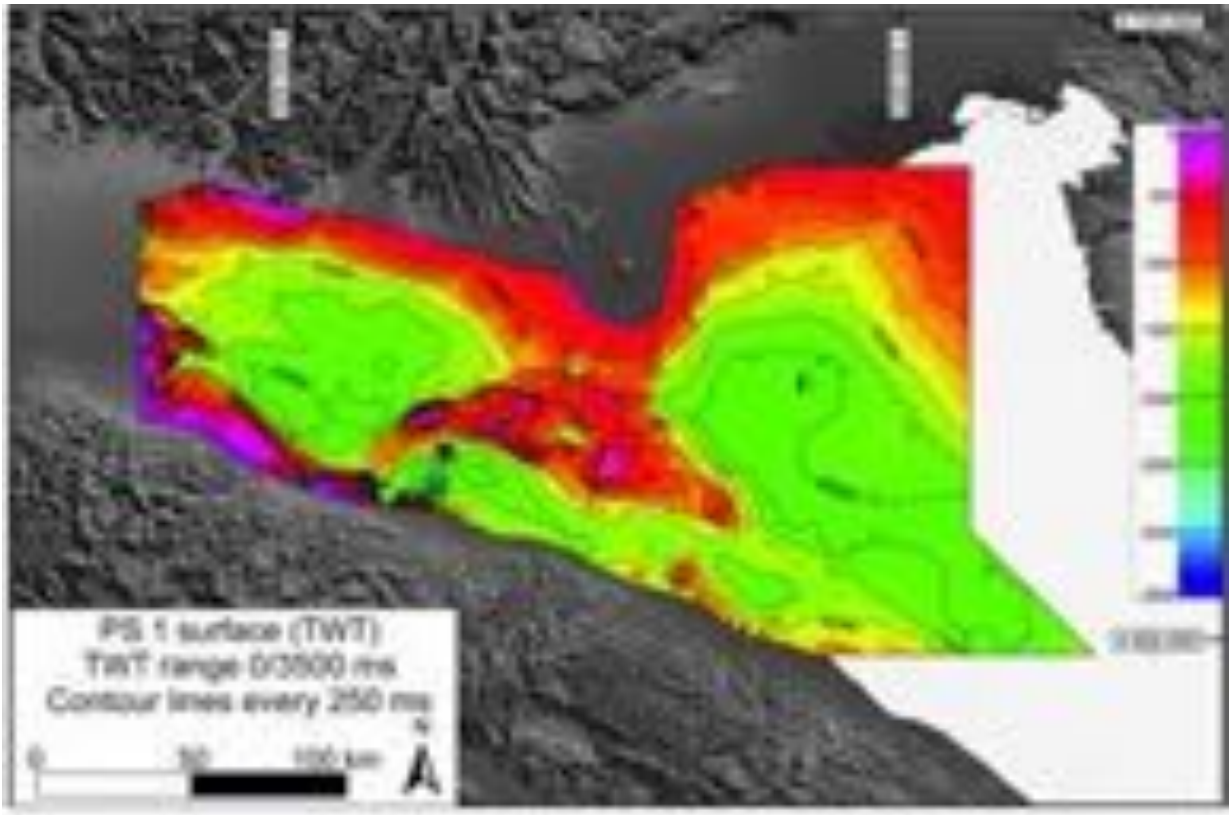

Figure 39. Map view of the 3D Calabrian surface (PS1), in time domain, interpolated after seismic interpretation.

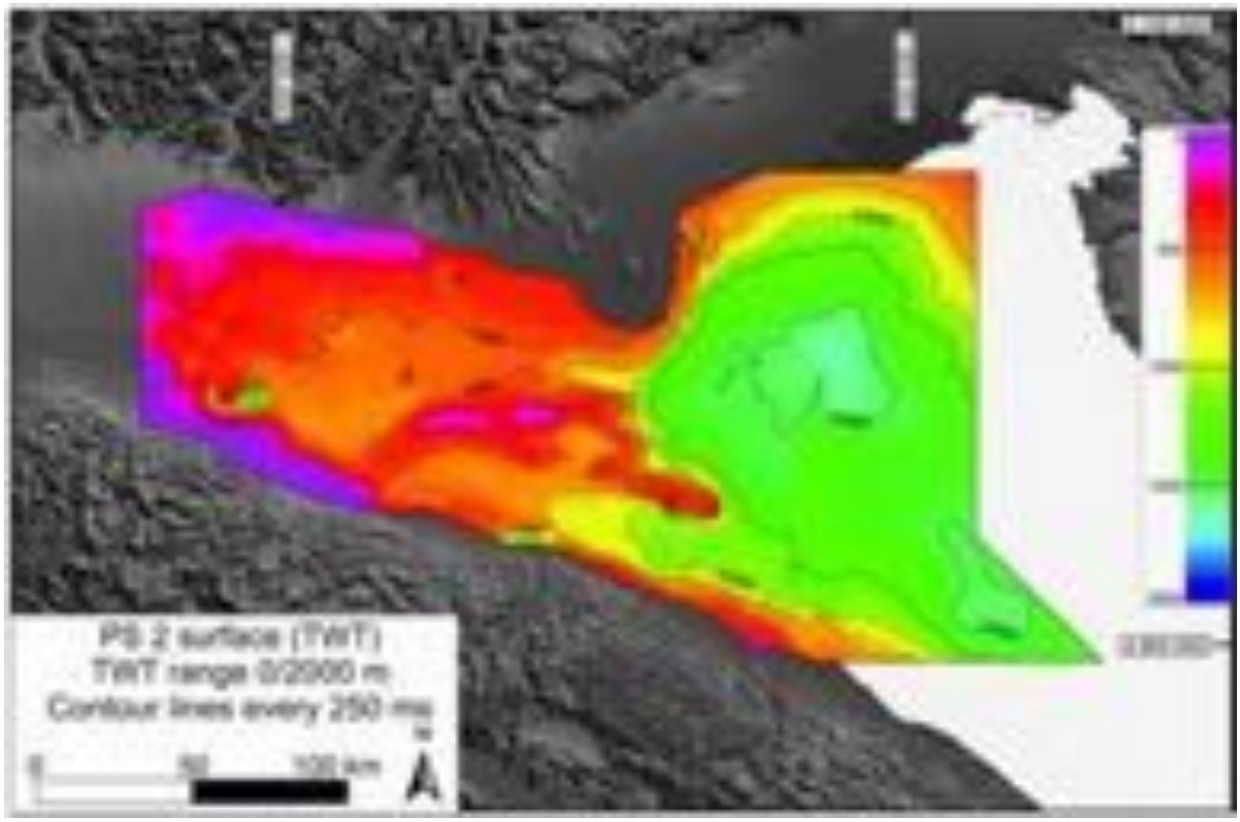

Figure 40. Map view of the 3D late Pleistocene surface (PS2 unc.), in time domain, interpolated after seismic interpretation.

3.5.2. Isobath-maps

In the following, the isobaths maps of the key-horizons with a basin scale extension and good lateral continuity, depth-converted by means of VEL-IO 3D tool by Maesano and D'Ambrogi (2017) are presented. These surfaces are all in the Plio-Pleistocene sedimentary volume: PL1, PL2, PL3, PL4, PS1 and PS2 (Figs. 41-46). Each of them will be briefly described, highlighting the most important/evident geometrical features, e.g. morphologic peculiarities. All horizons are characterized by onlap geometries on the marginal foreland sectors of the basin, i.e. Venetian foreland and Mantova Monocline (MM) and by correlative conformities in the deep portion, e.g. foredeep basin.

These maps define the overall architecture of the Pliocene-Pleistocene filling of the western Po Plain-Northern Adriatic region; they are released within contour lines and geographic references to be "user-friendly", in order to share them with the scientific community (both academy and industry). Colour scale range has been set differently for the maps for two main reasons, i) because maximum and minimum elevation values change significantly and ii) to appreciate small variations of the Pleistocene shallower horizons (i.e. PS1 and PS2) with smoothed morphologies than the Pliocene surfaces.

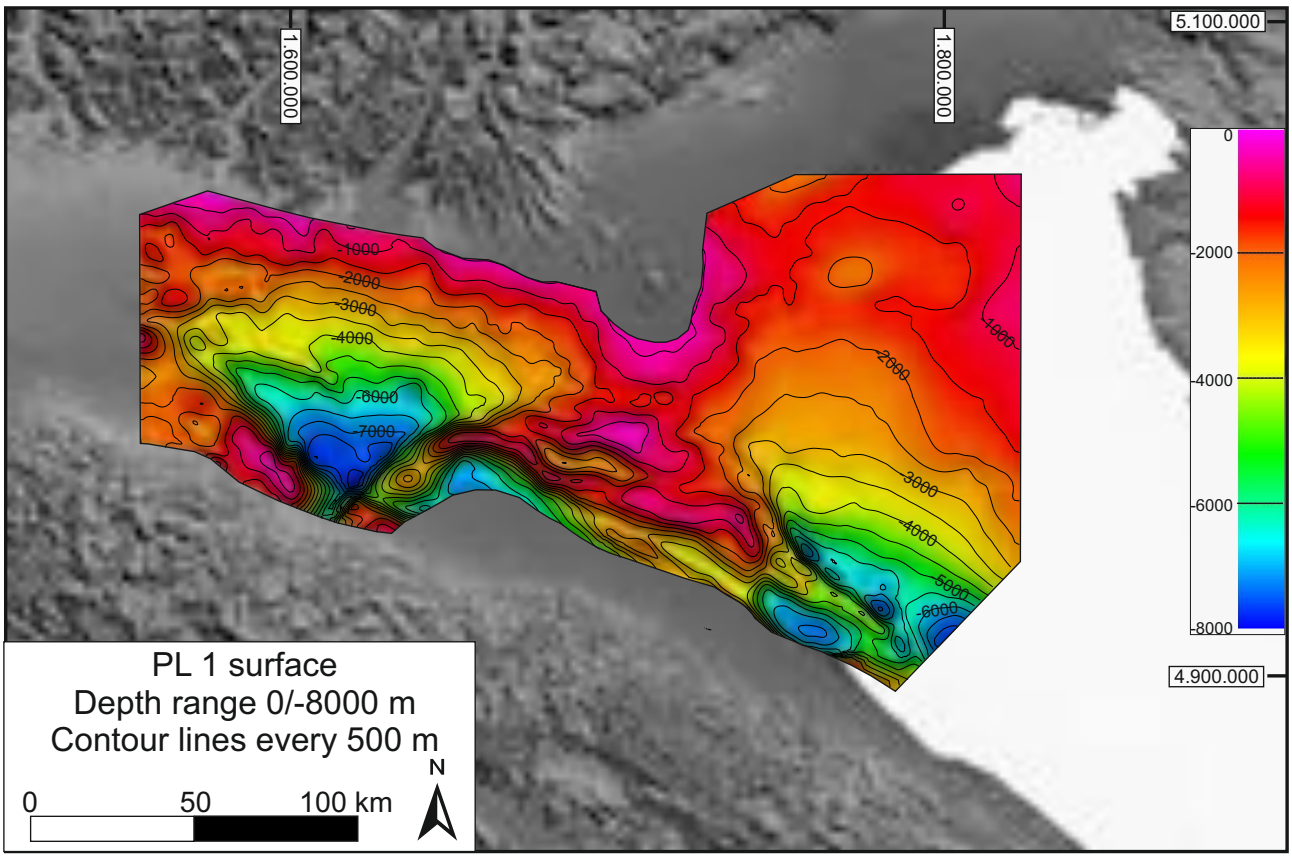

Figure 41. Isobath map of the base Pliocene unconformity (PL1). Black lines: contouring every 500 m.

The deepest subsurface is the base of the Pliocene (PL1 unc.) (Fig. 41); it is also the most deformed horizon. The base Pliocene can record different ages: the *Sphaeroidinellopsis* spp. acme interval is not present everywhere because of the increase hiatus along the onlap surface going towards basin margin, due to the Zanclean marine transgression.

This buried topography locally reaches the maximum depth of ca. 7 km (dark blue shades) in the junction between Emilia and Ferrara folds, the Ferrara syncline and Rimini offshore to the east.

Shallow articulated morphologies (0-2 km) correspond to the Ferrara arcs, northern foreland ramp and Trento Plateau. The north-eastern foredeep margin, Garda ramp and Mantova Monocline (MM), shows steep and irregular slopes (close contour lines) with incisions. The eastern foreland ramp (Venetian and the northern Adriatic Sea) is wider, gently S-dipping but with erosive features similar to the western incisions. The Trento Plateau (Mt. Lessini area) is a rigid carbonate substratum, neither involved into the southern Alpine nor in northern Apennine thrust and fold belt propagation.

In fig. 42, the Intra-Zanclean (PL2) surface, base of the EP allogroup is reported; it is dated between 3.94 and 4.13 Ma, because recognised in the upper MPl3 planktonic foraminifer biozone and into the MNN14-15 nannofossil biozone (*Reticulofenestra pseudoumbilicus*) (Eni's internal report).

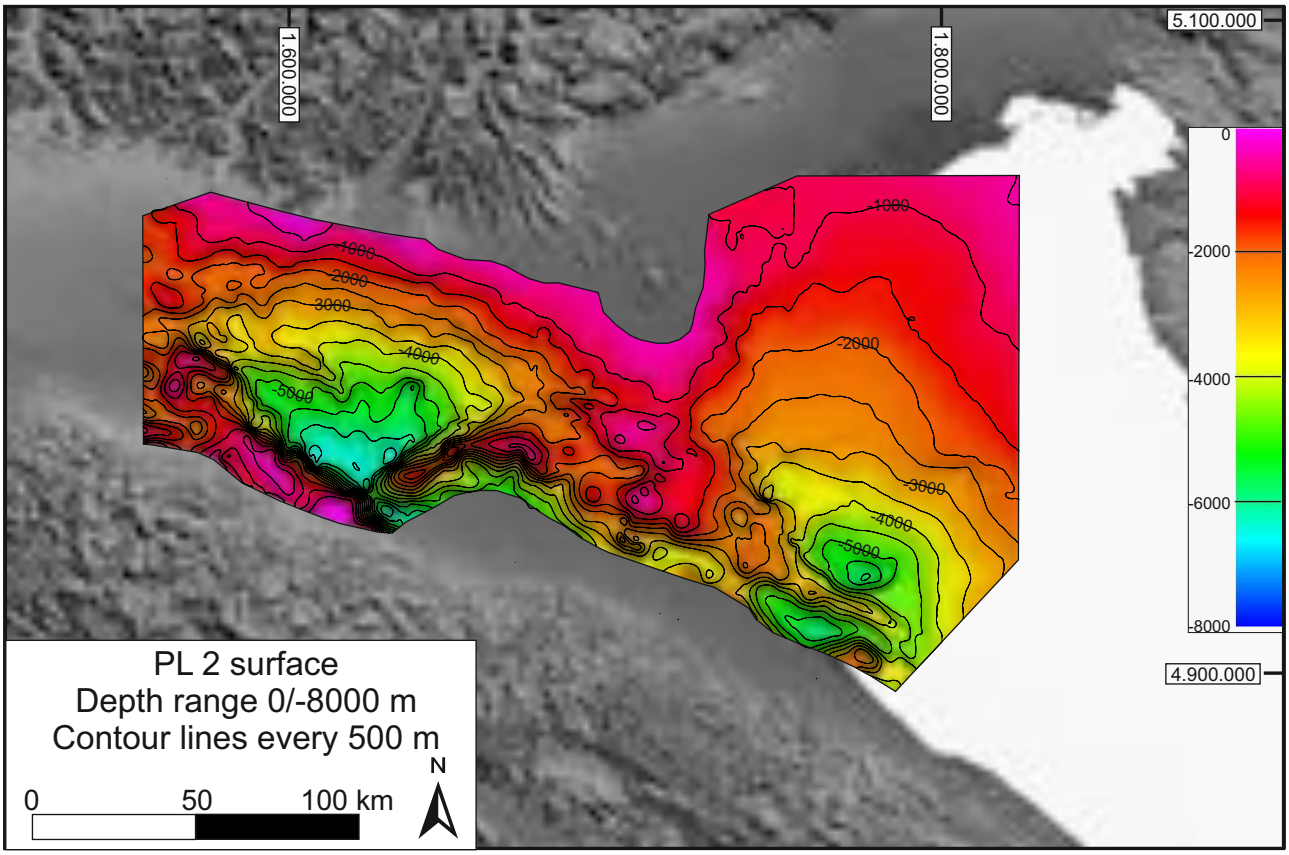

Figure 42. Isobath map of the Intra-Zanclean unconformity (PL2), base of EP allogroup. Black lines: contouring every 500 m.

Due to the progressive tectonic deformation and basin infill (the corresponding tectonic phase is one of the most intense), the depocenters are about 1-1.5 km shallower respect to the PL1 unc. The horizon maximum depth is 6-6.5 km. On the foreland and foreland ramp areas (MM, Trento Plateau and Venetian-northern Adriatic basin) the Intra-Zanclean-lower Piacentian deposits (sediments between PL2 and PL3 unconformities) onlapped directly the base Pliocene surface.

In fig. 43, the Intra-Piacentian (PL3) unconformity, dated 3.3 Ma (note: the colour scale range is different from the previous ones) is visible the foredeep progressive fragmentation, with two depocenters (eastern onshore and western in the Adriatic sector) and a deep piggy-back in the Ferrara subsurface.

The piggy-back is still partially connected with the depocenters by NW-SE oriented channels; the western is located in the subsurface corresponding to the actual Reggio Emilia town and the eastern near the town of Ravenna.

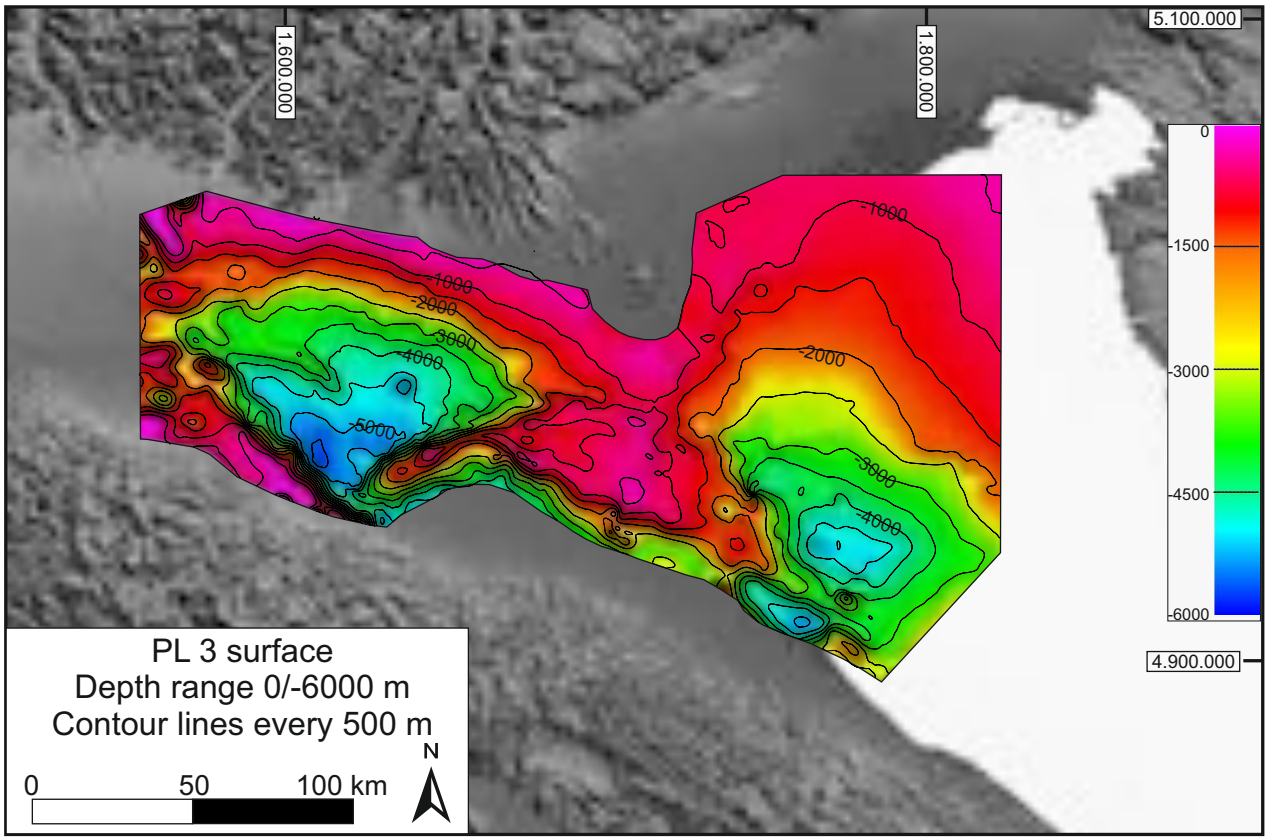

Figure 43. Isobath map of the Intra-Piacentian unconformity (PL3). Black lines: contouring every 500 m.

The base Gelasian (PL4) unconformity (Fig. 44), base of the LP allogroup, is dated at 2.4 Ma by means of biostratigraphy (lower MPl5c) (Ghielmi et al., 2010, 2013 and Eni's internal report) and corresponds to the last strong tectonic phase responsible for the complete isolation of the Ferrara thrust-top basin. The extended reddish colours (in the range of 0-1.5 km depth) highlight the complex thrust and fold Apennines' architecture and the shallower foreland areas. Maximum depths, in the range of 3-5 km, still correspond to the western onshore and eastern offshore depocenters observed

in the previous maps. The distance between contour lines is larger respect to the PL3, meaning a smoother and more regular geometry, due to the sedimentary infill.

The base Calabrian PS1 horizon (1.8-1.5 Ma) (Fig. 45) is related mainly to marine (Carola Fm.) to a transitional environment (Ravenna Fm. of the Pleistocene Prograding Complex). The tectonic activity is greatly reduced as evidenced by the decreasing morphological complexity of the Piadena anticline in the central part of the western depocenter, highly prominent during the Pliocene (note the colour scale range is 0-3 km). At the base Calabrian, the western depocenter does not record yet a continental shelf; the delta front prograding from W to E is still confines into the recent Piemonte region. Marine conditions persisted in the eastern sector. Aggradation and progradation of deltaic sediments of middle-late Pleistocene Prograding Complex upon this unconformity produced the later infill of the eastern part of the basin.

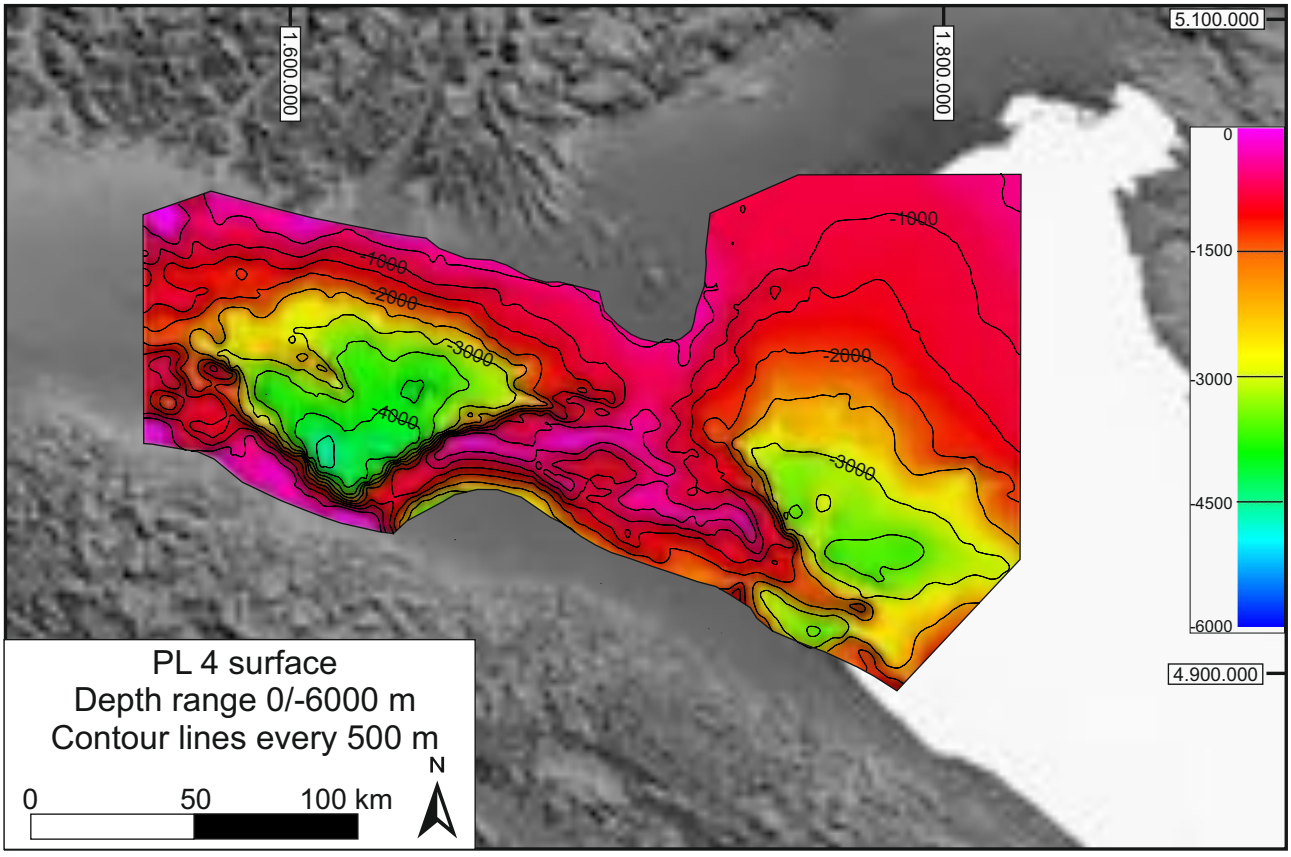

Figure 44. Isobath map of the base Gelasian unconformity (PL4), base of LP allogroup. Black lines: contouring every 500 m.

The infill of the western and central Po Plain can be considered complete, at the time of unconformity PS2 (0.87 Ma) (Fig. 46). The PS2 horizon (Ghielmi et al., 2010, 2013) coincides with the R surface traced in the Lombardia region (REGIONE LOMBARDIA & ENI, 2002; Muttoni et al., 2003) and Qc1 unconformity (Maesano and D'Ambrogi, 2015). This unconformity marks the transition from marine to continental sedimentation in a wide sector of the Po Basin, nearly corresponding to the present onshore sector (Muttoni et al., 2003; Ghielmi et al., 2010, 2013).

In this interpretation, at the time of the unconformity formation, the studied sector should have represented a continental shelf passing eastwards from continental area to coastal and marine facies in the Adriatic region, as confirmed by the paleo-coastline reconstruction of Ghielmi et al. (2010), Garzanti et al. (2011) and Scardia et al. (2012) (around 1 km depth). This upper key-horizon is characterised by low topographic gradients, generally controlled by the paleodrainage. In seismics, the corresponding reflector is a top-lap surface representing the transition to shallow marine and continental deposits (Muttoni et al., 2003).

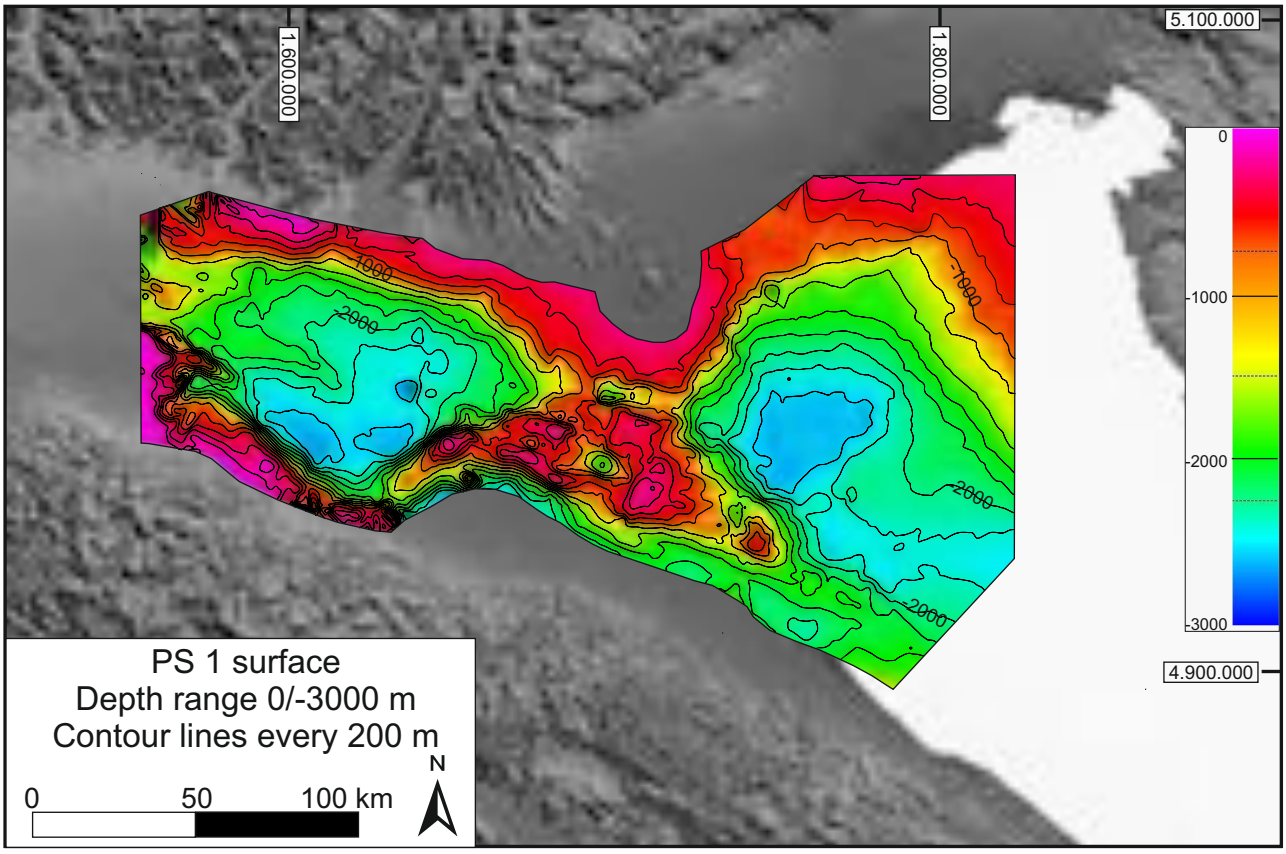

Figure 45. Isobath map of the base Calabrian unconformity (PS1). Black lines: contouring every 200 m.

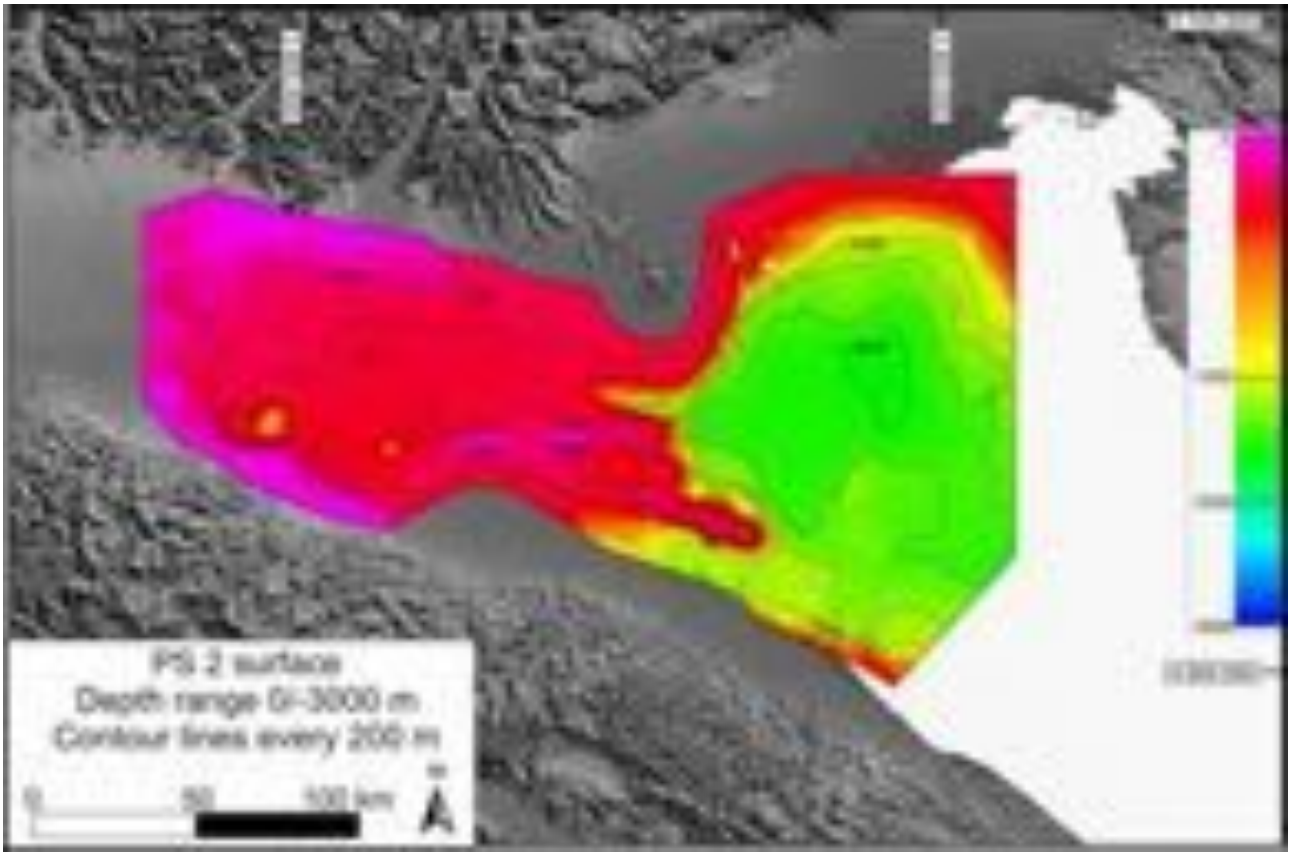

Figure 46. Isobath map of the late Pleistocene unconformity (PS2). Black lines: contouring every 200 m.

3.5.3. Isopach-maps

Following the morphological description of each depth-converted horizon, the actual not decompacted thickness of the sediment sequences are here represented through six isopach maps (Figs. 47 A-F). Each map is displayed with 1kmx1km cell grid and contours are every 300 meters.
These maps show, in a quantitative way, the depocenters migration through time in response to tectonic activity, climate change and subsequent change in sedimentary supply.
Each map describes the sediment thickness bounded by two mapped unconformities (i.e. sequences). The PL1 sequence (Fig. 47 A), for instance, is bounded at the base by the basal Zanclean PL1 unconformity and at the top by the Intra-Zanclean PL2 unc. (base of EP allogroup). This volume contains all formations (i.e. Canopo Fm., Santerno Fm.) deposited in that time span, confined by two horizons. The upper and most recent PS2 unit, includes sediments deposited from 0.87 Ma to recent. The unit is limited at the base by the PS2 unc. (or R Surface, Muttoni et al., 2003) and at the top by the present-day topography.
The color scale range is equal for all maps, in order to easy compare the areal distribution and magnitude variation of the thickness through time.
Fig. 47 A, B and C show three steps of the Po Plain-Northern Adriatic basin during the entire Pliocene epoch. Between 5.33-2.4 Ma, highest values remain in the narrow and elongated foredeep sector, parallel to the northern Apennine orogen. The maximum thickness (ca. 2 km) is recorded in the PL1 sequence, in the foredeep area; remarkable values in the range of 300-600 m are also present in the north-eastern sector, the Venetian-northern Adriatic basin. In this area in fact, between 5.33-4 Ma developed a S-prograding delta complex (Eraclea Fm.) fed from the eastern Alps.
The Pleistocene step-wise scenario starts with the Base Gelasian sequence (Fig. 47 D), genetically related to the last and strong Apennine migration phase that caused the complete separation of the elongated foredeep in two deep depocenters; the western basin with ca. 2 km thick sediments and the eastern one with ca. 1km of sediment thickness. In figs. 47 D, E is still well visible the piggy-back evolved behind Ferrara arcs, which was filled completely during the middle-late Pleistocene (upper PS1 sequence), when the Prograding Complex initiates to prograde towards east.
This important change of the basin, from marine to continental, started during the upper PS1 phase and characterized the PS2 sequence, after the Alpine glaciation onset at ca. 0.9 Ma (Muttoni et al., 2003). This last sequence was able to smooth the previously articulated morphologies, filling all the available onshore accommodation space.

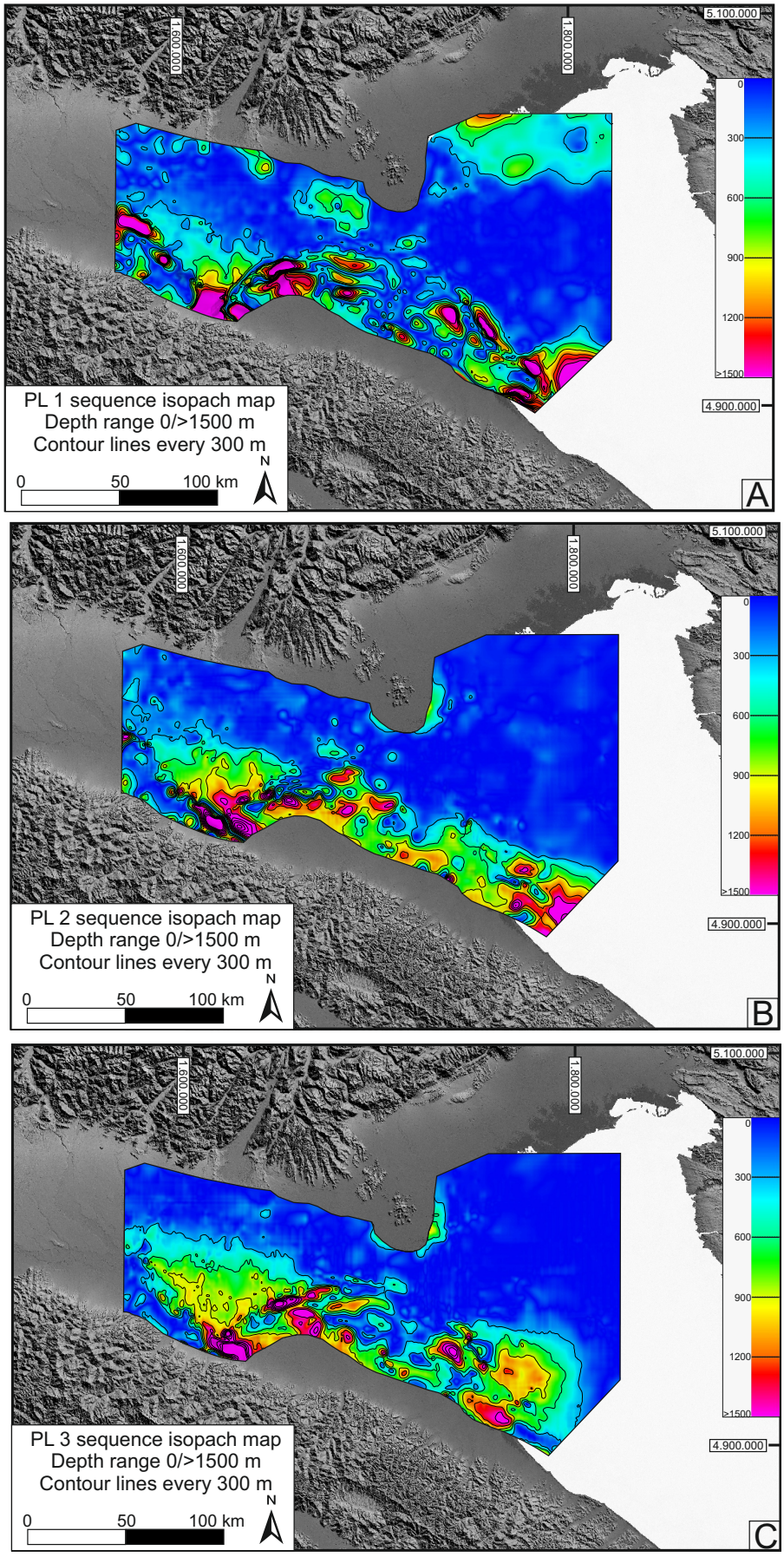

Figure 47. Isopach maps. A) Early Zanclean PL1 sequence (base Zanclean to ca. 4 Ma). B) Intra-Zanclean-Piacentian, PL2 sequence (ca. 4-3.3 Ma). C) Piacentian-Base Gelasian PL3 sequence (3.3-2.4 Ma). Black lines: contour lines every 300 m.

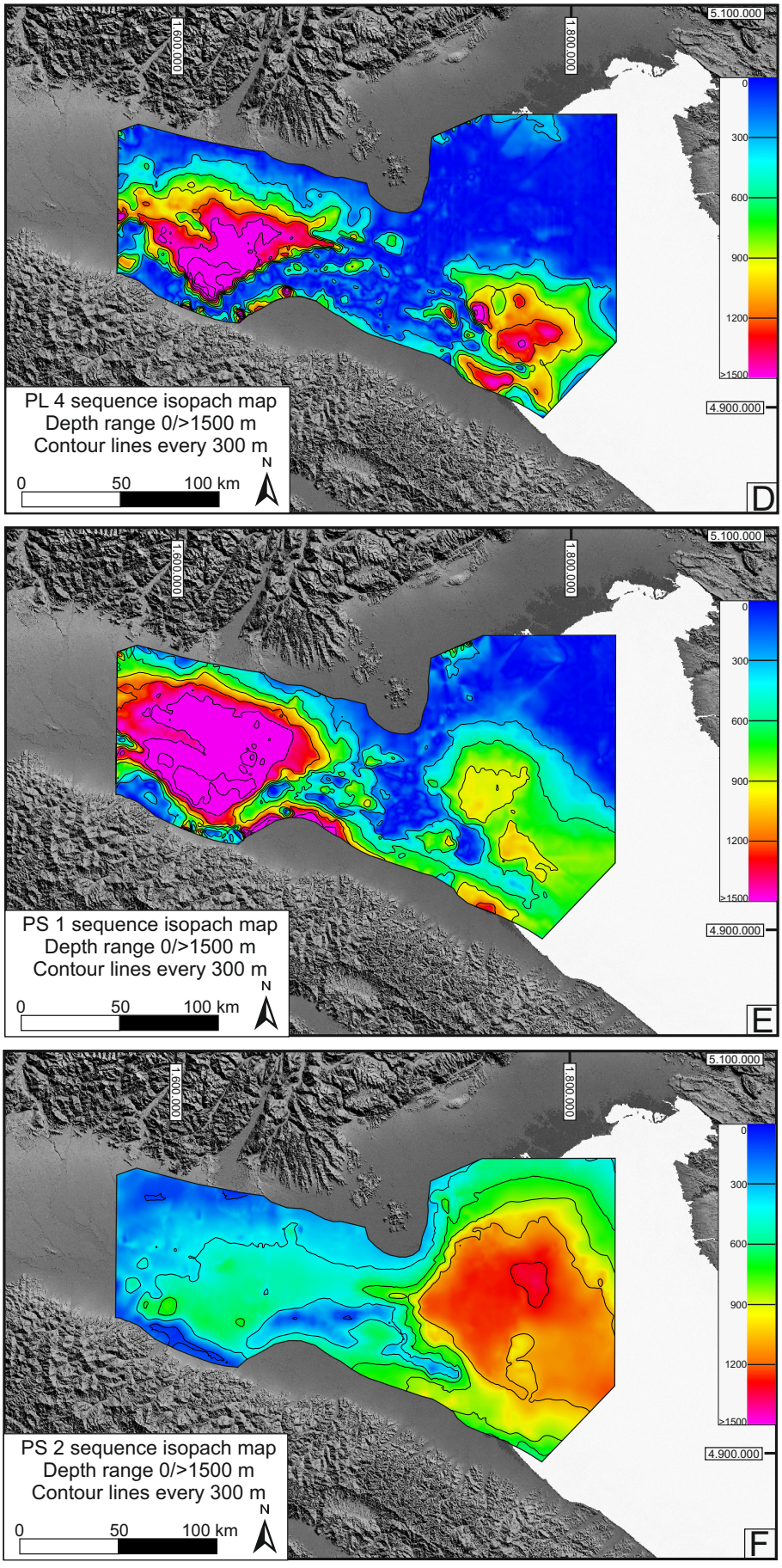

Figure 47. Isopach maps. D) base Gelasian-base Calabrian PL4 sequence (ca. 2.4-ca.1.5 Ma). E) middle-late Pleistocene PS1 sequence (1.5-0.89 Ma). F) late Pleistocene PS2 sequence (0.89 to recent time). Black lines: contour lines every 300 m.

3.6. Discussion

The isobath and isopach maps carried out in the present thesis represent the most detailed basin-scale picture of the Plio-Pleistocene succession of the Po Plain-Northern Adriatic Basin. Therefore, a comparison with the previous literature is possible only limitedly to a few sectors of the analysed basin.

The only surface available in literature and comparable, for areal dimension with the results from this Thesis, is base of Pliocene deposits from Structural Model of Italy (Bigi et al., 1989, 1992) (Fig. 48 A, B), that covers the entire Italian peninsula at 1:2,000,000 and 1:500,000 scale respectively. The base of Pliocene (Bigi et al., 1989, 1992) is equivalent to the interpreted base Pliocene PL1 horizon. On the contrary, in the Structural Model of Italy (Bigi et al., 1992) (Fig. 48 B) there is no reference to the used velocity model. Maesano and D'Ambrogi (2017) found that a homogeneous velocity value of 3000 m/sec allows obtaining the best fit with the base Pliocene surface from Bigi et al. (1992).The applied workflow with Vel-IO 3D tool (Maesano and D'Ambrogi, 2017) proposed in this study for the time-depth conversion and the construction of the final 3D model in depth domain has major impact on the horizons, respecting lateral and vertical velocity variations in order to reflect as much as possible the real morphology, especially in the sectors where no velocity data or well markers are available.

This comparison highlights a very close fit in the northern part of the study area (Southern Alps) and at the top of the Ferrara-Romagna Arc. Some differences, in the order of some hundred meters, are located in the central part of the study area, at the footwall of the Ferrara-Romagna Arc, possibly due to both the difficulties in the correlation of the unconformity and the use of a different time-depth conversion. However, moving to the south of the Ferrara-Romagna Arc, in the depocenter between Ferrara and Bologna, the discrepancies increase up to 2000 m. The maximum depth of the base Pliocene by Bigi et al. (1989) is 7 km (Fig. 48 A, C) and 9-9.5 km by Bigi et al. (1992) (Fig. 48 B). The equivalent PL1 interpreted in the present model reaches locally 7.5 km depth (Figs. 41, 49) but a definite calibration is not possible due to the lack of well log data recording the base Pliocene in the depocenters. These differences are related to the different velocity model adopted for the time-depth conversion. Since there is variability between the foreland and the thrust-top basin depocenter, the use of a single velocity value can produce inconsistent geometries on the surface of base of Pliocene and also affects the geometry of the thrust-related anticline. This consideration points out the importance of the use of a 3D optimized velocity model to obtain a 3D geological model consistent for applications that are deeply influenced by the accurate relative position and depth of the horizons and faults, for instance, seismotectonic analysis (Maesano and D'Ambrogi, 2016, 2017).

Before this Thesis, the GeoMol Project (European project run from 2012 to 2015) applied Vel-Io 3D

to the realization of a very high-resolution 3D model (private Eni database), in a small area located in the central Po Plain (Maesano & the Italian GeoMol Team, 2014; GeoMol Project report, 2015; Maesano and D'Ambrogi, 2016).

In fact, some surfaces are common to both models:

i) base Pliocene (PL) (Fig. 49A) and PL1 (Fig. 49B);

ii) Gelasian surface (GEL) (Fig. 50A) and PL4 (Fig. 50B);

iii) marine Quaternary (Qm1) (Fig. 51A) and PS1 (Fig. 51B);

iv) the uppermost continental Quaternary (Qc1) (Fig. 52A) and PS2 (Fig. 52B).

A good fit exists between the published maps and the corresponding maps worked out in this Thesis, which were based on the same dataset.

The only substantial difference is found in the Base Gelasian surface (Fig. 50 A, B). The surface by GeoMol Report (2015) (GEL, fig. 50 A) shows a very similar morphology but is considerably shallower than the analogue PL4 surface (Fig. 50 B) interpreted in this Thesis. On the basin margin, the vertical offset is ca. 1 km that reach 2 km towards the basin depocenter. This significant discrepancy might be linked to a different initial seismic interpretation of the Base Gelasian key-horizon and not to the velocity model because lower and upper surfaces are in good agreement after depth-conversion.

In this Thesis, the Base Gelasian unconformity has been interpreted in wells within the biozone MPl5c with *Globorotalia* gr. *crassaformis* (Eni internal report) and not into MPl6 biozone with *Globorotalia inflata*. Following these biostratigraphic constrains, it is not possible to agree with the previous interpretation proposed by GeoMol Team (GeoMol Project report, 2015).

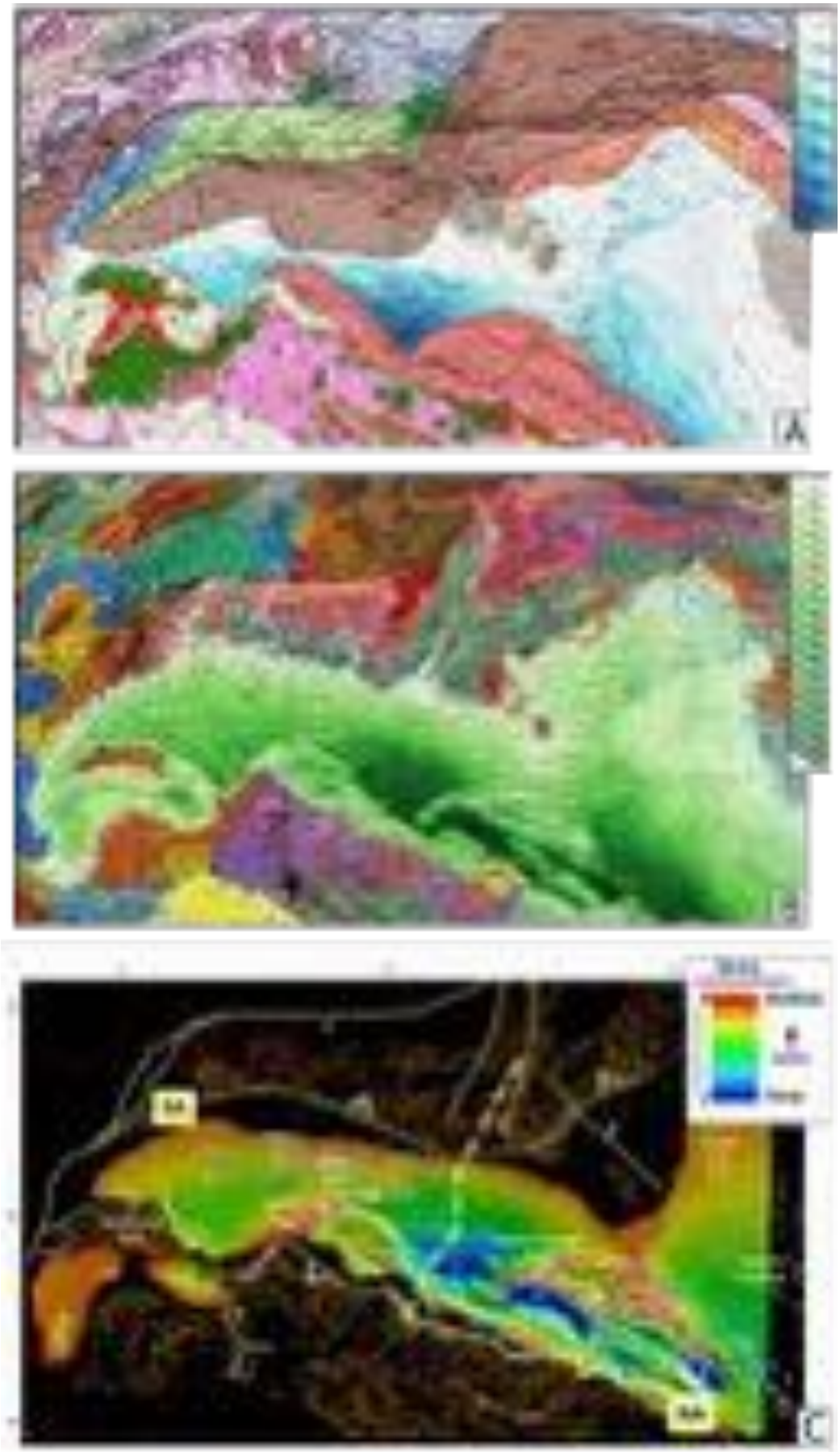

Figure 48. Published base Pliocene regional maps. A) Synthetic Structual-Kinematic Mao of Italy, 1:2,000,000 from Bigi et al. (1989). B) Structural model of Italy and Gravity Map, 1:5,00,00 by Bigi et al. (1992). C) 3D view of the map from Bigi et al., (1989) digitalized by Turrini et al., (2014).

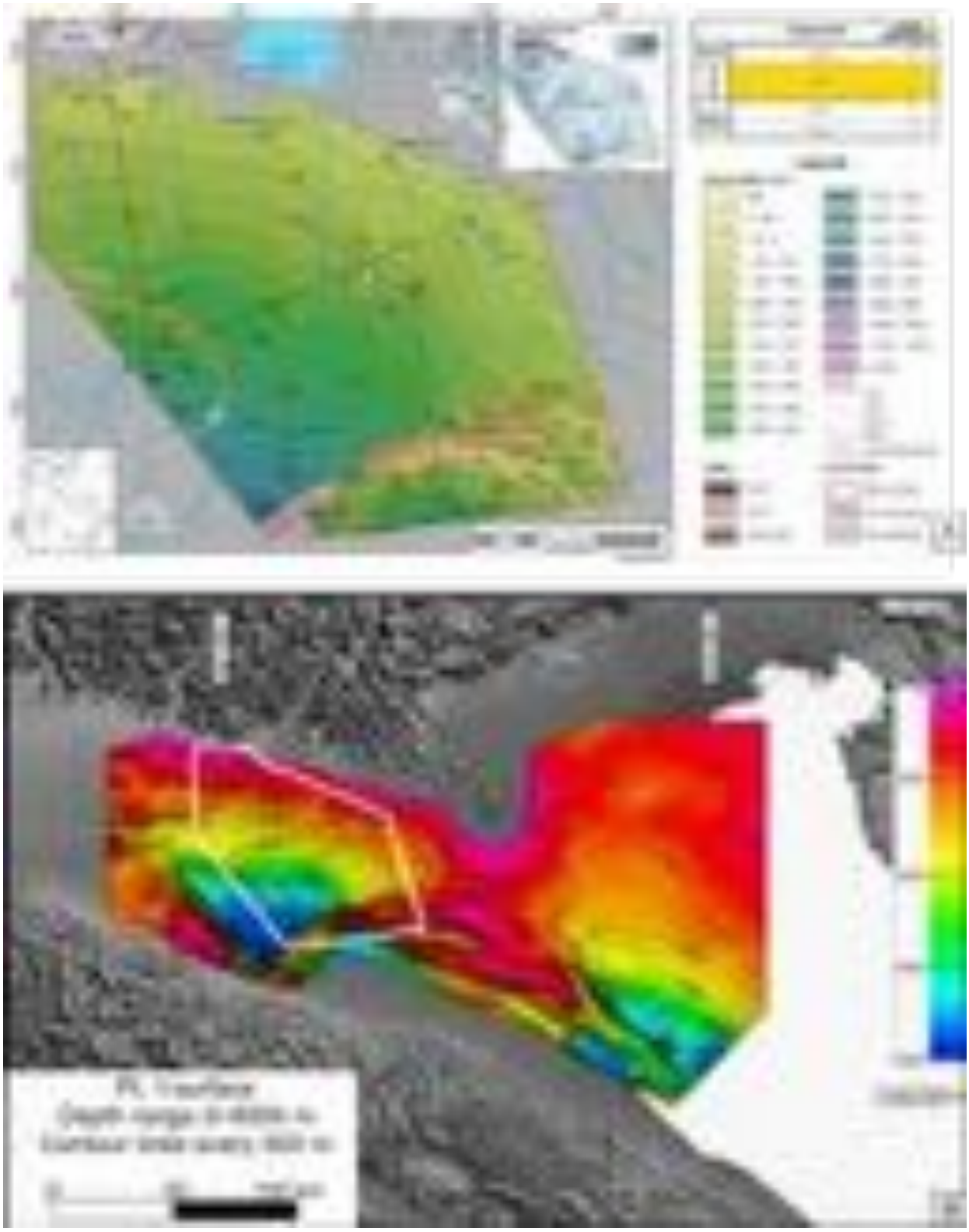

Figure 49. Comparison between the GeoMol 3D modelling of the base Pliocene (A) and the PL1 surface modeled in the present thesis (B). White line in box. B: GeoMol study area.

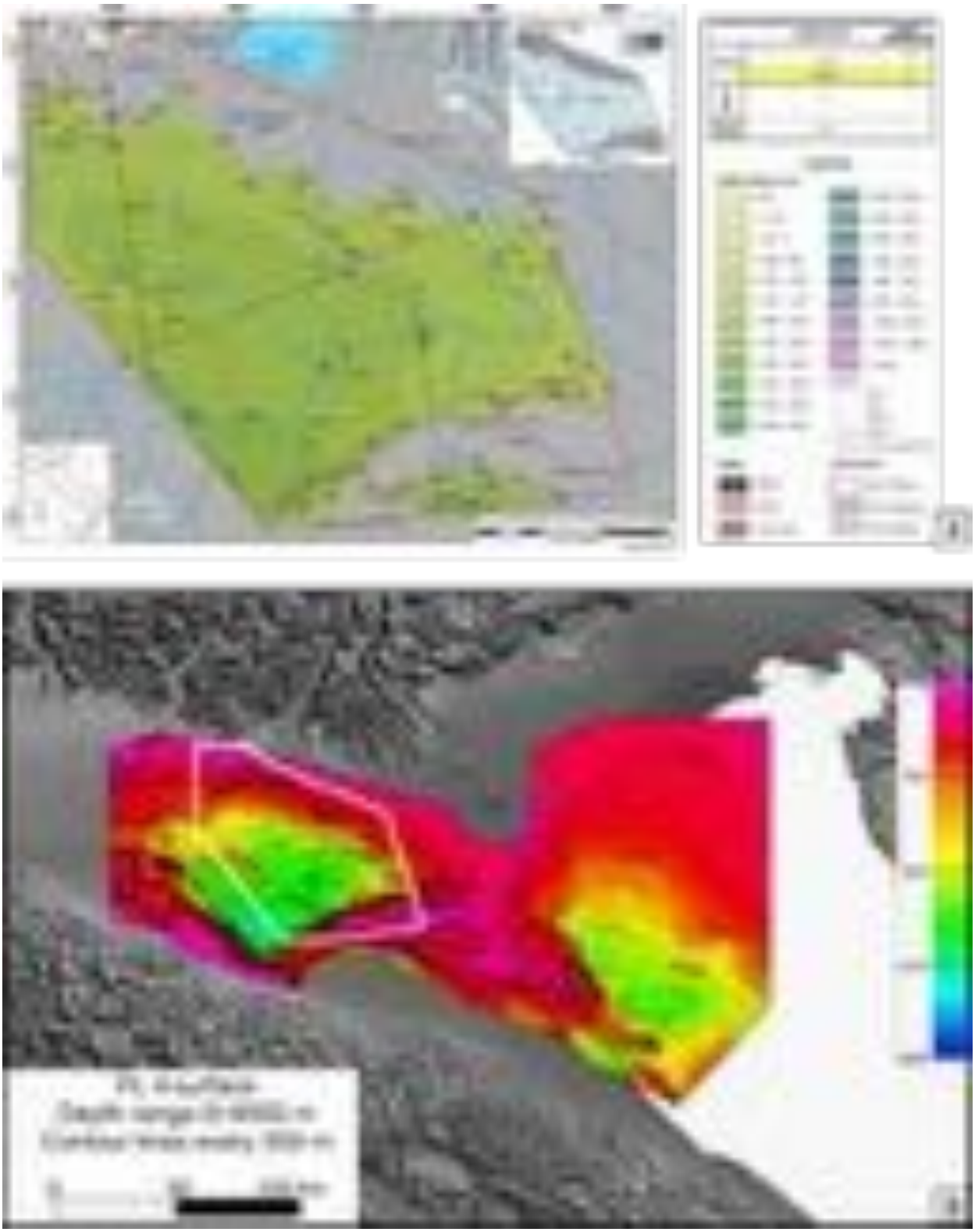

Figure 50. Comparison between the GeoMol 3D modelling of the Gelasian unconformity (A) and the PL4 surface modelled in the present thesis (B). White line in box B: GeoMol study area.

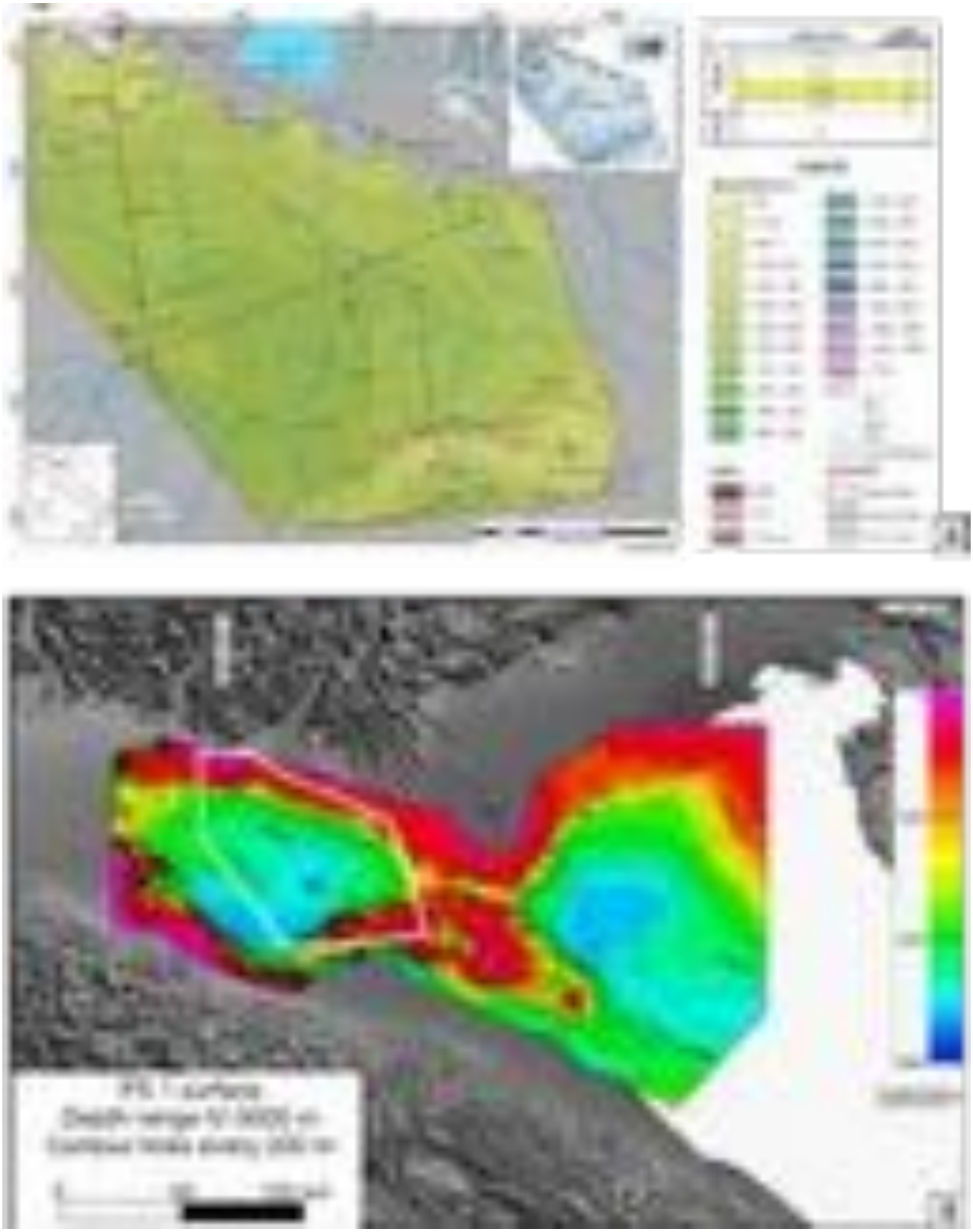

Figure 51. Comparison between the GeoMol 3D modeling of the base Calabrian (A) and the PS1 surface modelled in the present thesis (B). White line in box B: GeoMol study area.

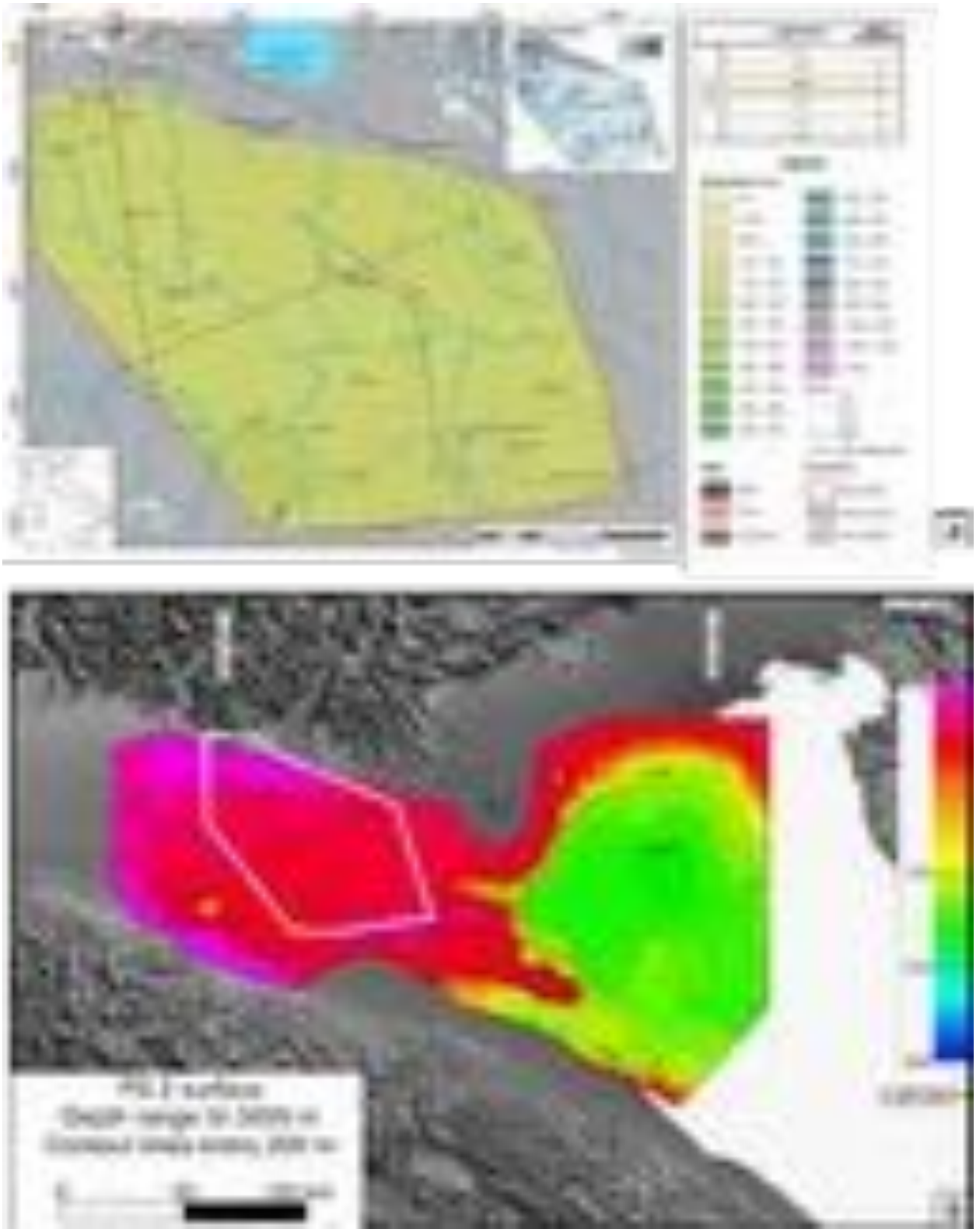

Figure 52. Comparison between the GeoMol 3D modeling of the late Pleistocene QC1 (A) and the PS2 surface modelled in the present thesis (B). White line in box B: GeoMol study area.

3.7. Conclusions

The principal aim of this project was to produce a high-resolution 3D stratigraphic model of the late Messinian-Pleistocene sedimentary infill of the Po Plain-Northern Adriatic basin (PPAF).

The model was worked out by means of seismic interpretation and well log analysis of a homogeneous dataset, entirely provided by Eni Upstream, applied to an uncommonly wide area (ca. 40,000 km^2) which has never been attempted to investigate before.

Through the interpretation of ca. 8,000 km seismic lines and hundreds of wells, seven surfaces have been interpolated and the Plio-Pleistocene horizons depth-converted with a calibrated velocity model, newly developed *ad hoc* with Vel-IO 3D software (Maesano and D'Ambrogi, 2016, 2017).

The results make finally possible to do an important step forward to the complete knowledge of the PPAF subsurface. Several potential applications in geoscience can be summarized as follows:

i) The isobath maps, every ca. 1 Ma, integrated with published data (Ghielmi et al., 1998, 2010, 2013; Maesano et al., 2015; Rossi et al., 2015) reveal the geological setting and the step-wise evolution of the basin through time. Collectively, all this information might be further used to support applications in basin analysis such as thermal history, geohistory and for exploiting subsurface resources (geothermal, gas storage).

ii) The isopach maps are useful to investigate the depocenters migration due to the Apennine tectonic activity and study the basin deformation.

iii) The calibrated 3D velocity model is also a fundamental input for any seismological studies, in particular for the analysis of ground motion shaking, i.e., relocating seismic events and seismological simulations.

iv) The workflow worked out by Maesano and D'Ambrogi (2016) is based on sequential 3D restoration-and-decompaction and can be easily applied to the present 3D model. The following results will be the calculation of sedimentation and uplift rates of the PPAF, highlighting the interaction between Plio-Pleistocene tectonics and sedimentation.

CHAPTER 4
RESTORED TOPOGRAPHY OF THE PO PLAIN-NORTHERN ADRIATIC REGION DURING THE MESSINIAN BASE-LEVEL DROP

4.1. Abstract

The Messinian Salinity Crisis (hereafter MSC) involved the isolation of the Mediterranean Sea from the Atlantic between 5.97-5.33 Ma. MSC caused a sea level fall whose maximum magnitude and regional distribution remains strongly debated, spanning between about 200 m to more than 1500 m. We present a new paleo-topographic reconstruction of the Po Plain-Northern Adriatic region during the intra-MSC peak desiccation event. It is based on the map of the latest Miocene unconformity traced in the subsurface through seismic and hydrocarbon well data. The map has been restored to its Messinian state by means of a flexural backstripping numerical modeling. The result supports the idea that a maximum water level drop of 800-900 m occurred in the studied region during the MSC. The resulting landscape is consistent with stratigraphic and sedimentologic data, with a modeled shoreline separating areas with marine deposits from subaerially eroded lands, two relatively deep marine depocenters (ca. 700 and 1300 m deep), and steep V-shaped incisions along the Southern Alps margin giving some clues on the MSC imprint on the present day Alpine drainage pattern. These results strongly suggest that during the maximum MSC base-level drop the Mediterranean region was divided in sub-basins with different base-level and water budgets.

4.2. Introduction

The Messinian Salinity Crisis (MSC) is one of the most extreme and debated Cenozoic environmental changes (Rouchy and Caruso, 2006; Roveri et al., 2014; Vai, 2016 and reference therein). Diagnostic evaporitic deposits (Selli, 1960) and erosional unconformities (Lofi et al., 2005, 2011a, b) across the entire Mediterranean enable to date this event between 5.33-5.97 Ma (Krijgsman et al., 1999; Manzi et al., 2013). Several erosional unconformities merge together into a single polygenic surface (usually referred to as the Messinian Erosional Surface - MES *sensu* CIESM, 2008; Lofi et al., 2011) in the upstream of deep and intermediate basins, thereby providing evidence for high erosion in the peripheral basins. Many of the key depositional units and erosional markers of the MSC, however, are buried underneath km-thick seawater and/or sediment columns (Lofi et al., 2011a, b; Urgeles et

al., 2011; Thinon et al., 2016), while other outcrops are strongly deformed by late-Cenozoic tectonics (e.g. Sicily, Butler et al., 1995).

Therefore, the magnitude of the strongest drawdown and the resulting paleogeography of the Mediterranean area during the MSC acme is still strongly debated (e.g. Blanc, 2006; Meijer and Krijgsman 2005; Jolivet et al., 2006; Clauzon et al., 2007; Garcia-Castellanos et al., 2009; Lofi et al., 2011a, b; Bache et al., 2012; Sternai et al., 2017).

In this paper, we analyse public and private (courtesy of Eni Upstream) subsurface data (Fig. 53 A) to carry out a 3D reconstruction of the subaerial and submarine landscape of the Po Plain-Northern Adriatic area of the Mediterranean during the maximum MSC sea-level drop, i.e. during the stage 2 of the crisis according to the scheme reported by Roveri et al. (2016, and references therein). Even if the isostatic response of the lithosphere to the MSC-related sea-level drop has been the subject of several studies (e.g. Ryan, 1976; Meijer and Grijgsman, 2005; Govers et al., 2009), previous works mainly focus on the Mediterranean-scale deformation rather than on the sub-basin-scale, moreover, the value of sea-level drop is crucial to these kinds of reconstructions. Here we rely on geological constraints from additional subsurface data relative to the Po Plain-Northern Adriatic basin during the MSC to produce new estimates tailored for the study area.

The restored paleotopography worked out through this modeling provides a completely new scenario that improves our understanding of the broader Mediterranean paleogeography during the MSC, giving also information about the role of this extreme environmental event in shaping the present-day river drainage pattern of the Po Plain region.

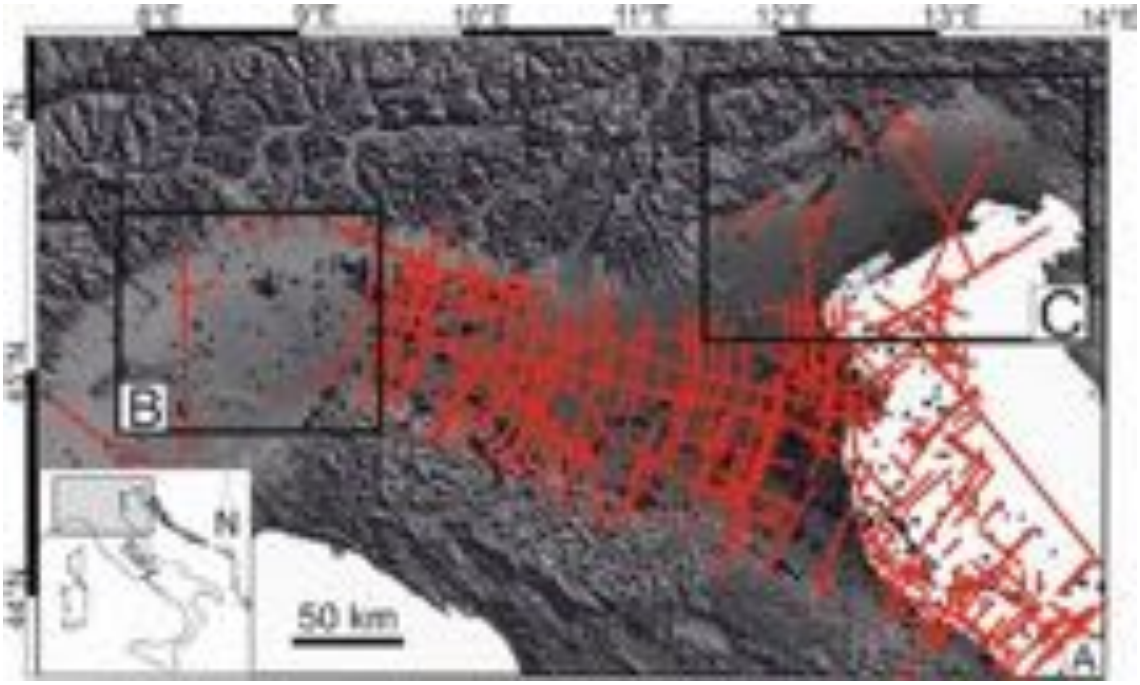

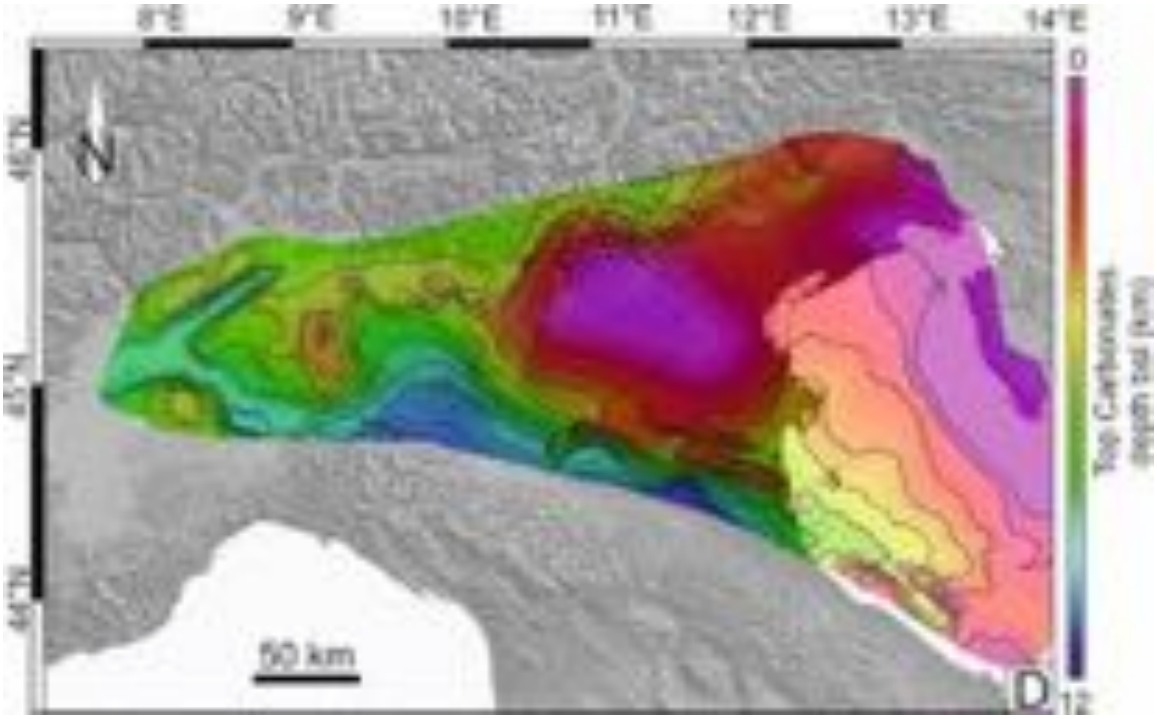

Figure 53. A) Study area and complete dataset. Red lines correspond to the Eni Upstream seismic grid, while black dots are wells and black lines correspond to the seismic profiles by public dataset. B) and C) represent the areas where the dataset has been integrated with observations from the literature. D) top Mesozoic carbonate surface modified from Turrini et al. (2014, 2016). Black lines are contour lines every 1 km.

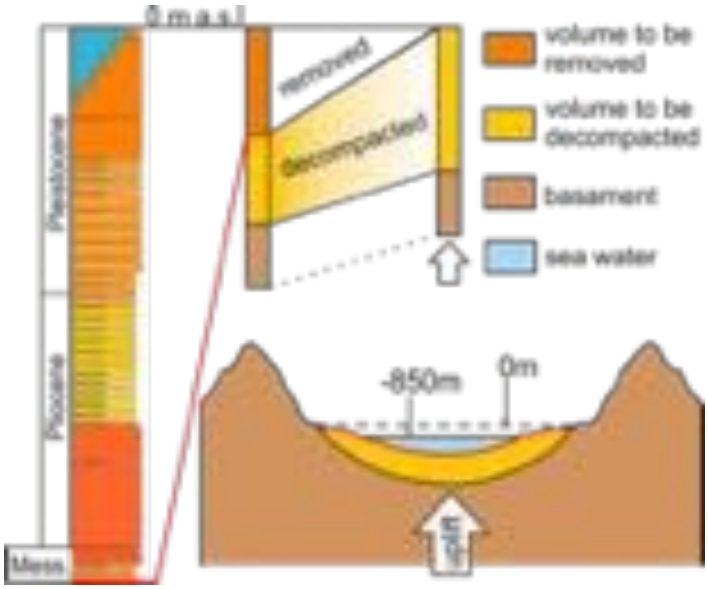

Figure 54. 1D and 2D conceptual model of the backstripping procedure. The volume to be decompacted is represented by the top Cretaceous-late Messinian sediments. The basement is the top of Mesozoic carbonate formations (Fig. 53D).

4.3. Geological setting and previous works

Tectonic shortening affected the Po Plain-Northern Adriatic region at different times and with variable directions during the Cenozoic. The middle-late Miocene to Pleistocene convergence in the Northern Apennines, in particular, resulted in the formation of the Western Po Plain Foredeep (WPPF) and the Po Plain-Northern Adriatic Foredeep Basins (PPAF) (Fantoni and Franciosi, 2010; Ghielmi et al., 2013; Rossi et al., 2015). Previous studies provide evidence for coastal onlaps as well as an intricate dendritic paleo-drainage network converging toward the Adriatic foredeep axis in the Adriatic offshore (Ghielmi et al., 2010, 2013; Rossi et al., 2015). Toscani et al. (2016), in addition, mapped the landward connections of two main late Messinian incised valleys in the Friulian-Venetian basin (FVB) onshore, which constrains the extent of subaerial fluvial erosion during the MSC Stage 2 (Fig. 55 A). Such connections within the FVB were also recognized in the proximal offshore by Donda et al. (2013) and Zecchin et al. (2017). Ghielmi et al., (2013) suggested a maximum relative sea level lowering in the Po Plain–Northern Adriatic region of less than 900 m. The isostatic response of the lithosphere to the MSC-related sea-level lowering has been the subject of several studies (e.g. Ryan, 1976; Meijer and Grijgsman, 2005; Govers et al., 2009). However, most previous works focus on the Mediterranean-scale rather than the local deformation. Here, we rely on geological constraints from additional data relative to the Po-Adriatic basin during the MSC, to produce new estimates tailored on the PPAF.

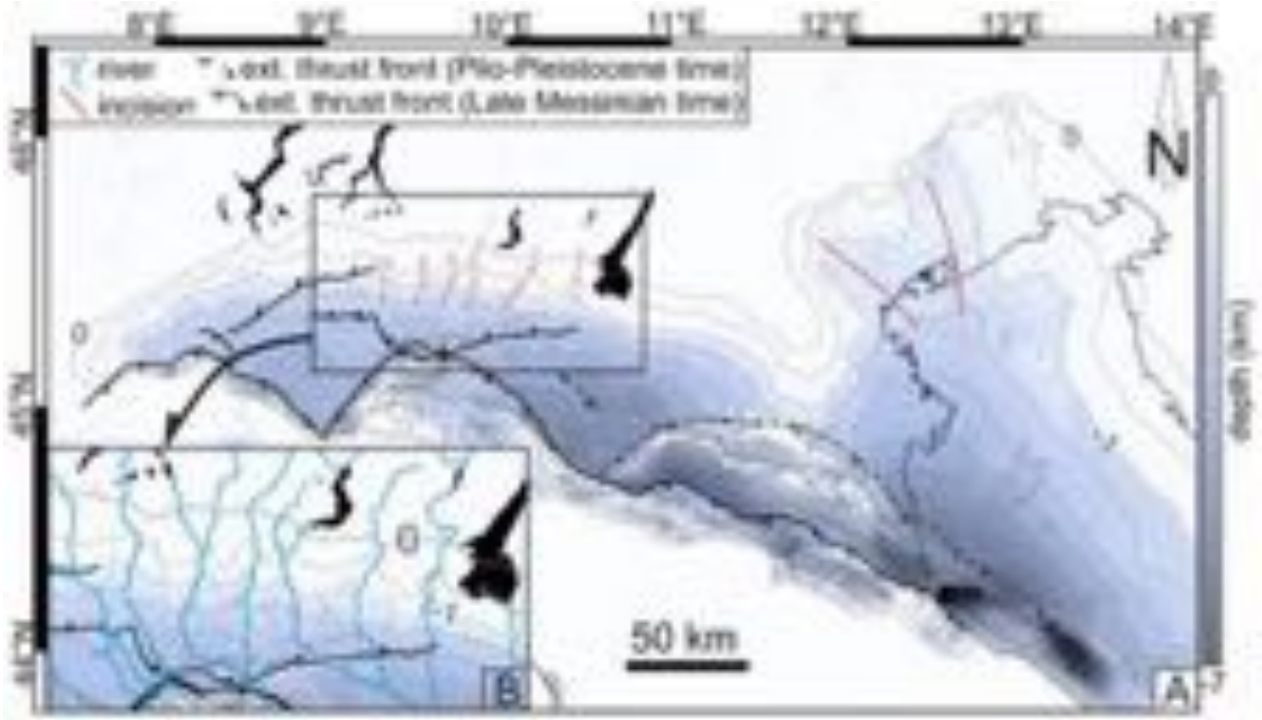

Figure 55. A) Depth-converted late Messinian unconformity with 500 m contouring. B) buried Messinian surface along the Southern Alps margin compared with the modern river network.

4.4. Dataset and methods

Our reconstruction of the paleotopography results from a vertical restoration of the latest Messinian unconformity through a backstripping procedure (Fig. 54), calculations made with TISC by Garcia-Castellanos et al. (2002, 2003). The analysis accounts for the decompaction and the 2D (planform) flexural isostatic adjustment associated with unloading of the post-Messinian sediments and the water column missing during the MSC acme.

The vertical restoration of the tectonic deformation of the basin has been carried out removing the vertical component of the main Plio-Pleistocene thrusts and anticlines of the Northern Apennines and Western Southern Alps, determined from published uplift data (Scrocca et al., 2007; Toscani et al, 2014; Maesano et al., 2015; Bresciani and Perotti, 2014). We also considered the additional erosional unload of the European Alps throughout the Plio-Quaternary (and the associated isostatic adjustment) by using the pre-glacial topography proposed by Sternai et al. (2012) to reconstruct the most plausible paleotopography of the Alpine chain. The sediment properties (i.e. initial porosity, exponential compaction coefficient and bulk density), were defined based on the analysis of well log data (unpublished data courtesy of Eni Upstream and ViDEPI public database). We performed a detailed parametric study involving, in particular, the amount of sea level lowering (0/-500/-800/-850/-900/-1500 m) and the lithospheric elastic thickness (between 10-45 km) to account for most previously proposed MSC scenarios (e.g., Manzi, 2005; Ryan and Cita, 1978; Urgeles et al, 2010 and reference therein) and rheological conditions (Moretti and Royden, 1988; Barbieri et al., 2004). The most relevant results are described and discussed in the following sections.

4.4.1. Workflow

We performed a backstripping-flexural analysis of the Po Plain-Northern Adriatic basin, constrained by new seismic and well log data (from Eni Upstream private data) and a novel workflow that we outline hereafter (Fig. 56). We apply the backstripping-flexural model to a detailed reconstruction of the stratigraphic architecture, considering also the tectonic deformation of the Po Plain-Adriatic Foreland Basin (PPAF) during the Messinian sea level drop.

Figure 56. Workflow chart followed in this study.

4.4.2. Tectonic correction

To model the morphology of the Po basin at the Latest Messinian time, we removed the vertical component of the Northern-Apennine thrust fronts showing a Plio-Pleistocene tectonic activity and the Pliocene uplift of the western Southern Alps thrusts. We derived the total uplift for each analyzed key-structure based on slip/uplift rates published by Scrocca et al. (2007), Maesano et al. (2015) and Bresciani & Perotti (2014) (Tab. 1).

Structure	References	Fault dip	Total slip (m)	Age Interval (Ma)	Vertical component to be removed (m)
MI	Scrocca et al., 2007	-	-	1.4 – 0	570
T5FF	Maesano et al., 2015	40°	1659	3.6 – 0	1059
T6FF	Maesano et al., 2015	25°	750	1.81 – 0	315
T9RF in	Maesano et al., 2015	30°	3178	3.6 – 0	1589
T9RF out	Maesano et al., 2015	30°	1425	3.6 – 0	815
T2EF	Maesano et al., 2015	40°	703	3.6 – 0	1400
T3EF	Maesano et al., 2015	40°	340	1.81 - 0	950
Romanengo anticline	Bresciani & Perotti, 2014 Maesano et al., 2015	-	-	5.33 - 0	1150

Tab.1. Structure code-name and location in Maesano et al. (2015); geometric features of the fault and the vertical component considering the age interval of the tectonic activity.

We used constraints from the literature (Perotti, 1991; Bigi et al. 1995; De Donatis, 2001; Toscani et al. 2014) to estimate the horizontal shortening in the Po basin since the late Messinian along the Apennine front. We found that the average shortening ranges between 10-20km along strike (Fig. 57), which is minor with respect to the size of the basin and, therefore, we neglect this correction in the peleogeographic reconstruction.

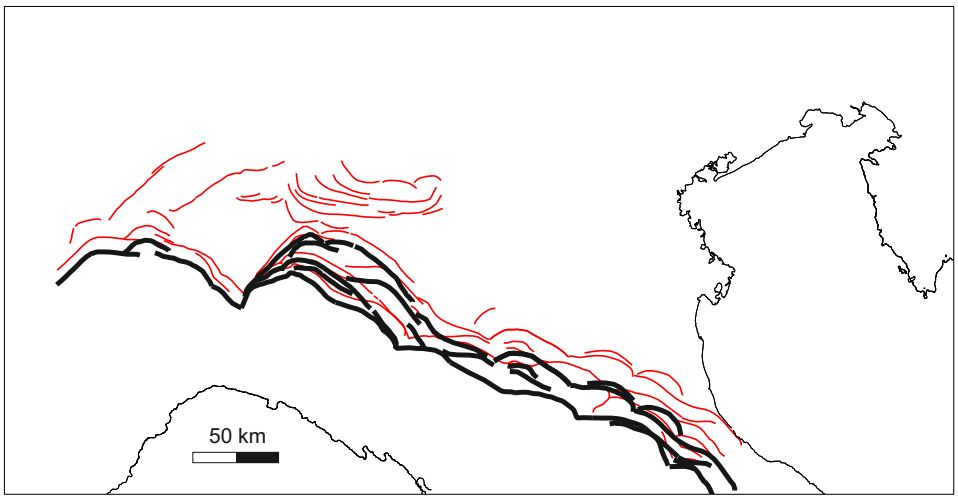

Figure 57. Red lines represent the late Messinian Southern-Alpine and Northern Apennine thrusts in their present-day position. In bold black, the restored late Messinian thrust fronts according with the shortening deduced by bibliography (see text).

4.4.3. Numerical Modeling

The backstripping follows the procedure by Sclater and Christie (1990) while flexural isostasy is performed by TISC program (Garcia-Castellanos et al., 2002, 2003). applying numerical solution from Van Wees and Cloetingh (1994), Watts (2001) and Turcotte and Schubert (2002).

The input dataset is composed by:

1) Topography (DEM) by GTOPO30 (https://lta.cr.usgs.gov/GTOPO30).

2) Late Messinian unconformity derived from regional scale interpretation and time-to-depth conversion of a net of seismic lines from Eni private dataset (Fig. 53 A) integrated with bibliographic data from Pieri and Groppi (1981), Bigi et al. (1992), Turrini et al. (2014) and Toscani et al. (2016) (Fig. 53 B, C respectively).

3) Top of Mesozoic carbonates, derived from Turrini et al. (2014, 2016) whose 500m depth-contouring have been digitized (Fig. 53 D).

We assigned a uniform surface porosity (Φ_0), bulk density and porosity-depth exponential coefficient (**c**) to the analyzed volumes. To characterize the lithologic properties of the modeled succession, we derived stratigraphic and electric log data over a hundred wells, from the Po Plain and Adriatic Sea (provided by Eni Upstream and ViDEPI database) (Fig. 53 A). The average lithologic properties to be used into the modelling calculation are similar to "Shaley Sandstone" lithotype, defined by Sclater & Christie (1980) (Tab. 2). The most representative lithologies into the Paleogene-late Messinian volume to are: the Paleogene-Miocene marine marls (i.e. Scaglia s.l and Gallare Group) and Miocene sandstones (i.e. Gonfolite Group and latest Tortonian-syn-evaporitic Messinian sand-poor turbidites of Bagnolo Fm.). We model this volume with a lithology-type of 75% shale and 25% sand; porosity fraction and lithologic properties are measured directly by modeling the proportion with Basin Mod2014 software, by Statoil (Tab. 2). We derived the mean bulk density from grain density values come by Sclater & Christie (1980) and BasinMod 2014 library (by Platte River Ass.).

The density of the removed seawater and the volume survived during the MSC drop, is assumed to be 1030 kg/m^3 like the current average seawater density at the surface (Beicher, 2000). We decided to use this value because the Po Plain during the MSC was not a fully evaporitic basin and there is not gypsum or halite precipitated into the WPPF and PPAF depocenters. The basement density was set to 2850 kg/m^3.

References	Lithology type	Lithology Mixing (%)	Φ_0 (fraction)	Exp Compac.Coeff (1/km)	Grain Density (kg/m^3)	Bulk density (kg/m^3)
Sclater & Christie, 1980	Sandstone	100% Sand	0,49	0,27	2650	2096
Sclater & Christie, 1980	Shale	100% Shale	0,63	0,51	2720	2140
Sclater & Christie, 1980	Shaley Sandstone	50% Sand 50% Shale	0,56	0,39	2680	2115
BasinMod 2014 library	Sandy Shales	75% Shale 25% Sand	0,563	0,45	2700	2149

Tab.2. Values from Basin Mod2014 software and used for decompaction and uplift calculation.

4.4.4. Topographic correction

During Pliocene time, the glacial activity was subordinated to tectonics due to the Northern Apennine migration (Toscani et al., 2014; Maesano et al., 2015) and Southern Alps uplift (Livio et al., 2009). Therefore it was not considered in this work.

During the last 2.6 Ma on the contrary, the tectonic component was negligible in the Alps (Fantoni & Franciosi, 2010) and the isostatic adjustments, due to the Quaternary glacial erosion, was particularly effective in the European Alps (e.g., Sternai et al., 2012).

To reconstruct the most plausible topography of the Alpine chain bordering the Po Plain-Northern Adriatic basin including the glacial-driven isostastic adjustment, we used the paleotopography of the European Alps prior to glaciations as reconstructed by Sternai et al. (2012) (Fig. 58).

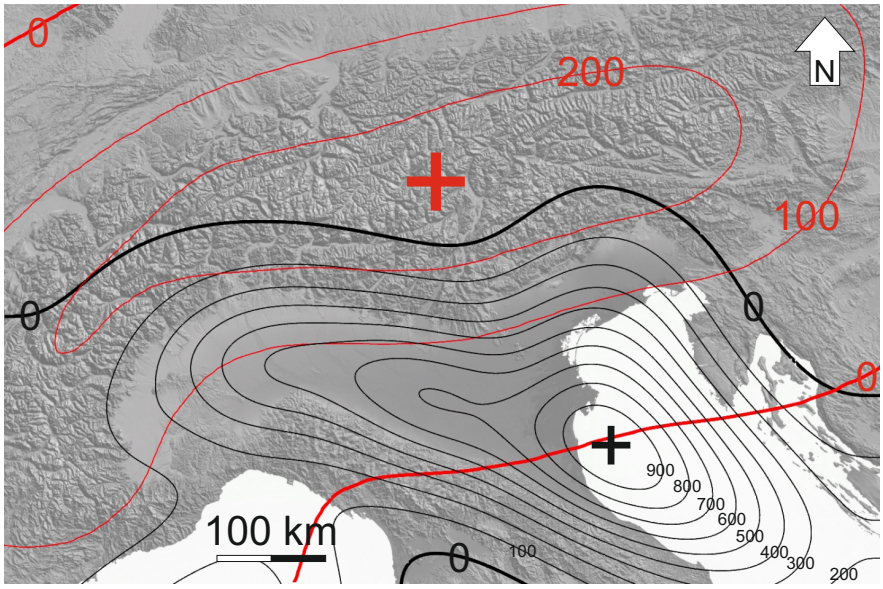

Figure 58. *Red contour lines: uplift from Sternai et al. (2012). Black contour lines: uplift resulted from the backstripping-flexural preferred model (Te 20 km and a sea level drop of 850 m).*

The uplift by Sternai et al., (2012) (Fig. 58) presents a very low gradient in the Po basin area and maximum value is focused on the alpine belt, approximately parallel to the northern peripheral bulge estimated in our modelling (corresponding to the black bold line 0 m), along the Alpine chain. Thus, the influence on Po-Adriatic basin uplift and coastline is minimal.

4.5. Results

The Alpine rivers carved deep valleys across the modern Po Basin and incised far into the Alps, the erosional surface can be followed into the Po Plain subsurface by means of seismic sections (Fig. 55 A, B). The comparison between the modern river network and the late Messinian buried incisions suggests that the Messinian erosional event controls the present-day drainage pattern of Southern-Alps (Fig. 55 B). Thus, the Southern-Alps drainage network dates back (at least) to the maximum drawdown during the MSC, confirming also a late Messinian origin (and not glacial) of the Alpine lakes crypto-depressions inferred by Bini et al. (1978) and Finckh, P.F. (1978).

In the case of no drawdown, the most of the Po Plain, the Friulian-Venetian basin (FVB) and the Northern Adriatic region remain below sea level throughout the entire MSC. On the contrary, assuming a sea-level fall up to 1500 m, the western Po Plain (WPPAF) and the Friulian-Venetian Basin are under continental conditions, implying subaerial exposure of marine structures such as the observed basinward-stepping coastal wedges (i.e: Fig. 9 in Ghielmi et al., 2013; Fig. 21 in Rossi et al., 2015).

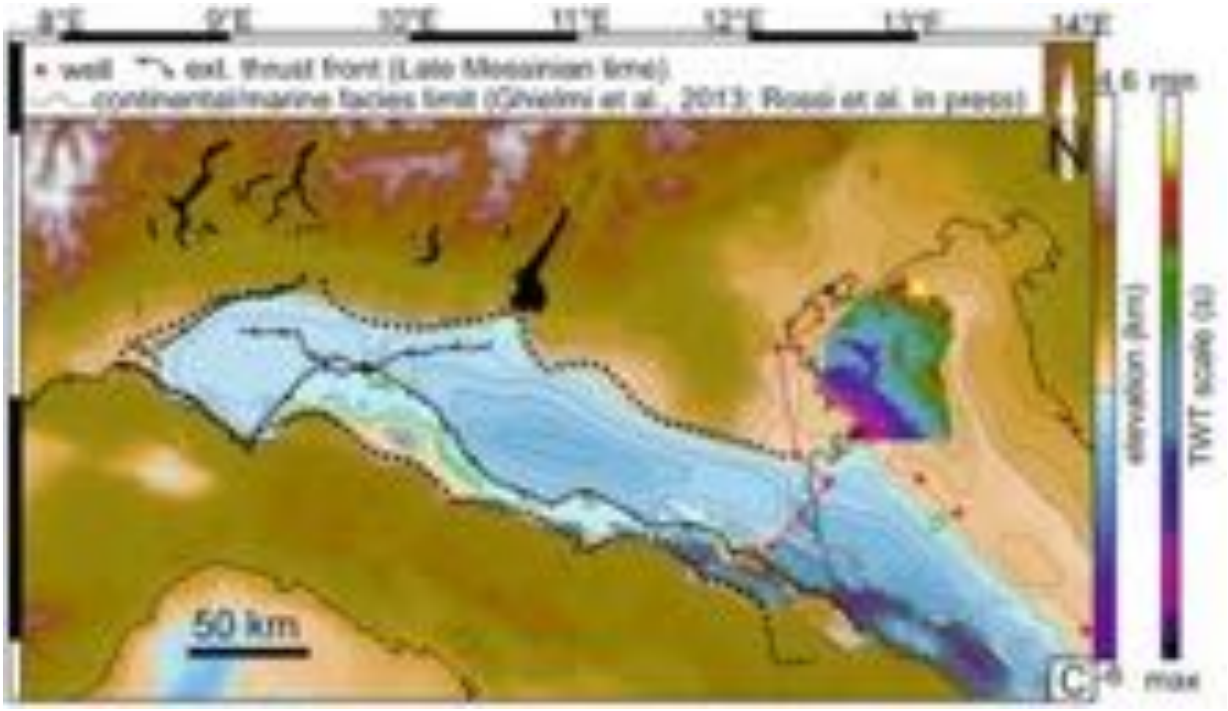

Figure 59. Restored late Messinian landscape applying a 850 m sea-level drop, 200 m contouring. In the inset TWT amplitude color map of a subaerial drainage network (after Ghielmi et al., 2013). Red line refers to the Fig.9 into Ghielmi et al. (2013) including a late Messinian marine-coastal system.

We find that the facies distribution recognized by Ghielmi et al. (2013) and Rossi et al. (2015; in press) is best matched when the relative sea level fall is imposed as ~800-900 m (Fig. 55 shows the case of relative sea-level lowering by 850 m).

Accordingly, to our preferred model, the maximum water depth in the western depocenter (WPPF) is nearly 700 m, while a wider WNW-ESE elongated depocenter (PPAF) was present to the east, with modeled paleobathymetry reaching up to 1300 m. In the eastern sector, the backstripping analysis shows the maximum uplift (995 m) in correspondence with the depocenter (Fig. 56).

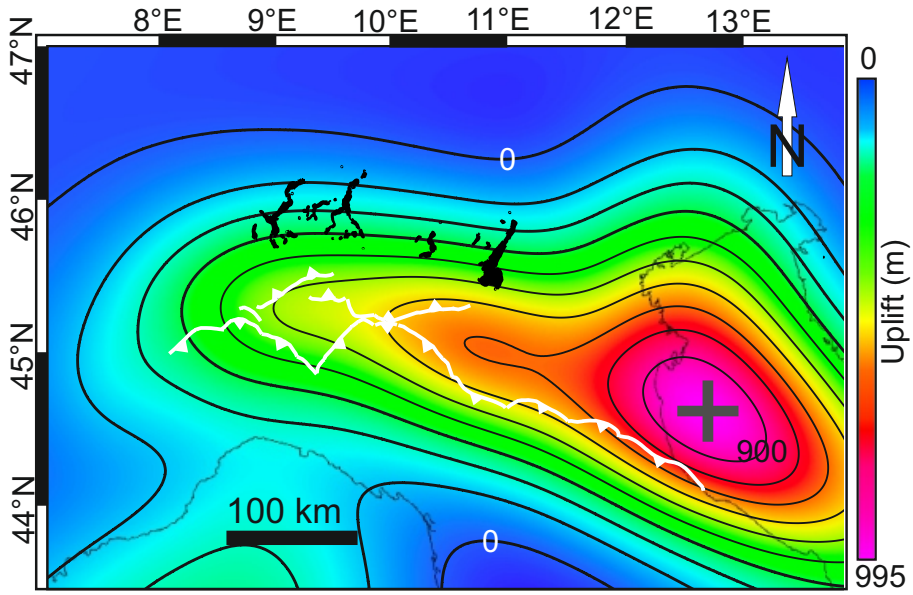

Figure 60. Map of the estimated isostatic uplift in response to sediment-water unloading

To the NE, the Friulian-Venetian Basin was exposed during the Messinian Stage 2. The proposed fluvial origin of the onshore incised valleys and offshore drainage network described by Donda et al. (2013), Ghielmi et al. (2013) and Toscani et al. (2016) agree with the landscape obtained from our preferred model. Consistently with our preferred model. a wide portion of the Mesozoic Istrian-Dalmatian platform was exposed (Velić et al., 2015), as suggested by unconformities interpreted from the Adriatic Sea (from NW to SE: Ornella 1, Raffaella 1, Gladiolo 1, Glenda 1 and Alessandra 1 wells, from public ViDEPI Project; Fig. 59).

4.5.1. Parametric study

The parametric study related to the uplift modeling focused on the: (1) sediments volume, (2) lithospheric elastic thickness (Te) and sea level fall.

1) Sediments volume: we tested different lithologic characteristics of the Cenozoic volume and the latest Messinian-Quaternary volume, considering different sand-clay proportions: 100% shale, 100% sand, 75% shale - 25% sand, 50% shale - 50% sand (Tab. 3).

2) Elastic thickness (Te): the lithospheric elastic thickness (Te) controls the flexural rebound of the plate under the basin; all values considered for the sensitivity analysis (10, 15, 20, 25 and 45 km) are

collected from bibliography (Moretti & Royden, 1988; Royden, 1988; Watts, 1992; Picotti et al., 1997b; Buiter et al., 1998; Kroon, 2002; Barbieri et al., 2004) (Tab. 3).

In our reference model, we assume an average constant elastic thickness of 20 km (Moretti & Royden, 1988; Barbieri et al., 2004).

3) The amount of sea level fall: 0, -500, -800, -850, -900 and -1500 m (Tab.3).

Cenozoic vol. Porosity	Te (km)	Uplift (m) (0 m drop)	Uplift (m) (-500 m drop)	Uplift (m) (-800 m drop)	Uplift (m) (-850 m drop)	Uplift (m) (-900 m drop)	Uplift (m) (-1500 m drop)
50-50	10	1047.4	1202.8	1292.8	1306.7	1320.4	1451.9
75sh-25s	10	1047.4	1202.9	1292.6	1306.6	1320.2	1452.1
100%shale	10	1047.4	1202.4	1289.9	1303.3	1316.3	1441
100%sand	10	1047.4	1203.2	1295.6	1310.2	1324.6	1467.3
50-50	15	890.6	1040.5	1121.4	1133.2	1144.6	1248.1
75sh-25s	15	890.6	1040.5	1121	1132.7	1144	1247.7
100%shale	15	890.6	1039.5	1116.4	1127	1138.1	1235.6
100%sand	15	890.6	1041.4	1126.1	1139	1151.4	1264.8
50-50	20	771.6	912.5	985.2	995.6	1005.4	1092.2
75sh-25s	20	771.6	912.4	984.6	994.9	1004.6	1091.3
100%shale	20	771.6	911	979.5	989.1	998.2	1079.7
100%sand	20	771.6	913.9	990.6	1002.1	1013	1108.5
50-50	25	677.2	807.6	872.9	882.2	891	966.6
75sh-25s	25	677.2	807.3	872.2	881.4	890.1	965.6
100%shale	25	677.2	805.8	867.3	875.9	883.9	954.7
100%sand	25	677.2	809.2	878.1	888.3	898.1	981.9
50-50	45	448.2	543.2	588.8	595.4	601.7	655.4
75sh-25s	45	448.2	543	588.2	603.4	601.1	654.4
100%shale	45	448.2	544.7	584.9	599.7	597.1	646.9
100%sand	45	448.2	541.7	592.6	608.3	606.4	665.7

Tab.3. *Table of Maximum Uplift variations under different input parameters. In this table, for easier reading, we vary the Cenozoic volume parameters only keeping the combinations with fixed porosity for latest Messinian-Quaternary sediments (as in Tab. 2).*

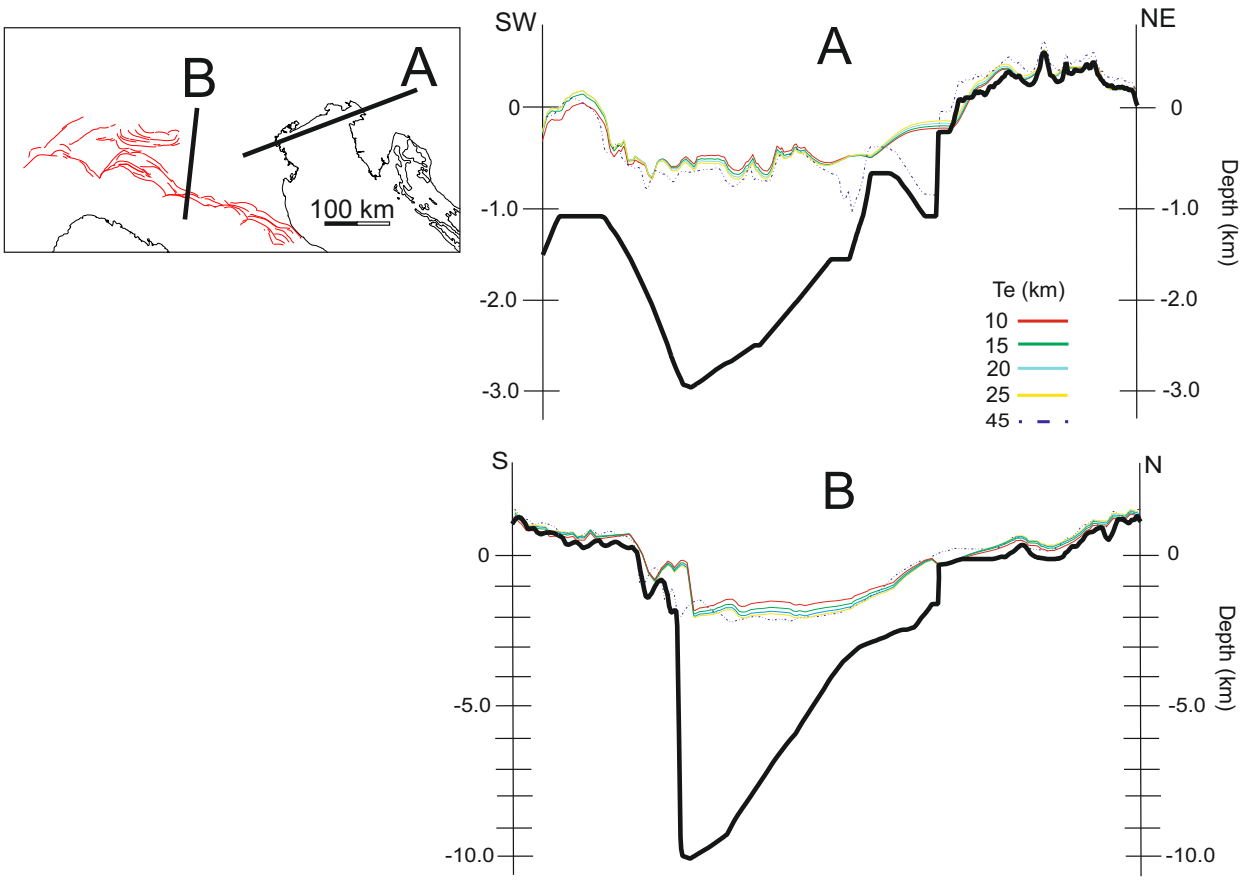

Figure 61. Profiles along the Po Plain foreland (A) and foredeep (B). Black bold line: basement of the model (corresponding to the top of the carbonate formations). Color lines: late Messinian surfaces modeled with different elastic thickness (Te) of the plate (others parameters like sea level drop and porosity remain fixed to show different uplift due to the Te variation only).

Sea level variation seems to be a relevant source of additional uplift only if its magnitude is significant. For given Te and porosity value, the uplift gains ca. 30% if we consider 1500 m sea level drop. Instead, for a sea level variation of only 100 m the uplift increases by 2% (< 30 m).

Furthermore, for a given Te and sea level drop, varying only porosities combinations of the Cenozoic-Quaternary volume, influence results by less than 20 m (Tab. 3).

The landscape resulting from models with Te=20 km considering no sea level drop and 1500 m drawdown are shown in figures 63 A, B respectively.

The shoreline migration for models with Te=10, 20, 45 and different sea level drops (0, -500, -800, -850, -900, -1500) is shown in Fig. 63 C, D, E.

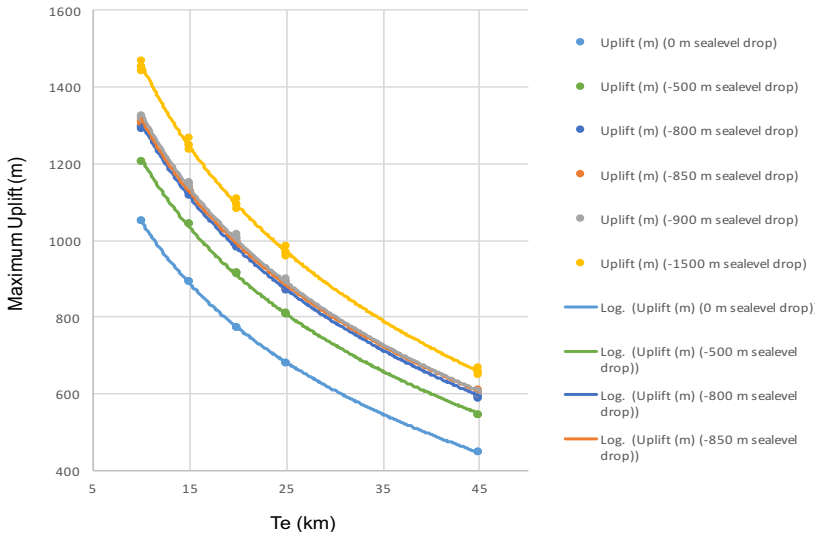

Figure 62. *Data from Tab.3 are plotted to describe the uplift values from Te, porosity ratio and sea level drop variations. All the trend lines are Logarithmic with* R^2*=0.99.*

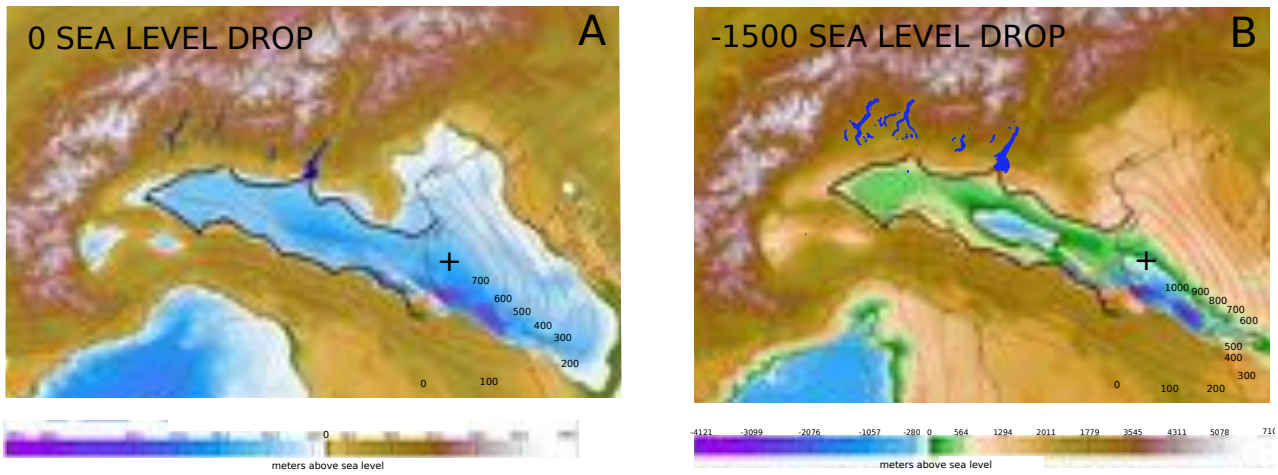

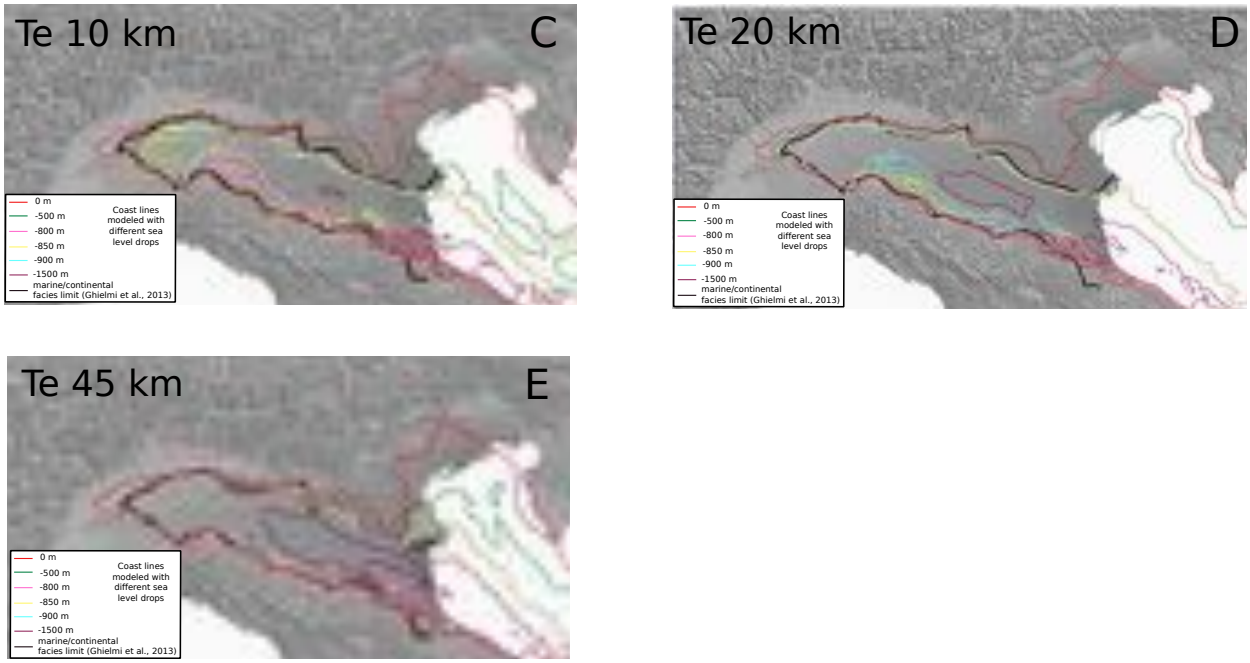

Figure 63. Paleogeographies by modeling two extreme cases (both with Te 20 km): (A) no sea level drop and (B) 1500 m drawdown. C, D, E: examples of shoreline shifts produced by modelling different drops on three different Te values.

4.6. Discussion

According to our best-fit model the main tracts of the restored late Messinian landscape with two major marine depocenters subject to deep-water turbiditic deposition throughout the Messinian contoured by exposed marine shelves and localized hypersaline basins on top on piggy-back northern Apennine basins (Artoni et al., 2007; 2010; Rossi et al., 2015). The proposed drop of 800-900 m is significantly lower than the 1300-1500 m drawdown suggested by several authors (e.g. Ryan and Cita, 1978; Gargani, 2004; Gargani and Rigollet 2007; Bache et al., 2009; Urgeles et al., 2010) based on morphological evidences from the Western Mediterranean (i.e., Gulf of Lions, Ebro margin) or by numerical modeling. Thus, during the MSC acme, we interpret the Po Plain-Northern Adriatic basin as a restricted elongated foreland basin physically disconnected from the rest of the Mediterranean by means of some thresholds, as suggested by Blanc (2006) according to independent hydrological balance considerations.

This result opens the question about where the morphological divide separating the Po Plain-Northern Adriatic basin from the rest of the Mediterranean basin could have been placed. With this respect, in agreement with the pioneeristic paper by Cita and Corselli (1990) and afterwards with Santantonio et al. (2013), and Pellen et al. (2017), we infer that a sill could have been probably located between the present day southern Italian peninsula and the southern Adriatic Sea. This interpretation agrees with the late Messinian geodynamic context of the Central Mediterranean region proposed by Jolivet et al. (2006) and Barone et al. (2006), in which the southern Italy-Adriatic Sea area was a tectonically active composite puzzle made of submerged/exposed continental blocks. Seismic data and well log analysis of southern Italy onshore and offshore (de Alteriis, 1995; Scrocca, 2010, Santantonio et al., 2013) reveal a stratigraphic hiatus of late Messinian age that further supports this scenario.

Although, the timing of closure and re-opening of the southern Adriatic sills during the late Messinian is beyond the purpose of this work. The presence of marine bio-events (e.g. the FO of *Turborotalita multiloba* and the *Neogloboquadrina acostanesis* sx/dx coiling change) in the pre-MSC sequences (Sierro et al., 2001; Blanc-Valleron et al., 2002; Gennari et al., 2013; Caruso et al., 2015), the reconstruction for the near Tertiary Piedmont Basin based on the Lower Evaporites gypsum (Dela Pierre, 2011) and the quasi-uniform $^{87}Sr/^{86}Sr$ values of the Lower Evaporites throughout the Mediterranean (Schildgen et al., 2014; Roveri et al., 2014) suggest that the Po-Adriatic basin should have been connected the rest of the Mediterranean at least during the pre-evaporitic and evaporitic phases (MSC stages 1 and 2). In turn, this suggests that the isolation of the Po Plain-Northern Adriatic region could have been reached only after the deposition of the Lower Evaporites, during the maximum sea-level drop correlated with the TG12 or both TG12 and TG14 glacial intervals

(Cosentino et al., 2013).

This means the integrated balance between river discharge, precipitation, evaporation and uplift rate could have changed quite rapidly and dramatically both through time and from place to place during the step wide base level change and should be taken into account to fully understand the Messinian evolution of this part of the Mediterranean basin. A high freshwater budget may prevent salt saturation and explain why halite or other high soluble K-rich salts did not accumulate in this region during MSC. The Po Plain-Northern Adriatic syn- and post-evaporitic Messinian deposits may indeed reflect a complex equilibrium between high fresh-water input provided by the large rivers draining the Alpine belt and the progressive increase in salinity due to the MSC. This would cause precipitation of gypsum and anhydrite only in restricted basins in the northern Apennine, like the TPB, piggy-back basin and/or very localized sectors of the Adriatic foreland (Rossi et al., 2002; Dela Pierre, 2011; Ghielmi et al., 2013; Rossi et al., 2015), coeval with massive deep-marine clastic deposition in the residual, quite deep depocenters (Rossi et al., 2015).

4.7. Conclusions

Within the uncertainty inherent to the modeling technique, the restored landscape obtained for the moment of the maximum sea-level drop occurred during the MSC in the Po Plain – Northern Adriatic Basin of the Mediterranean region allows drawing the following main conclusions.

- Our flexural-backstripping modeling best matches the available subsurface stratigraphic and facies distribution data when an 800-900 m drawdown is imposed; thus, the sea-level fall related to the MSC maximum lowstand in the study area is smaller than what was inferred for the eastern and western Mediterranean (about 1500 m or more), but also significantly larger than the one (about 200 m) proposed by other authors for the entire Mediterranean area.
- We argue that this result implies that, at a broader scale, the Mediterranean was divided into at least three sub-basins (Po Plain-Northern Adriatic, Western and Eastern Mediterranean Basins), with independent base-level evolutions and water budgets at least since the maximum MSC sea-level drop. This can be the reason for the lack of halite deposits in the Adriatic Sea.
- The buried late Messinian incised valleys cutting the Southern Alps margin fits quite well with the present-day fluvial network draining the not only the Southern Alps belt but also the Po River alluvial plain. This proves that the fluvial network draining the southern side of the Alps today dates back at least to the late Messinian, confirming previous interpretations suggesting the origin of South Alpine Lakes V-shaped valleys during the MSC drawdown. In addition,

the fact that many rivers running today in the Po alluvial plain follow Messinian deeply buried incised valleys suggests that the Messinian imprint is a controlling factor not only in the mountain valleys belt but also in the alluvial plain; we argue that this is probably due to differential subsidence between incised valley fills and interfluvial areas.

Finally, our results suggest that at least during a period of the MSC, different parts of the Mediterranean basin should have had independent base levels, water budgets and possibly similar but heterochronous evolution, as the effects of the MSC could have been recorded differently in each sub-basin at least during the main drawdown phase. Therefore, caution should be used in performing numerical model at the whole Mediterranean scale (i.e., salinity and water budget calculation). This is the reason because we support the generation and use of smaller-scale high-resolution stratigraphic models rather than Mediterranean-scale litho-stratigraphic correlations in the MSC studies.

CHAPTER 5
CHRONOLOGICALLY CALIBRATED PLIOCENE-PLEISTOCENE ARCHITECTURE OF THE COASTAL PRISM IN THE VENICE REGION: EVOLUTION UNDER CHANGING CONTROLLING FACTORS

5.1. Abstract

The Friulian-Venetian Basin (FVB) is the north-eastern portion of the wider Po Plain-Adriatic foreland, bounding the whole Italian peninsula to the east.
This work provides a new high-resolution chronostratigraphic framework integrated with 1-D backstripping analysis on available wells by means of new paleobathymetric data merged with seismics, direct (bottom cores) and indirect (electric well logs) sedimentological proxy analysis.
The reconstruction of the Plio-Pleistocene coastal prism accumulated in the Venice area is based on the proposed new age model, calibrated with a complete chronostratigraphic revision of the continuously cored Venezia 1 well and the sequence stratigraphic analysis, organised in allogroups and their lower rank units.
Results allow to discuss the engine and the causes (e.g. tectonic vs climate) for sediment production, provenance and stratigraphic evolution. For instance, the 1D backstripping modeling suggests a major tectonic control on sedimentation and basin accommodation space during the entire Pliocene-early Pleistocene time, strongly influenced by the northern Apennine thrust fronts migration. During middle-late Pleistocene on the contrary, climate forcing started to be the main factor controlling the sedimentation rate coupled with a progressive decrease of tectonic activity into the basin; during this time-span, 100 kyr Milankovitch-type cyclicity have been observed into sedimentary record, interpreted as orbitally-controlled transgressive-regressive cyclothems and correlated basinward by means of the well electric signals, lithological log analysis and seismics in the offshore area.

5.2. Introduction

The town of Venice and its lagoon have been included since 1987 in the UNESCO human heritage list. They are famous worldwide due both to the beautiful buildings of the town and its peculiar location into a barrier island lagoon system that developed 6-7 Kyr BP, during the Flandrian transgression occurred after the last glacial maximum (Brambati et al., 2003) (Fig. 64).

This transgression was the last step of the complex environmental evolution suffered by the Venice region after the reestablishment of an open marine condition occurred at the end of the Messinian salinity crisis. That environmental evolution was driven by the interplay of a several factors, such as:
i) a fairly continuous (but with a variable rate) subsidence experienced by the region during the whole Pliocene-Pleistocene time span (Carminati et al., 2005; Barbieri et al., 2007);
ii) the progressively decreasing tectonic activiyy linked to the Northern Apennines migration (Fantoni et al., 2002; Toscani et al., 2016 and references therein);
iii) the increasingly oscillating sea-level induced by the glacio-eustatic cycles (Miller et al., 2011) and;
iv) the changing sediment supply mostly due to climate change and the onset of alpine glaciations (Muttoni et al., 2003, 2007; Garzanti et al., 2011).
As a result, a complex coastal sedimentary prism has developed progressively filling the available accommodation space.
Here, we present a nwe, high-resolution, chronologically-calibrated reconstruction of the stratigraphic architecture of the Pliocene-Pleistocene sedimentary prism forming the stratigraphic substratum of the coastal area around Venice, providing a detailed picture of the paleo-environmental evolution of the area. It was obtained through the integration of published and unpublished seismic data, information from 13 hydrocarbon wells (courtesy by Eni Upstream), paleobathymetric constraints provided by micropaleontologic analyses and 1-D geohistory performed on 6 of these wells, combined with the high-resolution chronological calibration obtained by the correlation with the entirely revised Pliocene-Pleistocene reference section formed by the combination of the 915 m thick section provided by the continuously cored wells Venezia 1, and Venezia 1Bis, (hereafter VE1 and VE 1Bis; e.g. Kent et al., 2002 and references therein; Massari et al., 2004) and the close and correlatable stratigraphy of the Lido 1 hydrocarbon well (Barbieri et al., 2007).
The obtained reconstruction provides a key for onshore-offshore correlations in the Pliocene-Pleistocene sedimentary sequence of the Northern Adriatic region. However, it allows to discuss the relative role of the different factors controlling Pliocene-Pleistocene environmental evolution (e.g. climate instability) of a Venice coastal area and eventually provides a robust stratigraphic base necessary for intervention programs facing the problem of natural subsidence of Venice.

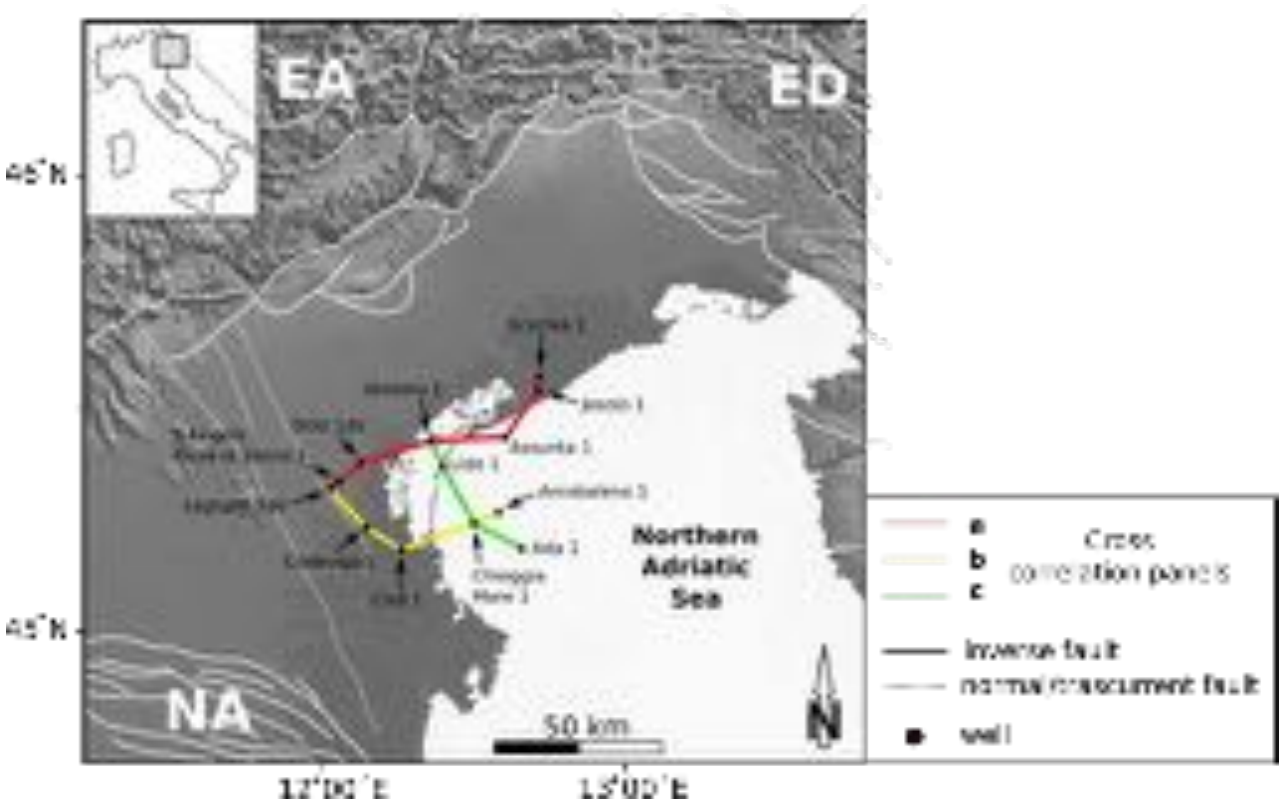

Figure 64. Map of the study area and well locations. EA: eastern Alps. ED: External Dinarides. NA: Northern Apennines. Red line: cross correlation panel A, explained in Fig. 77 A. Yellow line: cross correlation panel B, explained in Fig. 78 B. Green line: cross correlation panel C, explained in Fig. 78C.

5.3. Tectonic setting

Venice is located in the north easternmost sector of the Adria microplate (Fig. 64) at the boundary between the Friulian-Venetian Basin and the Norther Adriatic Basin (hereafter VFB and NAB respectively; Mancin et al., 2016; Toscani et al., 2016).

The starting point of the VFB and NAB evolution can be fixed at the paleotopographic arrangement inherited since the Mesozoic extensional evolution with the carbonate platform (Friulian platform), abruptly passing south-westwards to the deep Belluno Basin (Fantoni et al., 2002; Turrini et al., 2014; Toscani et al., 2016). From this starting point, the north-easternmost sector of the Adria microplate played the role of foreland basin for each of the collisional systems developed around it in different times. From the oldest to the youngest, the Dinaric, the eastern South Alpine and the Northern Apennines system (Fantoni et al., 2002; Caputo et al., 2010 and reference therein; Carminati and Doglioni, 2012 and reference therein).

Notwithstanding this complex tectonic setting, after Messinian time the deformation in the region was rapidly decreased and become almost absent during Pleistocene time (Fantoni et al., 2002), thus

preserving sediment filling geometries mostly driven by the balance between accommodation space and sediment supply (Carminati et al., 2005; Mancin et al., 2009, 2016; Toscani et al., 2016).

5.4. Stratigraphic framework

Several recent publications (Mancin et al., 2009; Ghielmi et al., 2010, 2013; Zecchin and Tosi, 2014; Rossi et al., 2015; Tosi et al., 2015; Toscani et al., 2016; Zecchin et al., 2016) provided new insights on the subsurface stratigraphy of the area. Specifically, Ghielmi et al. (2010, 2013) based on detailed well-log correlations on the Po Plain-Northern Adriatic Basin (PPAF), integrated with seismic interpretation of both 2D and 3D seismic surveys (from Eni private dataset), provided a new overall stratigraphic framework consisting of units bounded by regional scale unconformities and correlative conformities of different order and importance.

The basin reconstruction proposed in this thesis chapter is based on this stratigraphic framework, which is described as follows.

According to the cited authors, in the case of PPAF, allogroup boundaries are produced by major compressional tectonic phases and are usually related to the creation of new foredeep depocenters related to the north-east migration of the Northern Apennines fold-thrust belt. Allogroup boundaries can be recognised in wells and seismic from abrupt major changes in type and distribution of the depositional systems showing that the Apennines deformation strongly influenced the sedimentation by controlling the elevation and gradient of basin margins, the extension of the drainage areas, the location of the main clastic entry-points, and the extension, shape and depth of the deep-water depocenters (Ghielmi et al., 2010; 2013).

The entire Plio-Pleistocene sedimentary succession is bounded, at the bottom, by the regional scale erosive Messinian Unconformity Surface and by the present-day topographic surface at the top; according to the cited authors 3 allogroups can be distinguished (Fig. 65): LM (Late Messinian-Zanclean), EP (late Zanclean-base Gelasian) and LP (Gelasian-Holocene), divided by the PL2 (Intra-Zanclean) and PL4 (base Gelasian) major unconformities.

The allogroups can be further subdivided into lower rank unconformity bounded units: the largest of these sub-units are named Large-Scale Sequences (LSS). The LSS boundaries are as synchronous along the basin as the allogoup boundaries; in the foreland sector (e.g. the Adriatic Sea and Venice region) the LSS sedimentary units, bounded by tectonic or eustatic-driven sequence boundaries, correspond to relative sea level changes and significant lithofacies changes. In order to avoid confusion with previous papers, as for allogroups, we use here same names and color code for LSS boundaries (PL1, PL3, PS1, PS2a, PS2b; Fig. 65), even if, according to Gibbard et al. (2010) the base

of Quaternary has been moved to the base of the Gelasian, differently respect to the original papers of Ghielmi et al. (2010 and 2013).

Due to the late Messinian sea-level drop (Hsü et al., 1978; Roveri et al., 2014; Sternai et al., 2017 and reference therein), a huge subaerial erosion affected the Venetian-Northern Adriatic area, generating deep incised valleys and channels (Donda et al., 2013, 2015; Toscani et al., 2016) locally filled by few meters of latest Messinian fluvial conglomerates (Ghielmi et al., 2010, 2013; Rossi et al., 2015).

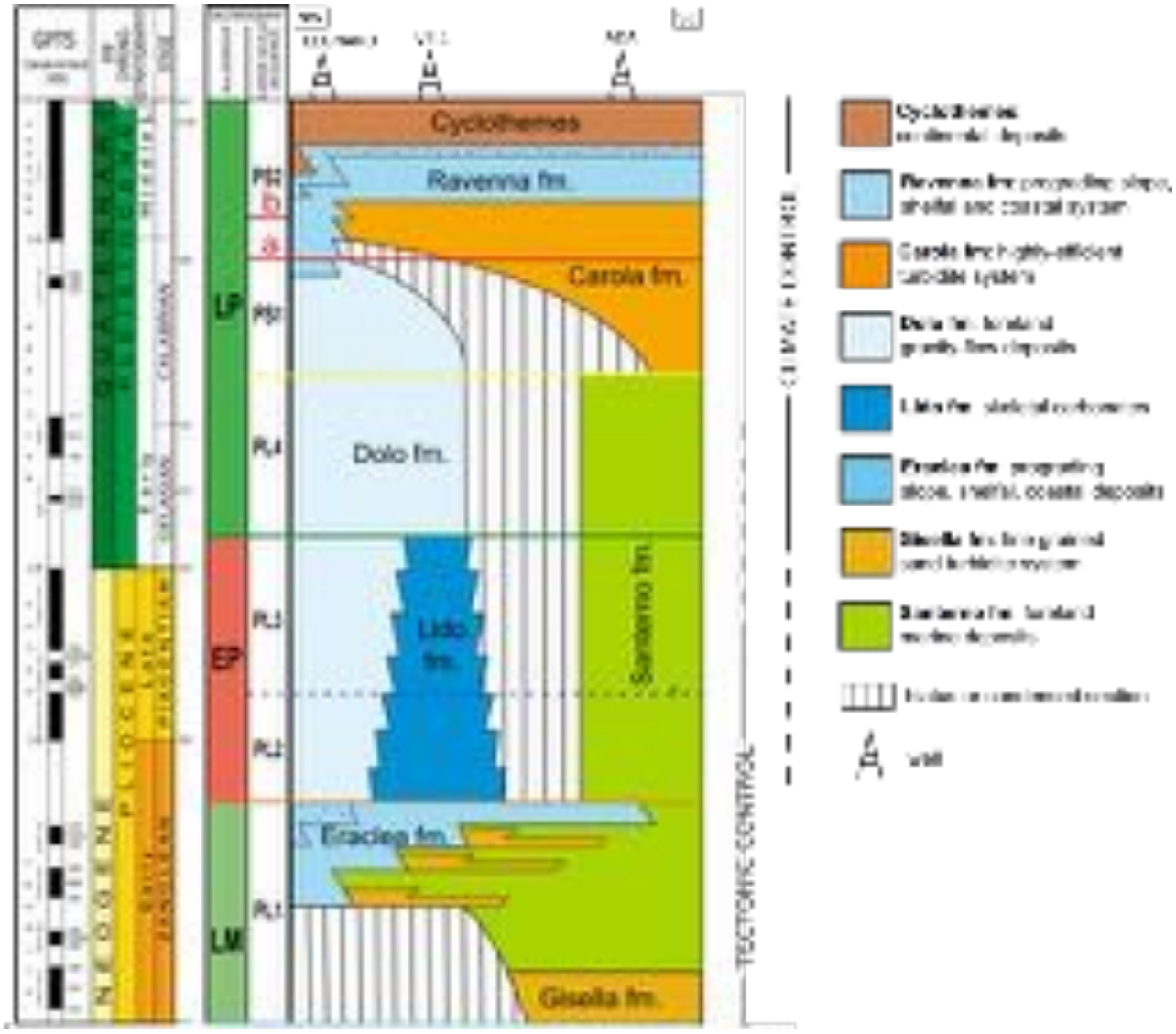

Figure 65. The Plio-Pleistocene stratigraphic framework of the study area along an idealized oblique transect located in the central portion of the basin, from NW to SE. Vertical scale in geologic time, Quaternary base updated after Gibbard et al. (2010) (modified from Ghielmi et al., 2013).

Regarding the studied area, in the early Pliocene, the foreland and foreland ramp were characterized by a non-depositional hiatus or by a condensed deposition of hemipelagic clay (Santerno Fm.) and a southward prograding shallow-marine complex (Eraclea fm.); Eraclea fm. evolves basinward into the foreland fine-grained turbidites system of Gisella fm. (contained also into the PL1 sequence), always confined into Messinian incised valleys (Ghielmi et al., 2013). During late Zanclean-Piacentian time

(PL2+PL3 sequences), shallow-water bioclastic packstones with an upward increasing in siliciclastic fraction were deposited in the area surrounded by Venezia-Lido-Assunta wells due to some favourable warm climatic conditions (last warm Pliocene peaks before the Quaternary climatic deterioration). These characteristic carbonates (Lido fm.) are yielding abundant *Amphistegina* generally associated with *Elphidium spp.* (Barbieri et a., 2007; Ghielmi et al., 2010, 2013). This particular calcarenite levels are widespread through the Mediterranean during the Pliocene (Di Bella et al., 2005 and reference therein); in Italy, coeval levels are recorded in the northern Apennines piggy-back basins (Capozzi and Picotti, 2003; Ghielmi et al., 2010, 2013), central Italy (De Amicis 1886; Conti et al., 1983; Barberi et al., 1994; Iaccarino et al., 1994) and Sicily (Catalano et al., 1998). This foramol carbonate platform (Lido fm.) is locally overlain the Zanclean shallow-water sandstones of Eraclea fm., heteropic and overlaid by the early Plio-middle Pleistocene foreland gravity-flow deposits of Dolo fm.

In the middle Pleistocene (PS1 and PS2 sequences), a drowning (started since the base Gelasian time) of the basin to bathyal depth led to mostly turbidite sedimentation (Carola fm.) (Massari et al., 2004; Ghielmi et al., 2010, 2013; Zecchin and Tosi, 2014) followed by a generalized south-eastward progradation trend in response to the sediment delivered by the paleo-Po River (PS2 sequence). This overall regressive evolution is represented by a thick succession of slope silty clays overlaid by shelfal, coastal and fluvio-deltaic silts and sands of the Ravenna fm.

Since the late Pleistocene, cyclic alternation between shallow-marine to continental deposits resulting from glacio-eustatic changes became the dominant stratigraphic style (Kent et al., 2002; Stefani, 2002; Massari et al., 2004 and reference therein). These cycles form the uppermost unit (UNIT I in Massari et al. 2004) characterised by at least five cycles, including marine shelf and coastal deposits recording maximum flooding stages and related slope ramp sediments (Barbieri et al., 2007).

Thanks to the multidisciplinary method and high-resolution seismics and well log data, eventually, it was possible to detail the middle-late Pleistocene sandy complex, commonly known as “Sabbie di Asti” (Lindquist, 1999; Mancin et al., 2009; Zecchin and Tosi 2014; Toscani et al., 2016; Zecchin et al., 2016; Zecchin et al., 2017). Indeed, sedimentary bodies with different depositional facies and environmental meaning are usually labelled as "Sabbie di Asti".

5.5. Methods and dataset

5.5.1. Chronostratigraphic calibration

In order to reconstruct a high-resolution chronologically calibrated evolution of the Plio-Pleistocene sedimentary prism in the coastal area around Venice, we accounted for published seismic data (Muttoni et al., 2003; Ghielmi et al. 2010, 2013; Zecchin et al., 2014) and 2D lines from Eni's private database (Figs. 66, 67, 68, 69) integrated with well logs in the area roughly bounded by the perimeter formed by Eraclea, Assunta 1, Lido 1, Dolo 1, S. Angelo Piove di Sacco 1, Legnaro 1 dir, Codevigo 1, Civé 1and Arcobaleno 1 wells (from public ViDEPI project), integrated by unpublished supplementary information (well logs; courtesy of Eni Upstream) deriving from Jesolo 1, Ada 1 and Chioggia Mare 1 wells. These wells were chosen because they provide the most complete Plio-Pleistocene stratigraphic sections through the basin. Well logs represent concise and detailed plots of formation parameters versus depth. In particular it is also possible to extract the relationship between porosity, permeability and fluids saturations. Stratigraphic data and well logs are particularly useful in providing additional information for interpreting depositional environments and seismic sequences: abrupt changes in gamma-ray and sonic logs (only available in Arcobaleno 1 well), spontaneous potential (SP) and resistivity (common to all wells) correspond to sharp lithological breaks associated with unconformities and sequence boundaries (Krassay, 1998; Catuneanu, 2006) (Fig. 70).

The chronological calibration was achieved through a complete revision of the 1-km long reference stratigraphic section provided by the continuously cored Venezia 1 well (CNR, 1971), integrated with the nearest correlatable onshore Lido 1 well and by well log data with other onshore (Legnaro 1 dir, Civè 1, Dolo 1 and S. Angelo Piove di Sacco 1) and offshore wells (Assunta 1, Arcobaleno 1, Ada 1 and Chioggia Mare 1). The updated high-resolution age model from the Venice-Lido section was also correlated with the Global Sea level curve by Miller et al. (2005) and the standard isotopic oxygen curve by Lisiecki and Raymo (2005) (Fig. 71). In addition, the transgressive-regressive cyclothemes occurring at the top of VE-1 well (0-300 m deep, referred as UNIT I in Massari et al. 2004) and recognizable in other 8 wells and seismic sections (Eni E&P dataset), were used to date the uppermost cyclic unit deposited during the last 600 kyr.

Biostratigraphic dating of PS2a and PS2b unconformities were also calibrated in the Adriatic offshore and correlated in the Venetian basin by mean of seismics and well log data. In detail, PS2a, also named the "Red surface" (Regione Lombardia and ENI-AGIP, 2002; Garzanti et al., 2011) dated onshore by Muttoni et al. (2003), in offshore it is always included into the MNN19f nannofossil biozone. The PS2b surface, in turn in the Po basin onshore corresponds to the base of the youngest

prograding sequence and was confidently traced in the Adriatic offshore at ca. 600 kyr, just above the last occurrence of *Gephyrocapsa* sp. 3 (Eni Upstream data). This younger depositional sequence is best recognized at the eastern edge of the Po Plain, e.g. in the Venetian area (Kent et al., 2002).

Figure 66. (Next page) Location map and 2D seismic profiles modified from Ghielmi et al. (2010, 2013). Well logs are projected on the seismic lines only if very close to the profile (e.g. less than 2 km distance). The interpreted key horizons represent allogroup and large scale sequence (LSS) boundaries also recognised in Ghielmi et al. (2010, 2013. In this Thesis, they are expressed with the same name and colour code as in Ghielmi et al. (2010, 2013). Light blue: base PL1 Zanclean sequence. Orange: base of EP allogroup and intra-Zanclean PL2 sequence. Blue: Piacentian PL3 sequence, clearly traceable only in seismic profile C, in the Venetian offshore. Dark green: base of LP allogroup and Gelasian PL4 sequence. Yellow: early Calabrian PS1 sequence. Red: Pleistocene PS2a sequence. Dark red: late Pleistocene PS2b sequence. The uppermost horizon PS2b, dated ca. 600 kyr, is newly interpreted in this Thesis. Formations names and stratigraphic details are shown in Fig. 65.

A) 2D seismic section of the Plio-Pleistocene succession in the Venice Lagoon (modified from Ghielmi et al., 2013). Note i) the high amplitude Upper Messinian conglomeratic incised valley fill; ii) the local direction of progradation is towards south for the Lower Pliocene Progradation (Eraclea fm. into PL1 sequence) and towards the NE for the Middle Pleistocene Po Plain Prograding Complex; iii) in this area the prograding complex corresponds to the PS2b sequence and the PS2a sequence is represented by the Carola Fm. turbidites onlapping towards north on the Venetian foreland ramp; iv) the Pleistocene PS2a shelf break, between 1000-1100 ms, on the right side of the seismic profile. The Plio-Pleistocene succession lies on the Oligo-Miocene southwards prograding complex.
B) Regional composite seismic profile, modified from Ghielmi et al. (2013). The coastal wedges visible on the southern margin (latest Tortonian) are later onlapped by Plio-Pleistocene aggradational turbidite systems of the Po Plain-Adriatic Foreland basin, i.e., "inner" (PL3 sequence) and "outer" (PL4 sequence) Porto Garibaldi Fms., deposited during Piacentian-Calabrian time and middle-late Pleistocene Carola Fm. On the left side of the profile, between 600-1500 ms, the PS2a and PL1 shelf break are visible.

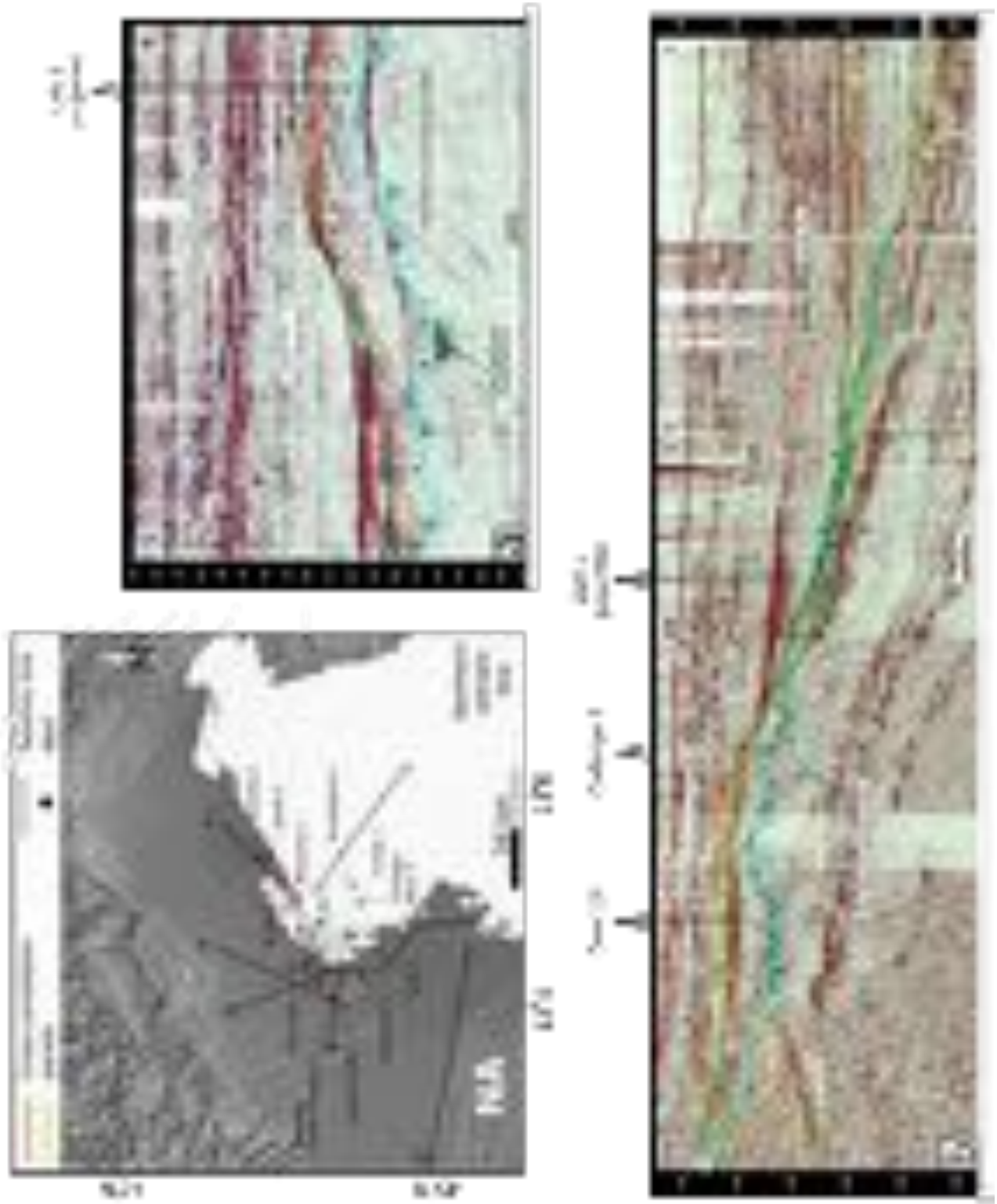

Figure 66. Location map of the seismic dataset analysed. Panels A-B-C are 2D seismic profiles modified from Ghielmi et al. (2010, 2013).

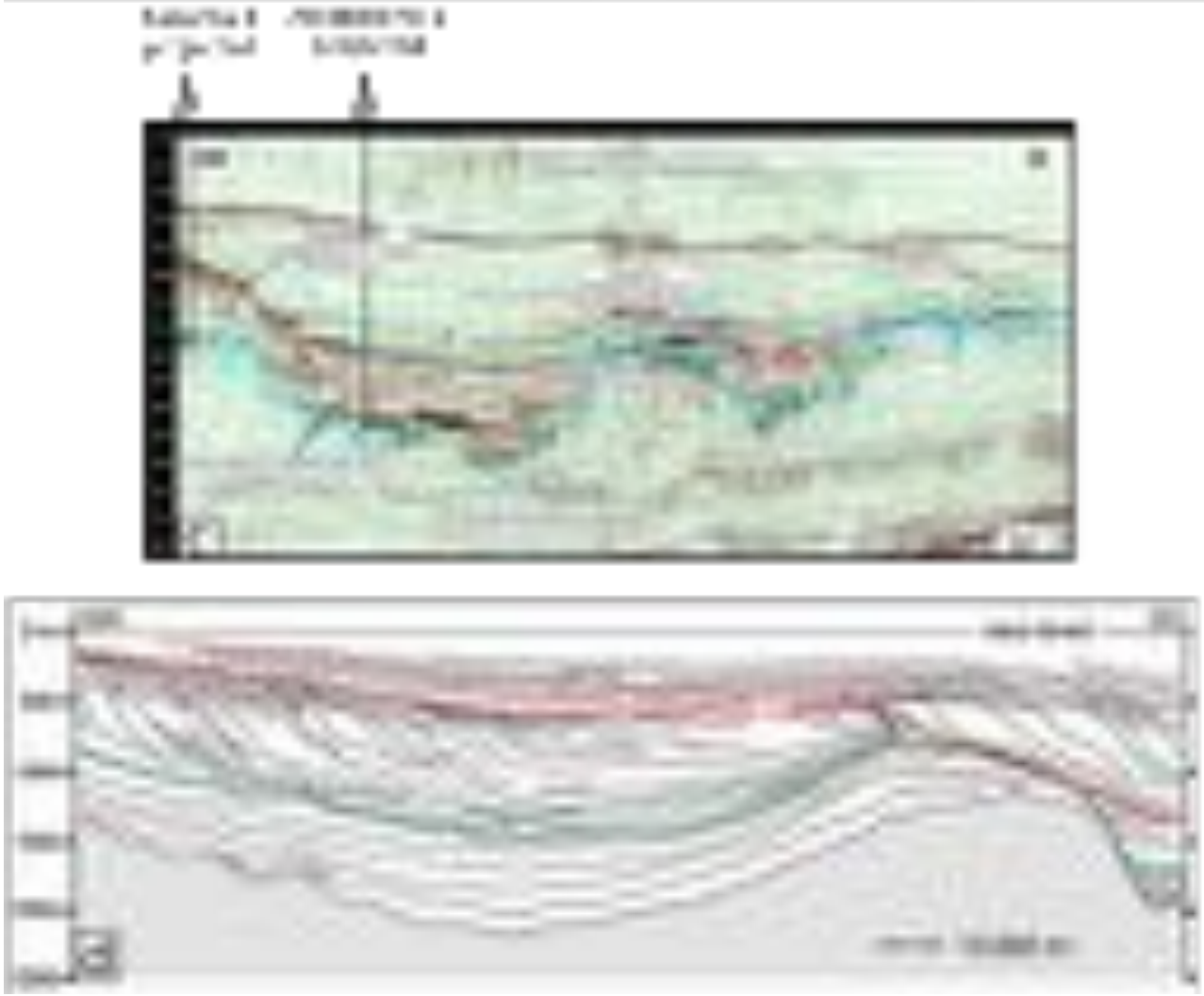

Figure 67. C) 2D seismic profiles modified from Ghielmi et al. (2010, 2013). D) linedrawing modified from Muttoni et al. (2003). See figure 66 for trace locations.
C) Seismic section, modified from Ghielmi et al. (2013). Note: i) the Lower Pliocene Progradation of Eraclea Fm. (PL1 sequence) whose local direction is towards SSE; ii) in this offshore foreland area the Early Pliocene turbidite sedimentation, Gisella Fm. (also included in the PL1 sequence) was confined into the Messinian paleo-valleys. These poorly-efficient turbidites, directly fed by the progradation, were deposited in a foreland setting; iii) in this area the LP allogroup boundary (PL4) is represented by a subaqueous surface of no deposition-condensation (Ghielmi et al., 2013). At this location, the hiatus/condensed section comprises the sediments of the PL4 and PS1 Sequences and the basal part of the PS2 sequence (Ghielmi et al., 2013). Here, the Piacentian PL3 sequence is present and confined into the offshore foreland; this unit is not expressed in the onshore sector.
D) linedrawing, modified from Muttoni et al. (2003) where is evident the shelf break of the PS2a horizon. The vertical axis is in depth domain (m). LP is the base of the Pleistocene allogroup which contains the Calabrian progradation phase, under the PS2a sequence boundary/basal surface produced in response to sea level lowering due to the Alpine glaciation during MIS 22.

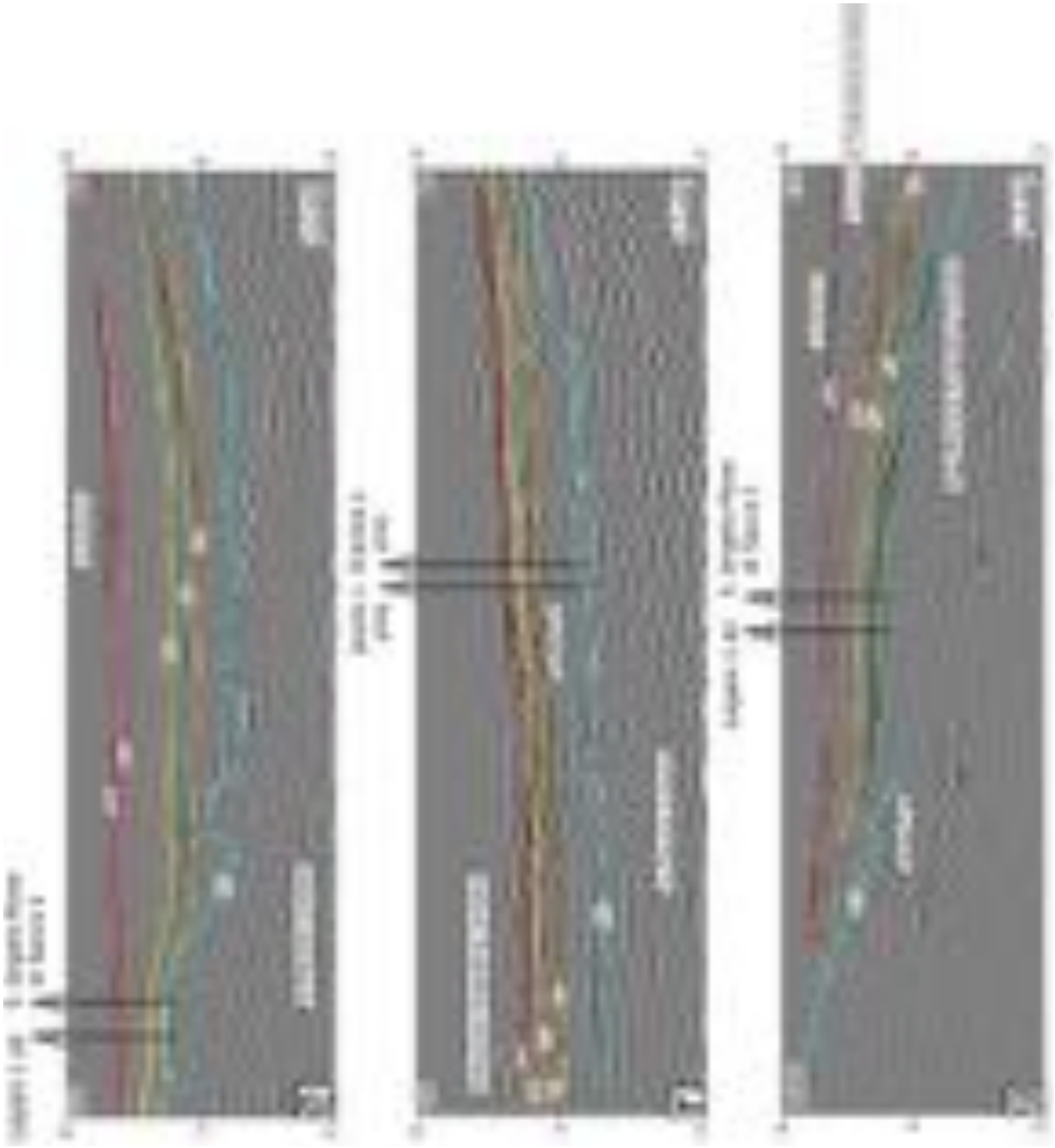

Figure 68. Seismic lines from Eni Upstream private dataset (vertical scales in TWT). See Fig. 66 for location. Wells are projected on the seismic lines only if very close to the profile (e.g. less than 2 km distance). The interpreted key horizons represent allogroup and large scale sequence (LSS) boundaries also recognised in Ghielmi et al. (2010, 2013). In this Thesis, they are expressed with the same name and colour code as in Ghielmi et al. (2010, 2013). Light blue: base PL1 Zanclean sequence. Orange: base of EP allogroup and intra-Zanclean PL2 sequence. Blue: Piacentian PL3 sequence, clearly traceable only in seismic profile C, in the Venetian offshore. Dark green: base of LP allogroup and base Gelasian PL4 sequence. Yellow: early Calabrian PS1 sequence. Red: Pleistocene PS2a sequence. Dark red: late Pleistocene PS2b sequence. The uppermost horizon PS2b, dated ca. 600 kyr, is newly interpreted in this Thesis. Formations names and stratigraphic details are shown in Fig. 65.

E) this section shows the inland closure and thinning of the Pliocene-middle Pleistocene sequences on the SW margin of the Venetian basin. Legnaro 1 dir and S. Angelo Piove di Sacco 1 wells record the condensed Pliocene succession and the late Pleistocene cyclothems. Since the seismic trace orientation is nearly parallel to the strike of the Pleistocene Prograding complex, this sequence appears horizontal or gently dipping. Instead, the early Pliocene Eraclea fm. (PL1 sequence) southwards progradation direction is visible.

F) here, is well visible the early Pliocene southwards prograding complex and the opposite Pleistocene northwards onlapping complex.

G) eastern Venetian basin higher margin where all the Plio-Pleistocene sequences pinch-out against the western sector. There is also visible the PS2a shelf-break.

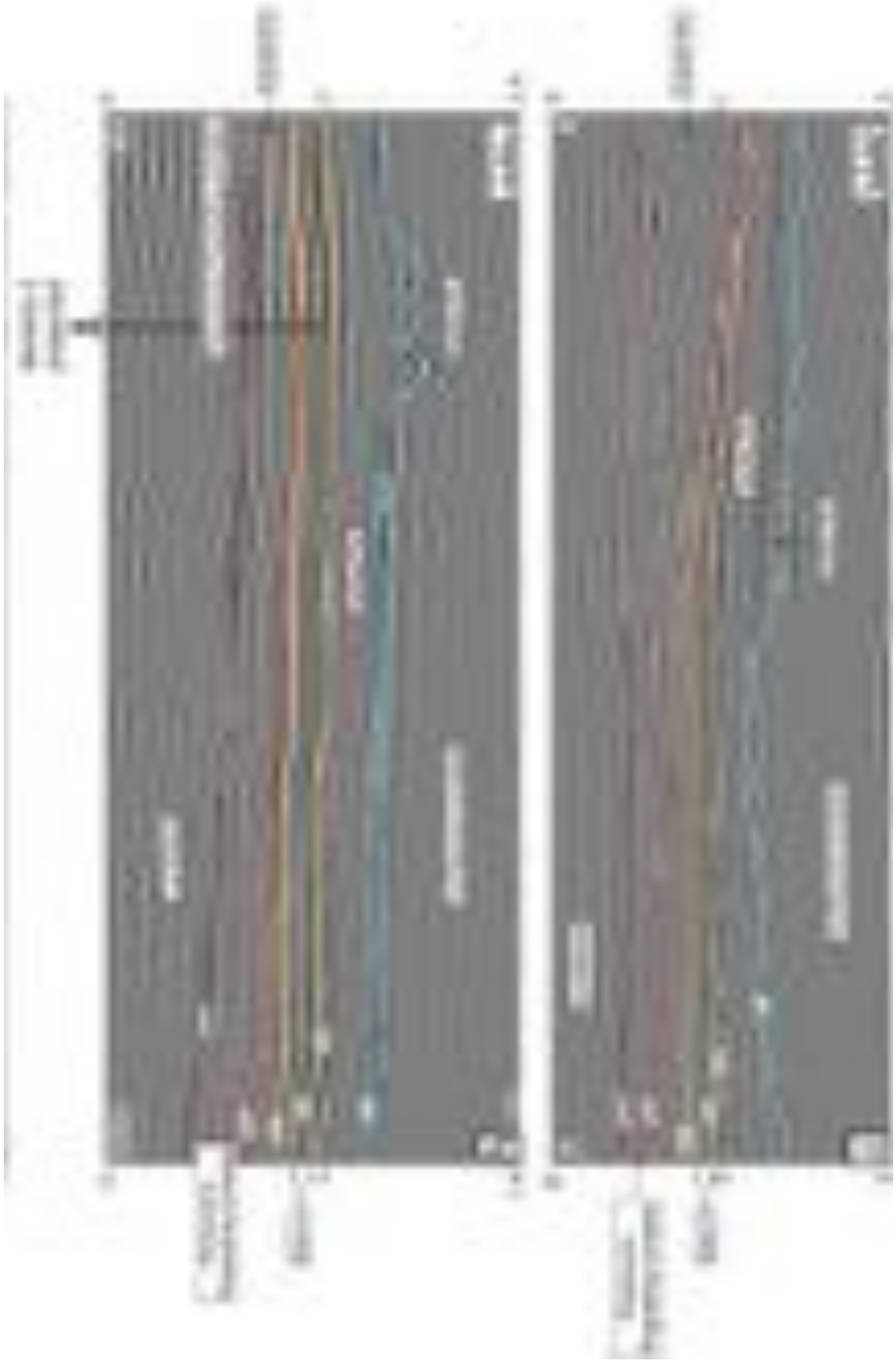

Figure 69. Seismic lines from Eni Upstream private dataset (vertical scales in TWT). See Fig. 66 for location. Wells are projected on the seismic lines only if very close to the profile (e.g. less than 2 km distance).
H) 2D seismic line from Eni dataset, modified and reinterpreted from Zecchin et al. (2014) according with the new chronostratigraphic interpretation of the Venetia 1 well and the Venetia-Friulian Plio-Pleistocene basin infilling, proposed in this Thesis.
I) here, is visible: i) the PS2a shelf break; ii) the PS2a sequence is made of the Pleistocene southwards Prograding Complex (visible on the left side of the profile) and the turbidites of Carola fm. onlapping towards north on the Pliocene-Calabrian eroded margin (similar features are visible in Fig. 66 A, B).

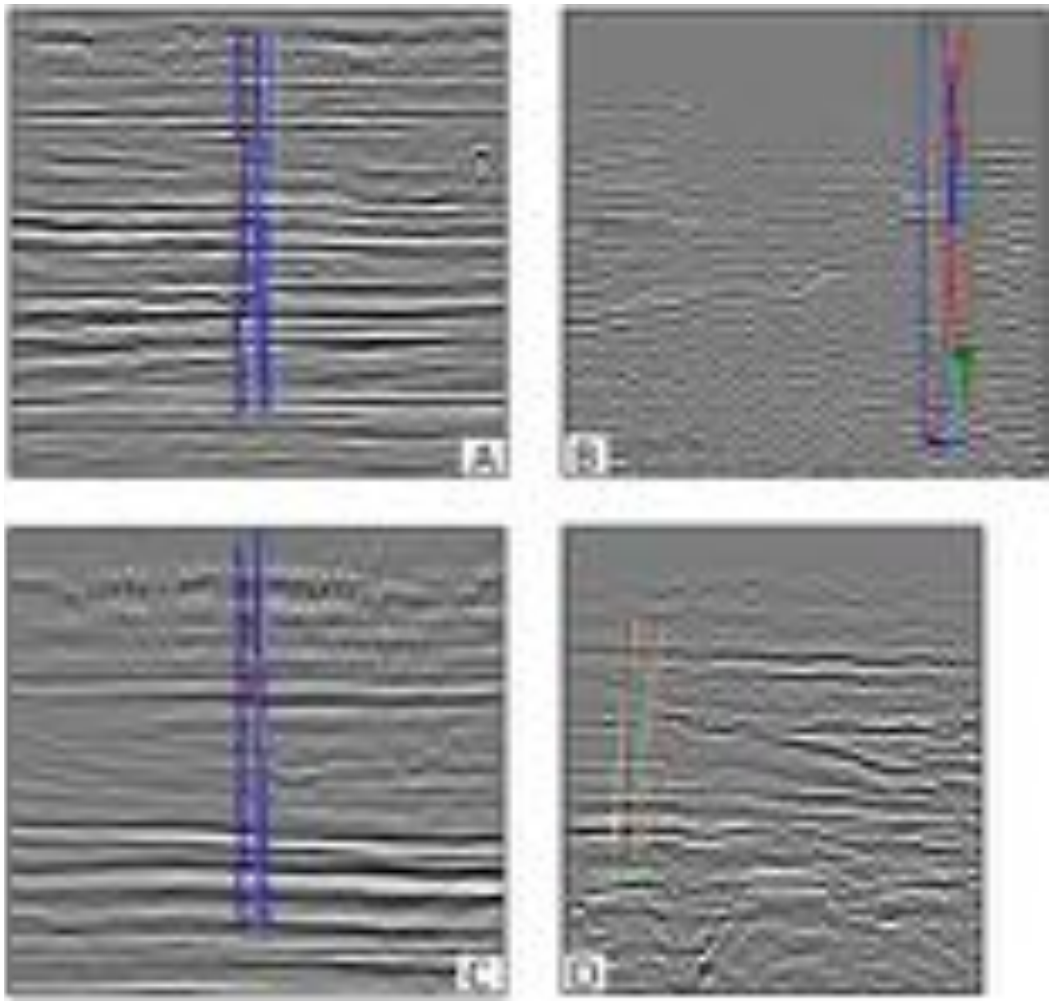

Figure 70. Examples of well logs projected on 2D seismic lines, from Eni private database. A) Lido 1 well. B) Assunta 1 well. C) Venezia 1 well. D) Dolo 1 dir well. Wells location in figs. 70 and 66.

5.5.2. Micropaleontological analysis

In order to refine the chronological frame and to obtain entirely new paleobathymetric information necessary to perform geohistory analysis, further micropaleontological analyses were performed (in collaboration with Nicoletta Mancin) on ca. 60 samples picked within the Plio-Pleistocene record of four key wells: Eraclea 1 and Jesolo 1 onshore, and Ada 1 and Assunta 1 offshore (core data courtesy of Eni Upstream).

Each rock sample (mostly cuttings integrated, limitedly to the Ada 1 well, by wall cores) was prepared as washed residue and analysed under a stereomicroscope in its foraminiferal content (both planktonic and benthic taxa) according to the analytical procedures described in Mancin et al. (2016). These data provide also an independent control on palaeodepth information that can be obtained by geometries (e.g. clinoforms) visible in seismics.

5.5.3. Geohistory

1D-backstripping analysis on the Plio-Pleistocene sequence where performed in order to investigate the sedimentation rate from the decompacted sedimentary succession and unravel some clues on the basin history, in this case on the interplay between sediment supply, tectonics and climate. This analysis was done using BasinMod2014 software (by Platt River Associates) on wells where palaeobathymetry data were available (Venice 1, Eraclea 1, Jesolo 1, Ada 1 and Assunta 1 wells) (Tab. 4, 5, 6, 7, 8).

The software follows the quantitative approach and algorithms proposed by Van Hinte (1978) and Allen and Allen (1990). The following input data were used for the geohistory analysis: ages of the sequence boundary (according with the new age model), unit present thickness, rock properties (i.e. lithology expressed in percentage of sand, shale and limestone from the well log analysis), porosity curve (only available in the case of the case of Venice 1, CNR 1971) and the average palaeo-water depth provided through micropaleontological analysis. Also, we used the global eustatic curves from Haq et al. (1987) and Miller et al. (2005) for late Quaternary, as a reference for global sea-level changes during the last 5 Ma.

Calculation are performed on individual units with different decompaction algorithms based on lithologic and facies analysis: exponential method (Sclater and Christie, 1981) for high sedimentation rate units (e.g. turbidites), reciprocal method for low sedimentation rate units (Falvey & Middleton, 1981) and the Baldwind & Butler (1985) equation for shales.

ADA 1 WELL							Paleobathymetry (m)		
Unit	**type**	**End age (Ma)**	**top depth (m)**	**Present thickness (m)**	**Lithology (%)**	**Decompaction algorithms**	**Min**	**Average**	**Max**
mis 5	Formation	0	0	127	sand 72 - shale 28	EXP	0	25	50
mis 7	Formation	0.123	127	50	sand 68 - shale 32	EXP	0	25	50
mis 9	Formation	0.217	177	43	sand 63 - shale 37	EXP	0	25	50
mis 11	Formation	0.325	220	55	sand 60 - shale 40	EXP	0	25	50
mis 13	Formation	0.41	275	100	sand 68 - shale 32	EXP	0	25	50
upper Ravenna	Formation	0.504	375	225	sand 74 - shale 26	EXP	100	150	200
lower Ravenna	Formation	0.53	600	70	sand 66 - shale 34	EXP	100	350	600
Upper Carola	Formation	0.58	670	100	sand 82 - shale 18	EXP	100	350	600
lower Carola	Formation	0.6	770	644	sand 68 - shale 32	EXP	600	800	1000
PS2a	Formation	0.87	1118414	66	sand 68 - shale 32	EXP	600	800	1000
PL4 - Upper Santerno	Formation	1.6	1118480	104	sand 92 - shale 8	EXP	200	600	1000
PL2	Formation	2.4	1118584	46	Shale 100	BB	600	1300	2000
PL1	Formation	4	1118630	67	Shale 100	BB	600	1300	2000

Tab.4. Input table for geohistory analysis of Ada 1 well. EXP: exponential method (Sclater and Christie, 1981). BB: Baldwind & Butler (1985) equation.

ASSUNTA 1 WELL							Paleobathymetry (m)		
Unit	**type**	**End age (Ma)**	**top depth (m)**	**Present thickness (m)**	**Lithology (%)**	**Decompaction algorithms**	**Min**	**Average**	**Max**
mis 5	Formation	0	0	100	sand 30 - shale 70	EXP	0	25	50
mis 7	Formation	0.123	100	45	sand 69 - shale 10	EXP	0	25	50
mis 9	Formation	0.217	145	40	sand 75 - shale 25	EXP	0	25	50
mis 11	Formation	0.325	185	35	sand 86 - shale 14	EXP	0	25	50
mis 13	Formation	0.41	220	90	sand 75 - shale 25	EXP	0	25	50
upper Ravenna	Formation	0.504	310	90	sand 33 - shale 67	EXP	100	150	200
lower Ravenna	Formation	0.53	400	140	sand 20 - shale 80	EXP	100	350	600
uppermost Carola	Formation	0.58	540	60	sand 70 - shale 30	EXP	100	350	600
upper Carola	Formation	0.6	600	175	sand 80 - shale 20	EXP	100	350	600
Carola - PS1	Formation	0.87	775	25	sand 20 - shale 80	EXP	100	350	600
Carola - PL4	Formation	1.7	800	73	sand 90 - shale 10	EXP	100	350	600
Lido - PL2	Formation	2.4	873	53	100 Limestone (grainstone)	RCP	0	50	100
PL1	Formation	3.9	926	499	sand 74 - shale 26	EXP	600	1300	2000

Tab.5. Input table for geohistory analysis of Assunta 1 well. Yellow values are data reconstructed from the adjacent Ada 1 well. EXP: exponential method (Sclater and Christie, 1981). RCP: reciprocal method (Falvey & Middleton, 1981).

ERACLEA 1 WELL							Paleobathymetry (m)		
Unit	**type**	**End age (Ma)**	**top depth (m)**	**Present thickness (m)**	**Lithology (%)**	**Decompaction algorithms**	**Min**	**Average**	**Max**
mis 5	Formation	0	0	95	sand 95 – shale 5	EXP	0	25	50
mis 7	Formation	0.123	95	32	sand 72 – shale 28	EXP	0	25	50
mis 9	Formation	0.217	127	22	sand 77 – shale 23	EXP	0	25	50
mis 11	Formation	0.325	149	41	sand 85 – shale 15	EXP	0	25	50
mis 13	Formation	0.41	190	100	sand 81 – shale 19	EXP	0	25	50
upper Ravenna	Formation	0.504	290	65	sand 83 – shale 17	EXP	100	150	200
upper Ravenna	Formation	0.53	355	130	sand 79 – shale 21	EXP	100	350	600
Carola	Formation	0.58	485	120	sand 82 – shale 18	EXP	100	350	600
Dolo	Formation	0.87	605	135	sand 87 – shale 13	EXP	100	350	600
Upper Eraclea	Formation	2.4	740	45	sand 82 - shale 18	EXP	100	350	600
Lower Eraclea	Formation	4	785	55	sand 90 – shale 10	EXP	0	50	100
lower Eraclea	Formation	4.09	840	100	sand 85 – shale 15	EXP	100	350	600
Gisella	Formation	4.25	940	160	sand 70 – shale 30	EXP	200	600	1000

Tab.6. Input table for geohistory analysis of Eraclea 1 well. Yellow values are data reconstructed from the adjacent Assunta 1 well. EXP: exponential method (Sclater and Christie, 1981).

JESOLO 1 WELL							Paleobathymetry (m)		
Unit	**type**	**End age (Ma)**	**top depth (m)**	**Present thickness (m)**	**Lithology (%)**	**Decompaction algorithms**	**Min**	**Average**	**Max**
Cyclothems	Formation	0	0	250	sand 88 - shale 12	EXP	0	25	50
upper Ravenna	Formation	0.5	250	65	sand 88 - shale 12	EXP	100	150	200
lower Ravenna	Formation	0.53	315	191	sand 82 - shale 18	EXP	100	350	600
Carola	Formation	0.6	506	119	sand 71 - shale 28	EXP	100	350	600
Dolo (Santerno)	Formation	0.87	625	115	sand 74 - shale 26	EXP	100	350	600
Upper Eraclea	Formation	2.4	740	115	sand 69 - shale 31	EXP	0	50	100
Lower Eraclea	Formation	4	855	80	sand 59 - shale 41	EXP	100	350	600
Gisella	Formation	4.25	935	135	sand 36 - shale 64	BB	200	600	1000

Tab.7. Input table for geohistory analysis of Jesolo 1 well. EXP: exponential method (Sclater and Christie, 1981). BB: Baldwind & Butler (1985) equation.

5.6. Results

5.6.1. High-resolution chronologic calibration

Pleistocene subsurface succession of the central Po Plain and northern Adriatic Sea is well time-constrained by biostratigraphic markers (Eni's internal studies) which combined with magnetostratigraphic analysis (Kent et al., 2002; Muttoni et al., 2003; Scardia et al., 2006, Garzanti et al., 2011), allows to track the main horizons through the entire basin.

In the Venetian basin instead, owing a very high core recovery (90%), the deep test core Venice 1 (CNR, 1971) has been described and analysed in detail (e.g. Kent et al., 2002; Massari et al., 2004; Barbieri et al., 2007 and reference therein). Specifically, the key-study by Kent and co-authors proposed two possible age models, due to the possible meanings given to the bioevent *Pseudoemiliana lacunosa* HO (highest occurrence) at 562.4m depth and its relation with the *Pseudoemiliana lacunosa* last-appearance datum (LAD) astro-chronologically calibrated at 0.467 Ma (Lourens et al., 2004, 2005; Raffi et al., 2006).

The two models result in different chronostratigraphic calibrations of the uppermost 600m of the Venice section, and particularly of the uppermost unit from 0 to 300m depth (UNIT I in Massari et al. 2004). This unit is poorly constrained by bioevents, as the only two robust chronological key-points are provided by the presence of Eemian pollens at -77.8m depth in correspondence with a transgressive-regressive surface, dated 0.123 Ma related to MIS 5.5 peak (Bassinots et al., 1994, Mullenders et al., 1996) and by a superficial paleosoil (named *Caranto,* at 7.7m depth) dated between 0.018-0.007 Ma through C^{14} (Bortolami et al., 1977). When *P. lacunosa* HO is considered to fit its LAD, the model outcome (Age Model 2 in Kent et al. 2002) shows an isolated uplift event during the late Pleistocene (in particular in the last 200 kyr; Kent et al. 2002) difficult to explain in the given tectonic setting. Furthermore, in the resulting time span there are too many transgressive-regressive cycles recorded in the Venice core to be easily correlated with major glacio-eustatic features occurring in the global curve. By contrast, if the highest occurrence of *P. lacunosa* in the Venice core occurred earlier respect to its LAD, the correlation of the transgressive-regressive events and the pollen datum (Mullenders et al., 1996; Kent et al., 2002) recorded by the Venice section fit with the most important global glacio-eustatic highstands and lowstands occurred during the last 500 kyr (Miller et al., 2005) and the subsidence trend does not show any late Quaternary isolated uplift peak (Kent et al., 2002).

Considering the absence of independent evidence for tectonic activity during late Pleistocene in the Venice area that could account for such uplift peak (Fantoni et al., 2002), suggested also by the gradual onlap of the Calabrian PS1 turbidites on the foreland ramp and by the undeformed sediments

of the PS2 Seq. deposited above (Ghielmi et al., 2013), we decided to not consider valid the *P. lacunosa* LAD and thus apply the Age Model 1 proposed by Kent et al. (2002), differently respect to several other recent papers (e.g. Barbieri et al., 2007; Zecchin and Tosi 2014; Zecchin et al., 2016; Zecchin et al., 2017).

According to this preliminary review, in this work a complete chronostratigraphic update of the Age Model 1 by Kent et al. (2002) was performed according with the most recent Neogene magneto-bio-cyclostratigraphy ATNTS 2004 by Lourens et al. (2004), Muttoni et al. (2003), Cita et al. (2008) and Bertini et al. (2010) and Eni's internal report.

The resulting new age model provides the chronological key-point to calibrate the time-surfaces in the entire Venetian- Northern Adriatic basin (Figs. 66, 67, Tab. 4, 5, 6, 7, 8).

A peculiar problem is the chronological calibration of the uppermost cyclic unit; due to the lack of magnetostratigraphic and biostratigraphic constraints, it can be achieved through the correlation with Marine Isotope Stages, (Shackleton, 1995; Lisiecki and Raymo, 2005, 2007) and the eustatic curve (Miller et al., 2005). Five lithologic cycles (cyclothems) made by marine-continental deposits are clearly recognizable in the Venice core. These cyclothems have been for the first time laterally correlated from onshore to offshore through well-log diagnostic expressions of TR cycles particularly clear looking at the resistivity curve, and available for all wells. This cyclicity is supposed to be driven by the strong late Quaternary climatic oscillations, punctuated by several major transgressive intervals; it is completely expressed in Legnaro 1 dir, S. Angelo Piove di Sacco 1 dir, Venezia 1, Lido 1, Assunta 1, Eraclea 1, Arcobaleno 1 and Ada 1 wells, and can be referred to the MIS 13, MIS 11, MIS 9, MIS 7, MIS 5e, MIS 1 of the global isotopic curve. Only northwestward (Legnaro 1 dir well) it is possible to recognize one older cycle, referable to the MIS 15. In Chioggia 1 and Dolo 1 wells only the 5^{th} cycle, referable to the MIS 13, is recorded due to the lack of the upper part of the section while, in Codevigo 1 and Jesolo 1 wells the available electric and lithologic record starts deeper than the cyclothems unit.

As a result, the proposed new age model linking each transgressive-regressive (TR) cycle to Milankovitch 100 kyr frequencies (Laskar et al., 2004) supporting the strong influence of allocyclic parameters on Venetian basin sedimentation during middle-late Pleistocene (Fig. 65).

Stage	***Depth in core (m)***	***Events***	***New Age (Ma)***	***MIS***	***New References***
Holocene	0-7.7		0.007-0.018	MIS 1	Kent et al., 2002 (age model 1); Massari et al., 2004
	7.7			Pleistocene/Holocene Hiatus	Kent et al., 2002 (age model 1); Massari et al., 2004
Taran-tian	7.7		0.018	MIS 2 (peak)	Kent et al., 2002 (age model 1); Massari et al., 2004
	77.8	Eemian flora	0.123	MIS 5.5 (peak)	Kent et al., 2002 (age model 1); Massari et al., 2004
Ionian	110	2nd Cycle	0.217	7	this work
	153	3rd Cycle	0.325	9	this work
	199	4th Cycle	0.410	11	this work
	248	5th Cycle	0.504	13	this work
	558.6-559.1	sapropel Sa	0.553	MIS 14	Lourens et al., 2004, 2005; Kent et al., 2002 (age model 1)
	560	PS2b	0.59	MIS 15	this work
	571.05-571.68	HO *Gephyrocapsa* sp.3	0.597	MIS 15	Lourens et al., 2004, 2005
	572.62-573.4	sapropel Sb	0.618	MIS 15/16	Lourens et al., 2004, 2005
	727.28	Brunhes/Matuyama	0.781	MIS 19	Lourens et al., 2004, 2005
	745	PS2a	0.87	MIS 22	Muttoni et al., 2003
	750-758	LO *Gephyrocapsa* sp. 3	0.963	MIS 25/26	Lourens et al., 2004, 2005
Calabrian	772	*Neogloboquadrina pachyderma* sx PE	1.21-1.22	MIS 36	Lourens et al., 2004; Cita et al., 2008
	778.98-780.86	HO Large *Gephyrocapsa* spp.	1.245	MIS 37/38	Cita et al., 2008; Raffi et al., 2006
	780	HIATUS			Massari et al., 2004
	783.23-783.5	sapropel VS03	1.378	MIS44	Laskar et al., 2004
	783.48-784.95	*Neogloboquadrina pachyderma* sx PB	1.367-1.37	MIS 44	Cita et al., 2008
	784.87-784.97	sapropel VS04	1.4	MIS 45	Laskar et al., 2004
	786.2-786.4	sapropel VS05	1.43	MIS 47	Laskar et al., 2004
	787.94-788.57	sapropel VS06	1.452	MIS 47	Laskar et al., 2004
	789.85-790.21	sapropel VS07	1.473	MIS 48/49	Laskar et al., 2004
	795.90-796.62	sapropel VS08	1.566	MIS 53	Laskar et al., 2004
	797.88-798.68	sapropel VS09	1.586	54/55	Laskar et al., 2004
	799.22-799.4	sapropel VS10	1.605	MIS 55	Laskar et al., 2004
	800.83-801.46	LO *Large Gephyrocapsa* spp.	1.608-1.62	MIS 55	Raffi et al., 2006; Cita et al., 2008
	800.95-801.52	sapropel VS11	1.624	MIS 56	Laskar et al., 2004
	802.32-802.59	sapropel VS12	1.644	MIS 57/58	Laskar et al., 2004
	806.04-806.07	sapropel VS13	1.663	MIS 58	Laskar et al., 2004
	808.04-808.54	sapropel VS14	1.718	MIS 60/61	Laskar et al., 2004
	809.4-809.98	LO *Gephyrocapsa oceanica* s.l	1.718	MIS 60/61	Massari et al., 2004
	808.89-809.35	sapropel VS15	1.738	MIS61	Laskar et al., 2004
	809.89-810.35	sapropel VS16	1.759	MIS 62/63	Laskar et al., 2004
	812.5-814.1	FCO *Neogloboquadrina pachyderma* sx	1.79	MIS 64	Cita et al., 2008
	812.42-812.67	sapropel VS17	1.8	MIS 65	Laskar et al., 2004; Bertini et al., 2010
	818	PS1	ca. 1.8		Ghielmi et al., 2010, 2013
Gelas ian	887.2	top Reunion	2.128	MIS 81	Kent et al., 2002; Lourens et al., 2005
	940	PL4	2.4	MIS 94	Ghielmi et al., 2010, 2013

Tab.8. Biomagnetostratigraphic age control points for the Venice succession from Kent et al. (2002) and Massari et al. (2004). Events depth in core by Massari et al. (2004). Sapropel layers of the Venice succession, with a correlation with Site 967 (Lourens et al., 1998a), Vrica section of Crotone Basin (Lourens et al., 1996b) are reinterpreted and correlated with insolation cycles from Laskar et al., (2004).

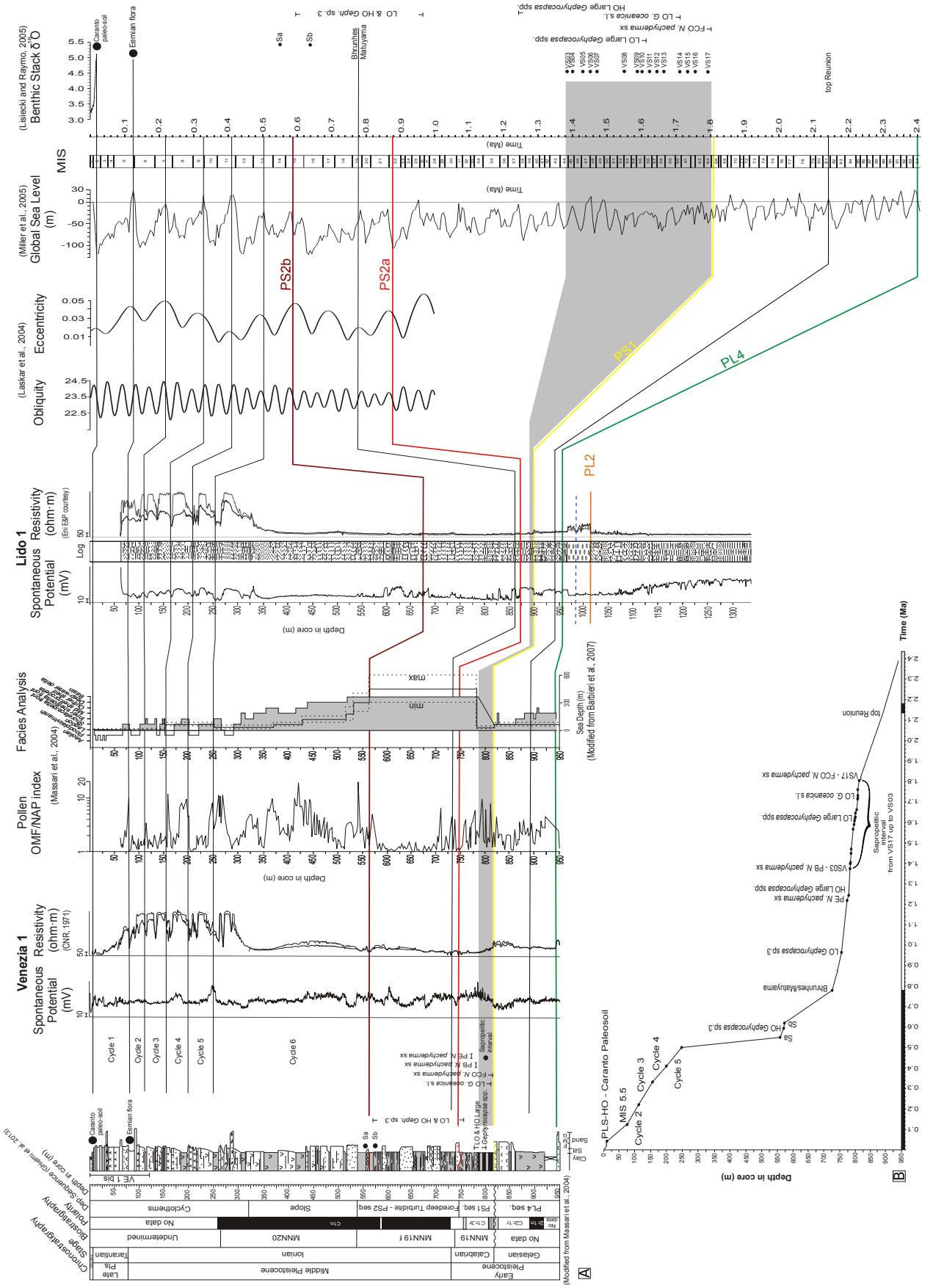

Figure 71. Chrono-magneto-bio-stratigraphic cross correlation section of Venezia 1 and Lido 1 wells. Name and colour code from Ghielmi et al. (2010, 2013). PL2: intra-Zanclean sequence boundary; PL3: intra-Piacenzian sequence boundary; PL4: Gelasian sequence boundary; PS1: early Calabrian sequence boundary; PS2a, PS2b: middle-upper Pleistocene sequence boundaries.
B) Age model of Venezia 1 well.

5.6.2. Paleobathymetry of Plio-Pleistocene depositional units

As a whole, samples picked in the studied depositional units contained quite abundant foraminiferal assemblages, diverse and well preserved. Displaced depth-constrained benthic species were quite rare and limited to particular stratigraphic intervals (e.g., Gisella and Santerno formations in the lower portion of the PL1 sequence, Figs. 66, 67); thus, foraminifera assemblages provided reliable paleo-water depth information.

The Zanclean PL1 sequence has been recorded in all the four studied wells (Figs. 72, 73, 74, 75). Foraminifera recovered in the foreland turbidites of the Gisella fm. were characterized by very abundant planktonic taxa, with percentages around 80% in the lower portion of the unit then sharply decreasing upwards, reaching values of 5% in the upper part (Assunta 1 well, Fig. 72). Benthic foraminifera were less abundant and represented by deep-water index species such as: *Oridorsalis umbonatus*, *Lenticulina* spp., *Marginulina spinulosa, Gyroidinoides neosoldanii*, and *Uvigerina peregrina,* indicative of middle-lower bathyal bathymetries (ca. 600-2000 m) and corresponding to a supposed average paleo-water depth of ca.1300 m. In the upper portion of the unit, the deepest benthic index species (e.g. *O. umbonatus*) disappeared and middle bathyal indexes (mostly *Lenticulina* and *Marginulina*) increased in abundance, indicating a probable decrease in the paleo-water depth, that reached values of ca. 600-1000 m. Note that towards NE, in the onshore Eraclea and Jesolo wells, similar turbiditic deposits contained quite different foraminiferal assemblages: planktonic taxa were less abundant whereas benthic taxa were dominated by shallower upper-middle bathyal indexes (*Lenticulina* and *Marginulina costata*), lacking also the deepest species *O. umbonatus*. This result has been interpreted as indicative of shallower bathymetries (ca. 200-1000 m) probably due to a deeper in the basin of the stated wells with respect to the Assunta 1 well. Southwards, in the Ada 1 well (Fig. 73), the time-equivalent fine-grained deposits of the Santerno fm. contained foraminiferal assemblages very similar to the ones recorded in the turbidites of the Gisella fm. (Assunta well). Planktonic taxa were quite abundant (ca. 60-70%) and benthic taxa were mostly represented by deep-water index species (*Oridorsalis umbonatus* and *Lenticulina* spp.) indicative of middle-lower bathyal bathymetries (ca. 600-2000 m) with a supposed paleo-water depth of ca. 1300 m.

Moving upwards in the upper PL1 sequence (Eraclea fm.), foraminifera assemblages progressively changed, testifying a probable shallowing upward paleobathymetric trend (Assunta 1, Eraclea 1 and Jesolo 1 wells, Figs. 72, 74, 75). In the lower portion of the Eraclea fm., corresponding to prograding slope deposits (Assunta 1and Eraclea 1 wells), foraminiferal assemblages were rare but still characterised by deep-water benthic species, such as the genera *Lenticulina* and *Marginulina* and the species *Uvigerina peregrina,* indicative of upper-middle bathyal bathymetries (average depth of

ca.600 m); these deep-water species were sometimes mixed with reworked upper neritic taxa (the genera *Ammonia*, *Amphistegina* and *Elphidium)* transported down-slope by currents. Up to top, within the shelf deposits of the upper Eraclea fm., most of the deep-water taxa were replaced by neritic indexes (e.g. miliolids, *Elphidium*, *Ammonia*) indicating a further progressive decreasing paleobathymetry that probably reached depths of ca. 100 m. Southwards, in the Ada 1 well (Fig. 73), foraminiferal assemblages from the time-equivalent basinal deposits of the Santerno fm. did not register any significant change, indicating a probable constant deep-water environment with a supposed average paleo-depth of ca. 1300 m during the whole PL1 sequence.

Even the upper Zanclean-Piacenzian PL2-PL3 sequence has been recorded in all the four studied wells although represented by different time-equivalent sedimentary units. Offshore, in the Assunta well, the PL2 sequence is formed by skeletal carbonates (Lido fm.) that laterally pass towards NE, in the onshore Eraclea 1 and Jesolo 1 wells, to terrigenous platform deposits (upper Eraclea fm.) while, towards SE, in the offshore Ada well, the time-equivalent sedimentation is represented by fine-grained basinal deposits belonging to the Santerno fm.. Foraminifera recovered in the PL2 sequence mirror this depositional variation; in particular foraminiferal assemblages from the carbonatic Lido fm. were dominated by upper neritic indexes (particularly the larger symbiont-bearing genus *Amphistegina*, in assemblage with *Elphidium* and the species *Asterigerinata planorbis*) together with very rare planktonics (usually less than 5%). This assemblage is indicative of average palaeo-water depths not exceeding 50 m, probably even shallower, around 20-25 m. Similar bathymetries can be hypothesised also for the time-equivalent shelf deposits recorded in the Eraclea and Jesolo wells containing very similar foraminiferal assemblages still dominated by the upper neritic indexes *Elphidium* and *Ammonia*. On the contrary, foraminifera from the basinal Santerno group were mostly represented by middle-lower bathyal indexes (*O. umbonatus*, *Heterolepa bellincionii*, *Gyroidinoides soldanii* and *Uvigerina peregrina*) still indicative of average paleo-depths of ca. 1300 m.

The Piacenzian-lower Gelasian PL3 sequence is highly condensed and difficult to recognize in the studied wells, while the overlaying Pleistocene PL4-PS2 sequences have been recorded in all the studied wells. In particular, foraminifera recovered in the Gelasian PL4 sequence, southwards represented by the Santerno group (Ada 1 well), showed a moderate decrease of lower bathyal indexes (*O. umbonatus* and *Lenticulina* spp.) coupled with an increase of middle-upper bathyal indexes (*H. floridana*, *H. bellincionii*, *G. soldanii* and *Bulimina marginata*) with respect to the assemblages from the underlying deposits of the PL2 sequence. This datum has been interpreted as indicative of shallower bathymetries probably with average palaeo-depths of ca. 600 m. To note, however, that these bathyal indexes were mixed with displaced upper neritic taxa (particularly the genus *Elphidium* in assemblage with miliolids, *Cibicides lobatulus* and *Asterigerinata planorbis*) probably transported

down-slope by currents. Due to high sedimentation rate, in such a depositional context, it is quite common that most of the foraminiferal faunas occurring within cuttings has been transported down slope by gravity currents, within the deeper faunas thus, we cannot definitely exclude a deeper bathymetry (ca. 1300 m) for these foreland deposits, similar to the one hypothesized for the underlying PL 2 sequence. Towards NE, the time-equivalent deposits of the PL4 sequence are represented by foredeep sand-rich turbidites (Carola fm.; Assunta 1 well) containing foraminiferal assemblages characterised by less abundant planktonics (ca. 10%) and lower neritic-upper bathyal indexes (*B. marginata*, *H. bellincionii*, *H. baltica*, *P. arimenensis*) indicative of average paleo-depths of ca. 350-400 m. Unfortunately, in the onshore Eraclea 1 well, the Pleistocene sequences were not sampled. In the very close Jesolo 1 well only one sample from the lowermost portion of the Carola fm. was collected at 740 m depth. This sample contained foraminiferal assemblages characterised by abundant lower neritic-upper bathyal indexes (*Heterolepa bellincionii*, *H. floridana*, *Hyalinea baltica*, *Planulina ariminensis*, *Pullenia bulloides* and *Uvigerina* spp.) identical to the ones recorded in the Assunta well and indicative of supposed average paleo-depths of ca. 350 m.

Moving upwards, within the PS1 and PS2 sequences (foredeep turbidites of the Carola fm.; Ada 1 well) foraminiferal assemblages gradually changed. At first, planktonic taxa increased in abundance (values of over 70%), particularly in the lower-middle portion of the unit (corresponding to the PS1 and PS2a sequences) and then, they sharply decreased (5-10%) in its upper part (lower PS2b sequence), testifying a probable increasing-decreasing paleobathymetric trend. Benthic foraminiferal assemblages support this interpretation. In the lower-middle portion of the Carola fm. (PS1-PS2a sequences, Ada 1 well) benthic taxa were mostly represented by middle bathyal indexes indicative of palaeo-depths of ca. 600-1000 m then replaced up to top in the lower PS2b sequence, by lower neritic-upper bathyal indexes that also strongly increased in abundance (*U. peregrina*, *H. baltica*, *Cassidulina neocarinata* and *Bulimina marginata*) testifying a progressive decrease of bathymetry with supposed paleo-depths of ca. 350 m. Similar results can be inferred from the time-equivalent turbiditic deposits of the upper Carola fm. recorded in the adjacent Assunta 1 well (Fig. 72).

The shallowest portion of the middle-upper Pleistocene PS2b sequence (corresponding to the deposition of the Ravenna fm. and upper Pleistocene cyclothems) has been studied in its foraminiferal content only in the Ada 1 well (Fig. 73). Foraminifera from the slope deposits forming the lower Ravenna fm. were identical to the ones recorded in the underlying turbidites of the upper Carola fm. and were characterised by less abundant planktonics (10-15%) in assemblages with abundant lower neritic-upper bathyal benthic index such as the species *Hyalinea baltica*, *Cassidulina neocarinata* and *Bulimina marginata*. Moving upwards in the shelf to coastal deposits of the upper Ravenna fm., the assemblages progressively changed (planktonics further decreased in abundance and upper

bathyal indexes disappeared or were replaced by lower neritic indexes) a paleobathymetric testifying decreasing trend with supposed palaeo-water depths of ca. 100-200 m. This regressive trend is accentuated in the overlying upper Pleistocene deposits (Cyclothems), where planktonic foraminifera were totally absent and benthic taxa were rare and exclusively represented by shallower upper neritic indexes such as the littoral genera *Ammonia* and *Elphidium* and the species *Cibicides lobatulus* indicative of very shallow bathymetries (0-50 m depth).

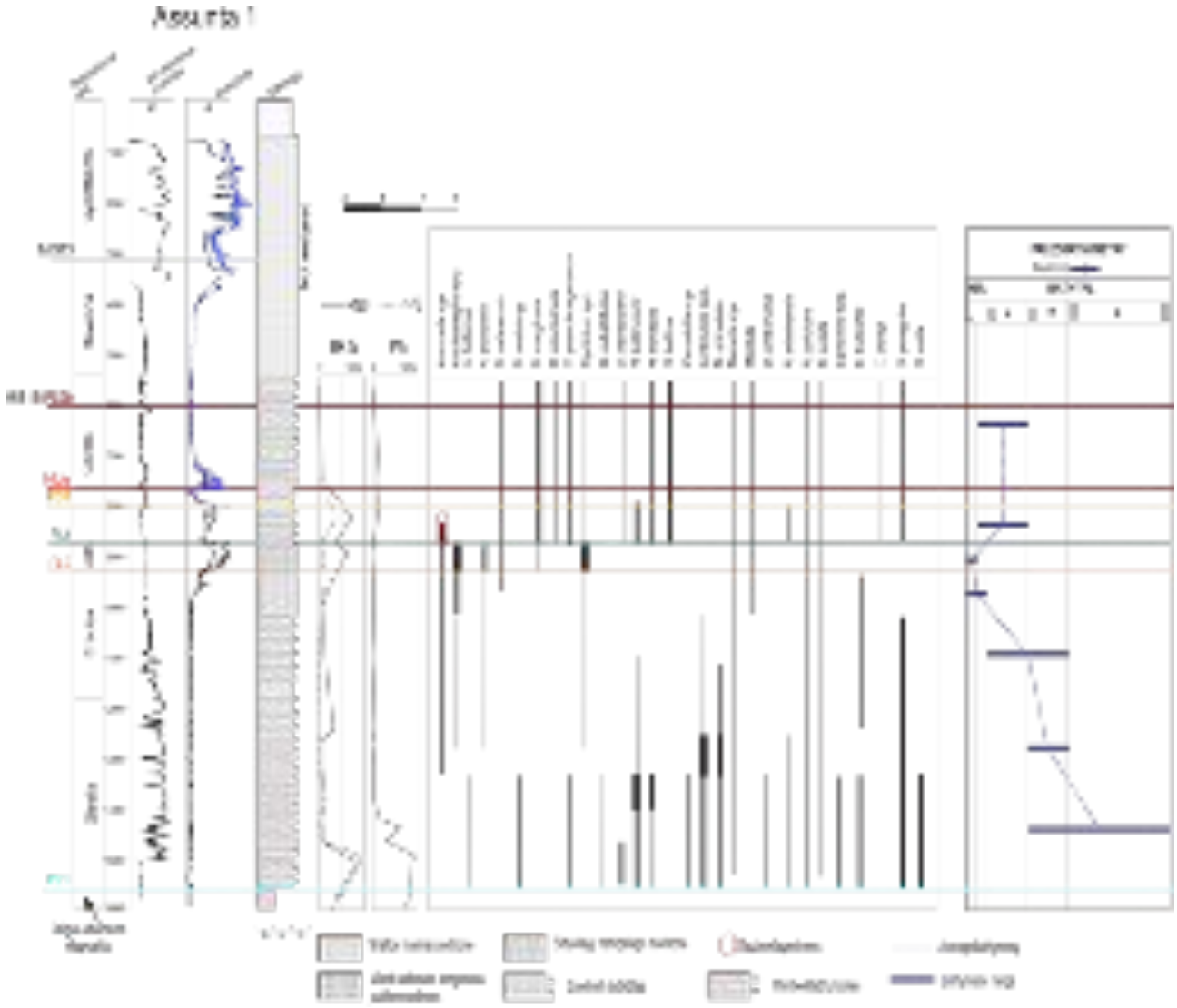

Figure 72. Biostratigraphic and paleobathymetry analysis of Assunta 1 well.

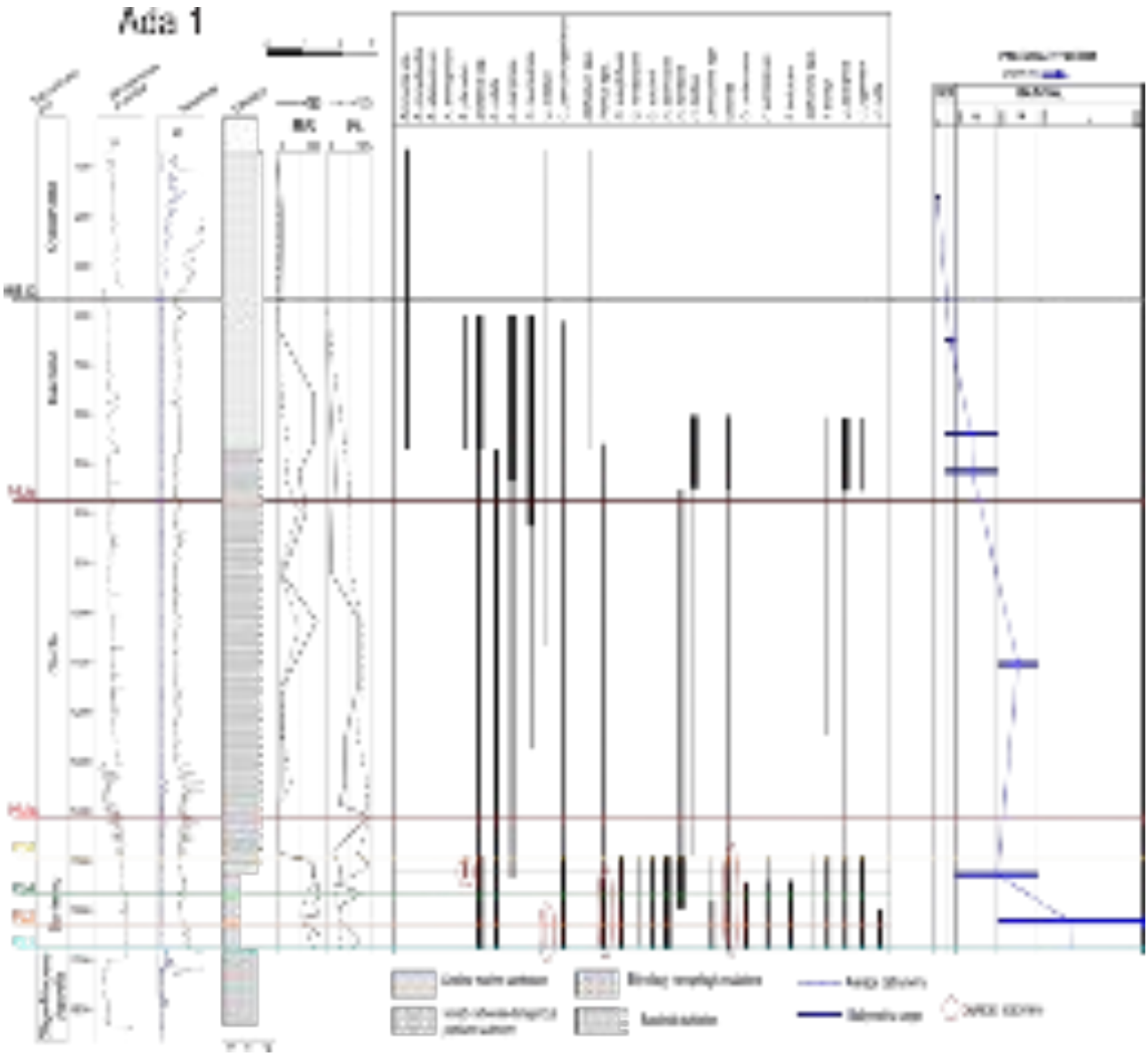

Figure 73. Biostratigraphic and paleobathymetry analysis of Ada 1 well.

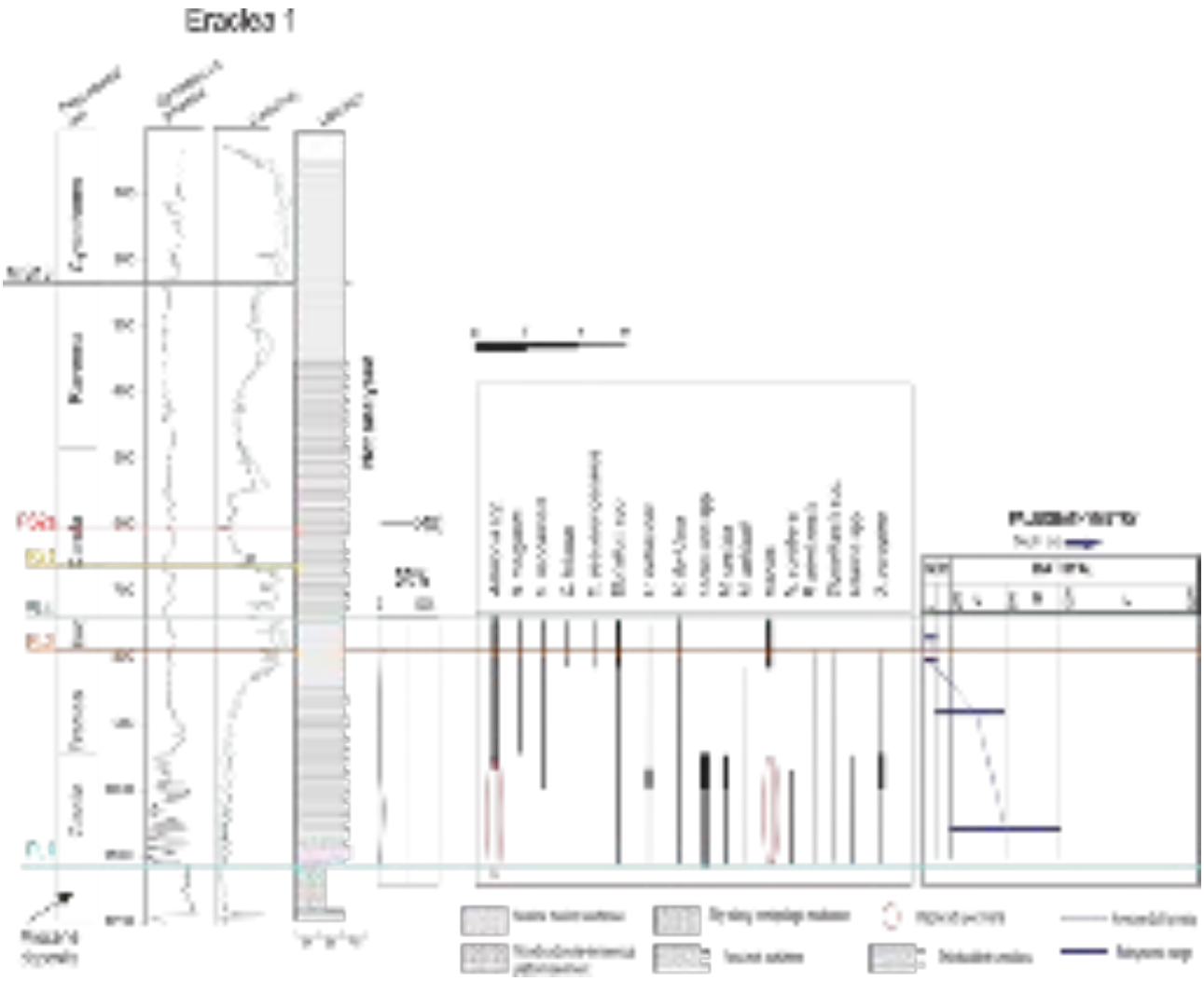

Figure 74. Biostratigraphic and paleobathymetry analysis of Eraclea 1 well.

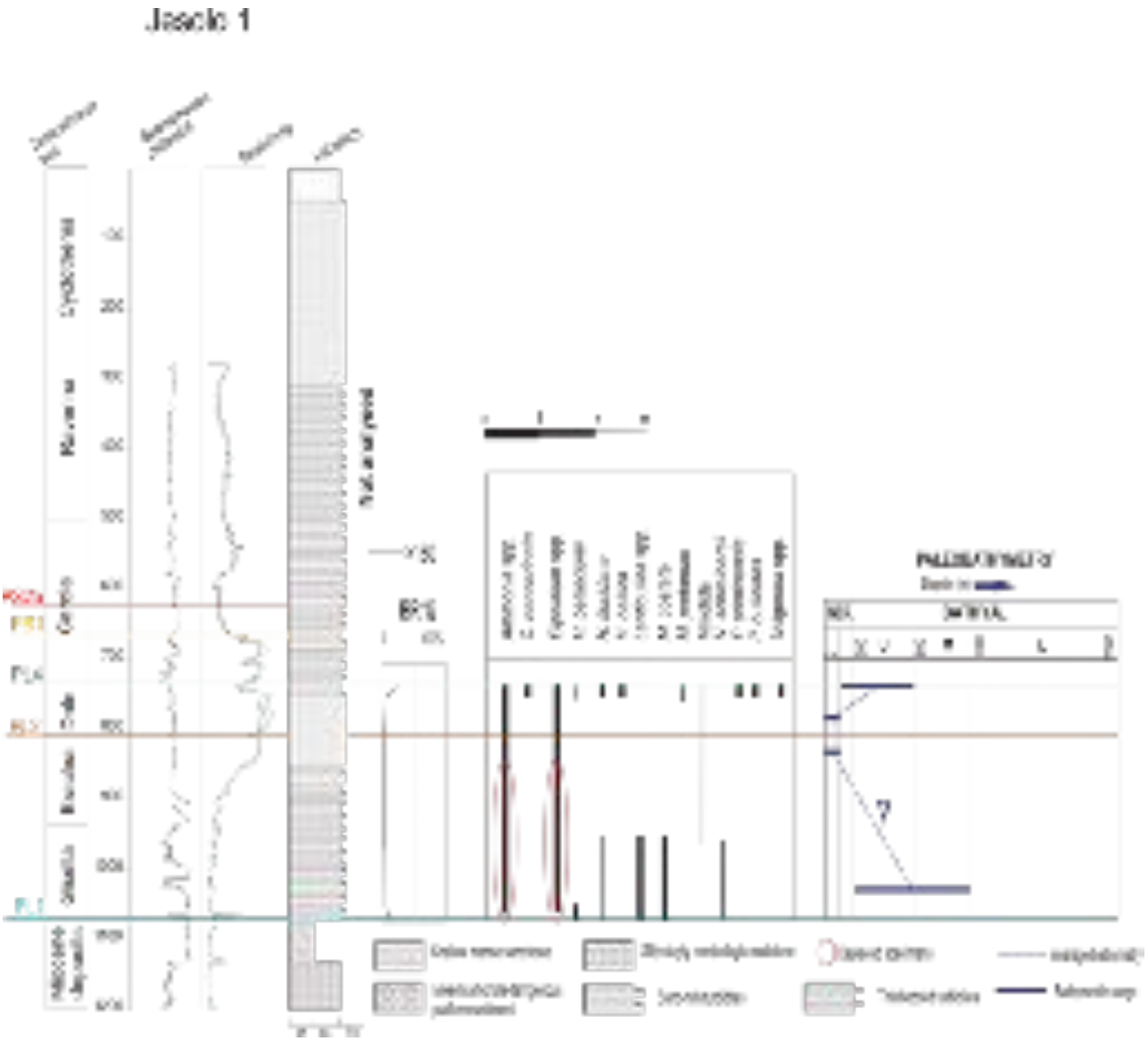

Figure 75. Biostratigraphic and paleobathymetry analysis of Jesolo 1 well.

5.6.3. Geohistory

The 1D-backstripping analysis was performed to extract decompacted sedimentation rates (m/Ma), in order to study the Venice coastal prism evolution during Pliocene-Pleistocene time.

Sedimentation rate curve is calculated on each well using average, minimum and maximum water depths from palaeobathymetry analysis. For sake of simplicity, here will be described only the curves obtained for the average palaeo-water depth (Fig. 76).

In this work, the total and tectonic subsidence will be not commented, because it is not the aim of this study to stress on the magnitude and deep-sources of the tectonic compound and subsidence and uplift response (e.g., slab retreating).

In the Venetian-Friulian and Northern-Adriatic basins the base of the Zanclean PL1 sequence cannot be completely described for two reasons: i) the sedimentation was highly condensed during the Zanclean regional mega flooding, occurred in the Mediterranean basin at the end of the Messinian Salinity Crisis (Garcia-Castellanos et al., 2009); ii) not the entire well dataset reach the bottom Pliocene.

The average sedimentation rate starts with a peak of ca. 500 m/Ma (maximum value ca. 1000 m/Ma recorded in Assunta 1 well), presumably correlated to the early Zanclean prograding prograding shelf-slope deposits of Eraclea Fm.. The prograding geometry is well visible in the seismic lines in figures 66, 67, 68, 69. In turn, at the end of the Zanclean PL2-PL3 sequence, low average sedimentation rates (ca. 400 m/Ma in average) are recorded. A higher peak during Piacenzian, about 1000-1500 m/Ma average value (maximum value of 2000 m/Ma recorded in Assunta 1 well), precedes a long period with lower rates (average lower than 100 m/Ma). This low sedimentation rate occurred for almost 2 Ma, until middle-late Quaternary. In fact, during Gelasian time, the PL4 sedimentary unit was lithologically represented by the condensed foreland clays of Dolo fm. and foramol carbonate platform (Lido fm.)

Following these low values, a sedimentation rate high peak increased from Calabrian, recording the turbidite sediments of Carola fm. and the Po Plain Prograding Complex (PS2 sequence).

Sedimentation rate increased rapidly from 900 kyr up to the highest average value of 7000 m/Ma, reached between 600-500 kyr (the highest value of ca. 10,000 m/Ma is recorded in Ada 1 well). During the last 500 kyr, sedimentation rates decreased, oscillating between ca. 500 and 1000 m/Ma in average.

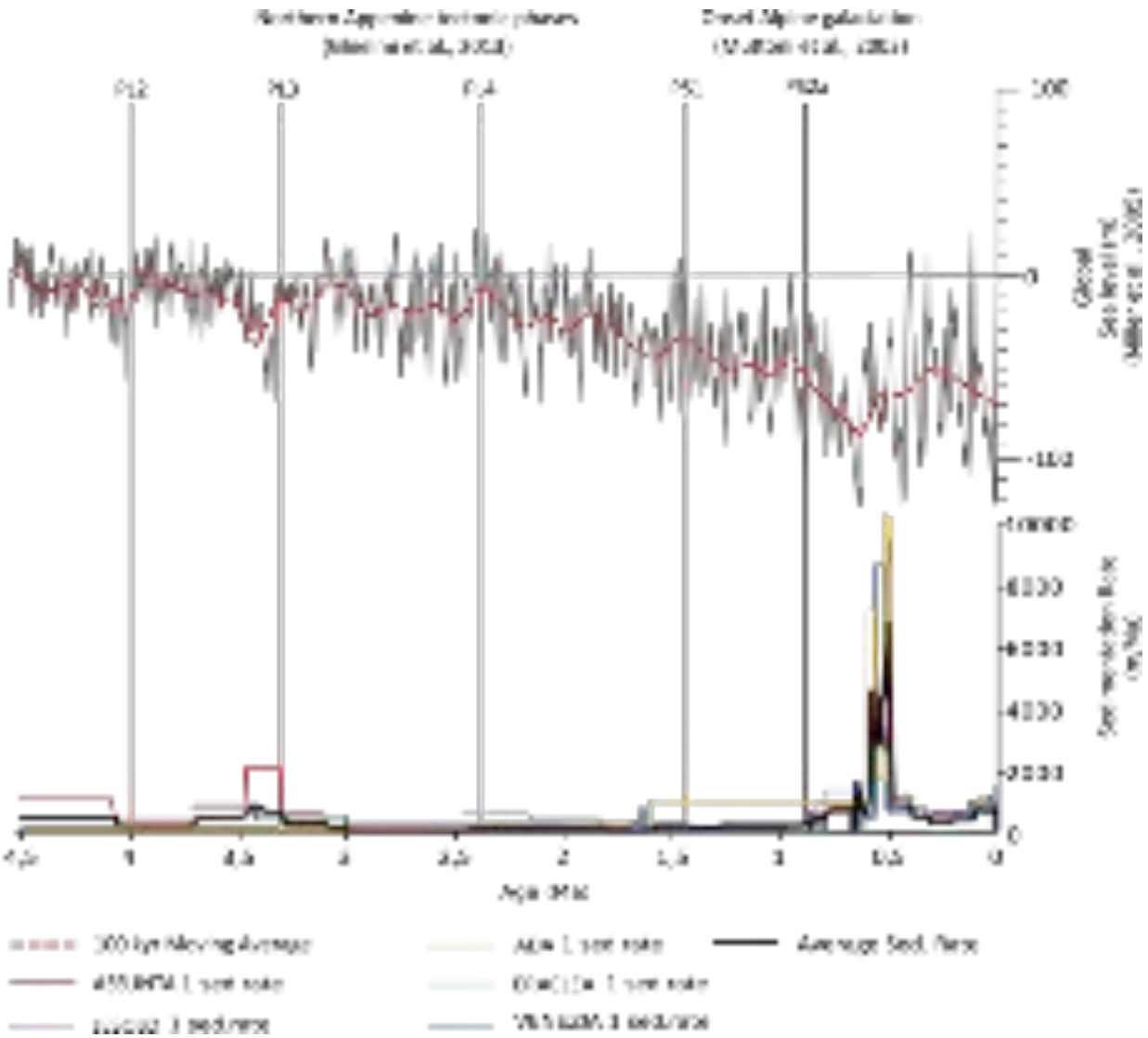

Figure 76. At the top of the figure is represented in dark grey the global sea level curve from Miller et al. (2005) and the dashed red curve is the same curve with a moving average window every 100 kyr. The lower part of the figure shows the geohistory outputs. Solid black bold line is the average sedimentation rate, obtained from decompacted thickness, of the analysed wells: Assunta 1, Ada 1, Eraclea 1, Jesolo 1 and Venezia 1 wells.

5.6.4. Shelf edge trajectories

We plotted the well-log correlations into three cross correlation panels (Figs. 77, 78), including complementary information on shelf break geometries provided by seismic interpretation (Fig. 66, 67, 68, 69), parallel and transversal oriented to the main sedimentary prograding bodies present in the study area (i.e., PL1 sequence with Eracela fm., and PS2 seq. with the Middle Pleistocene Po Plain Prograding Complex). Thus, the three resulting subsurface panels can be considered as depth-calibrated geological profiles, useful to trace shelf edge migration and progradation directions since the base Zanclean marine transgression to late Pleistocene (Figs. 79, 80).

In Fig. 79, shelf edge at PL1, PS2a, PS2b time-sequence (Ghielmi et al., 2010; Scardia et al., 2012; Ghielmi et al., 2013) are shown in map view. In Fig. 80 in turn, it is possible to quantify the basin-scale Plio-Pleistocene regressive cycle through the horizontal km-shift of the shelf edge (landward or basinward).

Since late Miocene the PPAF was a deep, subsiding foredeep basin: during the early Zanclean (PL1 sequence) the Emilia-Romagna and Ferrara arcs were not structured yet and the central-eastern Po Plain appeared as a Northern Adriatic gulf, with a shelf break ca. WNW-ESE oriented, parallel to the foredeep axes (Ghielmi et al., 2010, 2013).

In the VFB instead, a coeval early Zanclean complex (Eraclea fm.) developed prograding towards S-SE; PL1 sequence shelf break curved northwards into the recent Adriatic offshore, 25-50m far from the present coastline (Figs. 79, 80). The Eraclea fm. shelf edge and slope are visible in seismic (Figs. 66, 67, 68, 69), we interpret the sandstones in Codevigo 1, Lido 1, Legnaro 1 dir, S. Angelo Piove di Sacco 1, Assunta, Jesolo 1 and Eraclea 1 wells as shelf and coastal deposits into PL1 unit.

During the Pleistocene, due to Gelasian and Calabrian tectonic phases (forming LP allogroup with PL4, PS1 and PS2a sequences) the PPAF was affected by important geometrical modification due to the Emilia, Ferrara-Romagna syn-sedimentary thrust NE-migration together with a very high sedimentary input which progressively filled the fragmented foredeep depressions (Maesano and D'Ambrogi, 2016). This last Pleistocene tectonic PS2a phase (less intense than the previous ones) affected the PPAF contemporaneously with the onset of Alpine glaciation, dated 0.87 My according with Muttoni et al. (2003), causing a relative sea-level regression, continental exposure of the Venice shelf-slope break and early Pleistocene prograding complexes located far inland out from the study area (Figs. 79, 80).

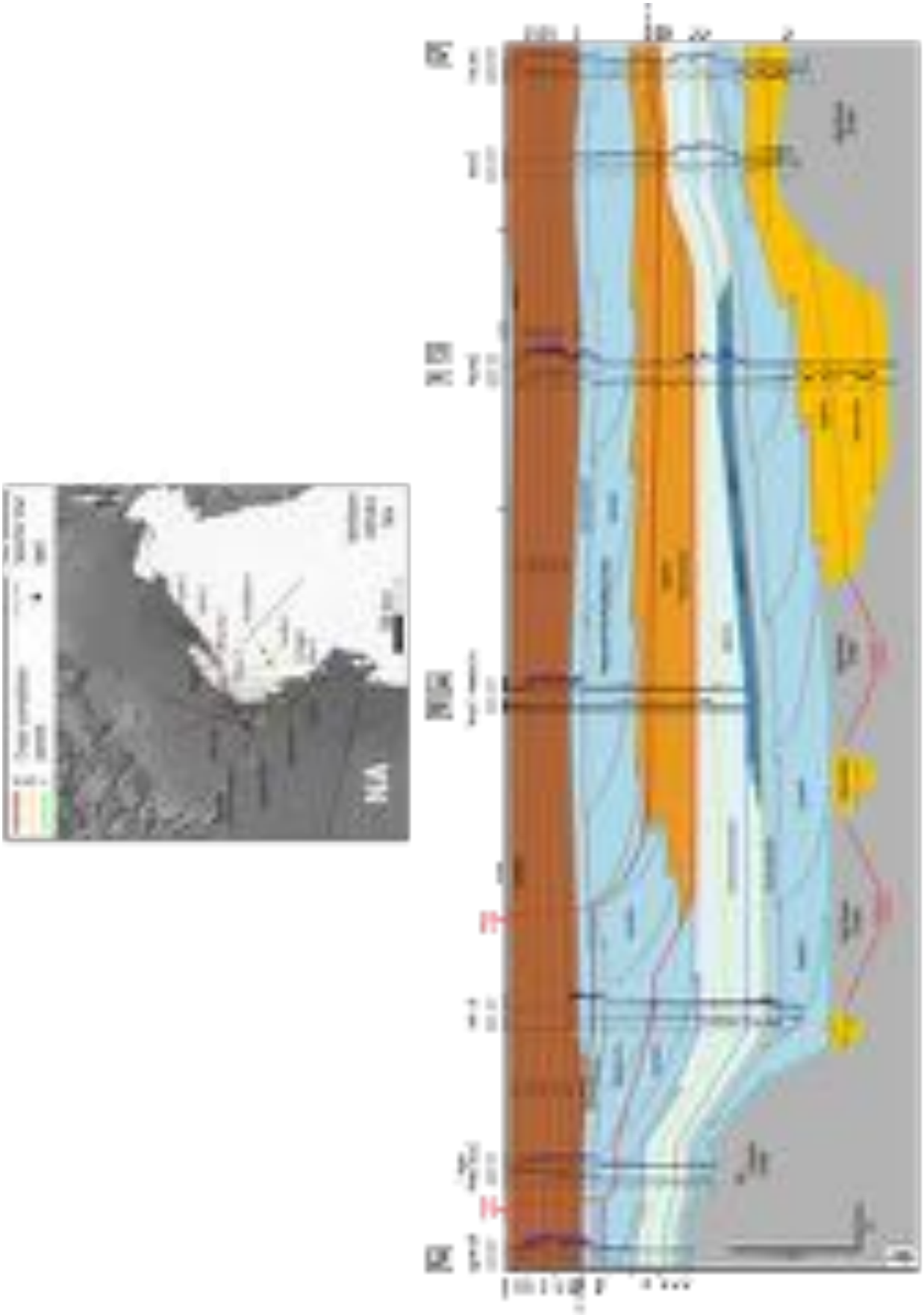

Figure 77. Cross correlation panels from well logs correlations. A) Transect ca. SW-NE. Colour code of the stratigraphy in Fig. 65.

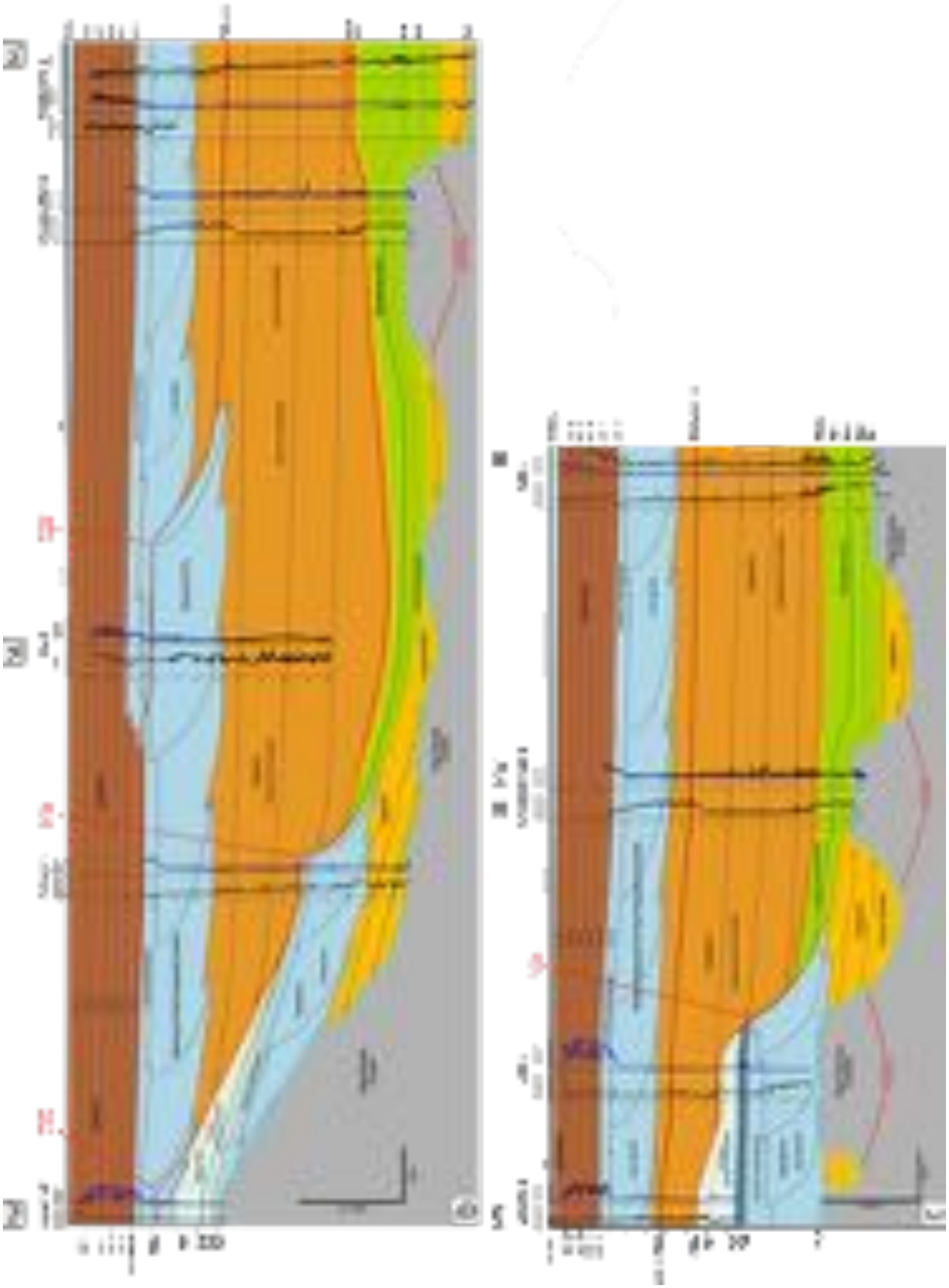

Figure 78. Cross correlation panels from well logs correlations. B) Transect ca. W-E. C) Transect ca. N-S. Wells and the transects locations in Fig. 77. Colour code of the stratigraphy in Fig. 65.

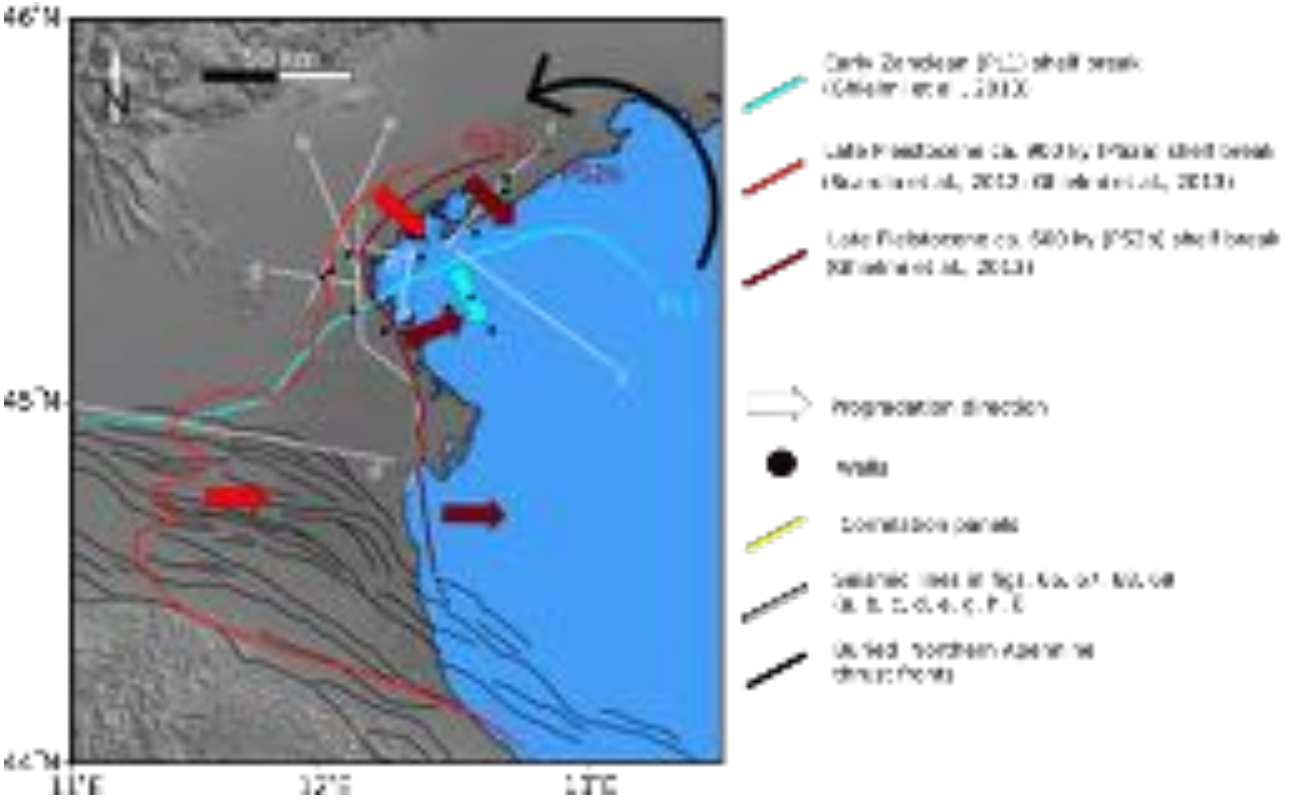

Figure 79. Shelf edges of the PL1, PS2a and PS2b sequences, reconstructed by means of seismic interpretation (Ghielmi et al., 2010, 2013; Scardia et al., 2012) shown in map view. Light blue, red and dark red arrows indicate the progradation direction at each time. Black arrow is useful to suggest the counter-clockwise shelf-edge rotation from Pliocene to late Pleistocene.

In the subsurface, seismic lines (modified from Ghielmi et al. 2013 and Muttoni et al. 2003) show the PS2a shelf edge, recorded only in the north-westernmost Legnaro 1 dir well at ca. -400 m from the datum level. The top of PS2a sequence, 0.6 Ma in age, corresponds to the base PS2b cyclic sequence. The PS2b shelf edge traced by seismic analysis and well log calibration in Ghielmi et al. (2010, 2013) (Figs. 66, 67, 68, 69), has been correlated by means of well-log data in agreement with the new age model and cyclostratigraphic interpretation proposed in this work. The PS2b shelf edge in the VFB, runs parallel to the PS2a, about 15 km basin ward, with foreset SE-progradation direction and curve geometry similar to the present Venetian coast. In the Po Plain area instead, during the same time step (900-600 kyr), a strong horizontal eastwards shift (ca. 100 km) occurred, reaching the final position at less than 10 km offshore from the today coastline (Figs. 72, 73).

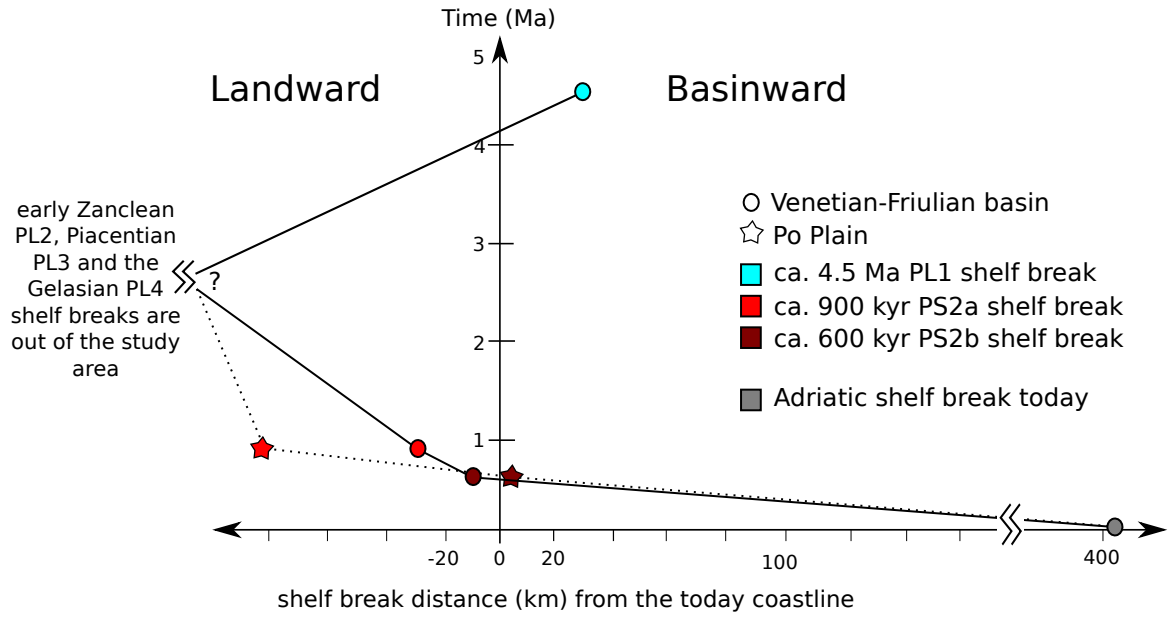

Figure 80. Quantification of the transgressive (landward) regressive (basinward) trend through Plio-Pleistocene time.

5.7. Discussion

4.7.1. Interplaying factors driving the Pliocene-Pleistocene sedimentation in the Venice area

The Plio-Pleistocene sequences accumulated in the study area document the depositional physiographic history of the Venetian-Friulian (VFB) and Northern Adriatic basin (NAB) and the main events that controlled the sedimentary rate and stacking pattern.

During the early Zanclean in the VFB developed a complete transitional setting (from continental to marine environment) but in the study area records only the shelf-slope and prograding complex (i.e., PL1 sequence with Eraclea fm.).

At the same time the southern margin of the Po Plain, the early Pliocene regional uplift occurred as the main consequence of the Northern Apennine PL1 tectonic phase, characterised by fold and thrust belt uplift, tilting and foredeep deepening (Ghielmi et al., 2010; 2013).

In the Po Plain, a following rapid uplift began since late Zanclean to Piacenzian time (PL2 and PL3 sequences), due to the external Apennine thrust fronts migration toward north-eastern sectors, and relative foreland bulge (Vai et al., 1987; Ghielmi et al., 2013; Maesano et al., 2015; Maesano and D'Ambrogi, 2016) located exactly in the FVB (Barbieri et al., 2007; Mancin et al., 2004; Mancin et al., 2016; Zecchin at al., 2017).

In the northern sector of the study area, PL2-PL3 sequence is lithologically represented by the foreland condensed clastic deposits of Dolo fm. and locally by a foramol carbonate platform (Lido fm.). The skeletal carbonate platform deposited into a limited zone, and survived into a fully clastic setting, due to local shallow-water condition (0-50 m palaeo-water depth). Condensed foreland sedimentation and localized carbonate production led to argue the occurrence of a paleo-high, probably related to a peripheral bulge concomitantly with a warm condition (Di Bella et al., 2005; Barbieri et al., 2007; Mancin et al., 2016). The chronostratigraphic constrain of the Lido carbonate platform comes from coeval and analogue deposits spread into Mediterranean basin (Di Bella et al., 2005 and reference therein). In particular, these relatively shallow-water skeletal packstones seem very similar to others lying on top of the highest Apennine structural fronts described by Capozzi & Picotti, (2003) and Roveri and Taviani (2003), deposited until late Pliocene cooling at about 2.7 Ma (Lisiecki & Raymo, 2005, 2007 and references therein).

In the Northern Apennine, the base Gelasian PL4 tectonic phase and related sequence boundary was outlined by the strong regional uplift due to the Emilia-Romagna thrusts fronts configuration and also depocenters deepening and foreland tilting (Ghielmi et al., 2013; Maesano et al., 2015; Maesano and D'Ambrogi, 2016). The unconformity at the top of Lido fm. can be interpreted as a tectonic-related regressive episode. A relative sea-level change, together with a climate cooling peak occurred at 2.7 Ma, contributed to carbonate production end.

The following base Calabrian PS1 tectonic activity produced large clastic volumes (km-thick), recorded in the Po basin foredeep (Ghielmi et al., 2010, 2013) but the Venetian foreland shows low to moderate sediment rates and fixed provenance area from the eastern Southern Alps (Stefani, 2002) for the entire Pliocene-early Pleistocene period. This means that sediments from the central and western Alps did not reach the Venetian foreland because they deposited and confined into deep Po basin foredeep, filling the available accommodation space.

Furthermore, the sediments eroded from the exposed southern Apennine margin and those reworked during the tectonic deformation, where probably stored into the evolving subaqueous piggy-back basins that worked as sediments traps.

Subsurface data analysis from Fantoni et al. (2001), Ghielmi et al. (2010, 2013) and Cazzini et al. (2015 and reference therein) show evidence of an overall compressive deformation decrease in the Po Plain-Norther Adriatic foreland basin (PPAF) area during the middle-late Quaternary. Turbidites of Carola fm. and Po Plain Prograding Complex (Ravenna fm.) (PS1 and PS2 sequences) rapidly advanced along the PPAF foredeep as far as its present-day position, reaching also the study area (Ghielmi et al., 2010, 2013; Zecchin and Tosi, 2014; Tosi et al., 2015; Toscani et al., 2016; Zecchin et al., 2017).

In the Venetian-Friulian basin, at least 700 m thick of Carola fm., was responsible for the sedimentary infill of the deeper portions of the basin and the consequent accommodation space reduction. PS1-PS2 sequences can be described as an overall basin-scale regressive cycle mainly driven by climatic changes coupled with large availability of siliciclastic sediments from western, central and eastern Southern Alps (Stefani, 2002). In fact, at about 1.8 Ma the average eustatic level started falling due to climate deterioration, characterised by long periods of sea-level lowering alternated with fast sea-level rise (Lisiecky and Raymo, 2005; Miller et al., 2005, 2011).

The glacial acme MIS 22 (Rohling et al., 1998; Miller et al., 2005, 2011), interpreted as the onset of major glaciation in the Alps region (Muttoni et al., 2003), was responsible for an intense continental erosion phase expressed with a huge clastic volume delivered into the Po-Adriatic basin. Consistently, into the VFB and NAB, the highest sedimentation rate is recorded (PS2a sequence).

The maximum peak (7000 m/Ma at 600-500 kyr, between MIS 16-12 lowstands) is in correspondence of an important basin facies shift: from foredeep turbidites to delta-type prograding deposits, typically marked by high accumulation rates. It is possible to infer that, the fast development and migration of the Po Plain Prograding complex shelf edge during the middle-late Quaternary (Fig. 79) is due to the favourable coupling between stable tectonic setting and high sedimentary supply derived from both eastern Southern Alps and Paleo-Po rivers (Barbieri et al., 2007; Garzanti et al., 2011), confirmed also by petrofacies analysis (Stefani, 2002).

This change in supply source, from a single western-central Southern Alps area (typical Po signal, Stefani et al. 2002) to mixed source within eastern Southern Alps (i.e., paleo-Brenta, paleo-Bacchiglione and paleo-Adige) may be due to the rapid northward shifting of the paleo-Po river into the Venetian basin, favoured by the progressive Po Plain accommodation space reduction of the western sector during the Calabrian (e.g., during the sedimentation of Carola fm.).

The strong ciclicity signal into the upper PS2b sequence, recognised in the Venice 1 core by Kent et al. (2002) and Massari et al. (2004), has been preserved into sedimentary record by low-to-absent tectonic activity and high sedimentation rates, favoured by compatible subsidence rates. The whole modern Adriatic Sea shelf setting generally meet those requirements (Patruno et al., 2015).

According with the presented new age model, 100 kyr frequency is the most efficient climate factor in modulating sea-level fluctuations and consequently the shape of the topmost sequence architecture into the VFB and NAB.

This climate frequency is indicative of the more extreme glacial events during the last ca. 1 Ma, with greater impact on the amplitude of sea-level changes (Shackelton, 1997; Raymo et al., 1997; Muttoni et al., 2003; Lisiecky and Raymo, 2005, 2007). Examples of similar overall progradational-regressive units providing evidence of 100 kyr sequences of the past 500-600 kyr, from diverse settings, have

been reported in several margins in the Mediterranean and nearby areas (Rabineau et al., 2005; Trincardi and Correggiari, 2000; Lobo et al., 2013 and reference therein), but they have never been described and dated in such detail in the Venetian-Friulian and Northern Adriatic basin.
The shelf-edge step-wise migration (Fig. 80) through the Plio-Pleistocene, highlights the incredibly fast south-east progradation occurred over the last 900 kyr. In fact, in the Adriatic Sea the progradation system is fed with sediments provided by Po river and all rivers draining the eastern Southern Alps. The clinoforms develop above a complete filled Po-Adriatic foredeep and foreland basin where the accommodation space can increase only by lower sediment compaction.

5.8. Conclusions

Combined seismics and well-log analysis with palaeobathymetry and subsidence trends, allowed to better understand the Venetian-Friulian basin and Northern Adriatic Sea evolution and controlling factors on sedimentation during Plio-Pleistocene time.
In summary:

- This work provides, for the first time, a reliable key for an onshore-offshore chronostratigraphic correlation of the Pliocene-Pleistocene sedimentary sequence in the Venetian-Friulian and Northern Adriatic region. It can be considered as a robust stratigraphic base necessary for future intervention programs, for instance the problem of natural subsidence of Venice.
- The influence of the migrating Northern Apennine fronts probably drives the accommodation space of the VFB for the entire Pliocene-Calabrian time.
- During middle-late Quaternary, the stratigraphic architecture was mainly driven by climatic-related processes (e.g., variation of sediment supply during climate change). The onset of major Alpine glaciations promoted an acceleration in both erosion and sediment supply, leading to a rapid progradation of paleo-Southalpine and paleo-Po alluvial fans.
- In the Venetian-Friulian and Northern Adriatic shelf, the PS2 progradational unit shows sequences with rhythmic variations in shape and thickness. The most evident cyclostratigraphic signature reflects a 100 kyr frequency, influenced by the middle-late Quaternary climatic cyclicity.
- Overall counter clockwise shelf-edge geometries rotation is evidenced. This is interpreted due to the Po basin accommodation space progressive reduction since Pliocene-middle Pleistocene. A relevant shelf-edge km-shift is occurred during PS2 phase, caused by the west-to-east progradation of the Po Plain Prograding Complex.

- It is possible to highlight the incredibly fast south-east shelf-edge migration (and relative progradation rate) in the Adriatic Sea, occurred during the last 900 kyr respect with the Plio-Pleistocene evolution.

CHAPTER 6

GENERAL CONCLUSIONS AND FUTURE OUTLOOKS

The results from this three-year Ph.D project can be briefly summarized as follows:

- Detailed 3D surfaces in TWT covering for the first time the entire central and eastern Po-Adriatic basin (ca. 40,000 km^2), obtained through interpretation of 2D lines (8,000 km in total) and subsequent interpolation.
- The 3D-model was depth-converted using a novel and calibrated velocity model; the obtained 3D depth-model allows to quantitatively study the subsidence of Po-Adriatic foredeep and its evolution during the Northern Apennine thrust front migration.
- Six chronologically calibrated isobath maps, every ca. 1 Ma, reflecting the step-wise morphological evolution of the basin.
- Six isopach maps for the Plio-Pleistocene units were calculated: these maps are useful tools to understand the depocenters thickness and their migration through time.
- Late Messinian paleotopography of the study area was reconstructed by means of backstripping-flexural modeling.
- The resulted landscape can sustain a new geological model of the Mediterranean basin evolution during the Messinian Salinity Crisis maximum drawdown. In fact, stratigraphic features and the modeling can prove that the Po plain-Northern Adriatic basin was an isolated basin where the marine environment was persevered under a water column hundreds of meters thick, even during the sea level fall. It was possible because of a sill located in the Southern Italy (Santantonio et al., 2013) that protected the Adriatic Sea from the estimated 1.5 km sea level fall, recorded along the western Mediterranean margin (i.e., Gulf of Lions, Lofi et al., 2005, 2011).
- 2D detailed chronostratigraphic correlations of the Venetian-Friulian and Northern Adriatic basin were performed by means of seismic interpretation and well log analysis. This study

will be very useful to correlate the Adriatic and Po basin subsurface sequences and increase the knowledge on the complete foredeep-foreland basin system and its evolution.

- 1D-backstripping analysis on five wells in the Venetian area in order to calculate the decompacted sedimentary rate through time and discuss climate VS tectonic efficiency in sediment production. In detail, in the Venetian-Northern Adriatic basin, the sedimentation rate during the last 1 Ma is higher than during Pliocene time. The results are useful to understand the erosion potential of different processes and sediment sources, both acting in a poorly deformed sedimentary basin. In this case, the basin architecture is strongly influenced, during Pliocene, by the Apennine orogeny which controlled the accommodation space available with flexural subsidence-uplift phases. During the middle-late Quaternary (time with negligible tectonic activity) the variability of the sedimentation rates is correlated to the onset of Alpine glaciation and change in sediment source from a single south-eastern Alpine input to the coupling with the huge Po Plain Prograding Complex (paleo Po river) from the west.

In conclusion, a number of results allow presenting, for the first time, the basin scale 3D architecture of the Po Plain-Northern Adriatic basin with a high-resolution and areal extension respect with the previously published studies.

Thanks to the high quality of the seismics and well log data, focus studies were performed to investigate more in detail some particular issues, for instance: i) effects of the dramatic regional event like the Messinian Salinity Crisis and ii) Quaternary climate instability.

Both these side-projects connect the local results found in the Po Plain-Northern Adriatic basin with Mediterranean-scale insights. In fact, geological processes like climate variability and lithospheric interplay are valid also for other places in the Mediterranean basin.

Nevertheless, none of the above-cited results would have been achieved without a continuous and fruitful collaboration among Academy (Italian and international) and industry. This apparently non-scientific result, indeed, deserves to be highlighted and take as a positive example for future collaborations between different partnerships.

Each of these represent the starting point for future outlooks and collaborations, some of which are already in progress. The 3D architecture in depth domain is also the base for further numerous scientific applications, such as:

1) structural history of the recent evolution of the basin. A dedicated study on the deformation of the upper and recentmost isobath surface, dated ca. 900 kyr, will contribute toward better understanding of the recent seismicity and quantifying the slip rates to produce seismic hazard reports.
2) fault restoration and decompaction for calculation of long term slip rates. This workflow has been successfully applied on a restricted area of the Po Plain by GeoMol team (2014) but a complete study of the whole basin is lacking.
3) sediment flux calculation might be worked out decompacting the 3D surfaces and calculating the restored volume of the successions. The sedimentary flux trend through time might me fundamental for estimating the erosion activity and give more information for mass balance study.
4) provenance analysis. The petrographic analysis coupled with a morphological description of the target surface will be decisive in provenance analysis and characterization of clastic bodies (i.e., potential reservoirs).
5) basin analysis thermal modeling, fundamental in Oil Industry to study the hydrocarbon generation study and for both Industry and Academia, for a higher understanding in geothermal model.

References

Allen P.A. & Allen J.R., 1990. Basin analysis, principles and applications. Blackwell Publishing, pp. 549.

Amore, M.R., Biffi, U., Capoferri, E., Ghielmi, M., Minervini, M., Rossi, M., 2004. Studio sedimentologico-stratigrafico della successione messiniano- pleistocenica della pianura lombarda. Eni-Agip Internal Report, San Donato Milanese (Italy).

Argnani, A., Ricci-Lucchi, F., 2001. Tertiary siliciclastic turbidite systems of the Northern Apennines. In: Vai, G.B., Martini, I.P. (Eds.), Anatomy of an Orogen: the Apennines and Adjacent Mediterranean Basins. Kluwer Academic Publishers, p. 327-350.

Argnani, A., Barbacini, G., Bernini, M., Camurri, F., Ghielmi, M., Papani, G., Rizzini, F., Rogledi, S., Torelli, L., 2003. Gravity tectonics driven by quaternary uplift in the Northern Apennines: insights from the La Spezia-Reggio Emilia geo-transect. Quat. Int., v.101-102, p. 13-26.

Artoni, A., 2003. Messinian events within the tectoni-stratigraphic evolution of the Southern Laga Basin (Central Apennines, Italy). Boll. Soc. Geol. It., v. 122, p. 447-465.

Artoni, A., Bernini, M., Papani, G., Rizzini, F., Barbacini, G., Rossi, M., Rogledi, S., Ghielmi, M., 2010. Mass-transport deposits in confined wedge-top basins: surficial processes shaping the Messinian orogenic wedge of Northern Apennine of Italy. Ital. J. Geosci. v. 129 (1), p. 101-118.

Bache F., Olivet J. L., Gorini C., Rabineau M., Baztan J., Aslanian D., Suc JP, 2009. Messinian erosional and salinity crises: View from the Provence Basin (Gulf of Lions, Western Mediterranean): Eart and Planetary Science Letters, v. 286, p. 139-157.

Bache F., Popescu S-M., Gorini C., Suc J-P., Clauzon G., Olivet J-L., Rubino J-L., Melinte-Dobrinescu M.M., Jolivet L., Jouannic G., Lerouz E., Aslanian D., Dos Reis A.T., Mocochain L., Dumurdzanov N., Zagorchev I., Sokoutis V.S., Csato I., Ucarkus G., Cakir Z., 2012, A two step process for the reflooding of the Mediterranean after the Messinian Salinity Crisis: Basin Research, v. 24, p. 125-153.

Baldwin, B. & Butler, C.O., 1985. Compaction curves. AAPG Bull., v. 69(4), p. 622-626.

Barbieri C., Bertotti G., Di Giulio A., Fantoni R. and Zoetemeijer R., 2004, Flexural response of the Venetian) foreland to the Southalpine tectonics along the TRANSALP profile: Terra Nova, v. 16, p. 273-280.

Barbieri C., Di Giulio A., Massari F., Asioli A., Bonato M. & Mancin N., 2007. Natural subsidence of Venice area during the last 60 My. Basin Research, v. 19 (1), p. 105-123.

Barberi F., Buonasorte G., Cioni R., Fiordalisi A., Foresi L., Iaccarino S., Laurenzi M.A., Sbrana A., Vernia L. & Villa I.M. (1994). Plio-Pleistocene geological evolution of the geothermal area of

Tuscany and Latium. Memorie Descrittive della Carta Geologica Italiana, v. 49, p. 77-134.

Barchi, M. and A. Bigozzi, 1995, Ipotesi sulla geometria e la genesi dei bacini euxinici del Trias superiore in Appennino Centrale: Studi Geologici Camerti, v. 2, p. 53-62.

Barone M., Critelli S., La Pera E., 2006. Stratigraphy and detrital modes of upper Messinian post-evaporitic sandstones of the Southern Apennines, Italy: evidence of foreland-basin evolution during the Messinian Mediterranean salinity crisis. International Geology Review, v. 48, p. 702-724.

Basili, R., Valensise, G., Vannoli, P., Burrato, P., Fracassi, U., Mariano, S., Tiberti, M. M., Boschi, E., 2008. The Database of Individual Seismogenic Sources (DISS), version 3: Summarizing 20 years of research on Italy's earthquake geology. Tectonophysics, 453, 1-4, 20-43

Bassetti M. A., Manzi V., Lugli S., Roveri M., Longinelli A., Ricci Lucchi F., Barbieri M., 2004. Paleoenvironmental significance of Messinian post-evaporitic lacustrine carbonatesin the northern Apennines, Italy. Sedimentary Geology, v. 172, p.1-18.

Bassinot, F.C., Labeyrie, L.D., Vincent, E., Quidelleur, X., Shackleton, N.J., Lancelot, Y., 1994. The astronomical theory of climate and the age of the Brunhes-Matuyama magnetic reversal. Earth Planet. Sci. Lett. v. 126, p. 91-108.

Becker, J. J. et al. Global Bathymetry and Elevation Data at 30 Arc Seconds Resolution: SRTM30_PLUS. 2009. Marine Geodesy, v. 32, p. 355-371.

Beicher, Robert J. Physics for Scientists and Engineers. Orlando: Saunders College, 2000.

Bello, M., Fantoni, R., 2002. Deep oil plays in the Po Valley: Deformation and hydrocarbon generation in a deformed foreland – AAPG Hedberg Conference, "Deformation History, Fluid Flow Reconstruction and Reservoir Appraisal in Foreland Fold and Thrust Belts" May 14-18, 2002, Palermo – Mondello (Sicily, Italy).

Bertello F., Fantoni R., Franciosi R., Gatti V., Ghielmi M., Pugliese A., 2010. From thrust-and-fold belt to foreland hydrocarbon occurrences in Italy. VINING, B. A. & PICKERING, S. C. (eds) Petroleum Geology: From Mature Basins to New Frontiers – Proceedings of the 7th Petroleum Geology Conference, p. 113–126.

Bertini A., Ciaranfi N., Marino M., Palombo M.R., 2010, Proposal for Pliocene and Pleistocene land-sea correlation in the Italian area. Quaternary International, v. 219, p. 95-108.

Bertotti G., Picotti V., Bernoulli D., Castellarin A., 1993. From rifting to drifting: tectonic evolution of the South-Alpine upper crust from the Triassic to the Early Cretaceous – Sedimentary Geology, v. 86, p. 53-76.

Bigi G., Castellarin R., Catalano R., Coli M., Cosentino D., Dal Piaz G. V., Lentini F., Parotto M., Patacca E., Praturlon A., Salvini F., Sartori R., ScandoneP., Vai G. B., 1986. Synthetic Structural-

kinematic map of Italy, 1:2,000,000. Consiglio Nazionale delle Ricerche, Progetto Finalizzato Geodinamica.

Bigi, G., Cosentino, D., Parotto, M., Sartori, R., Scandone, P., 1992. Structural Model of Italy and Gravity Map, 1:500,000. Quad. Ric. Scientifica, 114, 3, S.EL.CA Florence.

Bigi, S., F. Calamita, G. Cello, E. Centamore, G. Deiana, W. Paltrinieri, and M. Ridolfi, 1995a, Evoluzione messiniano-pliocenica del sistema catena-avanfossa nell'area marchigiano-abruzzese esterna: Studi Geologici Camerti, v. 1, p. 29-35.

Bini A., Cita M.B. and Gaetani M., 1978, Southern Alpine lakes – Hypotesys of an erosional origin related to the Messinian entrenchment: Marine Geology, v. 27, p. 271-188.

Blanc-Valleron M.M., Pierre C., Caulet J.P., Caruso A., Rouchy J.M., Cespuglio G., Sprovieri R., Pestrea S. and Di Stefano E., 2002, Sedimentary, stable isotope and micropaleontological records of paleoceanographic change in the Messinian Tripoli Formation (Sicily, Italy): Palaeogeography, Palaeoclimatology, Palaeoecology, v. 185, p. 255–286.

Blanc, P.L., 2006, Improved modelling of the Messinian Salinity Crisis and conceptual implication: Palaeogeography, Palaeoclimatology, Palaeoecology, v. 238, p. 349–372.

Boccaletti, M., Coli, M., Eva, C., Ferrari, G., Giglia, G., Lazzarotto, A., Merlanti, F., Nicolich, R., Papani, G., Postpischl, D., 1985. Considerations on the seismotectonics of the Northern Apennines. Tectonophysics, v. 117, p. 7–38.

Boccaletti, M., Corti, G., Martelli, L., 2010. Recent and active tectonics of the external zone of the Northern Apennines (Italy) – International Journal Earth Science (Geol Rundsch).

Bongiorni, D., 1987. La ricerca di idrocarburi negli alti strutturali mesozoici della Pianura Padana: l'esempio di Gaggiano – Atti Tic. Sc. Terra Vol. XXXI, pp. 125-141.

Bonini, L., Toscani, G., & Seno, S., 2014. Three-dimensional segmentation and different rupture behavior during the 2012 Emilia seismic sequence (Northern Italy). Tectonophysics, v. 630, p. 31-42.

Bortolami, G.C., Fontes, J.Ch., Markgraf, V., Salie'ge, J.F., 1977. Land, sea and climate in the northern Adriatic region during late Pleistocene. Palaeogeogr. Palaeoclimatol. Palaeo- ecol. v. 21, p. 139-156.

Brambati, A., Carbognin, L., Quaia, T., Teatini, P. & Tosi, L. 2003. The Lagoon of Venice: geological setting, evolution and land subsidence. Episodes, v. 26, p. 264–268.

Bresciani I. and Perotti C.R, 2014, An active deformation structure in the Po Plain (N Italy): The Romanengo anticline: Tectonics, v. 33, p. 2059-2076.

Burrato P., Ciucci F., Valensise G., 2003. An inventory of river anomalies in the Po Plain, Northern Italy: evidence for active blind thrust faulting. Annals of Geophysics, v. 46, p. 865-882.

Butler W.H.R., Lickorish W.H., Grasso M. and Pedley H.M., 1995. Tectonics and sequence stratigraphy in Messinian basins, Sicily: Constraints on the initiation and termination of the Mediterranean salinity crisis: GSA Bulletin, v. 107, p. 425–439.

Capozzi, R. & Picotti, V., 2003. Pliocene sequence stratigraphy, climatic trends and sapropel formation in the Northern Apennines (Italy). Palaeogeogr. Palaeoclimatol. Palaeoecol., v. 190, p. 349-371.

Carminati, E., Doglioni, C., Scrocca, D., 2003. Apennines subduction-related subsidence of Venice (Italy). Geophys. Res. Lett. v. 30 (13), 1717.

Carminati E., Doglioni C. & Scrocca D., 2005. Magnitude and causes of Long-Term subsidence of the Po Plain and Venetian region. In: Fletcher C.A. & Spencer T., "Flooding and Environmental Challenges for Venice and its Lagoon: State of Knowledge". Cambridge University Press.

Carminati, E., Scrocca, D., Doglioni, C., 2010. Compaction-induced stress variations with depth in an active anticline: Northern Apennines, Italy. Journal of Geophysical Research, 115, B02401.

Carminati, E., Doglioni, C., 2012. Alps vs. Apennines: the paradigm of a tectonically asymmetric Earth. Earth- Science Reviews, v. 112, p. 67-96.

Caruso A., Pierre C., Blanc-Valleron M.M. and Rouchy J.M, 2015. Carbonate deposition and diagenesis in evaporitic environments: The evaporative and sulphur-bearing limestones during the settlement of the Messinian Salinity Crisis in Sicily and Calabria: Palaeogeography, Palaeoclimatology, Palaeoecology, v. 429, p. 136-162.

Casati, P., Bertozzi, P., Cita, M.B., Longinelli, A., Damiani, V., 1976. Stratigraphy and paleoenvironment of the Messinian "Colombacci" formation in the periadriatic trough; a pilot study. In: Catalano, R., Ruggieri, G., Sprovieri, R. (Eds.), Messinian Evaporites in the Mediterranean. Memorie della Società Geologica Italiana, v. 16, pp. 173-194.

Casero P., Rigamonti A., Iocca, M., 1990. Paleogeographic relationship during Cretaceous between the Northern Adriatic area and the Eastern Southern Alps; Mem.Soc.Geol.It. v. 45, p. 807-814.

Casero, P., 2004. Structural setting of petroleum exploration plays in Italy. In: Geology of Italy (Ed. by U. Crescenti, S. D'Offizi, S. Merlino & L. Sacchi), Spec.Vol. It. Geol. Soc., IGC 32th Florence 2004, pp.189-199.

Cassano, E., Anelli, L., Fichera, R., & Cappelli, V., 1986. Pianura Padana, interpretazione integrata di dati Geofisici e Geologici. In: 73 Congresso Soc. Geol. It., Roma.

Castellarin, A., 2001. Alps-Apennines and Po Plain-Frontal Apennines relationships. In: Vai G. B. and Martini I. P. (Eds.), Anatomy of an Orogen. The Apennines and adjacent Mediterranean Basins, Kluver, London, p. 177- 196.

Castellarin, A., Cantelli, L., 2010. Geology and evolution of the Northern Adriatic structural triangle

between Alps and Apennines – Rend. Fis. Acc. Lincei, v. 21, (Suppl 1):S3-S14;

Catalano R., Di Stefano E., Infuso S., Sulli A., Vitale F.P. & Vail P.R. (1998). Sequence and system tracts calibrated by high- resolution bio-chronostratigraphy: the central Mediterranean Plio-Pleistocene record. *In* de Graciansky P.C., Jacquin T. & Vail P.R. (eds.), Mesozoic-Cenozoic Sequence Stratigraphy of Western European Basins, *SEPM Special Publication*, 60: 157-179.

Catuneanu, O., 2006. Principles of Sequence Stratigraphy. Elsevier, Amsterdam, p. 386.

Catuneanu, O., Abreu, V., Bhattacharya, J.P., Blum, M.D., Dalrymple, R.W., Eriksson, P.G., Fielding, C.R., Fisher, W.L., Galloway, W.E., Gibling, M.R., Giles, K.A., Holbrook, J.M., Jordan, R., Kendall, C.G.St.C., Macurda, B., Martinsen, O.J., Miall, A.D., Neal, J.E., Nummedal, D., Pomar, L., Posamentier, H.W., Pratt, B.R., Sarg, J.F., Shanley, K.W., Steel, R.J., Strasser, A., Tucker, M.E., Winker, C., 2009. Towards the standardization of sequence stratigraphy. Earth-Science Rev. v. 92, p. 1-33.

Cazzini F., Dal Zotto O., Fantoni R., Ghielmi M., Ronchi P., Scotti P., 2015. Oil and Gas in the Adriatic Foreland Italy. Journal of Petroleum Geology, v. 38 (3), p. 255-279.

CIESM (Commission Internationale pour l'Exploration de la Mer Mediterranee, Monaco), 2008. The Messinian Salinity Crisis from Mega-Deposits to Microbiology: A Consensus Report. CIESM Workshop Monograph, v. 33, p. 1-168.

Cita, M.B., Wright, R.C., Ryan, W.B.F., Longinelli, A. (Eds.), 1975. Messinian Paleonvironments. Initial Reports of the DSDP, vol. 42. U.S. Government, Washington, pp. 1003-1035.

Cita, M.B. and Corselli, C., 1990, Messinian paleogeography and erosional surfaces in Italy: an overview: Palaeogeogr., Palaeoclimatol., Palaeoecol., v. 77, p. 67-82.

Cita M.B., Capraro L., Ciaranfi N., Di Stefan E., Lirer F., Maiorano P., Marino M., Raffi I., Rio D., Sprovieri R., Stefanelli S., Vai G.B., 2008. The Calabrian Stage redefined. Episodes, v. 31 (4), p. 408-418.

CNR, 1971, Relazione sul pozzo Venezia 1-CNR. Consiglio Nazionale delle Richerche, Venice.

Conti M.A., Parisi G. & Nicosia U., 1983. Un orizzonte ad *Amphistegina* nel Pliocene di Orvieto e sue implicazioni neotettoniche. Bollettino della Società Geologica Italiana, v. 102 (1), p. 113-122.

Cosentino, D., R. Buchwaldt, G. Sampalmieri, A. Iadanza, P. Cipollari, T. F. Schildgen, L. A. Hinnov, J. Ramezani, and S. A. Bowring, 2013, Refining the Mediterranean ''Messinian gap'' with high-precision U-Pb zircon geochronology, central and northern Italy: Geology, v. 41, p. 323–326.

Cuffaro, M., Riguzzi, F., Scrocca, D., Antonioli, F., Carminati, E., Livani, M., Doglioni, C., 2010. On the geodynamics of the northern Adriatic plate. Rendiconti Fisiche Acca- demia Lincei 21 (Suppl. 1), S253–S279.

D'Ambrogi, C., Pantaloni, M., Borraccini, F., De Donatis, M., 2004. 3D geological model of the

sheet 280 Fossombrone (Northern Apennines) - Geological Map of Italy 1:50,000. In: Pasquarè, G., Venturini, C., Groppelli, G., (Eds.), Atlas Mapping geological in Italy. APAT, S.E.L.CA, Firenze, 193-198.

D'Ambrogi, C., Doglioni, C., 2008. Struttura delle Vette Feltrine. Rendiconti online Soc. Geol. It. v. 4, p. 37-40.

D'Ambrogi, C., Scrocca, D., Pantaloni, M., Valeri, V., Doglioni., 2010. Exploring Italian geological data in 3D; Journal of the Virtual Explorer, Electronic Edition, ISSN 1441-8142, volume 36, paper 33. In: (Eds.) Marco Beltrando, Angelo Peccerillo, Massimo Mattei, Sandro Conticelli, and Carlo Doglioni, The Geology of Italy, 2010.

Dal Piaz, G.V., Bistacchi, A., Massironi, M., 2003. Geological outline of the Alps. Episodes, v. 26, p. 175–180.

de Alteriis, G. and Aiello, G., 1993, Stratigraphy and tectonics offshore of Puglia (Italy, Southern Adriatic Sea): Mar. Geol., v.13, p. 233-253.

de Alteriis, G., 1995, Different foreland basins in Italy: examples from the central and southern Adriatic Sea: Tectonophysics, v. 252, p. 349–373.

De Amicis G.A. (1886). Il calcare ad Amphistegina nella provincia di Pisa, ed i suoi fossili. Atti della Società Toscana di Scienze Naturali, Memorie, v. 7, p. 200-247.

De Donatis, M., 2001, Three-dimensional visualization of the Neogene structures of an external sector of the Northern Apennine, Italy: AAPG Bulletin, v. 85-3, p. 419-431.

De Donatis, M., 2001. Three-dimensional visualisation of the Neogene structures of an external sector of the northern Apennines, Italy. AAPG Bulletin, v. 95(3), p. 419-431.

De Donatis, M., Jones, S., Pantaloni, M., Bonora, M., Borraccini, F., D'Ambrogi, C., 2002. A National Project on Three-Dimensional Geology of Italy: Sheet 280 - Fossombrone in 3D. Episodes v. 25(1), p. 29-32.

Dhont, D., Luxey, P., Chorowicz, J., 2005. 3-D modeling of geologic maps from surface data. AAPG Bulletin 89(11).

Di Bella, L., Carboni, M.G. & Pignatti, J., 2005. Paleoclimatic signi¢cance of the Pliocene Amphistegina levels from the Tyrrenian margin of Central Italy. Boll. Soc. Paleontol. Ital., v. 44(3), p. 219-229.

Di Manna, P., Guerrieri, L., Piccardi, L., Vittori, E., Castaldini, D., Berlusconi, A., Bonadeo, L., Comerci, V., Ferrario, F., Gambillara, R., Livio, F., Lucarini M., Michetti, A., 2012. Ground effects induced by the 2012 seismic sequence in Emilia: implications for seismic hazard assessment in the Po Plain. Annals of Geophysics, 55, No 4.

DISS Working Group, 2015. Database of Individual Seismogenic Sources (DISS), Version 3.2.0: A

compilation of potential sources for earthquakes larger than M 5.5 in Italy and surrounding areas. http://diss.rm.ingv.it/diss/, © INGV 2015 - Istituto Nazionale di Geofisica e Vulcanologia.

Doglioni, C., and E. Carminati. 2002. The effects of four subductions in NE Italy. Transalpine Conference, Mem. Scienze Geol. v. 54, p. 1–4.

Donda F., Civile D., Forlin E., Volpi V., Zecchin M., Gordini E., Merson B., De Santis L., 2013, The northernmost Adriatic Sea: A potential location for CO_2 geological storage?. Mar. Petr. Geol., v. 42, p. 148-159.

Donda, F., Civile, D., Forlin, E., Volpi, V., Zecchin, M., Gordini, E., Merson, B., De Santis, L., 2013. The northernmost Adriatic Sea: a potential location for CO2 geological storage? Mar. Petroleum Geol. v. 42, p. 148-159.

Donda, F., Forlin, E., Gordini, E., Panieri, G., Buenz, S., Volpi, V., Civile, D., De Santis, L., 2015. Deep-sourced gas seepage and methane-derived carbonates in the Northern Adriatic Sea. Basin Res. v. 27, p. 531-545.

Emergeo Working Group, 2013. Liquefaction phenomena associated with the Emilia earthquate sequence of May-June 2012 (Northern Italy). Nat. Hazards Earth Syst. Sci., v. 13, p. 935- 947.

Eni, S.p.A. 2009. The Italian Petroleum Research History. www.eni.it

Falvey D.A. & Middleton M.F., 1981. Passive continental margins: evidence for prebreakup deep crustal metamorphic subsidence mechanism. Oceanol. Acta, 103-114.

Fantoni, R., Massari, F., Minervini, M., Rogledi, S. & Rossi, M., 2001. Il Messiniano del margine subalpino-padano: relazioni tra contesto strutturale e stratigra¢co-deposizionale. Geol. Insubr., v. 6(1), p. 95-108

Fantoni, R., Castellani, D., Merlini, S., Rogledi, S. and Venturini, S., 2002, La registrazione degli eventi deformativi cenozoici nell'avampaese Veneto-Friulano: Mem. Soc. Geol. It., v. 57, p. 301-313.

Fantoni, R., Bersezio, R. & Forcella, F. (2004) Alpine structure and deformation chronology at the Southern Alps-Po Plain border in Lombardy. Boll. Soc. Geol. Ital., v. 123, p. 463-476.

Fantoni, R. And Franciosi, R. 2008. 8 geological sections crossing Po Plain and Adriatic foreland. Rend. Soc. Geol. It, 3/1, Riassunti dell'84° Congresso Nazionale Sassari 15-17 settembre 2008 (Italy), p. 367-368.

Fantoni, R. and Franciosi, R., 2010a, Mesozoic extension and Cenozoic compression in Po Plain and Adriatic foreland: Sassi, F.P. (Ed.), Nature and Geodynamics of the Lithosphere in Northern Adriatic. Rend. Fis. Acc. Lincei., v. 21, p. 181-196

Fantoni, R., Franciosi, R., 2010b. Tectono-sedimentary setting of the Po Plain and Adriatic foreland. Rend. Lincei v. 21 (1), S197–S209.

Fernandez, O., Munoz, J.A., Arbues, P., Falivene, O., Marzo, M., 2004. Three-dimensional reconstruction of geological surfaces: An example of growth strata and turbidite systems from the Ainsa basin (Pyrenees, Spain). AAPG Bulletin, v. 88(8), p. 1049-1068.

Fernandez, O., Jones, S., Armstrong, N., Johnson, G., Ravaglia, A., Munoz, J.A., 2009. Automated tools within workflows for 3D structural construction from surface and subsurface data. Geoinformatica, v. 13, p. 291-304.

Finckh, P.F., 1978. Are southern alpine lakes former Messinian canyons? - Geophysical evidence for preglacial erosion in the Southern alpine lakes. Marine Geology, v. 27, p. 289-302

Garcia-Castellanos D, Fernàndez M., Torné M., 2002, Modelling the evolution of the Guadalquivir foreland basin (South Spain): Tectonics, v. 21, p. 1018.

Garcia-Castellanos D., Estrada F., Jiménez-Munt I., Gorini C., Fernández M., Vergés J. and De Vicente R., 2009, Catastrophic flood of the Mediterranean after the Messinian salinity crisis: Nature Letter, v. 462, p. 778-781.

Garcia-Castellanos, D., Verg.s, J., Gaspar-Escribano, J., and Cloetingh, S., 2003, Interplay between tectonics, climate, and fluvial transport during the Cenozoic evolution of the Ebro Basin (NE Iberia): Journal of Geophysical Research, v. 108, p. 2347

Gargani J., Rigollet C., 2007, Mediterranean Sea level variations during the Messinian salinity crisis: Geophysical Research Letters, v. 34, L10405

Garzanti E., Vezzoli G. & Andò S., 2011. Paleogeographic and paleodrainage changes during Pleistocene glaciations (Po Plain, Northern Italy). Earth-Science Rev., v. 105, p. 25-48.

Gelati E., Dimanti F., Prence J., Cane H., 1987. The stratigraphic record of Neogene events in the Tirana Depressione, Rivista italiana di Pelontologia e Stratigrafia, v. 103, p. 81-100.

Gennari R., Manzi V., Angeletti L., Bertini A., Biffi U., Ceregato A., Faranda C., Gliozzi E., Lugli S., Menichetti E., Rosso A. and Roveri M., 2013, A shallow water record of the onset of the Messinian salinity crisis in the Adriatic foredeep (Legnagnone section, northern Apennines). Palaeogeography, Palaeoclimatology, Palaeoecology, v. 386, p. 145-164

GeoMol Team, 2015. GeoMol – Assessing Subsurface Potentials of the Alpine Foreland Basins for Sustainable Planning and use of Natural Resources. Project Report, p.188. (Augsburg, LfU)

Ghielmi, M., Rogledi, S., Rossi, M., 1998. Studio stratigrafico-sedimentologico dell'area padana: sedimentologia, stratigrafia fisica e play concept della successione Messiniano-Pleistocenica. Eni-Agip Internal Report, San Donato Milanese (Italy).

Ghielmi, M., Nini, C., Livraghi, L., Minervini, M., Rogledi, S., Rossi, M., Sules, O., Visentin, C., 2008. Modern Po PlaineAdriatic foredeep (Italy): geological framework and hydrocarbon

exploration. In: 70th EAGE Conference & Exhibitione Workshop n. 3: Hydrocarbon Plays and Future Potential of the Circum-Mediterranean Region, 9-12 June 2008, Rome (Italy).

Ghielmi M., Minervini M., Nini C., Rogledi S. and Rossi M., 2013, Late Miocene-Middle Pleistocene sequences in the Po Plain - Northern Adriatic Sea (Italy): The stratigraphic record of modification phases affecting a complex foreland basin: Marine and Petroleum Geology, v. 42, p. 50-81

Ghielmi, M., Minervini, M., Nini, C., Rogledi, S. and Rossi, M., 2010, Sedimentary and tectonic evolution in the eastern Po Plain and northern Adriatic Sea area from Messinian to Middle Pleistocene (Italy): Sassi, F.P. (Ed.), Nature and Geodynamics of the Lithosphere in Northern Adriatic. Rend. Fis. Acc. Lincei, v. 21, p. 131-166.

Gibbard L.P., Head M.J., Walker J.C. & The Subcommission On The Quaternary Stratigraphy, 2010. Formal ratification of the Quaternary System/Period and the Pleistocene series/epoch with a base at 2.58 Ma. J. Quat. Sci., v. 25 (2), p. 96-102.

Govers R., Meijer P., Krijgsman W., 2009, Regional isostatic response to Messinian Salinity Crisis events: Tectonophysics, v. 463, p. 109-129.

Haq B.U., Hardenbold J. & Vail P.R., 1987. Chronology of fluc- tuating sea levels since late Triassic. Science, v. 235, p. 1156-1167.

Hsü K.J., Montadert L., Bernoulli D., Cita M.B., Erickson., Garrison R.E., Kidd R.B., Mèlierés F., Müller C. and Wright R., 1977, History of the Mediterranean Salinity Crisis: Nature, v. 267, p. 399-403.

Iaccarino S., Vernia L., Battini P. & Gnappi G. (1994). Osservazioni stratigrafiche sul bordo orientale del Bacino di Radicofani (Toscana meridionale). *Memorie Descrittive della Carta Geologica d'Italia*, v. 49, p.151-168.

Jadoul, F., Rossi, P.M., 1982. Evoluzione paleogeografico-structturale e vulcanismo triassico nella Lombardia centro-occidentale. In A. Castellarin & G.B. Vai: Guida alla geologia del Sudalpino centro-occidentale. Guide geol.reg. S.G.I., p. 143-155, Bologna.

Jolivet L., Augier R., Robin C., Suc JP and Rouchy J.M, 2006, Lithospheric-scale geodynamic context of the Messinian salinity crisis: Sedimentary Geology, v. 188–189, p. 9–33

Kaufmann, O., Martin, T., 2008. 3D geological modelling from boreholes, cross-sections and geological maps, application over former natural gas storages in coal mines. Comput. Geosci. v. 34, p. 278–290.

Kent, D.V., Rio, D., Massari, F., Kukla, G., Lanci, L., 2002, Emergence of Venice during the Pleistocene. Quaternary Science Reviews, v. 21 (14-15), p. 1719-1727.

Krijgsman, W., Hilgen, F. J., Raffi, I., Sierro, F. J. and Wilson, D. S., 1999, Chronology, causes and progression of the Messinian salinity crisis: Nature, v. 400, p. 652–655.

Kuhlemann J., Frisch W., Sz´ekely B, Dunkl I. and K´azm´er M., 2002, Post-collisional sediment budget history of the Alps: tectonic versus climatic control: Int. J. Earth Sci. (Geol. Rundsch.), v. 91, p. 818–37.

Kummerow, J., Kind, R., Oncken, O., Giese, P., Ryberg, T., Wylegalla, K., Scherbaum, F., TRANSALP Working Group, 2004. A natural and controller source seismic profile through the Eastern Alps: TRANSALP. Earth and Planetary Science Letters, v. 225, p. 115–129.

Laskar L.J., Robutel P., Joutel F., Gastineau M., Correia A.C.M., Levrard B., 2004. A long term numerican solution for the insolation quantities of the Earth. Astron. Astrophys., v. 428, p. 261-285.

Lindquist, S.J., 1999. Petroleum systems of the Po Basin province of northern Italy and the northern Adriatic Sea: Porto Garibaldi (biogenic), Meride/Riva di Solto (thermal), and Marnoso Arenacea (thermal): U.S. Geological Survey Open-File Report 99-50-M, 19 p., 15 figs., 3 tables.

Lisiecki, L.E. & Raymo, M.E. (2005) A Pliocene-Pleistocene stack of 57 globally distributed benthic d18O records. Paleoceanography, v. 20, p. 1-17.

Lisiecki, L.E. & Raymo, M.E. (2007) Plio -Pleistocene climate evolution: trends and transitions in glacial cycle dynamics. Quatern. Sci. Rev., v. 26, p. 59-69.

Livio, F.A., Berlusconi, A., Michetti, A.M., Sileo, G., Zerboni, A., Trombino, L., Cremaschi, M., Mueller, K., Vittori, E., Carcano, C., Rogledi, S., 2009a. Active fault-related folding in the epicentral area of the December 25, 1222 (Io=IX MCS) Brescia earthquake (Northern Italy): Seismotectonic implications. Tectonophysics, v. 476 (1–2), p. 320–335

Lobo F. J., Ridente D., 2013. Milankovitch cyclicity in modern continental margins: stratigraphic cycles in terrigenous shelf settings. Boletín Geológico y Minero, v. 124 (2): p. 169-185

Lofi J., Christian Gorini C., Berné S., Clauzon G., A. T. Dos Reis, Ryan W.B.F., Michael S. Steckler M.S., 2005, Erosional processes and paleo-environmental changes in the Western Gulf of Lions (SW France) during the Messinian Salinity Crisis: Marine Geology, v. 217, p. 1-30

Lofi J., Deverchere J. et al., 2011a, Atlas of the Messinian seismic markers in the Mediterranean and Black Sea. Commission for the Geological Map of the World/Mem. de la Soc. Geol. de France, v. 179, pp 72

Lofi J., Sage F., Déverchère J., Loncke L., Maillard A., Gaullier V., Thinon I., Gillet H., Guennoc P., and Christian Gorini C., 2011b. Refining our knowledge of the Messinian salinity crisis records in the offshore domain through multi-site seismic analysis: Bull. Soc. géol. Fr., v. 182, p. 163-180

Lourens, L.J., 2004, Revised tuning of Ocean Drilling Program Site 964 and KC01 (Mediterranean) and implications for the $\delta^{18}O$, tephra, calcareous nannofossil, and geomagnetic reversal chronologies of the past 1.1 Myr. Paleoceanography, v. 19 (3), p. 1-20.

Lourens, L.J., Hilgen, F.J., Laskar, J., Shackleton, N.J., and Wilson, D.S., 2005. The Neogene Period, *in* Gradstein, F.M., Ogg, J.G., and Smith, A.G., eds., A Geologic Time Scale 2004: Cambridge, UK, Cambridge Univer- sity Press, p. 409–440.

Maesano, F. E., Toscani, G., Burrato, P., Mirabella, F., D'Ambrogi, C., Basili, R., 2013. Deriving thrust fault slip rates from geological modeling: examples from the Marche coastal and offshore contraction belt, Northern Apennines, Italy, Marine Petr. Geol., v. 42, p. 122-134.

Maesano, F.E. & Italian GeoMol Team, 2014. Integrating data sources for 3D modeling: the Italian activity in the GeoMol Project. Rendiconti Online Soc. Geol. It., v. 30, 28-32.

Maesano F.E., D'ambrogi C., Burrato P. and Toscani G., 2015, Slip-rates of blind thrust in slow deforming areas: examples from the Po Plain (Italy): Tectonophysics, v. 643, p. 8-25.

Maesano, F.E., D'Ambrogi, C., 2016. Coupling sedimentation and tectonic control: Pleistocene evolution of the central Po Basin. Ital. J. Geosci. v. 135 (3).

Maesano, F.E., D'Ambrogi, C., 2017. Vel-IO 3D: A tool for 3D velocity model construction, optimization and time-depth conversion in 3D geological modeling workflow. Computers and Geosciences, 99, pp. 171-182.

Mancin N., Brandolese S., Cobianchi M., 2004. Micropaleontology and geohistory of the southeastern Po Plain Cenozoinc succession (subsurface data). Atti Ticinensi si Scienze della Terra, v. 45. p. 61-68.

Mancin, N., Di Giulio, A., Cobianchi, M., 2009. Tectonic vs. climate forcing in the Cenozoic sedimentary evolution of a foreland basin (Eastern Southalpine system, Italy). Bas. Res., v. 21, 6, p. 799-823.

Mancin N., Barbieri C., Di Giulio A., Fantoni R., Marchesini A., Toscani G. & Zanferrari A., 2016. The Friulian-Venetian Basin Ii: Paleogeographic Evolution From micropaleontological constraints. Ital. J. Geosci., v. 135 (3), p. 460-473.

Manzi V., Gennari R., Hilgen F., Krijgsman W., Lugli S., Roveri M. and Sierro F.J., 2013, Age refinement of the Messinian salinity crisis onset in the Mediterranean: Terra Nova, v. 25, p. 315-322.

Manzi V., Lugli S., Ricci Lucchi F., Roveri M., 2005, Deep-water clastic evaporites deposition in the Messinian Adriatic foredeep (northern Apennines, Italy): did the Mediterranean ever dry out?: Sedimentology, v. 52, p. 875-902.

Masetti, D., Fantoni, R., Romano, R., Sartorio, D., Trevisani, E., 2012. Tectonostratigraphic evolution of the Jurassic extensional basins of the eastern southern Alps and Adriatic foreland based on an integrated study of surface and subsurface data. AAPG Bulletin, v. 96, no. 11, pp. 2065– 2089.

Massari, F., Rio, D., Serandrei Barbero, R., Asioli, A., Capraro, L., Fornaciari, E., Vergerio, P.P.,

2004, The environment of Venice area in the past two million years. Palaeogeography, Palaeoclimatology, Palaeoecology, v. 202 (3-4), p. 273-308.

Matano F., Barbieri M., Di Nocera S., Torre M., 2005, Stratigraphy and strontium geochemistry of Messinian evaporite-bearing successions of the southern Apennines foredeep, Italy: implications for the Mediterranean salinity crisis and regional palaeogeography: Palaeogeography, Palaeoclimatology, Palaeoecology, v. 217, p. 87–114.

Mattavelli, L., Novelli, L., 1987. Origin of the Po basin hydrocarbons – Mémoires de la Société Géologique de France, nouvelle série. v. 151, p. 97-106.

Mattavelli, L., Grigo, D., Orlando, M., Rossi, M., 1992. Neogene tectono-sedimentary evolution and hydrocarbon occurrence in the Adriatic Sea. Paleot. I Evol. 24-25, p. 377-391.

Meijer, P.T., Krijgsman, W., 2005. A quantitative analysis of the desiccation and re-filling of the Mediterranean during the Messinian Salinity Crisis. Earth and Planetary Science Letters, v. 240, p. 510–520.

Mellere, D., Stefani, C. & Angevine, C., 2000. Polyphase tectonics through subsidence analysis: the Oligo-MioceneVenetian and Friuli Basin, North-East Italy. Basin Res., v. 12, p. 159-182.

Miller K.G., Kominz M.A., Brownimg J.V., Mountains G.S., Katz M.E., Sugarman P.J., Cramer B.S., Christie-Bilck N. & Pekar S.F., 2005. The Phanerozoic record of global sea-level change. Science, v. 310, p. 1293-1298.

Miller, K.G., G.S. Mountain, J.D. Wright, and J.V. Browning. 2011. A 180-million-year record of sea level and ice volume variations from continental margin and deep-sea isotopic records. Oceanography, v. 24(2), p. 40–53,

Minervini, M., 1999. Comparazione tra le serie Messiniane Veneta e Lombarda: caratterizzazione sedimentologica e geochimica. Unpublished Msc thesis, Padova University, Italy.

Minervini, M., Ghielmi, M., Rogledi, S., Rossi, M., 2008. Tectono-stratigraphic framework of the Messinian-to-Pleistocene succession in the Western Po Plain Foredeep (Italy). In: 84° Congresso Nazionale della Società Geologica Italiana, Sassari (Italy), 15-17 September 2008, pp. 562-563.

Molnar P., 2004, Late Cenozoic increase in accumulation rates of terrestrial sediment: How might climate change have affected erosion rates?: Annual Review of Earth and Planetary Sciences, v. 32, p. 67-89.

Moretti I. and Royden L., 1988, Deflection, gravity anomalies and tectonics of dubly subducted contineltal lithosphere: Adriatic and Ionian Seas: Tectonics, v. 7, p. 875-893.

Mosca, P., Polino, R., Rogledi, S., Rossi, M., 2010. New data for the kinematic interpretation of the Alps– Apennines junction (Northwestern Italy) - Int J Earth Sci (Geol Rundsch), v. 99, p. 833–849.

Müllenders, W., Favero, V., Coremans, M., Dirickx, M., 1996. Analyses polliniques des sondages a Venise (VE1, VE1bis, VE2). Aardkund Mededel 7, 87-117.

Mutti, E., 1985. Turbidite systems and their relations to depositional sequences. In: Zuffa, G.G. (Ed.), NATO ASI Series, Series C. Reidel Publishing Co., Amsterdam, pp. 65-93.

Mutti, E., Davoli, G., Figoni, M., Sgavetti, M., 1994. Part 1: conceptual stratigraphic framework. In: Mutti, E., Davoli, G., Mora, S., Sgavetti, M. (Eds.), The Eastern Sector of the South-Central Folded Pyrenean Foreland: Criteria for Stratigraphic Analysis and Excursion Notes (2nd High-Resolution Sequence Stratigraphy Conference, 20-26 June 1994, Tremp, Spain), pp. 3-16.

Muttoni, G., Carcano, C., Garzanti, E., Ghielmi, M., Piccin, A., Pini, R., Rogledi, S. & Sciunnach, D., 2003. Onset of major Pleistocene glaciations in the Alps. Geology, v. 31(11), p. 989-992.

Muttoni, G., Ravazzi, C., Breda, M., Pini, R., Laj, C.,Kissel,C.,Mazaud, A. & Garzanti, E., 2007. Magnetostratigraphic dating of an intensification of glacial activity in the southern Italian Alps during Marine Isotope Stage 22. Quatern. Res., v. 67, p. 161-173.

Norman, S.E., and Chase, C.G., 1986, Uplift of the shores of the western Mediterranean due to Messinian desiccation and flexural isostasy: Nature, v. 322, p. 450–451.

Panza, G.F., Pontevivo, A., Chimera, G., Raykova, R., Aoudia, A., 2003. The lithosphere–asthenosphere: Italy and surroundings. Episodes, v. 26, p. 169–174.

Patruno S., H G. J., Jacksnon C. AJ., 2015. Quantitative characterisation of deltaic and subaqueous clinoforms. Earth-Science Reviews, v. 142. p. 79-119.

Pellen, R., Popescu SM., Suc JP. Melinte-Dobrinescu M. C., Rubino JL., Rabineau M., Marabini S., Loget N., Casero P., Cavazza W., Head M. J., Aslanian D., 2017. The Apennine foredeep (Italy) during the latest Messinian: Lago Mare reflects competing brackish and marine conditions based on calcareous nannofossils and dinoflagellate cysts. Geobios (2017)

Perotti, C. R., 1991, Osservazioni sull'assetto strutturale del versante padano dell'Appennino Nord-Occidentale: Atti Ticinensi di Scienze della Terra, v. 34, p. 11-22.

Picotti, V., R. Capozzi, G. Bertozzi, F. Mosca, A. Sitta, and M. Tornaghi, 2007. The Miocene petroleum system of the Northern Apennines in the central Po Plain (Italy), in Thrust Belts and Foreland Basins, From Fold Kinematics to Hydrocarbon System, edited by O. Lacombe et al., pp. 117 – 131, Springer Verlag, Berlin.

Picotti V. & Pazzaglia F.J., 2008. A new active tectonic model for the construction of the Northern Apennines mountain front near Bologna (Italy). J. Geophys. Res., 113, B08412.

Pieri, M., Groppi, G., 1981. Subsurface geological structure of the Po Plain (Italy): C.N.R. Progetto Finalizzato Geodinamica, v. 414, p. 1-13.

Ponza, A., Pazzaglia, F.J., Picotti, V., 2010. Thrust-fold activity at the mountain front of the Northern Apennines (Italy) from quantitative landscape analysis. Geomorphology, v. 123 (3–4), p. 211–231

Rabineau, M., Berné, S., Aslanian, D., Olivet, J.L., Joseph, P., Guillocheau, F., Bourillet, J.F., Ledrezen, E., Granjeon, D., 2005. Sedimentary sequences in the Gulf of Lion: A record of 100,000 years climatic cycles. Mar. Pet. Geol. v. 22, p. 775–804.

Raffi, I., Backman, J., Fornaciari, E., Pälike, H., Rio, D., Lourens, L., Hilgen, F., 2006, A review of calcareous nannofossil astrobiochronology encompassing the past 25 million years. Quaternary Science Reviews, v. 25 (23-24), p. 3113-3137.

Raymo, M.E., 1997. The timing of major climate terminations. Paleoceanography 12, 577-585.

Regione Emilia-Romagna & Eni-Agip, 1998. Riserve idriche sotterranee nella Regione Emilia-Romagna. Di Dio G. (ed.), 119 pp., 9 sheets, S.EL.CA., Firenze.

Regione Lombardia & Eni-Agip, 2002. Geologia degli Acquiferi Padani della Regione Lombardia. Carcano C. & Piccin A. (eds.), 130 pp., 9 sheets, S.EL.CA., Firenze.

Rohling, E.J., Fenton, M., Jorissen, F.J., Bertrand, P., Ganssen, G., Caulet, J.P., 1998. Magnitudes of sea-level lowstands of the past 500,000 years. Nature, v. 394, p. 162-165.

Ronald Abraham, J., Lai, C.G., Papageorgiou, A. (2015). Basin-effects observed during the 2012 Emilia earthquake sequence

Rossi, M., Rogledi, S., 1988. Relative sea-level changes, local tectonic setting and basin margin sedimentation in the interference zone between two orogenic belts: seismic stratigraphic examples from Padan foreland basin, northern Italy. In: Nemec, W., Steel, R.J. (Eds.), Fan Deltas: Sedimentology and Tectonic Settings. Blackie and Son, Glasgow, pp. 368-384.

Rossi, M., Rogledi, S., Barbacini, G., Casadei, D., Iaccarino, S., Papani, G., 2002. Tectono-stratigraphic architecture of Messinian piggyback basins of northern Apennines: the Emilia folds in the Reggio-Modena area and comparison with the Lombardia and Romagna sectors. Boll. Soc. Geol. It. 1, p. 437-447.

Rossi M., Minervini M., Ghielmi M., and Rogledi S., 2015, Messinian and Pliocene erosional surfaces in the Po Plain-Adriatic Basin: Insights from allostratigraphy and sequence stratigraphy in assessing play concepts related to accommodation and gateway turn arounds in tectonically active margins: Marine and Petroleum Geology, v. 66, p. 192-216

Rossi M., Rogledi S., Barbacini G., Casadei D., Iaccarino S., Papani G., 2002, Tectono-stratigraphic architecture of Messinian piggyback basins of Northern Apennines: the Eminilia folds in the Reggio-Modena area and comparison with Lombardia and Romagna sectors: Boo. Geol. It., v. 1, p. 437-447.

Rouchy J.M. and Caruso A., 2006, The Messinian salinity crisis in the Mediterranean basin: a

reassessment of the data and an integrated scenario: Sedimentary Geology, v. 188, p. 35-67.

Roveri, M., Manzi, V., Bassetti, M.A., Merini, M., Ricci Lucchi, F., 1998. Stratigraphy of the Messinian postevaporitic stage in eastern Romagna (northern Apennines, Italy). Giorn. Geol. Bologna (Italy). V. 60, p. 119-142.

Roveri, M., Flecker, R., Krijgsman, W., Lofi, J., Lugli, S., Manzi, V., Sierro, F.J., Bertini, A., Camerlenghi, A., De Lange, G., Govers, R., Hilgen, F.J., H€Ubscher, C., Meijer, P.T.H. and Stoica, M., 2014, The Messinian Salinity Crisis: Past And Future Of A Great Challenge For Marine Sciences: Marine Geology, v. 352, p. 25–58.

Ryan W.B.F. and Cita M.B, 1978, The nature and distribution of Messinian Erosional Surfaces; indicators of a several-kilo- meter-deep Mediterranean in the Miocene: Marine Geology, v. 27, p. 193–230.

Ryan W.B.F., 1976, Quantitative evaluation of the depth of the western Mediterranean before, during and after the Late Miocene salinity crisis: Sedimentology, v. 23, p. 791-813.

Santantonio, M., Scrocca, D. And Lipparini, L., 2013. The Ombrina-Rospo Plateau (Apulian Platform): Evolution of a Carbonate Platform and its Margins during the Jurassic and Cretaceous. Marine Petroleum Geology, v. 42, p. 4-29.

Sarti M, Bosellini A, Winterer EL, 1993. Basin geometry and architecture of the a Tethyan passive margin (Southern Alps, Italy): implications for rifting mechanisms. In: Watkins JS et al (eds) Geology and Geophysics of continental margins AAPG Mem. v. 53, p. 241–258.

Scardia G., Festa A., Monegano G., Pini R., Rogledi S., Tremolada F., Galadini F., 2015. Evidence for late Alpine tectonics in the Lake Garda area (northern Italy) and seismogenetic implications. GSA bulletin, v. 127, p. 113-130.

Scardia G., De Franco R., Muttoni G., Rogledi S., Caielli G., Carcano C., Sciunnach D. & Piccin A., 2012. Stratigraphic evidence of a Middle Pleistocene climate-driven flexural uplift in the Alps. Tectonics, 31, TC6004.

Scardia G., Muttoni G. & Sciunnach D., 2006. Subsurface magnetostratigraphy of Pleistocene sediments from the Po Plain (Italy): Constraints on rates of sedimentation and rock uplift.

Sclater, J.G. & Christie, P.A., 1980. Continental stretching: an explanation of the post mid Cretacoeus subsidence of the Central North Sea Basin. J. Geophys. Res., v. 85, p. 3711-3739.

Scrocca D., 2010, Southern Apennines: structural setting and tectonic evolution: (Eds.) Marco Beltrando, Angelo Peccerillo, Massimo Mattei, Sandro Conticelli, and Carlo Doglioni, Journal of the Virtual Explorer, v. 36, pp. 13.

Scrocca D., Carminati E., Doglioni C. and Marcantoni D., 2007, Slab Retreat and Active Shortening along the Central-Northern Apennines. In: Lacombe O., Roure F., Lavé J. and Vergés J. (eds.),

Thrust Belts and Foreland Basins: SE-25, Frontiers in Earth Sciences. Springer Berlin Heidelberg, p. 471-487.

Selli R., Su un libello-guida nel Messinian romagnolo-marchigiano, 1952. Atti 7 Convegno Nazionale del Metano, Taormina, p.192-195.

Selli R, 1954. Il Bacino del Metauro. Giornale di Geologia, v. 24 (2), p. 1-294, Bologna.

Selli R., 1960. Il Messiniano Mayer-Eymar, 1867, Proposta di un neostratotipo: Giornale di Geologia, v. 28, p. 1-33.

Sierro F.J., Hilgen F.J., Krijgsman W., Flores J.A., 2001, The Abas composite (SE Spain): a Messinian reference section for the Mediterranean and the APTS: Palaeogeography, Palaeoclimatology, Palaeoecology, v. 168, p. 141-169.

Shackleton, N.J., 1995, New data on the evolution of Pliocene climate variability, in Vrba, E., Denton, G.H., Partridge, T.C., Burckle, L.H., eds., Palaeoclimate and evolution with emphasis on human origins: Yale University Press, New Haven, p. 242–248.

Shackelton, N. J., 1997. The deep-sea record and the Pliocene boundary. In: Partridge, T. C. (Ed.), The Plio-Pleistocene boundary. Quaternary International. v. 40, p. 33-36.

Stefani C., 2002. Variation in terrigenous supplies in the Upper Pliocene to recent deposits of the Venice area. Sedimentary Geology, v. 153 (1-2), p. 43-55.

Sternai P., Caricchi L., Jolivet L., Garcia-Castellanos D., Sheldrake T., Castelltort S., Magmatic pulse driven by sea-level changes associated with the Messinian Salinity Crisis, 2017. Nature Geoscience.

Sternai P., Herman F., Champagnac J.D, Fox M., Salcher B. and Willett S.D, 2012. Pre-glacial topography of the European Alps: Geology, v. 40, p. 1067-1070.

Thinon I., P. Guennoc P., Serrano O., Maillard A., Lasseur E., Réhault J.P., 2016, Seismic markers of the Messinian Salinity Crisis in an intermediate-depth basin: data for understanding the Neogene evolution of the Corsica Basin (Northern Tyrrhenian Sea): Marine and Petroleum Geology.

Toscani, G., Seno, S., Fantoni, R., Rogledi, S., 2006. Geometry and timing of deformation inside a structural arc; the case of the western Emilian folds (Northern Apennine front, Italy). Boll. della Soc. Geol. Ital. v. 125 (1), p. 59–65.

Toscani, G., Burrato, P., Di Bucci, D., Seno, S., Valensise, G., 2009. Plio-Quaternary tectonic evolution of the Northern Apennines thrust fronts (Bologna-Ferrara section, Italy): seismotectonic implications. Ital. J. Geosci. (Boll. della Soc. Geol. Ital.), v. 128 (2), p. 605–613.

Toscani G., Bonini L., Ahmad M.I., Bucci D.D., Di Giulio A., Seno S. and Galuppo C., 2014, Opposite verging chains sharing the same foreland: Kinematics and interactions through analogue

models (Central Po Plain, Italy): Tectonophysics, v. 633, p. 268-282.

Toscani G., Marchesini A., Barbieri C., Di Giulio A., Fantoni R., Mancin N and Zanferrari A., 2016, The Friulian-Venetian Basin I: architecture and sediment flux into a shared foreland basin: Ital. J. Geosci., v. 135, p. 444-459.

Tosi L., Teatini P., Brancolini G., Zecchin M., Carbognin L., Affato A., Baradello L., 2015. Three-dimensional analysis of the Plio-Pleistocene seismic sequences in the Venice Lagoon (Italy). Journal of the Geological Society, London. v. 169, p. 507-510.

Trincardi F. and Correggiari A, 2000. Quaternary forced regression deposits in the Adriatic basin and the record of composite sea-level cycles. From: Hunt, D. & Gawthorpe, R. L. (eds) Sedimentary Responses to Forced Regressions. Geological Society, London, Special Publications, v. 172, p. 245-269. The Geological Society of London 2000.

Turcotte, D. L., and G. Schubert, 2002, Geodynamics, Cambridge Univ. Press, New York, 456 pp.

Turrini C., Lacombe O. & Roure F., 2014. Present-day 3D structural model of the Po Valley basin, Northern Italy. Marine and Petroleum Geology, v. 56, p. 266-289.

Turrini, C., Angeloni, P., Lacombe, O., Ponton, M., Roure, F., 2015. Three-dimensional seismo-tectonics in the Po Valley basin, Northern Italy Tectonophysics, v. 661, p. 156-179.

Turrini C., Toscani G., Lacombe O., Roure F. 2016. Influence of structural inheritance on foreland-foredeep system evolution: An example from the Po valley region (northern Italy). Marine And Petroleum Geology, vol. 77, p. 376-398.

Urgeles R., Camerlenghi A., Garcia-Castellanos D., De Mol B., Garcés M., Vergés J. And Hardman M., 2010, Newconstraints on theMessinian sealevel drawdown from 3D seismic data of the Ebro Margin, western Mediterranean: Basin Research, v. 23, p. 123-145.

Vai G.B., 2016, Over half a century of Messinian salinity crisis: Boletin Geologico y Minero, v. 127, p. 625-641.

Vail, P.R., Mitchum, R.M., Todd, R.G., Widmier, J.M., Thompson, S., Sangree, J.B., Bubb, J.N., Hatlelid, W.G., 1977. Seismic stratigraphy and global change of sea level. In: Payton, C.E. (Ed.), Seismic Stratigraphy Applications to Hydrocarbon Exploration. AAPG Memoir v. 26, p. 49-212.

Van Hinte J.E., 1978. Geohistory analysis-application of Micropaleontology in Exploration Geology. Bull. Am. Assoc. Petrol. Geol., v. 62 (2), p. 201-222.

Van Wees J.D., and Cloetingh S.A.P.L, 1994, A finite-difference technique to incorporare spatial cariations in rigidity and planar faults into 3-D models for lithospheric flexure: Geophysical Journal International, v. 1, p. 179-195.

Velić, J., Malvić, T., Cvetković, M., Velić, I., 2015, Stratigraphy and petroleum geology of the Croatian part of the Adriatic Basin: J. Pet. Geol., v. 38, p. 281–300.

Watts, A.B., 2001, Isostasy and flexure of the lithosphere: Cambridge, UK, Cambridge University, Press, 458 p.

Wegmann K.W. & Pazzaglia F.J., 2009. Late Quaternary fluvial terraces of the Romagna and Marche Apennines, Italy: Climatic, lithologic, and tectonic controls on terrace genesis in an active orogen. Quat. Sci. Rev., v. 28, p. 137-165.

Willett, S.D, 2010, Messinian Late Neogene Erosion of the Alps: A Climate Driver?: Annu. Rev. Earth Planet. Sci, v. 38, p. 411-437.

Zecchin, M., Tosi, L., 2014. Multi-sourced depositional sequences in the neogene to quaternary succession of the Venice area (northern Italy). Mar. Petroleum Geol. v. 56, p. 1-15.

Zecchin, M., Praeg, D., Ceramicola, S., Muto, F., 2015. Onshore to offshore correlation of regional unconformities in the Plio-Pleistocene sedimentary successions of the Calabrian Arc (central Mediterranean). Earth-Science Rev., v. 142, p. 60-78.

Zecchin M, Donda F., Forlin E., 2017, Genesis of the Northern Adriatic Sea (Northern Italy) since early Pliocene: Mar. Petr. Geol., v.79, p. 108-130.

In Press

Rossi M., Minervini M., Ghielmi M., Rogledi S. (in press), The Po Plain-Adriatic Basin. In Lofi J. (Ed.): Seismic Atlas of the "Messinian Salinity Crisis" Markers in the Mediterranean and Black Seas - vol. 2.

Software

BasinMod 2014, Platte River Associates.

Move™ 2017, by Midland Valley Exploration Ltd.

DecisionSpace®, Landmark, by Halliburton

TISC, https://sites.google.com/site/daniggcc/software/tisc

Web Sites

Eni, S.p.A. 2009. The Italian Petroleum Research History. www.eni.it

GTOPO30 by U.S. Geological Survey, https://lta.cr.usgs.gov/GTOPO30

ViDEPI Project, http://www.videpi.com

GeoMol Project: www.geomol.eu